Neural Plasticity

Neural Plasticity and Neuropathic Pain 2021

Lead Guest Editor: Xue-Qiang Wang
Guest Editors: Yazhuo Kong, Deborah L. Falla, Zhi Jie Zhang, Hao-Yu Hu, and Yu-Long Bai

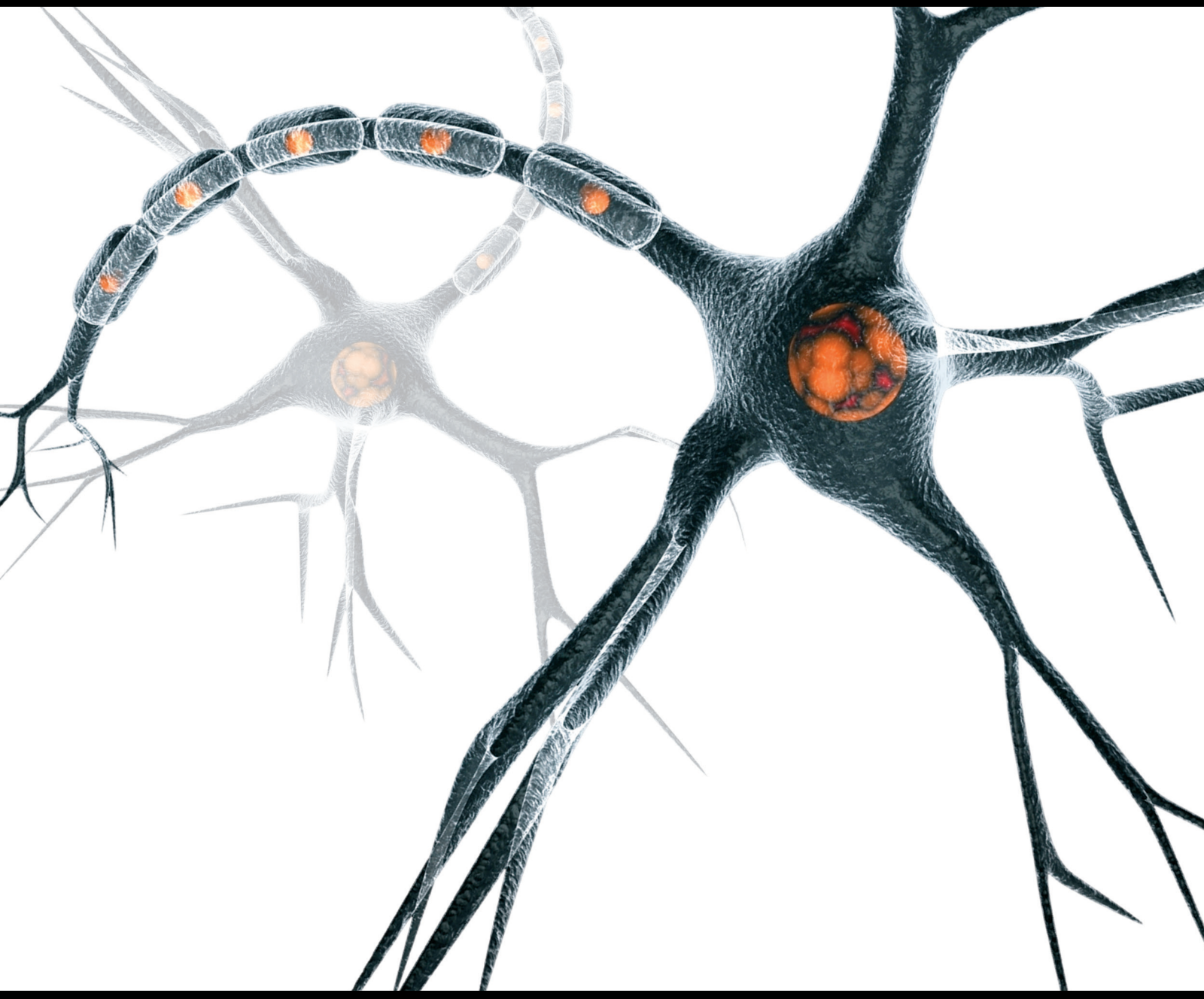

Neural Plasticity and Neuropathic Pain 2021

Neural Plasticity and Neuropathic Pain 2021

Lead Guest Editor: Xue-Qiang Wang
Guest Editors: Yazhuo Kong, Deborah L. Falla, Zhi Jie Zhang, Hao-Yu Hu, and Yu-Long Bai

Contents

Short-Term Spinal Cord Stimulation or Pulsed Radiofrequency for Elderly Patients with Postherpetic Neuralgia: A Prospective Randomized Controlled Trial
Lei Sheng, Zihao Liu, Wang Zhou, Xiaojun Li, Xin Wang, and Qingjuan Gong
Research Article (8 pages), Article ID 7055697, Volume 2022 (2022)

LANCL1 as the Key Immune Marker in Neuropathic Pain
Yu Shi, XueFei Zhang, Qian Fang, Hongrui Zhan, Xianglong Wang, Xiyan Huang, Tao Fan, Wei Liu, and Wen Wu
Research Article (11 pages), Article ID 9762244, Volume 2022 (2022)

Hindawi
Neural Plasticity
Volume 2022, Article ID 5253527, 11 pages
https://doi.org/10.1155/2022/5253527

Research Article

Analysis of Muscular Electrical Activity and Blood Perfusion of Upper Extremity in Patients with Hemiplegic Shoulder Pain: A Pilot Study

Minghong Sui,[1,2] **Naifu Jiang**,[2,3] **Luhui Yan**,[1] **Chenxi Zhang**,[1] **Jiaqing Liu**,[1] **Tiebin Yan**,[4] **and Guanglin Li**[2,3]

[1]*Department of Rehabilitation Medicine, Huazhong University of Science and Technology Union Shenzhen Hospital (Shenzhen Nanshan People's Hospital), Shenzhen 518052, China*
[2]*CAS Key Laboratory of Human-Machine Intelligence-Synergy Systems, Shenzhen Institute of Advanced Technology (SIAT), Chinese Academy of Sciences (CAS), and the SIAT Branch, Shenzhen Institute of Artificial Intelligence and Robotics for Society, Shenzhen 518055, China*
[3]*Guangdong-HongKong-Macao Joint Laboratory of Human-Machine Intelligence-Synergy Systems, Shenzhen 518055, China*
[4]*Department of Rehabilitation Medicine, Sun Yat-sen Memorial Hospital, Sun Yat-sen University, Guangzhou 510120, China*

Correspondence should be addressed to Guanglin Li; gl.li@siat.ac.cn

Received 24 December 2021; Revised 1 July 2022; Accepted 9 September 2022; Published 27 September 2022

Academic Editor: Xue-Qiang Wang

Background. Hemiplegic shoulder pain (HSP) is a common symptom for post-stroke patients, which has a severely adverse impact on their rehabilitation outcomes. However, the cause of HSP has not been clearly identified due to its complicated multifactorial etiologies. As possible causes of HSP, the abnormality of both muscular electrical activity and blood perfusion remains lack of investigations. *Objective*. This study aimed to analyze the alteration of muscular electrical activity and blood perfusion of upper extremity in patients with HSP by using surface electromyography (sEMG) and laser speckle contrast imaging (LSCI) measurement techniques, which may provide some insight into the etiology of HSP. *Methods*. In this observational and cross-sectional study, three groups of participants were recruited. They were hemiplegic patients with shoulder pain (HSP group), hemiplegic patients without shoulder pain (HNSP group), and healthy participants (Healthy group). The sEMG data and blood perfusion data were collected from all the subjects and used to compute three different physiological measures, the root-mean-square (RMS) and median-frequency (MDF) parameters of sEMG recordings, and the perfusion unit (PU) parameter of blood perfusion imaging. *Results*. The RMS parameter of sEMG showed significant difference ($p < 0.05$) in the affected side between HSP, HNSP, and Healthy groups. The MDF parameter of sEMG and PU parameter of blood perfusion showed no significant difference in both sides among the three groups ($p > 0.05$). The RMS parameter of sEMG showed a statistically significant correlation with the pain intensity ($r = -0.691$, $p = 0.012$). *Conclusion*. This study indicated that the muscular electrical activity of upper extremity had a correlation with the presence of HSP, and the blood perfusion seemed to be no such correlation. The findings of the study suggested an alternative way to explore the mechanism and treatment of HSP.

1. Introduction

Hemiplegic shoulder pain (HSP) is a common symptom for post-stroked patients [1]. Almost up to 70% of post-stroked patients suffer from HSP, which can have an adverse impact on their rehabilitation outcomes [2]. In order to apply the appropriate therapeutic techniques for HSP, it would be necessary and essential to know the causes of HSP. Nonetheless, the causes of HSP have not been clearly identified due to the complicated multifactorial etiology [3]. As a possible cause, the abnormality of muscle contractions has been investigated in a number of previous studies [4–7].

The stroke-induced weakness, spasticity, and sensory impairment of shoulder muscles are regarded as the relevant

factors for shoulder pain [4]. These factors are usually measured via subjective scale [5–12]. Modified Ashworth scale (MAS) and tone assessment scale (TAS) are commonly used to evaluate the muscle tone (spasticity) for hemiplegic patients, while manual muscle testing (MMT) is a highly reliable method for assessing muscle strength [5–7]. Besides, the Fugl-Meyer Assessment for upper extremity (FMA-UE), motor evaluation scale for upper extremity in stroke (MESUPES), and reaching performance scale (RPS) are often applied to assess the upper extremity function in hemiplegic patients [8, 9]. In addition, there are also some objective measures for HSP. For example, the goniometer is used to measure range of motion (ROM; flexion, abduction, internal and external rotation) and the hand grip/held dynamometry and fixed force gauge are used to measure the muscle force [10–12]. However, these methods could not directly assess the activities of individual muscles, which would limit the understanding of the muscle functions in patients with HSP. Surface electromyography (sEMG) provides an objective tool that can be used to assess the activities of individual muscles by measuring the muscular electrical activities. By analyzing sEMG data from relevant muscles related to different types of pains, the strength and endurance of individual muscle contractions would be evaluated, which can provide more detailed electrophysiological information under the mechanism of the neuromuscular etiology of many clinical pains such as low back pain, neck pain, and patellofemoral pain [13–16]. Therefore, it should be also a good way to analyze the mechanism of HSP by using sEMG signals.

On the other hand, the arterial, venous, and lymphatic circulatory pumps of the affected upper extremity require to be activated to facilitate adequate blood flow [17]. Failure of any one of these pumps can lead to the development of regional pain syndrome. The immobility of the hemiplegic shoulder may enhance its development [18]. Consequently, the abnormal alteration of local blood flow may account for the reason of HSP. The laser speckle contrast imaging (LSCI) is a fast, full-field, cheap, and relatively simple imaging method [19]. It can give 2-dimension blood perfusion maps of large surfaces. Compared with other measurement techniques for blood flow such as functional near-infrared spectroscopy (fNIRS) and functional magnetic resonance imaging (fMRI), the LSCI is simpler to operate and more robust [19]. The duration of its preparation and data collection is short. Some studies showed the blood flow/perfusion around targeted muscles could be measured by using LSCI, so that the muscle microcirculation could be analyzed [20, 21]. The LSCI also showed some good findings for assessment of pain-related blood perfusion [22, 23]. Thus, the LSCI would be an additional way to reveal the mechanism of HSP.

It is well known that the abnormal contractions of shoulder muscles in patients with HSP are often observed, which might be produced by the changes of both electrophysiology and blood perfusion. Nonetheless, currently, there is lack of investigation on these two physiological responses when contracting muscles in HSP. Thus, in this study, we aimed to investigate the relationship between the HSP and the two physiological responses (electrophysiology and blood perfusion) by using sEMG recordings and LSCI imaging. For comparison purpose, the hemiplegic patients without shoulder pain (HNSP group) and healthy participants (Healthy group) were also involved in this study. The findings of this study would be helpful to further understand the etiology of HSP and to improve the effectiveness of treatment for patients with HSP.

2. Materials and Methods

2.1. Experimental Design. In this observational and cross-sectional pilot study, three groups of participants, hemiplegic patients with shoulder pain (HSP), hemiplegic patients without shoulder pain (HNSP), and healthy subjects (Healthy), were recruited. The clinical characteristics and physiological characteristics of each participant were recorded once by an investigator. Five commonly used clinical characteristics including scores of Fugl-Meyer Assessment for Upper Extremity (FMA-UE), Manual Muscle Testing (MMT), Modified Ashworth Scale (MAS), Range of Motion (ROM) for shoulder flexion and abduction, and Visual Analogue Scale (VAS) for shoulder pain intensity were collected from the affected upper extremity in hemiplegic patients. The physiological responses of both sEMG and blood perfusion were recorded from both affected and non-affected upper extremities in the HSP and HNSP groups and both left and right upper extremities in the Healthy group. The experimental procedure was performed in accordance with the Declaration of Helsinki and was approved by the Institutional Ethics Committee (IRB number: 032502). This study was also registered with the Chinese Clinical Trial Registry (ChiCTR2000029051).

2.2. Participants. The calculation of sample size in this study was based on data from primary measures (sEMG and blood perfusion) instead of VAS. Unlike VAS for which there are abundant studies, there are few studies on sEMG and blood perfusion in the area of hemiplegic shoulder pain. As such, we have to conduct a trial at first to estimate the appropriate sample size. Through the trial, the measures showed a large difference among Healthy group and two patient groups, which led to a large effect size (8.1458). Generally, a large effect size can result in a small sample size [24]. In our study, we used the G∗Power 3.1.9.2 software to calculate the sample size with the above-mentioned effect size (8.1458), alpha (α, 0.05), and power (1-β, 0.95), and finally calculated that a sample size of 6 is sufficient for each group. Thirteen hemiplegic patients with shoulder pain and fourteen hemiplegic patients without shoulder pain were recruited from the Huazhong University of Science and Technology Union Shenzhen Hospital (Mar. 2020-Mar. 2021). And thirteen healthy subjects participated in this study as a control group. The same inclusion criteria for both HSP group and HNSP group were aged 18-80 years; first stroked or previous stroked without sequelae; stroked that appeared within one year; limb dysfunction on only one side of the body; stable vital signs; no severe heart, lung, liver, or kidney dysfunction; no coagulation dysfunction. The HSP group was also

required to meet the criteria that VAS score of shoulder pain ≥ 4 points. The exclusion criteria for all groups were a history of rotator cuff injury; periarthritis, shoulder surgery, or shoulder trauma; malignant tumor; quadriplegia; severe speech or cognitive dysfunction; mental illness; pain caused by cancer, menopause, or fracture; severe dizziness or a pacemaker. All participants gave their written informed consent before testing.

2.3. Physiological Measurements

2.3.1. sEMG Recordings. The shoulder movement is associated with muscles such as biceps brachii, subscapularis, deltoid, pectoralis major, supraspinatus, and infraspinatus [25]. In this study, the sEMG recordings from biceps brachii muscle were selected as a proxy based on the following considerations. (a) Hemiplegic shoulder pain typically appears among stroke patients in the second Brunnstrom stage [2], in which severe muscle spasticity, widely considered the cause of such pain, is often seen in the flexors of these patients [26]. During flexors, the most significant level of spasticity is seen in both biceps brachii and subscapularis, according to previous studies [26] and our clinical observations. Subscapularis is a deep muscle and it is limited to measure its electrophysiological signal by using a surface electrode. Thus in this study, the recordings from biceps brachii were chosen as a proxy. (b) During experiments, we need the patients to do some shoulder movements and maintain the postures for a certain duration for learning electrophysiological mechanism of hemiplegic shoulder pain. For stroke patients with hemiplegic shoulder pain, the flexion and abduction of their shoulder are often difficult to maintain for long enough. On the contrary, the flexion of their elbow is much easier to maintain [26], which mainly controlled by biceps brachii. This is another reason why the recordings from biceps brachii were chosen as a proxy in this study.

Then, a pair of bipolar surface electrodes (Ag/AgCl electrode, diameter: 1 cm, inter-electrode distance: 2 cm) were attached to the skin over the biceps brachii. Another one electrode was placed on the bony part of upper extremity as the ground (GND). The placement of the electrodes is shown in Figure 1(a). Before the sEMG electrodes were attached, the skin preparation for sEMG was done according to the following procedures: cleaning the site with alcohol, shaving the electrode site (if the skin surface at the sensor location was covered with noticeable hair), and lightly abrading the skin with fine sandpaper. 8 seconds of sEMG data were recorded when the participant performed a maximum voluntary isometric contraction (MVIC). The MVIC was performed via elbow flexion with the lever arm of an isokinetic dynamometer (Humac2009 system, Human Norm, CA, USA). The participant was asked to repeat the MVIC three times with an interval resting time of 30 seconds to record the sEMG data. By using an EMG acquisition system (Mega ME6000, Mega Electronics, Kuopio, Finland), the sEMG signal was acquired at a sample rate of 1000 Hz.

2.3.2. Blood Perfusion Recordings. Blood perfusion was evaluated in the shoulder area with a PeriCam Perfusion Speckle Imager (PSI) System (Perimed, Stockholm, Sweden) for analysis of complete occlusion after stroke induction (Figure 1(b)). This system provides images using Laser Speckle Contrast Analysis (LASCA) technology, and data on both the dynamics and the spatial distribution of the perfusion throughout the procedure are displayed in real time. The measurement of blood perfusion is based on the speckle pattern of blood cells, which has a relationship with the concentration and mean velocity of the blood cells. The detailed measuring principle of LASCA is displayed in the Supplemental file (available here). A lot of studies have validated the LASCA for showing blood perfusion, by comparing the LASCA with other perfusion measurement tools (e.g., single laser Doppler flowmetry analysis) [27, 28]. Due to the limitation of photon penetration depth, the LASCA technology can only be used to measure the superficial blood perfusion than the deep blood perfusion.

During the procedure, environmental temperature was controlled to approximately 26°C ±1°C and the relative humidity between 50% and 60% whereas the evaluated field was not exposed to direct light. The PSI parameter was set as follows: image acquisition rate, 50 Hz; normal resolution, 0.5 mm; 1 frame per second; 20 ±1 cm of working distance; 5 cm ×5 cm of region of interest (ROI). PIMSoft v1.5.8078 (Perimed, Stockholm, Sweden) was used for recording, saving, and analysis of data. By applying the LASCA technology and using the PIMSoft software, the average perfusion unit (PU) was computed to measure the blood perfusion. It is an arbitrary unit, because it is from the speckle contrast. The higher the PU value, the greater the perfusion observed.

2.4. Clinical Measurements

2.4.1. FMA-UE. FMA-UE is a reliable assessment scale to quantitatively evaluate the stroke patients' motor function of upper extremity [29, 30]. It includes 33 items which was divided into 4 subscales: shoulder/elbow (18 items), wrist (5 items), hand (7 items), and coordination/speed (3 items). Each item is scored between 0 and 2 (0 indicates the movement cannot be performed, 1 indicates it is performed partially, and 2 indicates it can be performed fully) with a total score range of 0-66.

2.4.2. MMT. MMT is a clinical procedure for grading the strength of individual muscle or muscle group. The MMT for bicep brachii of affected arm was performed with the patient in the lying position [31]. The MMT score was transformed to 0-12 scale according to the previous study (i.e., 5 score would transform to 12, 5- to 11, 4 to 10, and so forth) [32].

2.4.3. MAS. MAS is a 6-point scale to measure the abnormality in muscle tone. The MAS of bicep brachii of affected arm in all hemiplegic patients was recorded. For data analysis, the 1+ value of MAS was assigned as 2 while 2 was assigned as 3 and so forth [33].

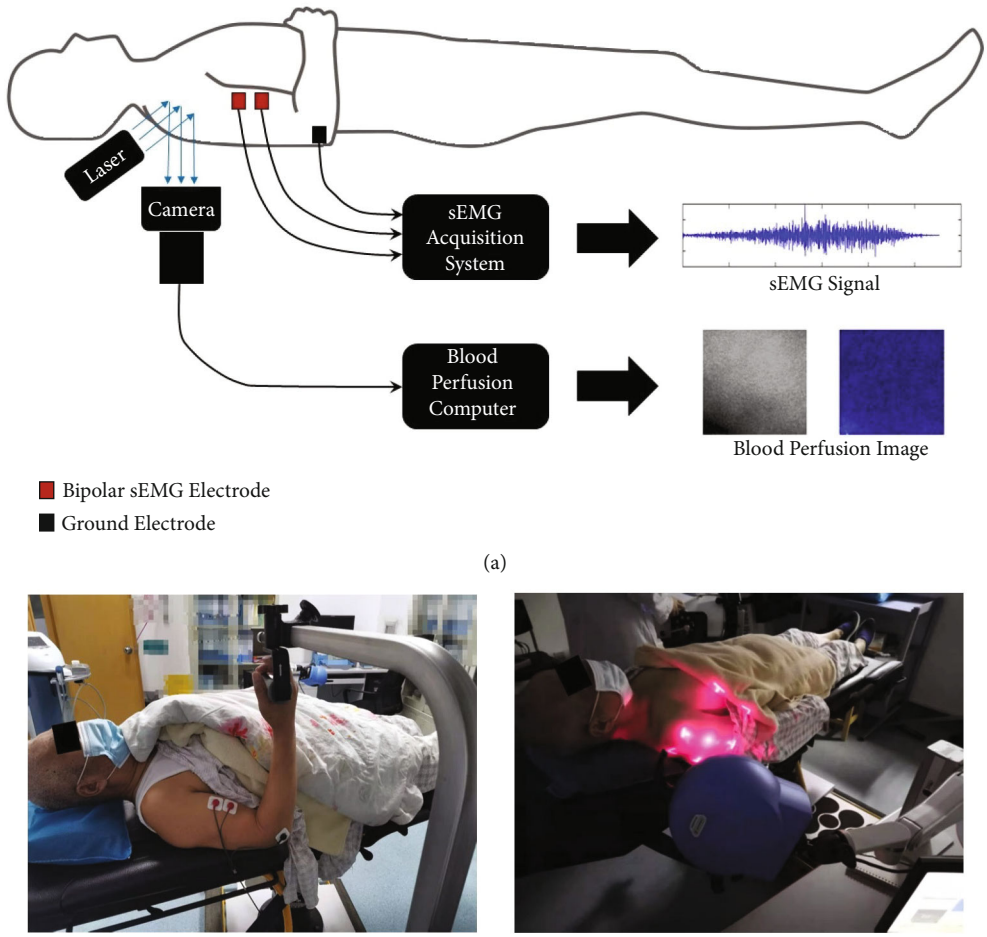

Figure 1: Physiological measurements (sEMG and blood perfusion) of the upper extremity. (a) Design of physiological measurements. (b) Measurement of sEMG in patients. (c) Measurement of blood perfusion in patients.

2.4.4. ROM. The ROMs of the shoulder in two different directions (shoulder flexion and shoulder abduction) were measured by a goniometer.

2.4.5. VAS for Shoulder Pain Intensity. VAS is a subjective measure of pain intensity. The range of VAS was from 0 (no pain at that moment) to 10 (worst imaginable pain at that moment).

2.5. Data Analysis. Three seconds of stable sEMG data was extracted from original eight seconds of data, in order to remove the movement artifact caused by the paraplegia and pain. Then, a bandpass filter with a range from 10 Hz to 500 Hz and a notch filter of 50 Hz were applied to eliminate the artifact and noise. The root-mean-square (RMS) and median-frequency (MDF) during the three-time MVIC-maintaining period were computed and averaged, using a custom script on MATLAB 2016b (The MathWorks Inc., USA).

RMS is used to measure the amplitude of EMG. It is computed as follows:

$$\mathrm{RMS} = \sqrt{\frac{1}{N}\sum_{k=1}^{N} x_k^2} \quad k = 1, 2, \cdots, N, \tag{1}$$

where x_k is the kth sampled sEMG data point; N is the sampling number of data points.

MDF is a frequency at which the EMG power spectrum is divided into two regions with equal amplitude. The definition of MDF of sEMG data is given by:

$$MDF = \sum_{j=1}^{MDF} P_j = \frac{1}{2}\sum_{j=1}^{M} P_j, \tag{2}$$

where P_j is the EMG power spectrum at the frequency bin j; M is the length of frequency bin.

2.6. Statistical Analysis. SPSS 19.0 (IBM, Armonk, NY, USA) was applied to conduct all statistical analyses. The normality of the data set was assessed with the Shapiro–Wilk test. The demographic variables and clinical characteristics variables were compared with χ^2 test and one-way analysis of variance (ANOVA). The RMS value and MDF value from sEMG data and the PU value for blood perfusion were all compared between left and right side in healthy subjects, by using paired T test. The difference of these physiological variables among Healthy group, HSP group, and HNSP group was explored using a one-way ANOVA test. Because the homogeneity of variance was violated (Levene's test), this one-way ANOVA test was applied with the Brown-Forsythe correction. The post-hoc analysis was carried out using the Games-Howell test. Because the affected side of stroke patients can be either side, it will produce a bias when managing any side of the healthy subject for the comparison analysis. Thus, we used the average physiological variables of the left and right side of the healthy subjects for analysis. It can help reduce the bias. Pearson's correlation coefficients were used to determine the linear correlation between pain score (VAS) and physiological measurements (sEMG parameters and blood perfusion parameters). Two-tailed p values were set at 0.05.

3. Results

3.1. Demographic and Clinical Baseline Characteristics. We recruited 13 healthy subjects (Healthy group), 13 hemiplegic patients with shoulder pain (HSP group), and 14 hemiplegic patients without shoulder pain (HNSP group) in this study. Most of demographic and clinical baseline characteristics among groups showed no significant difference. Only the ROM of flexion and ROM of abduction showed significant difference between HSP and HNSP groups. The bias caused by the inconsistency of dominant side can be avoided because all subjects were right-handed and the hemiplegic side between the HSP and HNSP groups did not show a significant difference using the χ^2 test. The details are displayed in Table 1.

3.2. Comparison of Physiological Responses between Left and Right Side in Healthy Group. By using a paired T test, the RMS and MDF values from sEMG data showed no significant difference between left and right side in Healthy group (RMS: $p = 0.297$, MDF: $p = 0.215$). Similarly, the PU value for blood perfusion showed no significant difference between sides in Healthy group ($p = 0.112$). The details are displayed in Figure 2.

3.3. Comparison of Physiological Responses between HSP, HNSP, and Healthy Groups. When comparing the physiological responses among the affected side in the HSP group, affected side in the HNSP group, and the left-right-average side in Healthy group, the one-way ANOVA test with Brown-Forsythe correction showed a significant difference of RMS value of sEMG ($F(2,15.891) = 23.443$, $p < 0.000$). The follow-up post-hoc comparison using the Games-Howell test indicated that RMS of sEMG in the HNSP group had significantly higher mean value than that in the HSP group ($p = 0.045$), and RMS of sEMG in the Healthy group was significantly higher than that in the HSP group ($p < 0.001$) and HNSP group ($p = 0.002$). On the other hand, there was no significant difference on the MDF value of sEMG ($F(2,36.020) = 2.560$, $p = 0.091$) and PU value of blood perfusion ($F(2,34.800) = 0.099$, $p = 0.906$). The details are displayed in Figure 3.

After the Pearson correlation analysis between the pain score (VAS) and physiological measurements (sEMG parameters and blood perfusion parameters), only the RMS value of sEMG showed a statistically significant correlation with the VAS of pain intensity ($r = -0.691$, $p = 0.012$). The details are displayed in Figure 4.

When comparing the physiological responses among the non-affected side in the HSP group, affected side in the HNSP group, and the left-right-average side in Healthy group, the one-way ANOVA test with Brown-Forsythe correction showed a significant difference of RMS value of sEMG ($F(2,22.130) = 11.600$, $p < 0.001$). The follow-up post-hoc comparison using the Games-Howell test indicated that RMS of sEMG in the HNSP group had significantly higher mean value than that in the HSP group ($p = 0.011$), RMS of sEMG in the Healthy group was significantly higher than that in the HSP group ($p = 0.001$), but not significantly different with that in the HNSP group ($p = 0.116$). On the other hand, there was no significant difference on the MDF value of sEMG ($F(2,36.433) = 0.859$, $p = 0.432$) and PU value of blood perfusion ($F(2,32.447) = 0.883$, $p = 0.423$). The details are displayed in Figure 5.

For the Pearson correlation analysis, no significant correlation was shown between pain score and physiological measurements. The details are displayed in Figure 6.

4. Discussion

This study adopted sEMG recording and LSCI techniques to measure the muscular electrical activity and blood perfusion of upper extremity in participants with and without HSP. The RMS parameter of sEMG showed significant difference ($p < 0.05$) in the affected side between HSP, HNSP, and Healthy groups. The MDF parameter of sEMG and PU parameter of blood perfusion showed no significant difference in both sides among the three groups ($p > 0.05$).

The RMS parameter from sEMG reflects the intensity of muscular electrical activity [34]. The findings in this study indicate that the single pain symptom has a correlation with the reduction of activities of both affected and non-affected shoulder muscles (HSP vs. HNSP in the affected side: $p = 0.045$; HSP vs. HNSP in the non-affected side: $p = 0.011$), while the single hemiplegia symptom has a correlation only with the reduction of affected shoulder muscular electrical activity (HNSP vs. Healthy in the affected side: $p = 0.002$). The similar findings for the relationship between the hemiplegia and the limbs' muscles can be found in previous studies. Kallenberg, LA et al. found the RMS of motor unit action potential (MUAP) of the affected side is larger and more variable than those of the non-affected side in chronic hemiparetic stroke patients [35]. Chokroverty, S et al. observed the

Table 1: Participant's baseline characteristics.

	Healthy group (n =13)	HSP group (n =13)	HNSP group (n =14)	p value
Male/female (n)	10/3	12/1	14/0	0.129∗
Age (years)	54.0 (14.8)	61.9 (10.3)	57.4 (12.2)	0.283#
Weight (kg)	67.0 (7.4)	71.3 (13.2)	74.0 (13.5)	0.291#
Height (cm)	167.0 (5.5)	169.5 (5.7)	170.0 (5.4)	0.400#
BMI (kg/m^2)	23.9 (1.8)	24.7 (3.5)	25.5 (3.3)	0.373#
Right dominant side/total subject number (n)	13/13	13/13	14/14	1.000∗
Left/right hemiplegic side (n)	N/A	6/7	6/8	0.863∗
Duration of hemiplegia (days)	N/A	91.8 (60.0)	77.4 (52.4)	0.514#
FMA-UE	N/A	32.5 (19.4)	38.1 (21.2)	0.486#
MMT	N/A	7.2 (3.3)	8.1 (2.2)	0.453#
MAS	N/A	0.7 (0.8)	1.1 (1.2)	0.334#
ROM for flexion (degree)	N/A	61.2 (50.9)	120.9 (59.3)	0.023#
ROM for abduction (degree)	N/A	69.1 (57.6)	120.9 (59.3)	0.030#
VAS (0-10)	N/A	4.85 (0.99)	N/A	N/A

HSP means hemiplegic patients with shoulder pain, HNSP means hemiplegic patients without shoulder pain, BMI means body mass index, FMA-UE means Fugl-Meyer assessment for upper extremity, MMT means manual muscle testing, MAS means modified Ashworth scale, ROM means range of motion, VAS means visual analogue scale. * means χ^2 test, # means one-way analysis of variance (ANOVA). N/A means not applicable. Data except male/female (n) expressed as mean (standard deviation).

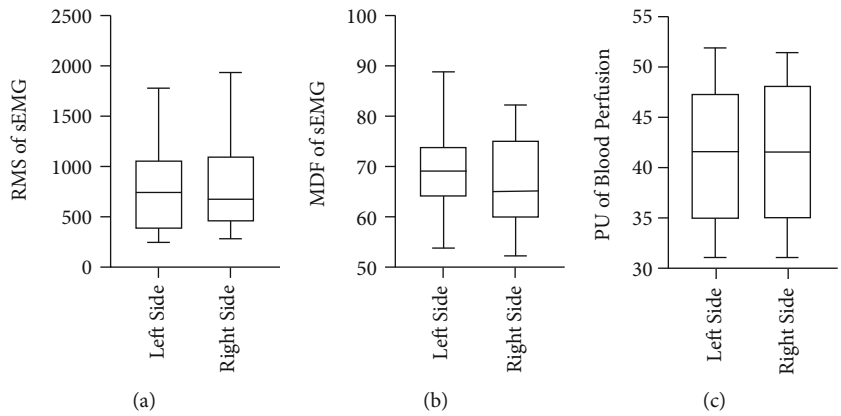

Figure 2: Comparison of sEMG parameters and PU value between left side and right side in the healthy subjects. (a) RMS parameter of sEMG. (b) MDF parameter of sEMG. (c) PU value of blood perfusion.

brachial plexus latencies to biceps and deltoid muscles were longer in the affected than in the non-affected sides in some hemiplegic patients [36]. For the relationship between the hemiplegic shoulder pain and the RMS value of bilateral shoulder muscles, there may be three reasons. Firstly, the bilateral disuse muscle atrophy can cause muscle imbalance and potentially cause instability around the shoulder [37]. It might also explain the reason for the pain. Secondly, the cross corticospinal tract from the brain to the muscles may account for this finding. Passing by pyramidal decussation, some of the fibers continue ventrally, forming the corticospinal tract anterior or medial and the remaining crosses to form the corticospinal tract side [38]. The injury or intervention to the hemisphere can also affect the ipsilateral corticospinal tract more or less [39]. Thirdly, the pain sensitization of peripheral/central neural network may affect the control from the spine/brain to the muscles. The pain threshold can decrease with the sensitization in the muscle tissue [40]. It can induce a higher muscle response (amplitude of endplate spikes).

For MDF from sEMG, there is no significant difference among HSP group, HNSP group, and Healthy group in both affected side and non-affected side. Some researchers also found the global MDF of sEMG did not show a significant difference in mean value between the two sides for stroke patients [35, 41]. The MDF generally reflects the recruitment firing rate, which can indirectly assess the muscle fatigue (i.e., muscular endurance) [42]. Fatigue reliably produces a decrease of the frequency feature of sEMG and increase of amplitude feature of sEMG for some specific muscles during static contraction [43, 44]. It indicated the fatigue-related changes in myoelectric properties

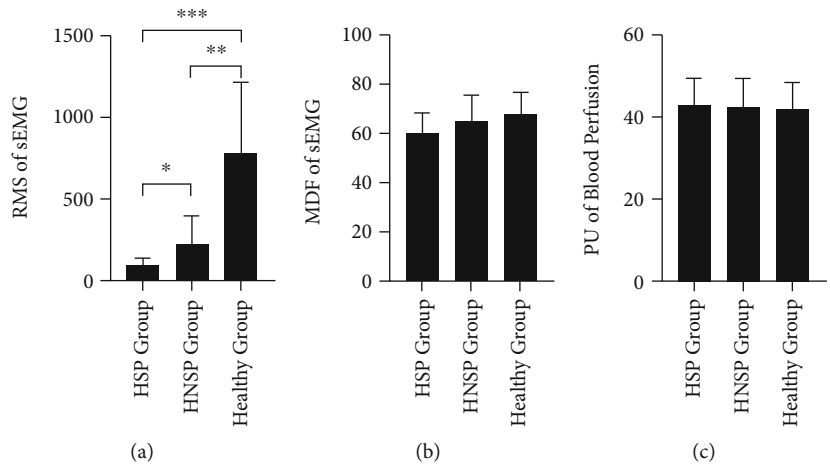

Figure 3: Comparison of sEMG parameters and PU value in the affected side among HSP, HNSP, and Healthy groups. (a) RMS parameter of sEMG. (b) MDF parameter of sEMG. (c) PU value of blood perfusion. * means $p < 0.05$. ** means $p < 0.01$. *** means $p < 0.001$.

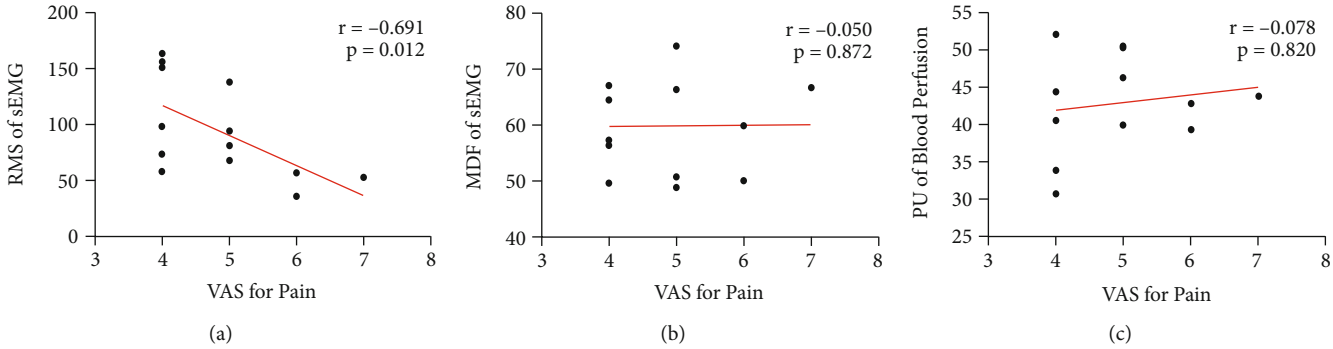

Figure 4: Linear correlation between VAS for shoulder pain intensity and physiological measurements (sEMG parameters and blood perfusion parameters) in the affected side of HSP patients. (a) Correlation between VAS and RMS parameter of sEMG. (b) Correlation between VAS and MDF parameter of sEMG. (c) Correlation between VAS and PU value of blood perfusion.

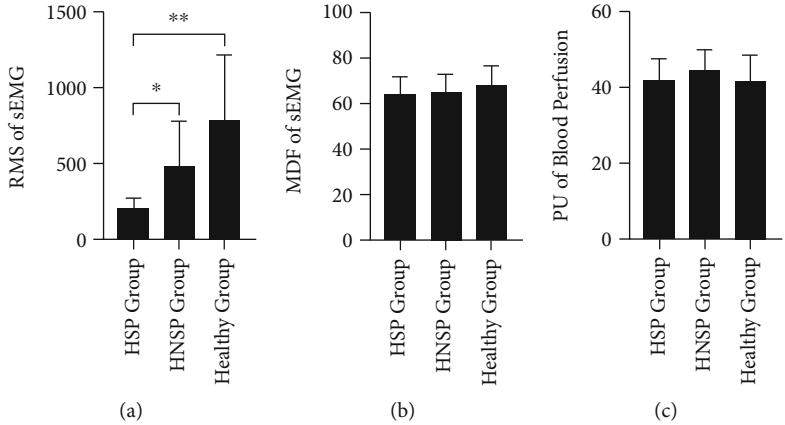

Figure 5: Comparison of sEMG parameters and PU value in the non-affected side among HSP, HNSP, and Healthy groups. (a) RMS parameter of sEMG. (b) MDF parameter of sEMG. (c) PU value of blood perfusion. * means $p < 0.05$. ** means $p < 0.01$.

involved a decrease of conduction velocity (CV) of motor unit action potential (MUAP) [45]. The finding in this study may imply the hemiplegic shoulder pain has no relationship with the alteration of fatigue characteristics of shoulder muscles.

The local superficial blood perfusion in the shoulder, not only in the affected side but also in the non-affected side, did not show any difference among groups. This finding is different with previous ones for hemiplegic limb. Naver, H et al. and Wandklyn, P et al. found both the temperature

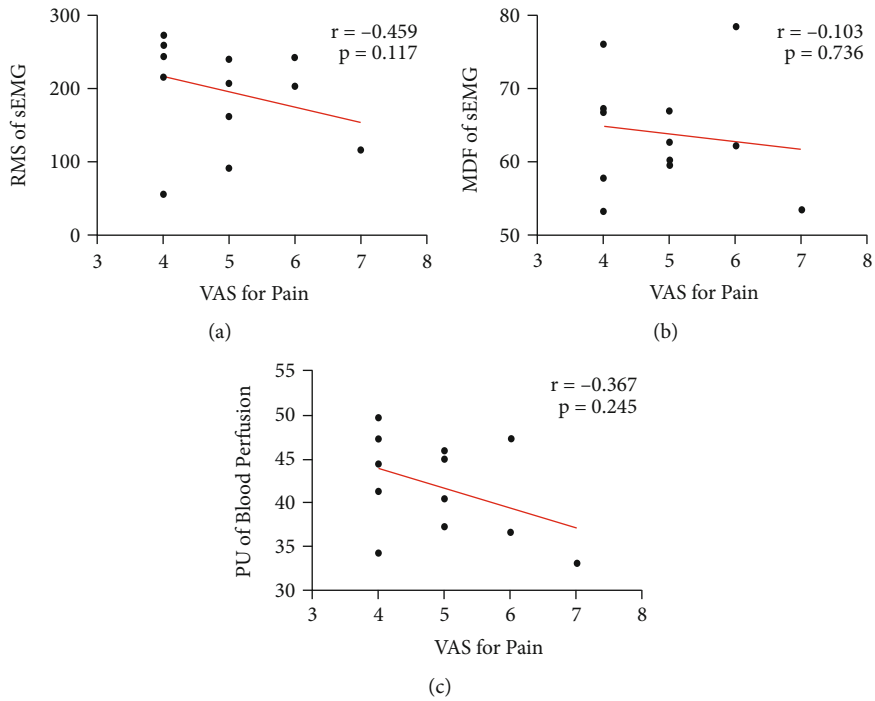

Figure 6: Linear correlation between VAS for shoulder pain intensity and physiological measurements (sEMG parameters and blood perfusion parameters) in the non-affected side of HSP patients. (a) Correlation between VAS and RMS parameter of sEMG. (b) Correlation between VAS and MDF parameter of sEMG. (c) Correlation between VAS and PU value of blood perfusion.

and blood flow of hand in the hemiplegic side decreased by using the plethysmograph [46, 47]. WC Adams et al. found the blood flow of affected and non-affected feet in the stroke patients was lower than that in the control subjects [48]. They inferred that the reduction of blood flow in hemiplegic limb was likely due to the muscle atrophy. It seemed, in this study, the shoulder pain could increase the superficial blood flow which was decreased by the hemiplegia. Because the LSCI technique can only detect the superficial blood flow [49], it is difficult to conclude whether the local blood flow including superficial and deep blood flow could or could not be affected by the HSP. Further studies using the measurement technique for deep blood flow are required in the future.

There are still several limitations in this study. Firstly, only the sEMG of biceps brachii was collected due to the limited contractions of most shoulder muscles in hemiplegic patients displayed in our previous pilot study. Some advanced techniques such as high-density sEMG and muscle synergy analysis should be used in the future. Secondly, the process of patient recruitment, the proportion of female stroke patients is found to be obviously smaller than that of male patients. In the future, we will try to investigate whether this difference of gender proportion is statistically existed and explore its possible reasons. More patients including female ones will be recruited in further studies in the future. Thirdly, the investigation on the relationship between the periphery neuromuscular system and the central nervous and microcirculation system is missing so the mechanism of HSP cannot be comprehensively explored. This will be investigated in the further study. Fourthly, the shoulder radiography and MRI were not measured in this study. They can be used to assess the degrees of osteoarthritis, rotator cuff tendinits, and tear, which may be the potential causes of hemiplegia shoulder pain [50]. In the further, we will apply these measurement technologies to investigate the mechanism of the hemiplegia shoulder pain. Fifthly, the influence of the duration of hemiplegia on the sEMG as well as the hemiplegic shoulder pain was not investigated. It will be explored in the future study. Finally, the psychological factor was not taken into account in this study. Different psychological state may modulate the pain recording which may cause a bias. We will collect the psychological data (e.g., beck depression inventory questionnaire) in the future.

5. Conclusions

By using sEMG and LSCI techniques, it was found the RMS and MDF parameters from sEMG signal in the affected shoulder muscles of HSP group showed significant difference with the Healthy group, while the PU value for blood perfusion showed no significant difference among groups. The muscle imbalance (or muscle dysfunction), caused by the muscle atrophy, impaired motor control, or abnormality of peripheral/central nervous activity, can lead to the instability around the shoulder and the change of sEMG signal. It might explain the reason for the hemiplegic shoulder pain. The findings of the study suggested an alternative way to explore the mechanism and treatment of HSP.

Data Availability

The data used to support the findings of this study are available from Dr. Minghong Sui (email: meekoo@163.com) upon request.

Conflicts of Interest

The authors declare that there is no conflict of interest regarding the publication of this paper.

Authors' Contributions

All authors listed have made a substantial, direct, and intellectual contribution to the work and approved it for publication. Minghong Sui, Naifu Jiang, and Luhui Yan have contributed equally to this work and share first authorship.

Acknowledgments

This work was supported by projects granted from the Traditional Chinese Medicine Bureau of Guangdong Province (#20201314), the National Natural Science Foundation of China (#62001463, #81927804), the Guangdong Basic and Applied Basic Research Foundation (#2021A1515011918), the Shenzhen Science and Technology Program (#JCYJ20210324102010029), and the Open Project from the CAS Key Laboratory of Human-Machine Intelligence-Synergy Systems, Shenzhen Institute of Advanced Technology of China, Chinese Academy of Sciences (#2014DP173025).

Supplementary Materials

The detailed measuring principle of Laser Speckle Contrast Analysis (LASCA) is showed in the supplementary material. *(Supplementary Materials)*

References

[1] R. W. Bohannon, P. A. Larkin, M. B. Smith, and M. G. Horton, "Shoulder pain in hemiplegia: statistical relationship with five variables," *Archives of Physical Medicine and Rehabilitation*, vol. 67, no. 8, pp. 514–516, 1986.

[2] J. M. Vasudevan and B. J. Browne, "Hemiplegic shoulder pain: an approach to diagnosis and management," *Physical Medicine and Rehabilitation Clinics of North America*, vol. 25, no. 2, pp. 411–437, 2014.

[3] P. Kumar, "Hemiplegic shoulder pain in people with stroke: present and the future," *Pain Management*, vol. 9, no. 2, pp. 107–110, 2019.

[4] M. Murie-Fernández, M. Carmona Iragui, V. Gnanakumar, M. Meyer, N. Foley, and R. Teasell, "Painful hemiplegic shoulder in stroke patients: causes and management," *Neurología*, vol. 27, no. 4, pp. 234–244, 2012.

[5] N. Ciesla, V. Dinglas, E. Fan, M. Kho, J. Kuramoto, and D. Needham, "Manual muscle testing: a method of measuring extremity muscle strength applied to critically ill patients," *Journal of Visualized Experiments*, vol. 50, no. 50, p. 2632, 2011.

[6] S.-K. Lee, H.-O. Lee, and J.-I. Youn, "Evaluation of muscle tension in hemiplegia patients with a real-time monitoring system during high intensity laser therapy," *Journal of the Optical Society of Korea*, vol. 19, no. 3, pp. 277–283, 2015.

[7] R. R. Serrezuela, M. T. Quezada, M. H. Zayas, A. M. Pedrón, D. M. Hermosilla, and R. S. Zamora, "Robotic therapy for the hemiplegic shoulder pain: a pilot study," *Journal of Neuroengineering and Rehabilitation*, vol. 17, no. 1, p. 54, 2020.

[8] A. R. Hernández-Ortíz, R. Ponce-Luceño, C. Sáez-Sánchez, O. García-Sánchez, C. Fernández-de-las-Peñas, and A. I. de-la-Llave-Rincón, "Changes in muscle tone, function, and pain in the chronic hemiparetic shoulder after dry needling within or outside trigger points in stroke patients: a crossover randomized clinical trial," *Pain Medicine*, vol. 21, no. 11, pp. 2939–2947, 2020.

[9] X. Song, S. Chen, J. Jia, and P. B. Shull, "Cellphone-based automated Fugl-Meyer assessment to evaluate upper extremity motor function after stroke," *IEEE Transactions on Neural Systems and Rehabilitation Engineering*, vol. 27, no. 10, pp. 2186–2195, 2019.

[10] E. Alanbay, B. Aras, S. Kesikburun, S. Kizilirmak, E. Yasar, and A. K. Tan, "Effectiveness of suprascapular nerve pulsed radiofrequency treatment for hemiplegic shoulder pain: a randomized-controlled trial," *Pain Physician*, vol. 23, no. 3, pp. 245–252, 2020.

[11] R. W. Bohannon, "Measurement and nature of muscle strength in patients with stroke," *Journal of Neurologic Rehabilitation*, vol. 11, no. 2, pp. 115–125, 1997.

[12] L. Yang, J. Yang, and C. He, "The effect of kinesiology taping on the hemiplegic shoulder pain: a randomized controlled trial," *Journal of Healthcare Engineering*, vol. 2018, Article ID 8346432, 7 pages, 2018.

[13] N. Jiang, K. D. Luk, and Y. Hu, "A machine learning-based surface electromyography topography evaluation for prognostic prediction of functional restoration rehabilitation in chronic low back pain," *Spine*, vol. 42, no. 21, pp. 1635–1642, 2017.

[14] N. Jiang, J. Wei, G. Li, B. Wei, F. F. Zhu, and Y. Hu, "Effect of dry-electrode-based transcranial direct current stimulation on chronic low back pain and low back muscle activities: a double-blind sham-controlled study," *Restorative Neurology and Neuroscience*, vol. 38, no. 1, pp. 41–54, 2020.

[15] I. Lascurain-Aguirrebeña, D. J. Newham, X. Casado-Zumeta, A. Lertxundi, and D. J. Critchley, "Immediate effects of cervical mobilisations on neck muscle activity during active neck movements in patients with non-specific neck pain. A double blind placebo controlled trial," *Physiotherapy*, vol. 110, pp. 42–53, 2021.

[16] B. S. Neal, C. J. Barton, A. Birn-Jeffrey, M. Daley, and D. Morrissey, "The effects & mechanisms of increasing running step rate: a feasibility study in a mixed-sex group of runners with patellofemoral pain," *Physical Therapy in Sport*, vol. 32, pp. 244–251, 2018.

[17] L. Bender and K. McKenna, "Hemiplegic shoulder pain: defining the problem and its management," *Disability and Rehabilitation*, vol. 23, no. 16, pp. 698–705, 2001.

[18] R. B. Shepherd and J. H. Carr, "The shoulder following stroke: preserving musculoskeletal integrity for function," *Topics in Stroke Rehabilitation*, vol. 4, no. 4, pp. 35–53, 1998.

[19] W. Heeman, W. Steenbergen, G. van Dam, and E. C. Boerma, "Clinical applications of laser speckle contrast imaging: a

review," *Journal of Biomedical Optics*, vol. 24, no. 8, article 080901, 2019.

[20] J.-i. Takada, J. J. Miyamoto, C. Sato, A. Dei, and K. Moriyama, "Comparison of EMG activity and blood flow during graded exertion in the orbicularis oris muscle of adult subjects with and without lip incompetence: a cross-sectional survey," *European Journal of Orthodontics*, vol. 40, no. 3, pp. 304–311, 2018.

[21] D. L. Ron Clijsen, A. Schneebeli, C. Cescon, E. Soldini, L. Li, and M. Barbero, "Does the application of Tecar therapy affect temperature and perfusion of skin and muscle microcirculation? A pilot feasibility study on healthy subjects," *Journal of Alternative and Complementary Medicine*, vol. 26, no. 2, pp. 147–153, 2020.

[22] M. Ringkamp, M. Wooten, B. S. Carson, M. Lim, T. Hartke, and M. Guarnieri, "Laser speckle imaging to improve clinical outcomes for patients with trigeminal neuralgia undergoing radiofrequency thermocoagulation," *Journal of Neurosurgery*, vol. 124, no. 2, pp. 422–428, 2016.

[23] I. Unal-Cevik, "Temporal and spatial quantification of pain-related small fiber functionality assessed using laser speckle contrast analysis," *Pain Practice*, vol. 18, no. 7, pp. 824–838, 2018.

[24] S. J. Mulroy, J. K. Gronley, C. J. Newsam, and J. Perry, "Electromyographic activity of shoulder muscles during wheelchair propulsion by paraplegic persons," *Archives of Physical Medicine and Rehabilitation*, vol. 77, no. 2, pp. 187–193, 1996.

[25] S.-F. Lo, S.-Y. Chen, H.-C. Lin, Y.-F. Jim, N.-H. Meng, and M.-J. Kao, "Arthrographic and clinical findings in patients with hemiplegic shoulder pain[1]," *Archives of Physical Medicine and Rehabilitation*, vol. 84, no. 12, pp. 1786–1791, 2003.

[26] R. Slavin and D. Smith, "The relationship between sample sizes and effect sizes in systematic reviews in education," *Educational Evaluation and Policy Analysis*, vol. 31, no. 4, pp. 500–506, 2009.

[27] B. Ruaro, A. Sulli, E. Alessandri, C. Pizzorni, G. Ferrari, and M. Cutolo, "Laser speckle contrast analysis: a new method to evaluate peripheral blood perfusion in systemic sclerosis patients," *Annals of the Rheumatic Diseases*, vol. 73, no. 6, pp. 1181–1185, 2014.

[28] M. Draijer, E. Hondebrink, T. van Leeuwen, and W. Steenbergen, "Review of laser speckle contrast techniques for visualizing tissue perfusion," *Lasers in Medical Science*, vol. 24, no. 4, pp. 639–651, 2009.

[29] S. Ikbali Afsar, I. Mirzayev, O. Umit Yemisci, and S. N. Cosar Saracgil, "∗∗Virtual reality in upper extremity rehabilitation of stroke patients: a randomized controlled trial∗∗," *Journal of Stroke and Cerebrovascular Diseases*, vol. 27, no. 12, pp. 3473–3478, 2018.

[30] E. D. Hernández, C. P. Galeano, N. E. Barbosa et al., "Intra- and inter-rater reliability of Fugl-Meyer Assessment of Upper Extremity in stroke," *Journal of Rehabilitation Medicine*, vol. 51, no. 9, pp. 652–659, 2019.

[31] O. Mohamed, J. Perry, and H. Hislop, "Relationship between wire EMG activity, muscle length, and torque of the hamstrings," *Clinical biomechanics*, vol. 17, no. 8, pp. 569–579, 2002.

[32] E. Bye, J. Glinsky, J. Yeomans et al., "The inter-rater reliability of the 13-point manual muscle test in people with spinal cord injury," *Physiotherapy Theory and Practice*, vol. 37, no. 10, pp. 1126–1131, 2021.

[33] A. Sivaramakrishnan, J. M. Solomon, and N. Manikandan, "Comparison of transcutaneous electrical nerve stimulation (TENS) and functional electrical stimulation (FES) for spasticity in spinal cord injury - a pilot randomized cross-over trial," *The Journal of Spinal Cord Medicine*, vol. 41, no. 4, pp. 397–406, 2018.

[34] D. Renshaw, M. R. Bice, C. Cassidy, J. A. Eldridge, and D. W. Powell, "A comparison of three computer-based methods used to determine EMG signal amplitude," *International Journal of Exercise Science*, vol. 3, no. 1, pp. 43–48, 2010.

[35] L. A. Kallenberg and H. J. Hermens, "Motor unit properties of biceps brachii in chronic stroke patients assessed with high-density surface EMG," *Muscle & Nerve*, vol. 39, no. 2, pp. 177–185, 2009.

[36] S. Chokroverty and J. Medina, "Electrophysiological study of hemiplegia," *Archives of Neurology*, vol. 35, no. 6, pp. 360–363, 1978.

[37] L. Kalichman and M. Ratmansky, "Underlying pathology and associated factors of hemiplegic shoulder pain," *American Journal of Physical Medicine & Rehabilitation*, vol. 90, no. 9, pp. 768–780, 2011.

[38] U. Ziemann, K. Ishii, A. Borgheresi et al., "Dissociation of the pathways mediating ipsilateral and contralateral motor-evoked potentials in human hand and arm muscles," *The Journal of Physiology*, vol. 518, no. 3, pp. 895–906, 1999.

[39] N. Jiang, L. Wang, Z. Huang, and G. Li, "Mapping responses of lumbar paravertebral muscles to single-pulse cortical TMS using high-density surface electromyography," *IEEE Transactions on Neural Systems and Rehabilitation Engineering*, vol. 29, pp. 831–840, 2021.

[40] Y. M. Xu, H. Y. Ge, and L. Arendt-Nielsen, "Sustained nociceptive mechanical stimulation of latent myofascial trigger point induces central sensitization in healthy subjects," *The Journal of Pain*, vol. 11, no. 12, pp. 1348–1355, 2010.

[41] S. Angelova, S. Ribagin, R. Raikova, and I. Veneva, "Power frequency spectrum analysis of surface EMG signals of upper limb muscles during elbow flexion - a comparison between healthy subjects and stroke survivors," *Journal of Electromyography and Kinesiology*, vol. 38, pp. 7–16, 2018.

[42] S.-H. Liu, C.-B. Lin, Y. Chen, W. Chen, T.-S. Huang, and C.-Y. Hsu, "An EMG patch for the real-time monitoring of muscle-fatigue conditions during exercise," *Sensors*, vol. 19, no. 14, p. 3108, 2019.

[43] B. Gerdle, B. Larsson, and S. Karlsson, "Criterion validation of surface EMG variables as fatigue indicators using peak torque: a study of repetitive maximum isokinetic knee extensions," *Journal of Electromyography and Kinesiology*, vol. 10, no. 4, pp. 225–232, 2000.

[44] P. A. Ortega-Auriol, T. F. Besier, W. D. Byblow, and A. J. C. McMorland, "Fatigue influences the recruitment, but not structure, of muscle synergies," *Frontiers in Human Neuroscience*, vol. 12, no. 217, 2018.

[45] R. M. Enoka and J. Duchateau, "Muscle fatigue: what, why and how it influences muscle function," *The Journal of Physiology*, vol. 586, no. 1, pp. 11–23, 2008.

[46] P. Wanklyn, D. W. Ilsley, D. Greenstein et al., "The cold hemiplegic arm," *Stroke*, vol. 25, no. 9, pp. 1765–1770, 1994.

[47] H. Naver, C. Blomstrand, S. Ekholm, C. Jensen, T. Karlsson, and G. Wallin, "Autonomic and thermal sensory symptoms and dysfunction after stroke," *Stroke*, vol. 26, no. 8, pp. 1379–1385, 1995.

[48] W. C. Adams and F. J. Imms, "Resting blood flow in the paretic and nonparetic lower legs of hemiplegic persons: relation to local skin temperature," *Archives of Physical Medicine and Rehabilitation*, vol. 64, no. 9, pp. 423–428, 1983.

[49] L. Zhang, L. Ding, M. Li et al., "Dual-wavelength laser speckle contrast imaging (dwLSCI) improves chronic measurement of superficial blood flow in hands," *Sensors*, vol. 17, no. 12, p. 2811, 2017.

[50] M. Sui, N. Jiang, L. Yan et al., "Effect of electroacupuncture on shoulder subluxation in poststroke patients with hemiplegic shoulder pain: a sham-controlled study using multidimensional musculoskeletal ultrasound assessment," *Pain Research & Management*, vol. 2021, article 5329881, pp. 1–9, 2021.

Hindawi
Neural Plasticity
Volume 2022, Article ID 7670629, 17 pages
https://doi.org/10.1155/2022/7670629

Research Article

Combined-Acupoint Electroacupuncture Induces Better Analgesia via Activating the Endocannabinoid System in the Spinal Cord

Zhenhua Jiang,[1] Yuheng Li,[1,2] Qun Wang,[1] Zongping Fang,[1] Jiao Deng,[1] Xinxin Zhang,[1] Bowen Shen,[2] Zhixin Wu,[1] Qianzi Yang,[1] and Lize Xiong[1,3]

[1]*Department of Anesthesiology and Perioperative Medicine, Xijing Hospital, Fourth Military Medical University, Xi'an, Shaanxi Province 710032, China*
[2]*Department of Anesthesiology, The 960th Hospital of PLA, Jinan, China*
[3]*Department of Anesthesiology and Perioperative Medicine, Translational Research Institute of Brain and Brain-Like Intelligence, Shanghai Fourth People's Hospital Affiliated to Tongji University School of Medicine, the Shanghai Key Laboratory of Anesthesiology and Functional Modulation, Shanghai 200434, China*

Correspondence should be addressed to Qianzi Yang; qianziyang@hotmail.com and Lize Xiong; mzkxlz@126.com

Received 7 April 2022; Accepted 10 August 2022; Published 15 September 2022

Academic Editor: Xue-Qiang Wang

Electroacupuncture (EA) therapy has been widely reported to alleviate neuropathic pain with few side effects in both clinical practice and animal studies worldwide. However, little is known about the comparison of the therapeutic efficacy among the diverse EA schemes used for neuropathic pain. The present study is aimed at investigating the therapeutic efficacy discrepancy between the single and combined-acupoint EA and to reveal the difference of mechanisms behind them. Electroacupuncture was given at both Zusanli (ST36) and Huantiao (GB30) in the combined group or ST36 alone in the single group. Paw withdrawal mechanical threshold (PWMT) was measured to determine the pain level. Electrophysiology was performed to detect the effects of EA on synaptic transmission in the spinal dorsal horn of the vGlut2-tdTomato mice. Spinal contents of endogenous opioids, endocannabinoids, and their receptors were examined. Inhibitors of CBR (cannabinoid receptor) and opioid receptors were used to study the roles of opioid and endocannabinoid system (ECS) in EA analgesia. We found that combined-acupoint acupuncture provide stronger analgesia than the single group did, and the former inhibited the synaptic transmission at the spinal level to a greater extent than later. Besides, the high-intensity stimulation at ST36 or normal stimulation at two sham acupoints did not mimic the similar efficacy of analgesia in the combined group. Acupuncture stimulation in single and combined groups both activated the endogenous opioid system. The ECS was only activated in the combined group. Naloxone totally blocked the analgesic effect of single-acupoint EA; however, it did not attenuate that of combined-acupoint EA unless coadministered with CBR antagonists. Hence, in the CCI-induced neuropathic pain model, combined-acupoint EA at ST36 and GB30 is more effective in analgesia than the single-acupoint EA at ST36. EA stimulation at GB30 alone neither provided a superior analgesic effect to EA treatment at ST36 nor altered the content of AEA, 2-AG, CB1 receptor, or CB2 receptor compared with the CCI group. Activation of the ECS is the main contributor of the better analgesia by the combined acupoint stimulation than that induced by single acupoint stimulation.

1. Introduction

Neuropathic pain, defined as the chronic pain condition caused by a lesion or disease of the somatosensory nervous system [1], is a serious problem threatening the health of human. The prevalence rate of neuropathic pain in general population is estimated to be as high as 8% [2, 3]. Nearly 30% of people in the United States suffer from neuropathic

pain, resulting in an economic cost of 560-635 billion US dollars annually [4]. More importantly, the commonly used medications for neuropathic pain have a limited efficacy, and serious side effects are inevitable [5].

Acupuncture, which refers to stimulation of acupoints to modulate the body physiology [6, 7] and related techniques, such as electroacupuncture (EA), has been widely reported to alleviate pain in both clinical practice [8, 9] and animal studies [10–12] with few side effects. The National Institutes of Health (NIH) has clearly recommended acupuncture as an alternative therapy when conventional treatment is not satisfactory [10]. Meanwhile, increasing number of people have taken acupuncture treatment as part of medical care in management of pain. However, acupuncture schemes vary from studies and lack a standard practice. Acupoint selection determines the effect of acupuncture therapy to a large extent [13]. Although previous studies reported that stimulations at both single acupoint and multiple acupoints were effective in neuropathic pain treatment [14–18], such as single acupoint of ST36 [19, 20] or combinations of ST36 and GB30 [21, 22], very few researches compared the therapeutic efficacy among the diverse acupuncture schemes. To investigate whether there is a difference of analgesia between single- and combined-acupoint scheme is of great importance for simplifying and standardizing the practice of acupuncture.

It has been established that increase of excitability of spinal dorsal horn neurons and the synaptic strength between C fiber and spinal dorsal horn neurons contribute to neuropathic pain [23, 24]. Electroacupuncture has been proved to relieve neuropathic pain mainly at spinal level by involving endogenous opioids system, serotonin, norepinephrine, amino acids, and glia cell/cytokines [25]. Particularly, the endogenous opioid system in the spinal cord has been widely reported to participate in EA analgesia of neuropathic pain in humans and animals [10]. Besides, it has been acknowledged that low frequency (2-10 Hz) EA exerts a stronger analgesia than high frequency (100 Hz) EA in inhibiting inflammatory pain, which mediated by met-enkephalin, β-endorphin, and dynorphin, respectively [26], but whether this specificity applies to neuropathic pain remains unknown [25]. In addition, ECS also contributes to the EA analgesia [27]. The endocannabinoid system is composed of the endocannabinoids (anandamide, AEA; 2-arachidonoylglycerol, 2-AG), cannabinoid receptors (CB_1R, CB_2R), synthetase, and hydrolase of endocannabinoids [28, 29]. A preliminary study concluded that CB1R and CB2R are involved in the EA-induced analgesia and anti-inflammatory effects, respectively [27]. Although combined-acupoint EA could suppress inflammatory pain via regulating ECS, it produced analgesia in the supraspinal region. A very typical model of chronic pain is the chronic constriction injury of the sciatic nerve (CCI) in rats, which shows obvious mechanical allodynia. Whether ECS participates in the EA induced analgesia at the spinal cord is not clear. Thus, to investigate the analgesic effects and the underlying mechanism of EA treatment at single and combined acupoints may provide a structural and functional basis for developing more optimal EA strategy.

In the present study, we aim to answer the following questions: (1) Is combined-acupoint EA more effective than single-acupoint EA for analgesia in CCI-induced neuropathic pain? (2) What is the underlying analgesic mechanism of single-acupoint EA or/and combined-acupoint EA? Hence, we firstly established a chronic neuropathic pain model in rats and compared the analgesic efficacy of single-acupoint (ST36) and combined-acupoint (ST36 + GB30) EA through testing pain behaviors. In addition, we also examined the effects of single and combined EA on the pain information transmission in the spinal dorsal horn. Then, we further explored the mechanism underlying their analgesic effects using western blots, ELISA assays, and intrathecal injection methods. Elucidating the differences in EA-induced antinociception between single-acupoint and combined-acupoint schemes, as well as the underlying mechanism, may accelerate the development of drugs and provide better choices for patients that are refractory to conventional therapy.

2. Materials and Methods

2.1. Animals. Six weeks old male Sprague–Dawley rats weighing 167.8 ± 7.3 g (purchased from the Experimental Animal Center of the Fourth Military Medical University, Xi'an, Shaanxi, China) were used in the behavioral, immunohistochemistry, western blot, and ELISA experiments. Adult heterozygous male vGlut2-Cre mice (Jackson Laboratories) were crossed with Ai9 reporter mice (Jackson Laboratories) to generate vGlut2-tdTomato mice. Young adult (3–5 weeks old) male vGlut2-tdTomato mice were used for electrophysiological experiments. Animals were group-housed (4 per cage) at a temperature of 22-24°C, with a 12-hour light/dark cycle and free access to food and water. All rats were acclimatized to the laboratory conditions for at least 7 days before experimental manipulation in case their stress responses affected the experiment results. All animal experiments were approved by the Ethic Committee of the Fourth Military Medical University and followed the policies for the use of laboratory animals issued by the International Association for the Study of Pain. All efforts were made to minimize the number of animals used and their suffering.

2.2. Study Design. For rats, the whole study was divided into three steps. In the first step, rats were randomly divided into control, CCI, single, and combined groups ($n = 10$ per group). Sham operation was done in the control group, while the CCI model was established in the other 3 groups. After the CCI model were established, different treatments were applied to rats for 2 weeks: immobilization for the control and CCI group, ST36-acupoint EA for the single group, and ST36 + GB30-acupoint EA for the combined group. Paw withdrawal mechanical threshold of the rats, as well as the expression of endorphin, enkephalin, MOR, DOR, AEA, 2-AG, CB_1R, and CB_2R, were measured.

Secondly, rats were divided into CCI, single, high-intensity, combined, and sham-combined group randomly ($n = 8$ per group), and all the rats received CCI injury. Treatments in CCI, single, and combined group were the same as the

first step. Single-acupoint EA with high intensity stimulation was applied to high-intensity group, and sham-combined group was stimulated at sham acupoints. Paw withdrawal mechanical threshold was then measured to evaluate the analgesic effects in each group.

Thirdly, rats were randomly grouped into CCI, single, combined, and combined + CBR (cannabinoid receptor) inhibitor group ($n = 8$ per group), and all rats were conducted with CCI surgery. Except for immobilization and EA treatment, nonselective opioid antagonist naloxone was administrated to all animals intraperitoneally; CB_1R and CB_2R antagonists were applied intrathecally in the combined + CBR group. Mechanical threshold was then measured.

Finally, rats were randomly divided into CCI, ST36, and GB30 groups ($n = 8 - 10$). All rats were performed with CCI surgery. After the rats were immobilized and delivered EA treatment, PWMT as well as the expression of AEA, 2-AG, CB_1R, and CB_2R was measured.

For vGlut2-tdTomato mice, they were divided into control, CCI, single, and combined groups ($n = 6$). Control and CCI groups received sham and CCI surgery, respectively, and they are used for electrophysiological experiment at 10 days after operation. For combined (ST36 + GB30) and single (ST36) groups, they received CCI and EA treatment started at the 10 days after CCI. After the 6-consecutive days' treatment and 1-day off, they were used for electrophysiological experiment.

2.3. Neuropathic Pain Model. The chronic constriction injury (CCI) model was established as previously described to investigate the analgesic effect of electroacupuncture (EA) [30, 31]. Briefly, after the rat or vGlut2-tdTomato mouse was anesthetized with 1.5% isoflurane in oxygen, the left sciatic nerve was exposed. Four 4-0 chromic gut sutures were then tied to the sciatic nerve to induce the injury, and the surgical site was then closed with silk sutures. The behavioral test was conducted at 10 days after modeling to ensure the reliability of the pain phenotype.

2.4. EA Treatment. Rats were gently immobilized by our homemade fixing device without anesthesia. The vGlut2-tdTomato mice were anesthetized by 3.0% isoflurane and maintained by 1.5% isoflurane. The stainless-steel acupuncture needles (0.1 mm in diameter, Huatuo, Suzhou, China) were inserted into bilateral ST36, GB30, or nonacupoints according to the grouping. The needles were connected to the Huatuo SDZ-V Nerve and Muscle Stimulator (Huatuo), and then the dense-and-disperse mode stimulation was given at 2/10 Hz. Generally, the lowest intensity (1-2 mA) of EA which could evoke the vibration of the stimulated hindlimb was chosen for each acupoint. As to the high-intensity stimulation, the maximum intensity of EA that animals could tolerate was adopted. EA was given for 30 minutes per day. An EA treatment course included 6-consecutive days' treatment and 1-day off. EA treatment started at the 10 days after CCI.

2.5. Pain Behavioral Test. Paw withdrawal mechanical threshold (PWMT) was measured by von Frey filaments. Rats or mice were habituated in the experimental apparatus for 30 min, and baseline of PWMT was measured. After the CCI model was constructed, the EA treatment was performed. On Wednesday, Friday, and Sunday every week, animals were firstly treated with EA followed by detecting PWMT, which lasts for 2 weeks.

During the tests, each rat or mouse was placed in a chamber (15 cm × 15 cm × 15 cm) on a platform with 5 mm grids of iron wires throughout the entire area. The up-down method was used to evaluate mechanical allodynia as we previously did [32]. Briefly, the PWMT was determined by using von Frey hairs (Stoelting, Wood Dale, USA) applied to the central region of the plantar surface of the left hind paw in ascending order (rat: 2-26 g; mice: 0.008-2 g). Each filament was tested for 10 times at 10 s intervals. The PWMT was defined as the lowest force in grams that produced at least 5 withdrawal responses in 10 consecutive applications. All the tests were conducted by a researcher who is blind to the grouping.

2.6. Preparation of Sagittal Lumbar Spinal Cord Slice Attached with a Dorsal Root. According to the previous study [33], sagittal lumbar spinal cord slices (400- to 500 μm-thick) attached with a dorsal root were prepared. Briefly, young adult vGlut2-tdTomato mice from control, CCI, combined, and single groups were transcardially perfused with ice-cold sucrose artificial cerebrospinal fluid after deeply narcotized with pentobarbital sodium. Then, the sagittal lumbar spinal cord (400- to 500 μm-thick) with dorsal root was removed and cut by a vibrating microtome filled with ice-cold sucrose cerebrospinal fluid. Finally, lumbar spinal cord slice was incubated in the normal cerebrospinal fluid equilibrated with a mixture of 95% O_2 and 5% CO_2 at room temperature for 1 h.

2.7. Patch Clamp Whole Cell Recordings. According to our previous electrophysiology protocol [33], resistance of patch pipettes was maintained at 5 to 10 MΩ. Tight whole cell recordings were made from vGlut2-positive neurons located in lamina I and IIo of spinal cord slices and distinguished by the expression of tdTomato protein. At current-clamp mode, rheobase was recorded which refers to the current intensity of 40 ms duration resulting in the first action potential. Besides, the firing pattern was determined by depolarizing pulses of 1 s duration. Unmyelinated primary afferent C fiber evoked excitatory postsynaptic potential (eEPSP) was evoked by electrical stimulation of the dorsal root and judged by stimulation threshold and conduction velocities. Data were collected, digitized, and analyzed by the Axopatch 700B amplifier (Axon Instruments, USA), the Digitizer 1550B, and pCLAMP 10.7 software (Axon Instruments).

2.8. Western Blot Analysis. Once the rats were sacrificed, L4-L5 spinal cord tissue was rapidly removed and homogenized in strong RIPA buffer containing 1% protease inhibitors cocktail (Sigma-Aldrich, St Louis, USA) for 20 min and then centrifuged at 12000 rpm/min at 4°C for 15 min to collect supernatant. After protein concentration determined with

bicinchoninic acid (BCA) protein assay kit (Cwbiotech, Beijing, China), 40 micrograms of protein samples from different groups were loaded and separated on 10% SDS-PAGE gels and transferred to PVDF membranes (Merck Millipore, Billerica, MA, USA). Blocked with 5% bovine (Beyotime, Shanghai, China) in Tris-buffered saline (pH 7.4) with 0.1% Tween-20 for 2 h at room temperature, the membranes were then incubated overnight at 4°C with primary antibodies. The primary antibodies were rabbit anti μ-opioid receptor (1 : 1000, Abcam, ab10275, USA), rabbit anti-δ opioid receptor (1 : 1000, Alomone, AOR-014, USA), rabbit anti-cannabinoid receptor 1 (1 : 1000, Cayman Chemical, 101500, USA), rabbit anti-cannabinoid receptor 2 (1 : 1000, Cayman Chemical, 101550, USA), and rabbit anti-GAPDH (1 : 2000, GeneTex, GTX100118, USA). The blots were then incubated with HRP-conjugated secondary antibodies (1 : 8000, Abcam, ab97110, USA) for 2 h. Signals were detected using enhanced chemiluminescent reagent (ECL, Millipore, USA), and the bands were analyzed with the ChemiDoc XRS system (Bio-Rad, Hercules, USA). The quantification of band intensity was carried out using Image software. Band densities were normalized to individual GAPDH internal controls.

2.9. ELISA Assays. Rat ELISA kits (Westang, Shanghai, China) of endorphin, enkephalin, MOR, DOR, AEA, 2-AG, CB_1R, and CB_2R were used. Rat recombinant cytokine standards and samples of 100 μL were ran in duplicate according to the manufacturer's instructions. The optical density of each well was read at 450 nm.

2.10. Intrathecal Catheter Surgery and Drug Administration. To elaborate the difference of analgesic mechanism between single- and combined-acupoint EA, pharmacological experiments were performed. Specific drugs were injected intrathecally and intraperitoneally.

Intrathecal catheter surgery was performed as previously described [34]. After the rats were anesthetized with 1.5% isoflurane in oxygen inhalation, a PE-10 intrathecal catheter was implanted into the intrathecal space of the spinal cord at L4-L6 level. After filling the catheter with sterile endotoxin free PBS, rats were individually housed to protect the catheter from gnawing. Intrathecal injection of 2% lidocaine (10 μL) was performed at 3 days after surgery. A paralysis of the lower limbs occurred within 30 s and recovered within 30 min indicates the success of catheter implantation. Rats without signs of spinal cord damage were applied for experimentation.

The doses were chosen from the previous publication [35], and 10 μg CB_1R inhibitor AM281 (Sigma-Aldrich, A0980, USA) and 10 μg CB_2R AM630 (Cayman Chemical, 164178-33-0, USA) were diluted in 15 μL dimethyl sulfoxide (Sigma-Aldrich, 67-68-5, USA) and saline in a ratio of 1 : 1 and then injected through the intrathecal catheter 20 min prior to each EA treatment. Nonselective opioid inhibitor naloxone (1 mg/kg, Tocris Bioscience, UK) was administrated intraperitoneally 2 h prior to each EA treatment as previously reported [36].

2.11. Data Analysis. In the present study, statistical analyses were performed by GraphPad Prism 8.0 (GraphPad Software Inc., La Jolla, USA). All the data were expressed as mean ± SEM. The data of PWMT and numbers of spikes were analyzed by two-way repeated measures analysis of variance (ANOVA) followed by Bonferroni's post hoc analysis. The data of amplitude of eEPSP, rheobase, western blot, and ELISA assay were analyzed by one-way ANOVA and Bonferroni's post hoc analysis. All P values were two-sided, and $P < 0.05$ was considered significant.

3. Results

3.1. The Long-Term Analgesia of Combined-Acupoint EA Is Stronger than That of Single-Acupoint EA. To investigate whether there is any difference in the analgesic effect between EA stimulation at the single and two-combined acupoints, animals were randomly divided into four groups ($n = 10$ per group). Animals in the control group were conducted with sham surgery (the left sciatic nerve was exposed but with no chromic gut sutures tied to it). Animals in the CCI group were conducted with CCI modeling. In the single group, EA treatments were given at bilateral ST36 after CCI modeling. In the combined group, EA stimulation at bilateral ST36 and GB30 was performed after CCI modeling (Figure 1(a)).

As shown in Figure 1(b), the PWMT was dramatically decreased after CCI modeling. EA treatment at both ST36 and ST36 + GB30 significantly increased PWMT at 2, 4, 6, 9, 11, and 13 days after EA (single vs. CCI, $P < 0.05$; combined vs. CCI, $P < 0.001$, Figure 1(b)). Meanwhile, the PWMT of the combined group was higher than that of the single group (single vs. combined, $P < 0.01$), and this difference became statistically significant since the 2 days of EA and maintained until the 13 days. Area under the curve (AUC) of graphs (Figure 1(c)) suggested that the overall effect of alleviating mechanical allodynia was more effective in the combined-acupoint group (single vs. combined, $P < 0.001$). This behavioral result indicates that the long-term analgesic effect of combined-acupoint EA is better than that of single-acupoint EA.

In view of synaptic transmission being enhanced in the neuropathic pain conditions and spinal cord mechanism playing an important role in EA analgesia [25, 41], we also investigated changes of synaptic transmission between C fiber and excitatory projection neurons in the lamina I and IIo of vGlut2-tdTomato mice under control, CCI, combined-acupoint EA, and single-acupoint EA conditions (Figures 2(a) and 2(b)). We patched neurons expressing tdTomato in sagittal slices from vGlut2-tdTomato mice (Figure 2(c)). According to the electric strengths for activation of C-fiber and the conduction velocities for C-fiber transmission [33], 1.2 V stimulation of C fiber evoked EPSP was recorded and compared in control, CCI, single, and combined groups. As is shown, the amplitude of the evoked EPSP was higher in CCI mice than in control mice (CCI vs. control, $P < 0.05$, Figures 2(d), 2(e), and 2(h)). Compared with the CCI group, combined and single EA significantly and slightly decreased the amplitude of eEPSP, respectively

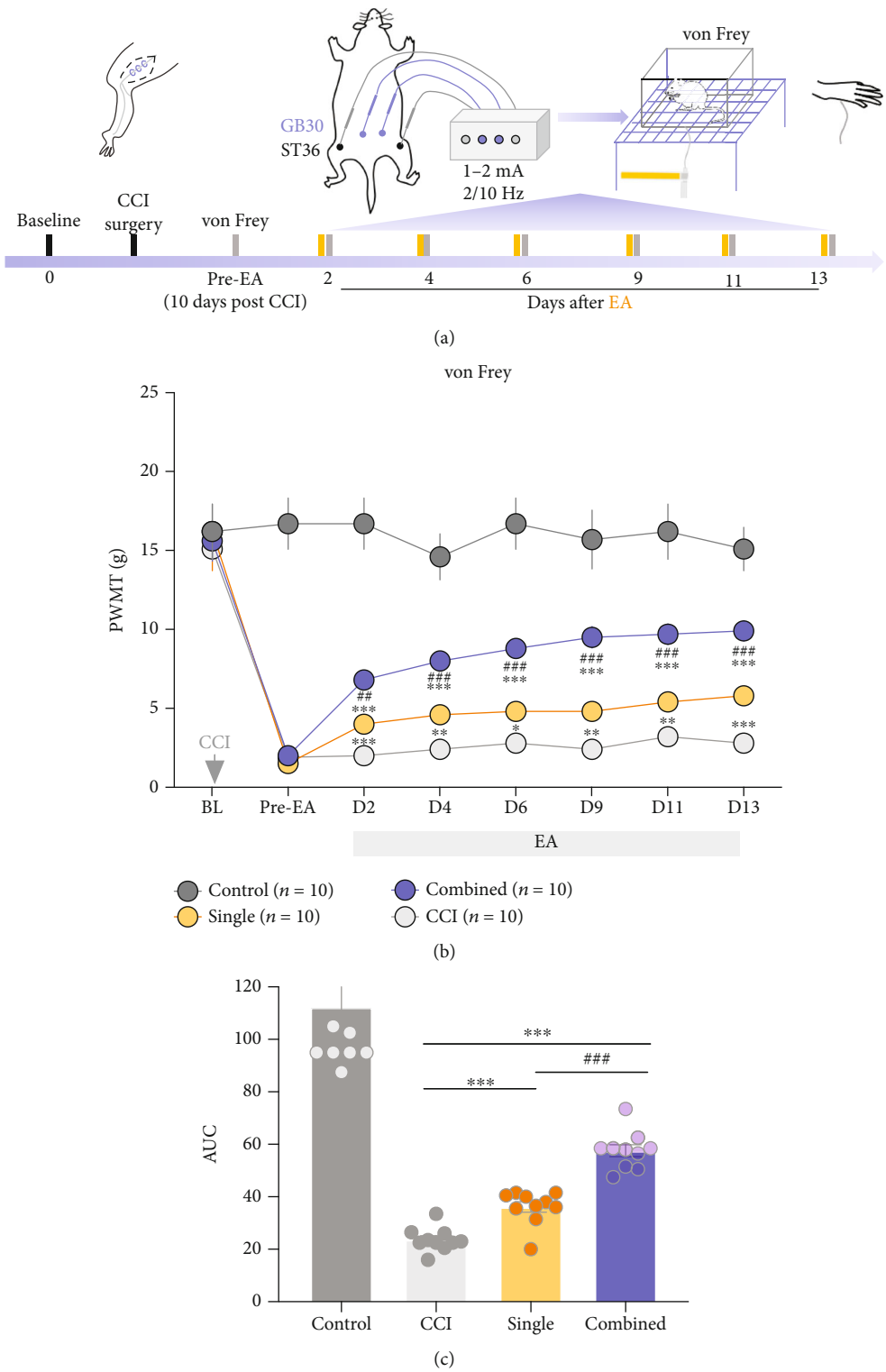

Figure 1: Combined-acupoint EA was more effective than single-acupoint EA in inducing the analgesic effects in CCI rats. (a) Schematic (top) and timeline (bottom) of the CCI model, pain behavior tests (von Frey), and EA stimulation. (b) Time course of CCI injury elicited remarkable mechanical allodynia in the CCI group. Both single-acupoint and combined-acupoint EA alleviated pain, as the paw withdrawal threshold was consistently decreased. The combined-acupoint EA exerted more effective antinociception than single-acupoint EA, and the statistical difference of analgesia between these two groups lasted from day 2 to day 13 of the EA treatment. Two-way ANOVA followed by Bonferroni's multiple comparisons test. (c) Area under the curve of graph b (from "BL" to D13). Student's unpaired t-test. All data are mean ± SEM, $^{*}P < 0.05$, $^{**}P < 0.01$, $^{***}P < 0.001$ vs. CCI; $^{\#\#}P < 0.01$, $^{\#\#\#}P < 0.001$ vs. single, $N = 10$ in each group. BL: baseline; CCI: chronic constriction injury; EA: electroacupuncture; AUC: area under curve; PWMT: paw withdrawal mechanical threshold; vs: versus; orange column indicated the EA; gray column indicates the von Frey measurement.

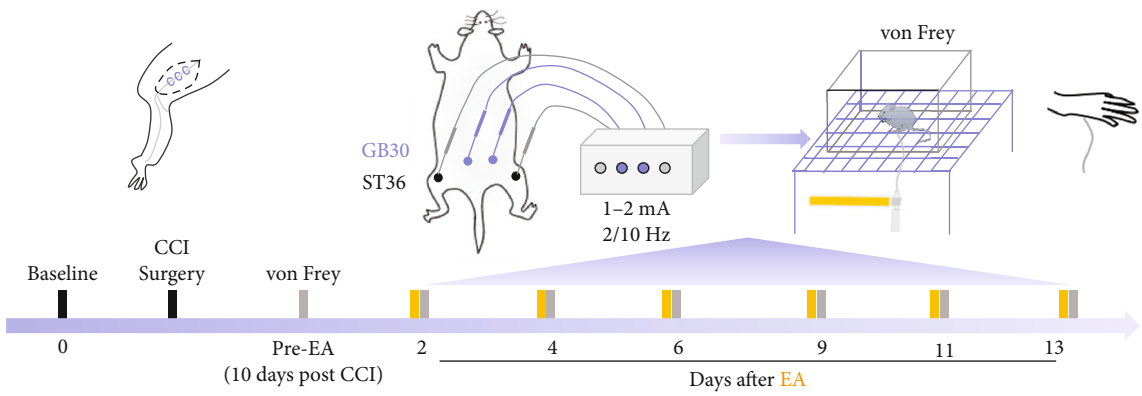

(a)

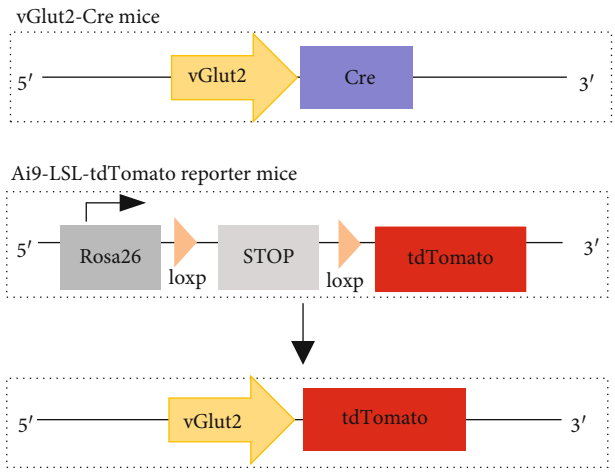

(b)

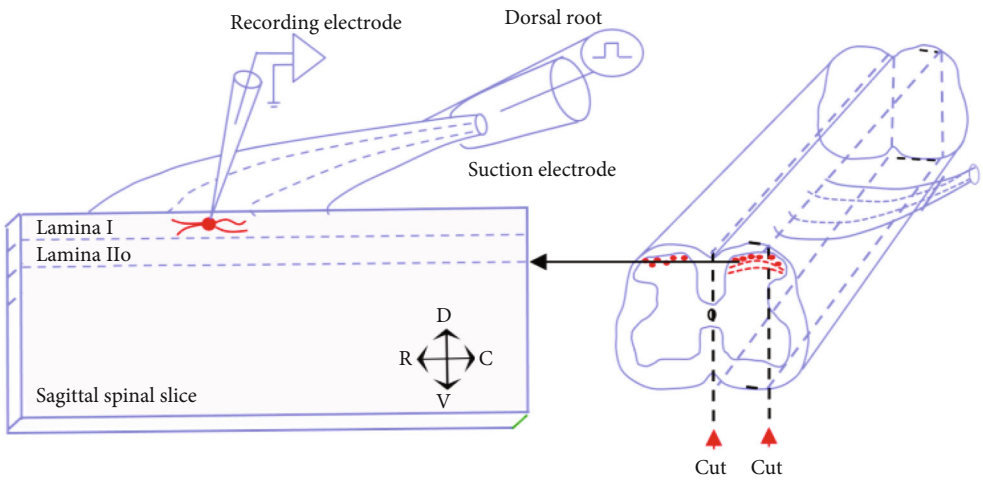

(c)

Figure 2: Continued.

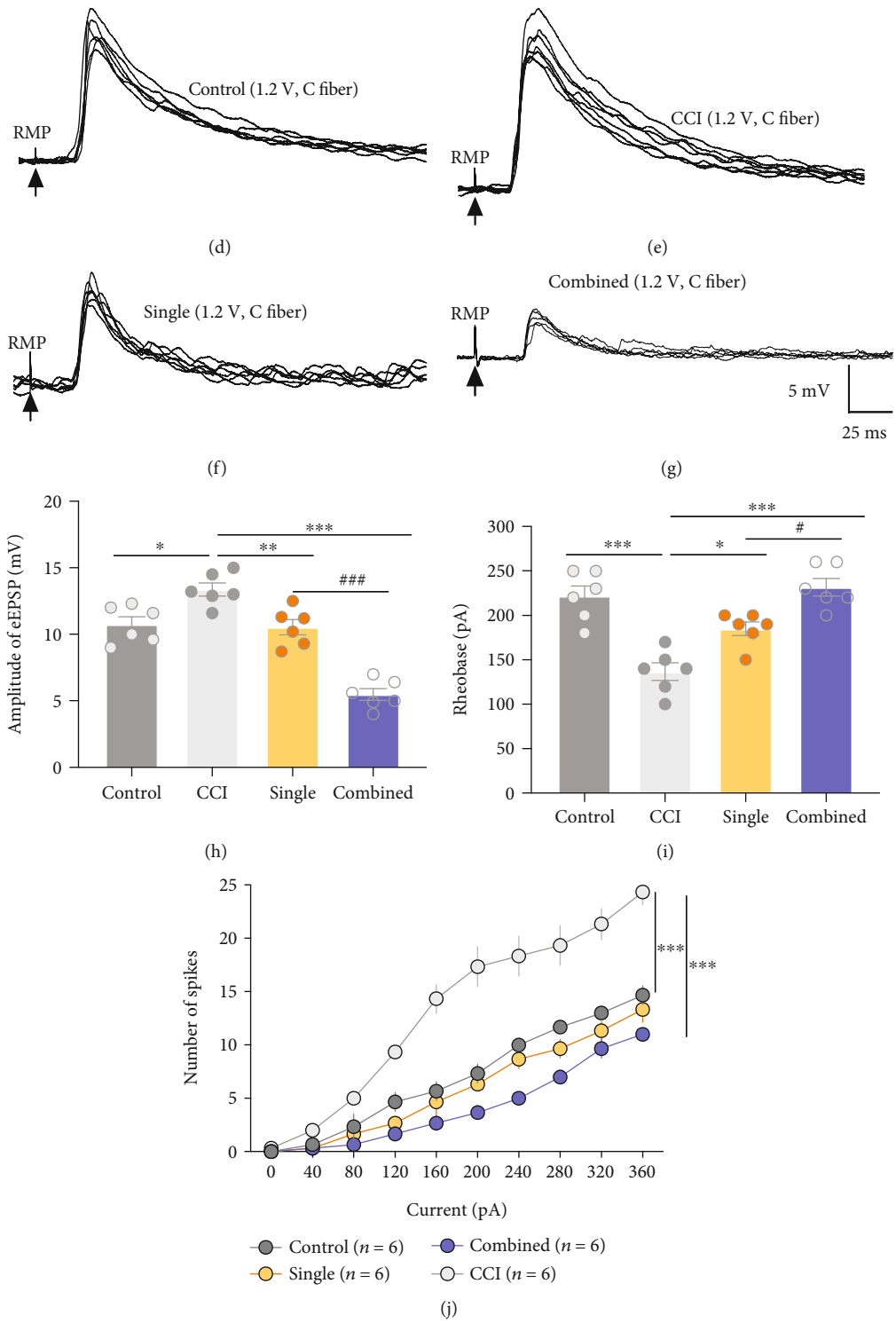

Figure 2: Continued.

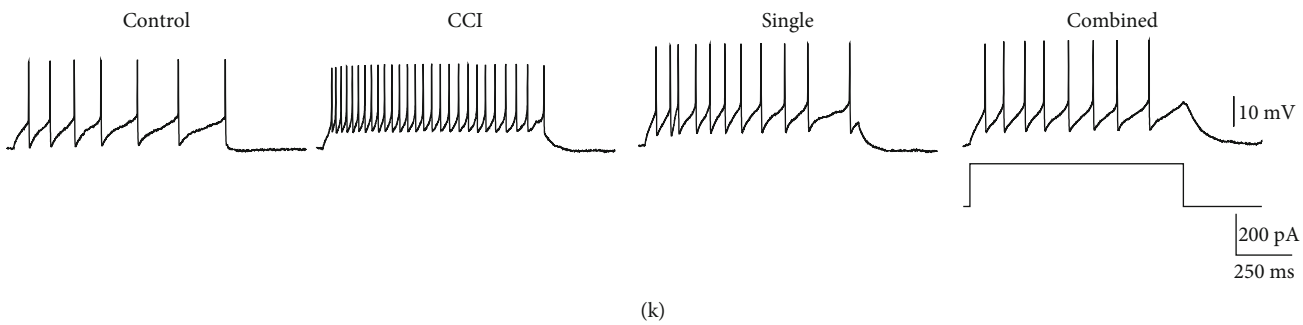

Figure 2: Combined-acupoint EA inhibit the synaptic transmission at the spinal level to a greater extent than Single-acupoint EA in mice. (a) Schematic (top) and timeline (bottom) of the CCI model, pain behavior tests (von Frey), and EA stimulation in control, CCI, combined, and single groups of vGlut2-tdTomato mice. (b) Schematic showing how to mate vGlut2-Cre and Ai9-LSL-tdTomato reporter mice to generate vGlut2-tdTomato mice to specific labeling of vGlut2-positive neurons in spinal dorsal horn. (c) Schematic showing the strategy for electrophysiological whole-cell recording of vGlut2-tdTomato-positive neurons in the lamina I and IIo of sagittal spinal slice attached dorsal root. Representative response of C-fiber evoked EPSP at 1.2 V stimulation of dorsal root in the control group (d) and in the CCI group at 10 days after CCI (e). Representative response of C-fiber evoked EPSP at 1.2 V stimulation of dorsal root in the combined group (f) and single group (g) at 10 days after CCI followed by 6 consecutive days and 1-day off EA treatment. (h) Amplitude of eEPSP recorded in the control, CCI, combined, and single groups. One-way ANOVA and Bonferroni's post hoc analysis. (i) Rheobase of vGlut2-tdTomato neurons in the control, CCI, combined, and single groups. One-way ANOVA and Bonferroni's post hoc analysis. (j) Number of spikes in response to 1000 ms depolarizing current injection of varying amplitude. Two-way repeated measures analysis of variance (ANOVA) followed by Bonferroni's post hoc analysis. (k) Representative tonic firing pattern in response to 1000 ms depolarizing 200 pA current injection. All data are mean ± SEM, $^{*}P < 0.05$, $^{**}P < 0.01$, $^{***}P < 0.001$ vs. CCI; $^{\#\#}P < 0.01$, $^{\#\#\#}P < 0.001$ vs. single, $N = 6$ in each group. RMP: resting membrane potential; CCI: chronic constriction injury; combined: ST36 + GB30; single: ST36; PWMT: paw withdrawal mechanical threshold; vs: versus; orange column indicated the EA; gray column indicates the von Frey measurement.

(combined vs. CCI, $P < 0.001$, Figures 2(e)–2(g)). Meanwhile, compared with single EA, combined EA reduced this amplitude to a greater extent (combined vs. single, $P < 0.001$, Figure 2(h)). Besides, we also detected the excitability of vGlut2-positive neurons in different groups. We found that CCI decreased the rheobase compared to the control group (CCI vs. control, $P < 0.001$, Figure 2(i)). Combined and single EA increased the rheobase compared to the CCI group (combined vs. CCI, $P < 0.001$; single vs. CCI, $P < 0.05$, Figure 2(i)). Tonic firing pattern was recorded in response to prolonged (1000 ms) depolarizing current injections of varying amplitudes (Figure 2(j)). As is shown, CCI increased the action potential firing frequency compared with the control groups under the same current injection amplitude including 200 pA (CCI vs. control, $P < 0.001$, Figures 2(j) and 2(k)). Similarly, action potential firing frequency was significantly inhibited after combined EA (combined vs. CCI, $P < 0.001$, Figures 2(j) and 2(k)). These results suggest that combined-acupoint EA inhibits the synaptic transmission at the spinal level to a greater extent than single-acupoint EA, laying a structural foundation for the behavioral results that combined-acupoint EA significantly alleviated neuropathic pain.

3.2. The Stimulation Intensity and Number of Stimulation Sites Are Not the Determinant for the Superior Analgesic Effect of the Combined-Acupoint EA. To further investigate whether the increased number of stimulation sites and the stimulation power in the combined-acupoint EA were the reason for the better analgesic effect, the animals were randomly divided into five groups. The interventions in CCI group, single group, and combined group were the same as those in the last experiment. In the high-intensity group, EA stimulation was given at the maximal tolerable intensity at the acupoint of ST36 (6-8 mA). In the sham-combined group, two nonacupoints (3 mm under ST36 or GB30) were stimulated simultaneously.

As shown in Figure 3, the PWMT of the single group was significantly higher than that of the CCI group at 6, 9, 11, and 13 days after EA (AUC, single vs. CCI, $P < 0.001$). EA stimulation at ST36 with high intensity also significantly alleviated the mechanical allodynia compared to the CCI group at 13 days after EA (AUC, high-intensity vs. CCI, $P < 0.01$). Besides, the PWMT of the combined group was also significantly higher than that of the CCI group from the 2 to 13 days after EA (AUC, combined vs. CCI, $P < 0.001$). The PWMT of the combined group was also higher than that of the high-intensity group or the single group (AUC, combined vs. high-intensity, $P < 0.001$; combined vs. single, $P < 0.01$). However, there was no significant difference between high-intensity and single group (AUC, high-intensity vs. single, $P > 0.05$), indicating that the increase of stimulation intensity may not be sufficient to enhance the analgesic effect of EA. Meanwhile, there was no statistical difference of PWMT between the sham-combined group and CCI group (AUC, sham-combined vs. CCI, $P > 0.05$), suggesting that increasing number of EA stimulation sites could not strengthen the analgesic effect either.

3.3. Both Single- and Combined-Acupoint EA Activated the Endogenous Opioid System. The endogenous opioid system has been widely reported to participate in the electroacupuncture inhibition of inflammatory and neuropathic pain

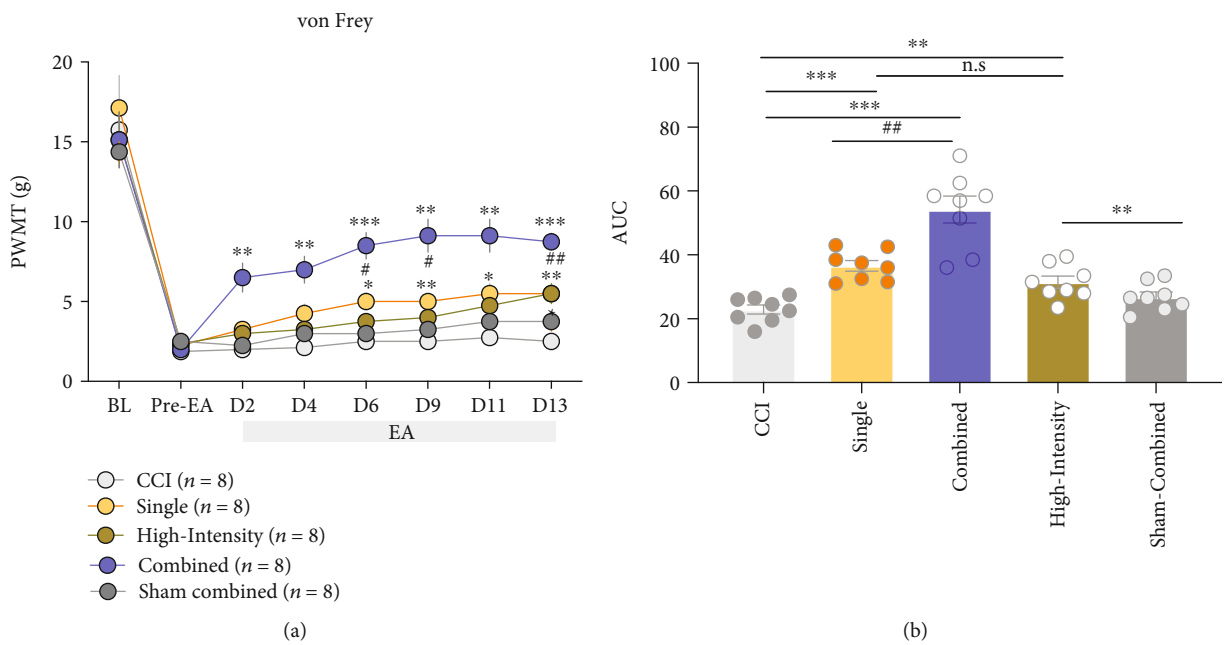

Figure 3: Increasing stimulation intensity or nonacupoint sites for single-acupoint EA did not mimic the analgesic effect of the combined-acupoint EA. (a) The paw withdrawal threshold after single-acupoint EA with high-intensity treatment (6-8 mA) was higher than that of CCI group and not different from that of the single-acupoint group but much lower than that of the combined-acupoint group. EA at two nonacupoints failed to suppress pain. Two-way ANOVA followed by Bonferroni's multiple comparisons test. (b) Area under the curve of graph a (from "BL" to D13). Student's unpaired t-test. All data are mean ± SEM, $^{*}P < 0.05$, $^{**}P < 0.01$, $^{***}P < 0.001$ vs. CCI; $^{\#}P < 0.05$, $^{\#\#}P < 0.01$ vs. combined; n.s.: not significant; $N = 8$ in each group. BL: baseline; CCI: chronic constriction injury; EA: electroacupuncture; AUC: area under curve; PWMT: paw withdrawal mechanical threshold; vs: versus.

through peripheral, spinal cord, and supraspinal mechanisms. In inflammatory pain, it has been reported that low frequency EA mainly exerts analgesic effect through met-enkephalin and β-endorphin, while high frequency EA relies on dynorphin for analgesia. However, it is unclear whether this specificity still applies to CCI-induced neuropathic pain. So, we compared the endogenous opioids levels and their corresponding receptors between the single-and combined-acupoint EA stimulation. Animals were grouped into control, CCI, single, and combined group randomly, and rats were sacrificed after the EA treatment at 6 days to obtain the spinal cord tissue. As is shown, the endogenous endorphin and enkephalin were increased in both single and combined groups (endorphin: single vs. CCI, $P < 0.01$, combined vs. CCI, $P < 0.001$, Figure 4(a); enkephalin: single vs. CCI, $P < 0.001$, combined vs. CCI, $P < 0.001$, Figure 4(b)). The ELISA assay showed that expressions of MOR and DOR in the spinal cord were significantly elevated in EA treated rats when compared with the CCI group (MOR: single vs. CCI, $P < 0.01$, combined vs. CCI, $P < 0.001$, Figure 4(c); DOR: single vs. CCI, $P < 0.001$, combined vs. CCI, $P < 0.001$, Figure 4(d)), which was also confirmed by the western blot tests (MOR: single vs. CCI, $P < 0.01$, combined vs. CCI, $P < 0.01$, Figures 4(e) and 4(g); DOR: single vs. CCI, $P < 0.05$, combined vs. CCI, $P < 0.05$, Figures 4(f) and 4(h)). These results demonstrated that both single-acupoint and combined-acupoint EA were able to activate the endogenous opioid system. However, the opioids did not contribute to the analgesic discrepancy between single-acupoint and combined-acupoint EA.

3.4. Combined-Acupoint Rather than Single-Acupoint EA Activated Endogenous Cannabinoid (eCB) System. The ECS was previously considered as a key factor for EA analgesia through peripheral and supraspinal mechanisms [27]. The ECS consists of endogenous ligands (AEA, 2-AG), cannabinoid receptor (CB_1R, CB_2R), synthase, and hydrolase. Hence, we quantified endogenous ligands and cannabinoid receptor level in the groups of single-acupoint and combined-acupoint EA. As illustrated in Figure 5, the combined-acupoint EA increased the release of AEA and 2-AG in comparison with single (AEA, 2-AG: combined vs. single, $P < 0.001$), while the AEA or 2-AG in the single-acupoint EA group did not show significant difference from those in CCI group (AEA, 2-AG: single vs. CCI, $P > 0.05$, Figures 5(a) and 5(b)). Meanwhile, combined-acupoint EA increased the expression of both cannabinoid receptor 1 and 2 protein (ELISA: CB_1R, CB_2R, and combined vs. CCI, $P < 0.001$; WB: CB_1R, CB_2R, and Combined vs. CCI, $P < 0.05$, Figures 5(c)–5(h)). However, single-acupoint EA did not exert such effect (single vs. CCI, $P > 0.05$, Figure 5). These findings indicated that the specific activation of the spinal cord eCB system might be the cause of the stronger analgesic effect induced by the combined-acupoint EA.

3.5. Activation of the Endocannabinoid System Related to the Better Analgesic Effect of the Combined-Acupoint EA. To further elucidate the role of ECS activation in the analgesic effect of combined-acupoint EA, rats with CCI model and intrathecal catheterization were randomly divided into 4 groups: CCI group, single group, combined group, and

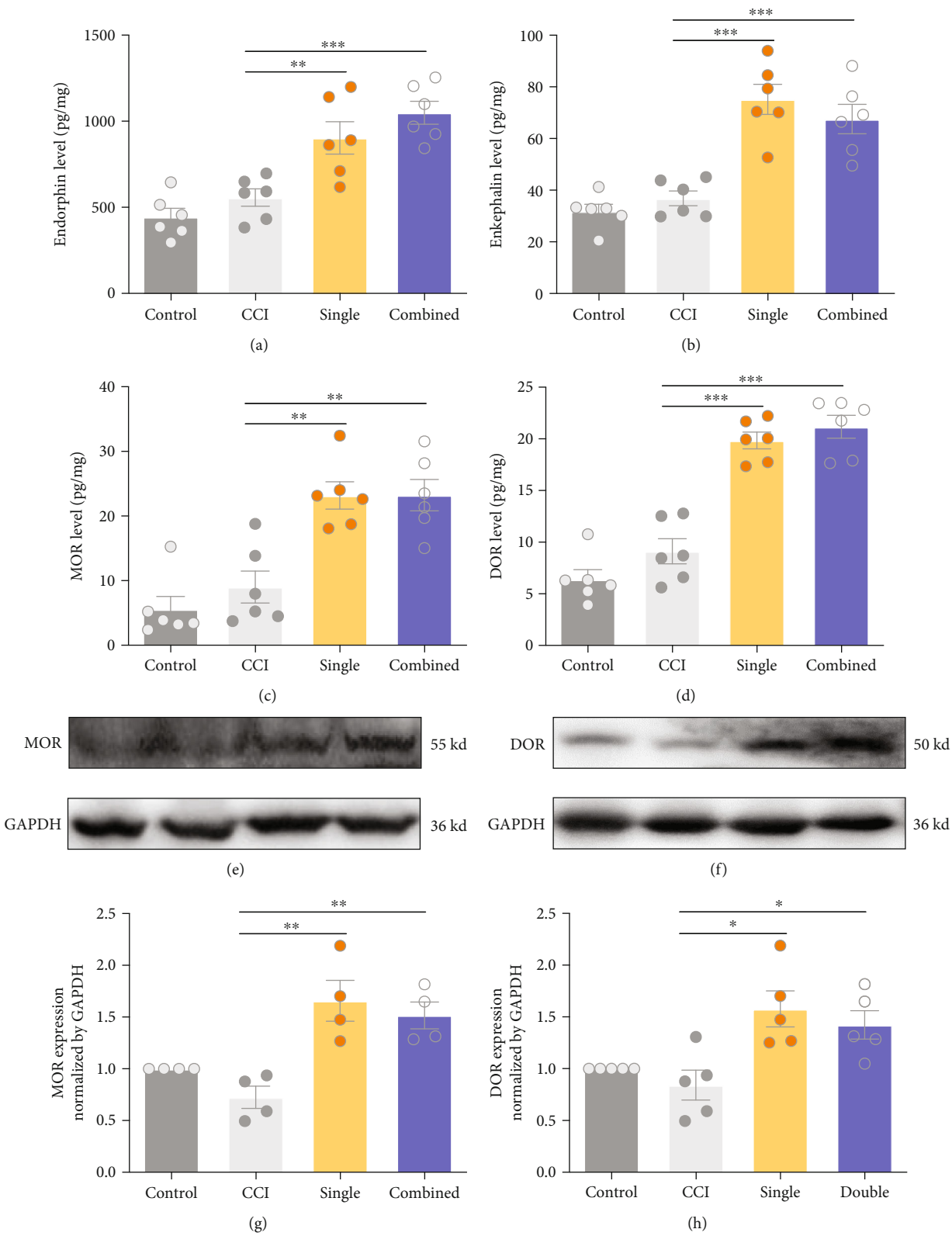

Figure 4: Both single and combined-acupoint EA activated endogenous opioid system. ELISA assay indicated the release of endorphin (a) and enkephalin (b) in both single and combined-acupoint EA groups increased at day 6 after EA treatment. ELISA assay showed that the expression of MOR (c) and DOR (d) was upregulated significantly in the single and combined groups. (e)–(h) The western blot analysis also confirmed the increased expression of MOR and DOR in both single-acupoint and combined-acupoint EA-treated rats. Student's unpaired t-test. All data are mean ± SEM, $^{*}P < 0.05$, $^{**}P < 0.01$, $^{**}P < 0.01$ vs. CCI; $N = 6$ in each group. CCI: chronic constriction injury; EA: electroacupuncture; MOR: μ-opioid receptor; DOR: δ-opioid receptor.

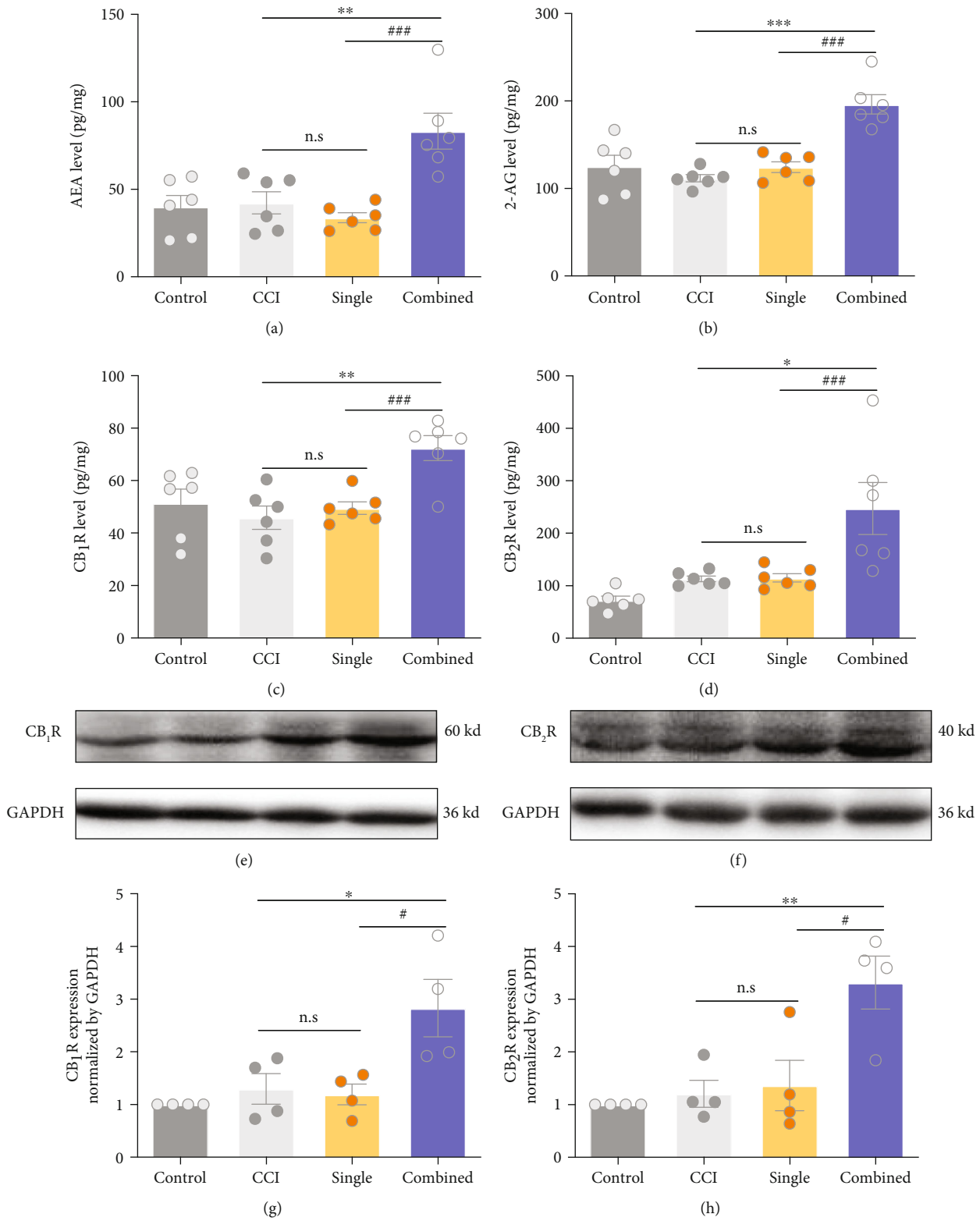

Figure 5: Combined-acupoint rather than single-acupoint EA activated the endogenous cannabinoid (eCB) system. ELISA assay revealed that combined-acupoint EA but not single-acupoint EA increased the release of AEA (a) and 2-AG (b) after 6 days' EA treatment. ELISA assay demonstrated that the expression of CB_1 (c) and CB_2 (d) receptor was only upregulated in combined-acupoint EA-treated group. The western blot analysis confirmed combined-acupoint EA but not single-acupoint EA increased the expression of CB_1 (e, g) and CB_2 (f, h) in the spinal cord. Student's unpaired t-test. All data are mean ± SEM, $^{*}P < 0.05$, $^{**}P < 0.01$, $^{**}P < 0.01$ vs. combined; $^{\#}P < 0.05$, $^{\#\#}P < 0.01$, $^{\#\#\#}P < 0.001$ vs. combined; n.s.: not significant; $N = 6$ in each group. CCI: chronic constriction injury; EA: electroacupuncture; AEA: anandamide; 2-AG: 2-arachidonoyl glycerol; CB_1: cannabinoid receptor 1; CB_2: cannabinoid receptor 2.

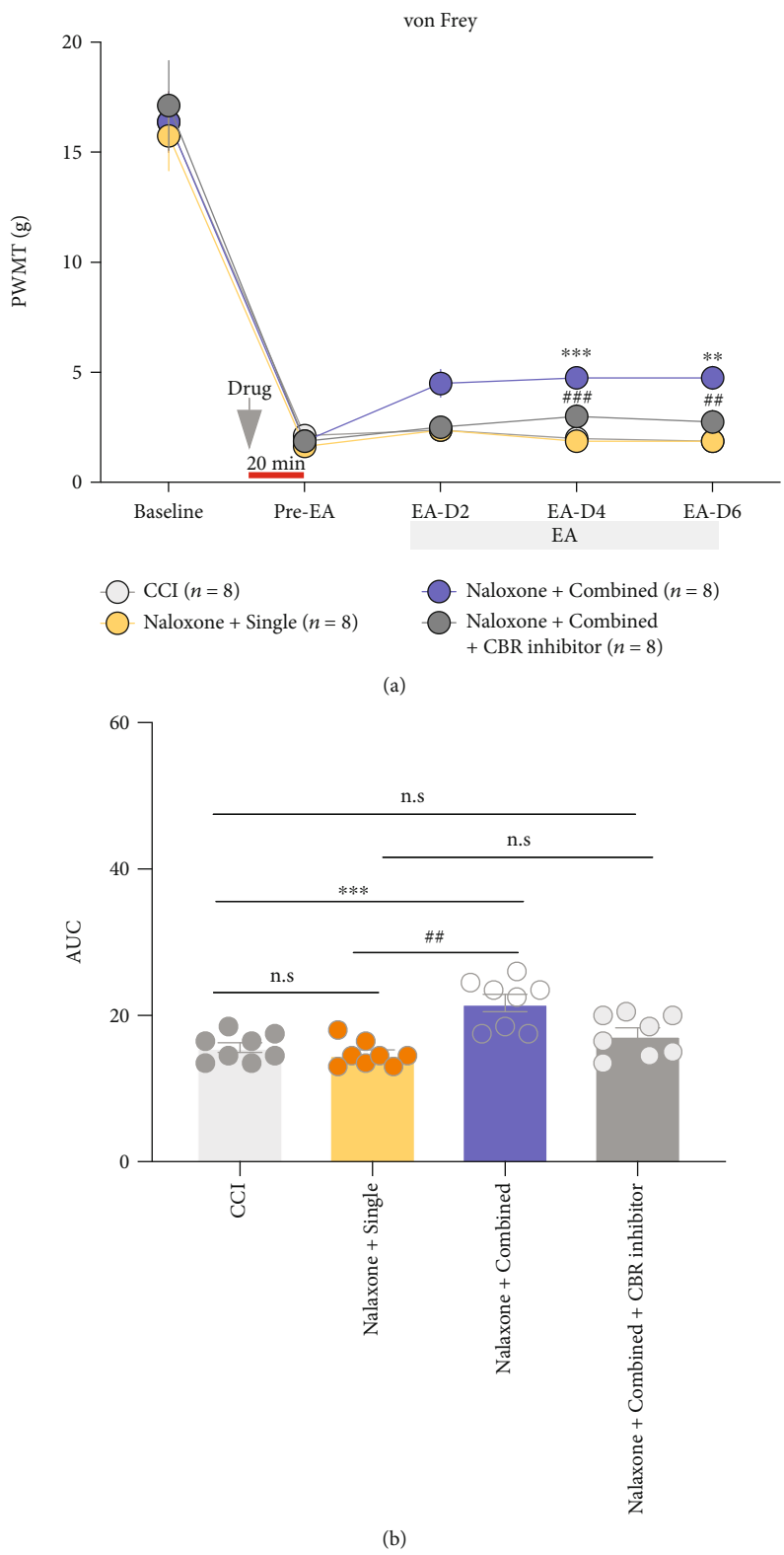

Figure 6: Intrathecal injection of cannabinoid receptor inhibitors blocked the analgesic effect of combined-acupoint EA. (a) Schematic and timeline showing pain behavior tests. All rats were injected with nonselective opioid receptor inhibitor naloxone. Naloxone completely inhibited the antinociceptive effect of single-acupoint EA but just partially reversed the analgesia induced by combined-acupoint EA. Coadministration of naloxone and CBR inhibitors eliminated the analgesic effect of combined-acupoint EA; two-way ANOVA followed by Bonferroni's multiple comparisons test. (b) Area under the curve of graph a (from "BL" to D6). Student's unpaired t-test. All data are mean ± SEM, $^{*}P < 0.05$, $^{**}P < 0.01$, $^{**}P < 0.01$ vs. CCI; $^{\#\#}P < 0.01$, $^{\#\#\#}P < 0.001$ vs. naloxone + single; n.s.: not significant; $N = 8$ in each group. CCI: chronic constriction injury; EA: electroacupuncture; PWMT: paw withdrawal mechanical threshold; CBR: cannabinoid receptor.

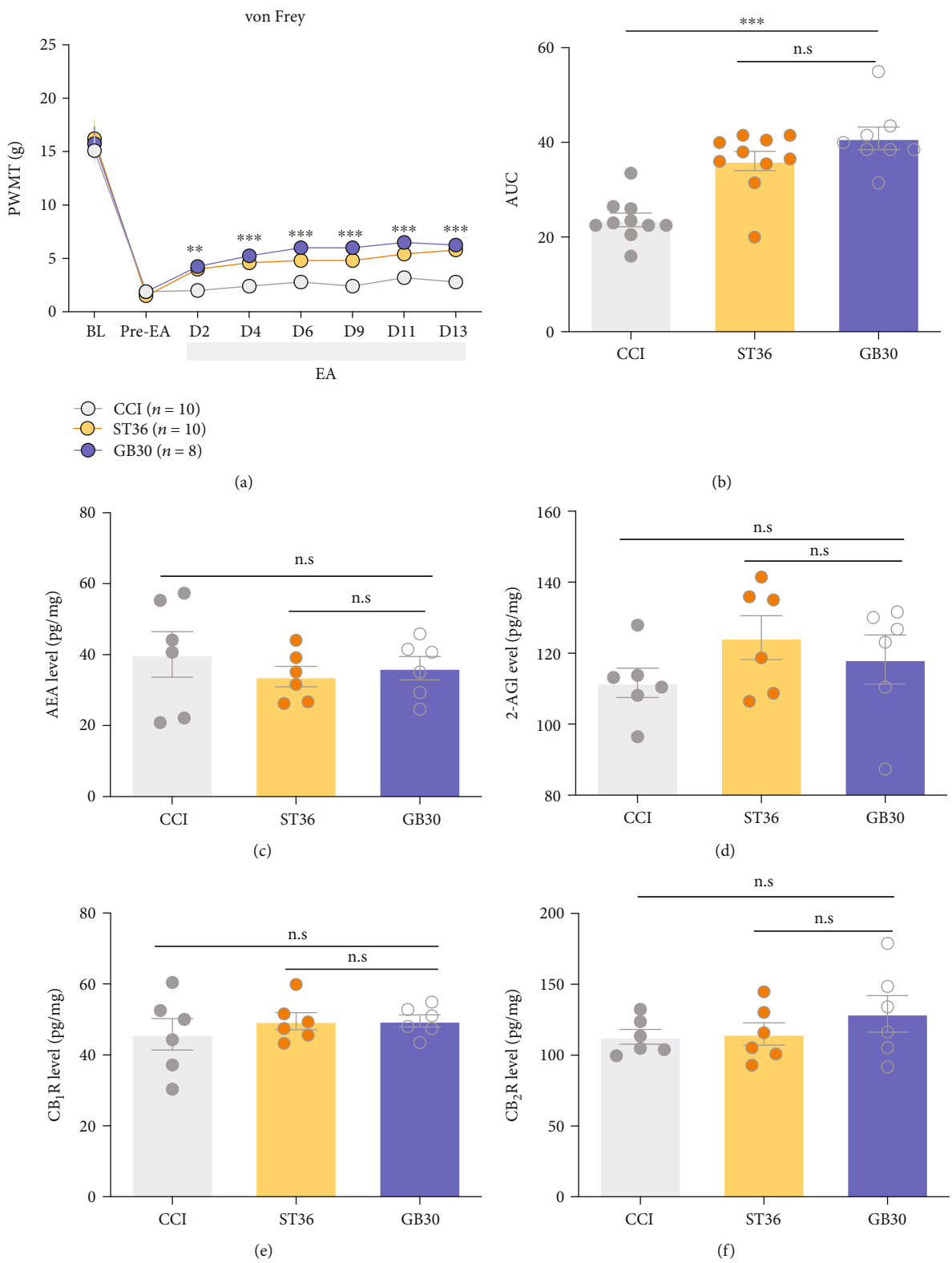

Figure 7: EA stimulation at single-acupoint GB30 was unable to provide a superior analgesic effect than ST36 in the ECS independent manner. (a) EA stimulation at GB30 provided a comparable analgesic effect to EA stimulation at ST36; two-way ANOVA followed by Bonferroni's multiple comparisons test. (b) Area under the curve of graph a (from "BL" to D13). Student's unpaired t-test. EA stimulation at GB30 did not elevate the AEA (c), 2-AG (d), CB_1R (e), and CB_2R (f) which activate the endocannabinoid system. All data are mean ± SEM, $^{**}P < 0.01$, $^{***}P < 0.001$ vs. CCI; n.s.: not significant; $N = 6$ in each group. CCI: chronic constriction injury; EA: electroacupuncture; eCB: endocannabinoid; AEA: anandamide; 2-AG: 2-arachidonoyl glycerol; CB_1: cannabinoid receptor 1; CB_2: cannabinoid receptor 2; ST36: Zusanli acupoint; GB30: Huantiao acupoint.

combined + CBR inhibitor group. All rats received the 2 mg/kg opioid inhibitor naloxone intraperitoneally prior to each EA treatment. At the same time, 10 μg AM281 and 10 μg AM630 were injected through the catheter to the combined + CBR inhibitor group. The PWMT of each rat was then measured at 2, 4, and 6 days after EA treatment.

As illustrated in Figure 6, the PWMT of rats in the combined group were significantly higher than that of CCI or single group at 4 (naloxone + combined vs. CCI, $P < 0.001$; naloxone + combined vs. naloxone + single, $P < 0.001$) and 6 days (naloxone + combined vs. CCI, $P < 0.01$; naloxone + combined vs. naloxone + single, $P < 0.01$). However, the PWMT in the single group was not different from that in the CCI group (naloxone + single vs. CCI, $P > 0.05$). When treated with cannabinoid receptor inhibitors, the pain alleviation effect of the combined-acupoint EA was blocked, as the PWMT of combined + CBR inhibitor was not different from CCI or single group (naloxone + combined + CBR inhibitor vs. CCI, $P > 0.05$; naloxone + combined + CBR inhibitor vs. naloxone + single + CBR inhibitor, $P > 0.05$, Figure 6(a)). The AUC results also showed that blocking the opioid receptor can completely block the analgesia effect of single EA (naloxone + single vs. CCI, $P > 0.05$); however, only simultaneously blocking both opioid and cannabinoid receptors can block the analgesia effect of combined EA (Figure 6(b)). These behavioral results illustrated that the endogenous opioid system was involved in the analgesia of both single-and combined-acupoint EA, while the eCB system was related to the superiority of analgesia induced by the EA stimulation at ST36 and GB30.

3.6. EA Stimulation at Single-Acupoint GB30 Was Unable to Provide a Superior Analgesic Effect than ST36 in the ECS Independent Manner. To further explore the mechanisms of ECS-mediated analgesia superiority of combined-acupoint EA, experiments about EA stimulation at GB30 alone were performed. Rats were randomly divided into CCI, ST36, and GB30 groups, which the latter two groups received the EA stimulation at ST36 and GB30, respectively. As is shown, EA stimulation at GB30 significantly alleviated the mechanical allodynia compared with the CCI group from the 2 days after EA stimulation (PWMT: GB30 vs. CCI, $P < 0.01$, Figure 7(a)), paralleled by the difference of overall effect reflected by the AUC (GB30 vs. CCI, $P < 0.001$, Figure 7(b)). However, compared with the single-acupoint stimulation at ST36, EA stimulation at GB30 alone did not provide a superior analgesic effect on the mechanical allodynia (PWMT: GB30 vs. ST36, $P > 0.05$, Figure 7(a); AUC: GB30 vs. ST36, $P > 0.05$, Figure 7(b)). Besides, EA stimulation at GB30 did not alter the content of AEA, 2-AG, CB_1, and CB_2 receptor compared with CCI (GB30 vs. CCI, $P > 0.05$, Figures 7(c)–7(f)) or ST36 (GB30 vs. ST36, $P > 0.05$, Figures 7(c)–7(f)) group, excluding the possibility that GB30 acupoint itself determined the analgesia superiority of combined-acupoint EA mediated by the ECS.

4. Discussion

The present study revealed that the analgesic effect of EA stimulation at combined acupoints ST36 and GB30 was stronger than that of EA stimulation at ST36 alone in the CCI animal model. Combined-acupoint EA significantly inhibited the synaptic transmission of pain information in the spinal dorsal horn compared to the single-acupoint EA to a greater extent. The increase of the stimulating intensity or number of stimulation sites did not enhance the analgesic effect of single-acupoint EA. Intraperitoneal naloxone injection could reverse the pain alleviation induced by single-acupoint EA, but not the combined-acupoint EA, unless inhibiting endogenous cannabinoid receptors. These findings provided evidence of the advantage of acupoints combination EA in the treatment of neuropathic pain and shed light on the underlying mechanism of acupuncture induced analgesia.

The current results demonstrated that combined-acupoint EA is more effective than single-acupoint EA in pain alleviation, which the PWMT of the combined group being significantly higher than the single group since the 2 days of EA treatment. This result corresponds to a previous study, in which combined-acupoint EA was demonstrated to provide stronger antinociception than single-acupoint EA did in an incisional pain model [37, 38]. Besides, the enhancement of synaptic transmission in the spinal cord is one of the mechanisms of neuropathic pain [23, 39]. Although related studies have reported that EA alleviates neuropathic pain by modulating the long-term synaptic plasticity in the spinal dorsal horn through field potential recording [40], they did not detect whether this effect is still applicable to explain the superiority of combined-acupoint stimulation. So, we further found that combined-acupoint EA produced superior analgesia through inhibiting the synaptic transmission between the nociceptive primary afferent and excitatory projection neurons using the whole-cell recording. Meanwhile, we also found higher-intensity stimulation, and the nonacupoint site stimulation failed to provide stronger analgesic effect, which indicated the stimulation at acupoint but not the electrical stimulus itself is responsible for achieving the better analgesic effect of combined-acupoint EA. However, whether EA induced analgesia depends on the power of the electrical stimulus is still controversial. Some studies reported that EA with higher intensity provided more powerful analgesia in healthy volunteers [41, 42]; however, some found mild EA was sufficient to produce analgesia in CFA induced inflammatory pain. The theory of "acupoint sensitization" may help to explain the paradoxical results. In this theory, acupoints are in "silent" state under physiological condition but are activated under pathological condition, which makes them more sensitive to external force, heat, light, electricity, and other stimuli [43].

The involvement of opioid substances in mediating acupuncture-induced analgesia was firstly demonstrated in the 1970s [44]. Acupuncture has been proved to activate all the three subfamilies of the endogenous opioid peptide, endorphin, enkephalin, and dynorphin. Low-frequency EA (2 Hz) mainly causes the release of endorphin and enkephalin, and high-frequency EA (100 Hz) dominates the activation of the dynorphin system in the inflammatory pain [26, 45]. In the present study, we found that the dense-

disperse mode at 2/10 Hz in the CCI-induced neuropathic pain model used for EA stimulation also induced the release of endorphin and enkephalin and upregulated their receptors MOR and DOR, followed by the contents of dynorphin being not elevated by EA treatment under the low-frequency, which is similar with inflammatory pain. This indicates that there may be no difference between the endogenous opioid system in regulating inflammatory pain and CCI-induced chronic pain.

The ECS is also a key factor in analgesia induced by EA [46]. Multiple studies have shown that acupuncture was able to activate CB1 receptor in the central nervous system [47, 48] and CB2 receptor in the peripheral [49, 50] to produce an analgesic effect. However, whether the ECS in the spinal cord participates in EA-induced analgesia remains unclear. In the current study, we found that EA at bilateral ST36 and GB30 rather than ST36 alone induced the release of both AEA and 2-AG and upregulated both CB_1 and CB_2 receptors in the spinal cord in the CCI animal model. There could be a possibility that the acupoint of GB30 was responsible for the activation of the ECS. However, our results showed that EA stimulation at GB30 alone neither provided a superior analgesic effect to EA treatment at ST36 nor altered the content of AEA, 2-AG, CB_1, or CB_2 receptor compared with the CCI group. This result suggested that the activation of ECS and the superior antinociception of combined-acupoint EA were not due to the simple combination of two acupoints' function but probably originated from a complex synergy effect of stimulating these two acupoints during neuropathic pain pathology. Up to now, most studies which reported the combined-acupoint EA could suppress pain via regulating ECS were done in the CFA model or knee osteoarthritis model in the supraspinal and peripheral level [51–54]. However, there were some studies showing single-acupoint EA could also activate the ECS to suppress acute pain elicited by heat stimuli [55, 56]. This inconsistency is probably caused by the heterogeneous mechanism of pain models. As explained by the theory of traditional Chinese medicine, single-acupoint acupuncture is mainly used to treat simple and emergency symptoms, while combined-acupoint acupuncture is used to cure complex and chronic diseases [56, 57]. The CCI neuropathic pain model we used in the current study is a kind of chronic pain model, in which no study ever reported the involvement of ECS activation in the single-acupoint EA. However, whether single-acupoint EA may have a transient regulatory effect on the ECS in the early stage after CCI modeling needs to be confirmed in further research. Moreover, it is generally known that ECS participates in the regulation of neuropathic pain at the spinal cord [58]. So, it is also very important to further study the role of ECS in modulating the inhibition of synaptic transmission in the spinal dorsal horn by different EA schemes. Certainly, we admit that there could be the influence of anatomical and physiological distinctions between rats and mice on the electroacupuncture. However, in clinical, patients receive the electroacupuncture normally in awake state. In order to perform the electroacupuncture to rodents without anesthesia, we used rats for most our studies, because rats could be easily immobilized in the home-made fixing platform without anesthesia, but it is harder to deliver electroacupuncture in mice at awake state. However, in the electrophysiological experiment, to specifically record the vGlut2-positive neurons, the vGlut2-tdTomato transgenic mice were used in respect of lacking of corresponding transgenic rats. Besides, to thoroughly elucidate how did ECS mediate analgesia discrepancy between the single and combined-acupoint EA, further exploration of the molecular and circuitry involving ECS in the spinal cord is needed.

5. Conclusion

In summary, the present study showed that the analgesic effect induced by combined EA stimulation at ST36 and GB30 is stronger than that induced by EA stimulation at ST36 alone in the CCI-induced neuropathic pain animal model. This superiority of analgesia is closely related to the specific activation of the ECS in the spinal cord by the combination of ST36 and GB30 stimulation, which provides a structural and functional basis for emphasizing electroacupuncture as an important complementary treatment.

Data Availability

The data supporting the findings of this study is available from the corresponding authors.

Conflicts of Interest

The authors declare that there is no conflict of interest.

Authors' Contributions

Lize Xiong and Qianzi Yang designed the experiments. Zhenhua Jiang, Yuheng Li, Qun Wang, Zongping Fang, Jiao Deng, Xinxin Zhang, Bowen Shen, and Zhixin Wu performed the experiments and analyzed the data. Zhenhua Jiang, Yuheng Li, and Lize Xiong wrote the manuscript. Lize Xiong and Qianzi Yang revised the manuscript and supported all aspects for this study. Zhenhua Jiang, Yuheng Li, and Qun Wang contributed equally to this work.

Acknowledgments

This study was supported by the funds from the National Basic Research Program of China (2014CB543202), the Major Program of the National Natural Science Foundation of China (No. 81590954, No. 82130121), National Natural Science Foundation of China (No. 82101295, No. 81701207), and Natural Science Foundation of Shandong Province (ZR202103030177). We would like to express our sincere gratitude to Prof. Yan Lu for his helpful comments and kind suggestions.

References

[1] T. S. Jensen, R. Baron, M. Haanpää et al., "A new definition of neuropathic pain," *Pain*, vol. 152, pp. 2204-2205, 2011.

[2] D. Bouhassira, M. Lantéri-Minet, N. Attal, B. Laurent, and C. Touboul, "Prevalence of chronic pain with neuropathic

characteristics in the general population," *Pain*, vol. 136, pp. 380–387, 2008.

[3] N. Torrance, B. H. Smith, M. I. Bennett, and A. J. Lee, "The epidemiology of chronic pain of predominantly neuropathic origin. Results from a general population survey," *The journal of pain : official journal of the American Pain Society*, vol. 7, pp. 281–289, 2006.

[4] Committee on Advancing Pain Research, Care, and Education; Board on Health Sciences Policy; Institute of Medicine, "A call for cultural transformation of attitudes toward pain and its prevention and management," *Journal of Pain & Palliative Care Pharmacotherapy*, vol. 25, pp. 365–369, 2011.

[5] L. E. Chaparro, P. J. Wiffen, R. A. Moore, and I. Gilron, "Combination pharmacotherapy for the treatment of neuropathic pain in adults," *Cochrane database of systematic reviews*, vol. 7, 2012.

[6] S. Liu, Z. F. Wang, Y. S. Su et al., "Somatotopic organization and intensity dependence in driving distinct NPY-expressing sympathetic pathways by electroacupuncture," *Neuron*, vol. 108, article e437, pp. 436–450, 2020.

[7] S. Liu, Z. Wang, Y. Su et al., "A neuroanatomical basis for electroacupuncture to drive the vagal-adrenal axis," *Nature*, vol. 598, pp. 641–645, 2021.

[8] F. Hui, E. Boyle, E. Vayda, and R. H. Glazier, "A randomized controlled trial of a multifaceted integrated complementary-alternative therapy for chronic herpes zoster-related pain," *Alternative Medicine Review*, vol. 17, pp. 57–68, 2012.

[9] E. Cerezo-Téllez, M. Torres-Lacomba, I. Fuentes-Gallardo et al., "Effectiveness of dry needling for chronic nonspecific neck pain: a randomized, single-blinded, clinical trial," *Pain*, vol. 157, 2016.

[10] S. Patil, S. Sen, M. Bral et al., "The role of acupuncture in pain management," *Current Pain and Headache Reports*, vol. 20, no. 4, pp. 1–8, 2016.

[11] S. W. Jiang, Y. W. Lin, C. L. Hsieh, and C. L. Hsieh, "Electroacupuncture at Hua Tuo Jia Ji acupoints reduced neuropathic pain and increased GABA(A) receptors in rat spinal cord," *Evidence-Based Complementary and Alternative Medicine*, vol. 2018, Article ID 8041820, 2018.

[12] C. P. Huang, Y. W. Lin, D. Y. Lee, and C. L. Hsieh, "Electroacupuncture relieves CCI-induced neuropathic pain involving excitatory and inhibitory neurotransmitters," *Evidence-Based Complementary and Alternative Medicine*, vol. 2019, Article ID 6784735, 2019.

[13] M. Armour and C. A. Smith, "Treating primary dysmenorrhoea with acupuncture: a narrative review of the relationship between acupuncture 'dose' and menstrual pain outcomes," *Acupuncture in Medicine*, vol. 34, pp. 416–424, 2016.

[14] M. Zhang, Q. Dai, D. Liang et al., "Involvement of adenosine A1 receptor in electroacupuncture-mediated inhibition of astrocyte activation during neuropathic pain," *Arquivos de Neuro-Psiquiatria*, vol. 76, pp. 736–742, 2018.

[15] S. S. Li, W. Z. Tu, C. Q. Jia et al., "KCC2-GABAA pathway correlates with the analgesic effect of electro-acupuncture in CCI rats," *Molecular Medicine Reports*, vol. 17, pp. 6961–6968, 2018.

[16] L. L. Ji, M. W. Guo, X. J. Ren, D. Y. Ge, G. M. Li, and Y. Tu, "Effects of electroacupuncture intervention on expression of cyclooxygenase 2 and microglia in spinal cord in rat model of neuropathic pain," *Chinese Journal of Integrative Medicine*, vol. 23, pp. 786–792, 2017.

[17] X. M. Chen, J. Xu, J. G. Song, B. J. Zheng, and X. R. Wang, "Electroacupuncture inhibits excessive interferon-γ evoked up-regulation of P2X4 receptor in spinal microglia in a CCI rat model for neuropathic pain," *British Journal of Anaesthesia*, vol. 114, pp. 150–157, 2015.

[18] J. Xu, X. M. Chen, B. J. Zheng, and X. R. Wang, "Electroacupuncture relieves nerve injury-induced pain hypersensitivity via the inhibition of spinal P2X7 receptor-positive microglia," *Anesthesia & Analgesia*, vol. 122, pp. 882–892, 2016.

[19] F. M. Teixeira, L. L. Castro, R. T. Ferreira, P. A. Pires, F. A. Vanderlinde, and M. A. Medeiros, "High-frequency electroacupuncture versus carprofen in an incisional pain model in rats," *Brazilian Journal of Medical and Biological Research*, vol. 45, pp. 1209–1214, 2012.

[20] N. Goldman, M. Chen, T. Fujita et al., "Adenosine A1 receptors mediate local anti-nociceptive effects of acupuncture," *Nature Neuroscience*, vol. 13, pp. 883–888, 2010.

[21] Y. P. Liu, Z. R. Luo, C. Wang et al., "Electroacupuncture promoted nerve repair after peripheral nerve injury by regulating miR-1b and its target brain-derived neurotrophic factor," *Frontiers in Neuroscience*, vol. 14, article 525144, 2020.

[22] H. Luo, Y. Zhang, J. Zhang et al., "Glucocorticoid receptor contributes to electroacupuncture-induced analgesia by inhibiting Nav1.7 expression in rats with inflammatory pain induced by complete freund's adjuvant," *Neuromodulation*, 2022.

[23] C. Luo, T. Kuner, and R. Kuner, "Synaptic plasticity in pathological pain," *Trends in neurosciences*, vol. 37, pp. 343–355, 2014.

[24] X. G. Liu and L. J. Zhou, "Long-term potentiation at spinal C-fiber synapses: a target for pathological pain," *Current Pharmaceutical Design*, vol. 21, pp. 895–905, 2015.

[25] R. Zhang, L. Lao, K. Ren, and B. M. Berman, "Mechanisms of acupuncture-electroacupuncture on persistent pain," *Anesthesiology*, vol. 120, pp. 482–503, 2014.

[26] J. S. Han, X. H. Chen, S. L. Sun et al., "Effect of low- and high-frequency TENS on Met-enkephalin-Arg-Phe and dynorphin A immunoreactivity in human lumbar CSF," *Pain*, vol. 47, pp. 295–298, 1991.

[27] I. J. MacDonald and Y. H. Chen, "The endocannabinoid system contributes to electroacupuncture analgesia," *Frontiers in Neuroscience*, vol. 14, article 594219, 2020.

[28] O. Aizpurua-Olaizola, I. Elezgarai, I. Rico-Barrio, I. Zarandona, N. Etxebarria, and A. Usobiaga, "Targeting the endocannabinoid system: future therapeutic strategies," *Drug Discovery Today*, vol. 22, pp. 105–110, 2017.

[29] M. Maccarrone, "Metabolism of the endocannabinoid anandamide: open questions after 25 years," *Frontiers In Molecular Neuroscience*, vol. 10, p. 166, 2017.

[30] G. J. Bennett and Y. K. Xie, "A peripheral mononeuropathy in rat that produces disorders of pain sensation like those seen in man," *Pain*, vol. 33, pp. 87–107, 1988.

[31] J. De Vry, E. Kuhl, P. Franken-Kunkel, and G. Eckel, "Pharmacological characterization of the chronic constriction injury model of neuropathic pain," *European Journal of Pharmacology*, vol. 491, pp. 137–148, 2004.

[32] Y. Li, Z. Fang, N. Gu et al., "Inhibition of chemokine CX3CL1 in spinal cord mediates the electroacupuncture-induced suppression of inflammatory pain," *Journal of Pain Research*, vol. 12, pp. 2663–2672, 2019.

[33] Q. Wang, X. Zhang, X. He et al., "Synaptic Dynamics of the Feed-forward Inhibitory Circuitry Gating Mechanical

Allodynia in Mice," *Anesthesiology*, vol. 132, no. 5, pp. 1212–1228, 2020.

[34] F. Xu, T. Li, and B. Zhang, "An improved method for protecting and fixing the lumbar catheters placed in the spinal subarachnoid space of rats," *Journal of Neuroscience Methods*, vol. 183, pp. 114–118, 2009.

[35] A. Romero-Sandoval, N. Nutile-McMenemy, and J. A. DeLeo, "Spinal microglial and perivascular cell cannabinoid receptor type 2 activation reduces behavioral hypersensitivity without tolerance after peripheral nerve injury," *Anesthesiology*, vol. 108, pp. 722–734, 2008.

[36] B. G. Hwang, B. I. Min, J. H. Kim, H. S. Na, and D. S. Park, "Effects of electroacupuncture on the mechanical allodynia in the rat model of neuropathic pain," *Neuroscience letters*, vol. 320, pp. 49–52, 2002.

[37] F. J. Cidral-Filho, M. D. da Silva, A. O. Moré, M. M. Córdova, M. F. Werner, and A. R. Santos, "Manual acupuncture inhibits mechanical hypersensitivity induced by spinal nerve ligation in rats," *Neuroscience*, vol. 193, pp. 370–376, 2011.

[38] L. N. Qiao, J. L. Liu, L. H. Tan, H. L. Yang, X. Zhai, and Y. S. Yang, "Effect of electroacupuncture on thermal pain threshold and expression of calcitonin-gene related peptide, substance P and γ-aminobutyric acid in the cervical dorsal root ganglion of rats with incisional neck pain," *Acupuncture in Medicine*, vol. 35, pp. 276–283, 2017.

[39] J. Sandkühler and X. Liu, "Induction of long-term potentiation at spinal synapses by noxious stimulation or nerve injury," *European Journal of Neuroscience*, vol. 10, pp. 2476–2480, 1998.

[40] G. G. Xing, F. Y. Liu, X. X. Qu, J. S. Han, and Y. Wan, "Long-term synaptic plasticity in the spinal dorsal horn and its modulation by electroacupuncture in rats with neuropathic pain," *Experimental Neurology*, vol. 208, pp. 323–332, 2007.

[41] P. Barlas, S. L. Ting, L. S. Chesterton, P. W. Jones, and J. Sim, "Effects of intensity of electroacupuncture upon experimental pain in healthy human volunteers: a randomized, double-blind, placebo-controlled study," *Pain*, vol. 122, pp. 81–89, 2006.

[42] H. X. Liu, J. B. Tian, F. Luo et al., "Repeated 100 hz tens for the treatment of chronic inflammatory hyperalgesia and suppression of spinal release of substance p in monoarthritic rats," *Evidence-Based Complementary and Alternative Medicine*, vol. 4, Article ID 397050, 75 pages, 2007.

[43] P. J. Rong, S. Li, H. Ben et al., "Peripheral and spinal mechanisms of acupoint sensitization phenomenon," *Evidence-Based Complementary and Alternative Medicine*, vol. 2013, Article ID 742195, 2013.

[44] B. Pomeranz and R. Cheng, "Suppression of noxious responses in single neurons of cat spinal cord by electroacupuncture and its reversal by the opiate antagonist naloxone," *Experimental Neurology*, vol. 64, pp. 327–341, 1979.

[45] J. S. Han, "Acupuncture: neuropeptide release produced by electrical stimulation of different frequencies," *Trends In Neurosciences*, vol. 26, pp. 17–22, 2003.

[46] L. W. Fu and J. C. Longhurst, "Electroacupuncture modulates vlPAG release of GABA through presynaptic cannabinoid CB1 receptors," *Journal of Applied Physiology*, vol. 106, pp. 1800–1809, 2009.

[47] J. H. Jang, J. Y. Park, J. Y. Oh et al., "Novel analgesic effects of melanin-concentrating hormone on persistent neuropathic and inflammatory pain in mice," *Scientific Reports*, vol. 8, p. 707, 2018.

[48] X. C. Yuan, B. Zhu, X. H. Jing et al., "Electroacupuncture potentiates cannabinoid receptor-mediated descending inhibitory control in a mouse model of knee osteoarthritis," *Frontiers in Molecular Neuroscience*, vol. 11, p. 112, 2018.

[49] T. F. Su, Y. Q. Zhao, L. H. Zhang et al., "Electroacupuncture reduces the expression of proinflammatory cytokines in inflamed skin tissues through activation of cannabinoid CB2 receptors," *European Journal of Pain*, vol. 16, pp. 624–635, 2012.

[50] F. Gao, H. C. Xiang, H. P. Li et al., "Electroacupuncture inhibits NLRP3 inflammasome activation through CB2 receptors in inflammatory pain," *Brain, Behavior, and Immunity*, vol. 67, pp. 91–100, 2018.

[51] J. J. Li, R. M. Chen, L. Liu et al., "Effects of electroacupuncture on the immunoreactivity of focal cutaneous CB2 receptor positive cells in arthritis rats," *Acupuncture Research*, vol. 32, pp. 9–15, 2007.

[52] Y. Shou, Y. Q. Zhao, M. S. Xu, and L. B. Ge, "Effects of repeated electroacupuncture on gene expression of cannabinoid receptor-1 and dopamine 1 receptor in nucleus accumbens-caudate nucleus region in inflammatory-pain rats," *Acupuncture Research*, vol. 36, pp. 18–22, 2011.

[53] J. Zhang, L. Chen, T. Su et al., "Electroacupuncture increases CB2 receptor expression on keratinocytes and infiltrating inflammatory cells in inflamed skin tissues of rats," *The journal of pain : official journal of the American Pain Society*, vol. 11, pp. 1250–1258, 2010.

[54] X. C. Yuan, Q. Wang, W. Su et al., "Electroacupuncture potentiates peripheral CB2 receptor-inhibited chronic pain in a mouse model of knee osteoarthritis," *Journal of Pain Research*, vol. 11, pp. 2797–2808, 2018.

[55] Y. H. Chen, H. J. Lee, M. T. Lee et al., "Median nerve stimulation induces analgesia via orexin-initiated endocannabinoid disinhibition in the periaqueductal gray," *Proceedings of the National Academy of Sciences*, vol. 115, pp. E10720–e10729, 2018.

[56] R. T. Almeida, T. R. Romero, M. G. Romero, G. G. de Souza, A. C. Perez, and I. D. Duarte, "Endocannabinoid mechanism for orofacial antinociception induced by electroacupuncture in acupoint St36 in rats," *Pharmacological Reports*, vol. 68, pp. 1095–1101, 2016.

[57] S. Zhang and L. Shi, "Thory and application of "between the parallel, or walk alone"," *Journal of Liaoning University of Traditional Chinese Medicine*, vol. 18, 2016.

[58] S. G. Woodhams, D. R. Sagar, J. J. Burston, and V. Chapman, "The role of the endocannabinoid system in pain," *Handbook of Experimental Pharmacology*, vol. 227, pp. 119–143, 2015.

Hindawi
Neural Plasticity
Volume 2022, Article ID 8057854, 8 pages
https://doi.org/10.1155/2022/8057854

Review Article

Translocator Protein 18 kDa (TSPO) as a Novel Therapeutic Target for Chronic Pain

Jie Liu,[1] Jingyao Huang,[1] Zhenjiang Zhang,[2] Rui Zhang,[1] Zhihao Zhang,[1] Yongxin Liu,[1] and Baoyu Ma[1]

[1]*Shandong Provincial Medicine and Health Key Laboratory of Clinical Anesthesia, School of Anesthesiology, Weifang Medical University, Weifang, China*
[2]*Department of Thoracic Surgery, Weifang People's Hospital, Weifang, China*

Correspondence should be addressed to Rui Zhang; zhangrui@wfmc.edu.cn

Received 11 April 2022; Revised 19 July 2022; Accepted 13 August 2022; Published 29 August 2022

Academic Editor: Xue-Qiang Wang

Chronic pain is an enormous modern public health problem, with significant numbers of people debilitated by chronic pain from a variety of etiologies. Translocator protein 18 kDa (TSPO) was discovered in 1977 as a peripheral benzodiazepine receptor. It is a five transmembrane domain protein, mainly localized in the outer mitochondrial membrane. Recent and increasing studies have found changes in TSPO and its ligands in various chronic pain models. Reversing their expressions has been shown to alleviate chronic pain in these models, illustrating the effects of TSPO and its ligands. Herein, we review recent evidence and the mechanisms of TSPO in the development of chronic pain associated with peripheral nerve injury, spinal cord injury, cancer, and inflammatory responses. The cumulative evidence indicates that TSPO-based therapy may become an alternative strategy for treating chronic pain.

1. Introduction

Chronic pain is a major public health issue, which seriously affects patients' quality of life and aggravates economic burdens on society. According to the International Association for the Study of Pain (IASP), chronic pain can be categorized as chronic primary pain and chronic secondary pain, (e.g., chronic cancer-related pain, chronic postoperative or post-traumatic pain, and chronic neuropathic pain) [1]. Opioids are powerful analgesics that are commonly used clinically. However, opioids can produce significant side effects, including respiratory depression, mental clouding, physical dependence, constipation, nausea, and vomiting [2, 3]. Despite increasing investigations into chronic pain mechanisms and therapeutic strategies [4, 5], current therapies for chronic pain management are severely insufficient or, as in the case of opioids, limited by serious side effects [6]. Therefore, exploring novel and effective analgesics for chronic pain treatment is crucial.

The translocator protein 18 kDa (TSPO) was discovered in 1977 as a peripheral benzodiazepine receptor [7]. This mitochondrial protein consists of 169 amino acids with five transmembrane domains [8], which is mainly localized in the outer mitochondrial membrane (OMM) [9]. TSPO can interact with specific mitochondrial proteins, like voltage-dependent anion channel (VDAC) and anion nucleotide translocator (ANT) [10–12], which are involved in the composition of mitochondrial permeability translocation pores and regulate development of physiological and pathological conditions [13], suggesting the key role of TSPO in cellular functions related to mitochondria. TSPO was initially designated as a peripheral-type benzodiazepine receptor, which is the binding site for benzodiazepines used to treat patients with anxiety, convulsions, or insomnia [7]. However, further research has shown that TSPO is widely expressed in most organs within the body, including the secretory and glandular tissues, kidney, heart, liver, and brain [8, 14, 15]. Its widespread distribution is consistent with its diverse

physiological functions, including membrane biogenesis, heme biosynthesis, redox balance, bioenergetics, cell proliferation, apoptosis, immunomodulation, and cholesterol binding and transport [8, 9, 16–20]. In the nervous system, TSPO has been investigated as a biomarker for various neuropathologies [21]. Recently, TSPO and its ligands have been found to be effective in neurodegeneration [22], neuroinflammation [23], and neuropathic pain [24]. These studies highlight the potential uses of TSPO and its ligands for neuroprotection, limiting neuroinflammation, promoting regeneration, and treating nervous system dysfunctions. Herein, we review the current evidence for the role of TSPO and its ligands in the development of chronic pain, including neuropathic pain, cancer pain, and inflammatory pain (Table 1) [24–26].

2. Possible Mechanisms of TSPO in Pain Processing

The mechanisms of chronic pain development involve a variety of factors, among which neuroinflammation is an important mechanism resulting in this process [8]. Glia cells, through interactions with neurons via transmitters, cytokines, or chemokines, participate in neuroinflammation [45]. In the spinal nerve ligation (SNL) model, microglia release chemokine CXC motif ligand 1 (CXCL1); its transport to neurons results in neuroinflammation, promoting the development of chronic pain [27]. After chronic complete Freund's adjuvant (CFA) injections, interleukin-6 (IL-6) released from activated astrocytes can also activate neurons by promoting neuroinflammation, resulting in chronic pain [25]. These results indicated the role of glia in neuroinflammation and chronic pain.

TSPO is upregulated concomitant with microglial activation, and strong colocalization between TSPO upregulation and activated microglia has been found during neuroinflammation in various disorders, including neurodegeneration [46], peripheral nervous system lesions [47], and brain damage [48]. Hence, TSPO has served as a marker of microglial activation and neuroinflammation and as a predictor of chronic pain in disorders like fibromyalgia [49] and neuropathic pain [33]. Recently, TSPO was reported to participant in neuropathic pain [50], and it was shown that the TSPO-positive allosteric modulator koumine alleviates inflammation and neuropathic pain by modulating microglial activation and polarization, along with astrocyte activation [30, 50]. Wei et al. [24] found that the agonistic TSPO ligands Ro5-4864 and FGIN-1-27 decrease tumor necrosis factor-α (TNF-α) levels released by spinal activated astrocytes, alleviating neuroinflammation in a rat chronic pain model. Thus, in addition to serving as a marker for activated microglia and neuroinflammation, TSPO plays a protective role in neuroinflammation, which may inhibit chronic pain.

TSPO may also participate in the development of chronic pain by mediating the synthesis of neurosteroids [51]. Neurosteroids play important roles in the structure and function of the nervous system [51], including inflammation, synaptic transmission, pain, consciousness, and cognition [52]. Numerous studies have shown that maintaining the normal structure and function of the nervous system is essential for preventing chronic pain development [11]. Neurosteroids are a class of steroid hormones that are widely distributed in the central and peripheral nervous systems [53]. TSPO transports cholesterol from the cytoplasm to the mitochondria, after which the cholesterol entering the mitochondria is catalyzed by a series of enzymes to produce steroid hormones [54]. This role of TSPO for steroid hormone synthesis is thus rate-limiting. Coronel et al. [34] found that expressions of TSPO and steroidogenic enzyme 5α reductase (I/II), which participate in steroid hormone synthesis [55], are significantly reduced and that progesterone injections reverse TSPO expression, in spinal cord injury (SCI). This demonstrated a correlation between TSPO and steroid hormone synthesis. Another group observed an increase in thalamic steroid hormone synthesis in the chronic phase of a rat pain model, which was accompanied by increased TSPO expression. Intrathalamic administration of steroid hormone, or AC-5216 (a TSPO agonist), reduced rats' pain symptoms; this effect was counteracted by administration of a TSPO inhibitor [56]. These studies suggest an inhibitory effect of steroid hormones on pain, and TSPO, as a rate-limiting enzyme for steroid hormone synthesis, may reduce pain by regulating neurosteroid synthesis (Figure 1).

3. The Role of TSPO in Chronic Pain

3.1. TSPO and Neuropathic Pain. The IASP defines neuropathic pain as pain caused by a lesion or disease of the somatosensory nervous system [57, 58]. Neuropathic pain is characterized by abnormal hypersensitivity to noxious stimuli (hyperalgesia) and abnormal pain responses to non-noxious stimuli (allodynia) [59]. A-δ fiber and C-fiber primary afferent neurons in the peripheral nervous system can transport pain signals to the central nervous system. Peripheral nerve injury (PNI) can activate sensitized neurons in these fibers. The latter also produce continuous pain stimulation signals [60], which can then transport to the dorsal horn of the spinal cord, further promoting central sensitization. Various animal models have been used to explore the mechanisms of neuropathic pain in PNI, SCI, and diabetes [61]. A growing volume of recent evidence indicates that TSPO plays a critical role in neuropathic pain.

3.1.1. TSPO and Peripheral Nerve Injury. Many studies have used animal models of PNI to explore novel strategies attenuating neuropathic pain and nerve regeneration. In early studies, TSPO improved peripheral nerve regeneration and functional recovery after nerve lesions [22, 28]. Daily intraperitoneal injections (i.p.) of etifoxine, an agonistic TSPO ligand, can promote axonal regeneration and improve functional recovery in rats with sciatic nerve injury (SNI) [22]. Another agonistic TSPO ligand, Ro5-4864, can substantially enhance adult facial motor neuron nerve regeneration and restore function after facial nerve axotomy [28]. In nerve stumps of SNI model rats, interleukin-1β (IL-1β) and IL-6 mRNA levels are significantly upregulated, while etifoxine treatment limits their increase in the proximal stumps [22].

Table 1: Role of TSPO and its ligands in chronic pain.

Model	TSPO/ligand	Mechanism	Reference(s)
SNL	TSPO	Inhibit CXCL1-CXCR2-dependent astrocyte-to-neuron signaling and central sensitization	[24, 27]
	Ro5-4864	Downregulate expression of TNF-α; alleviate mechanical allodynia and thermal hyperalgesia	[27, 28]
	FGIN-1-27	Downregulate expression of TNF-α, alleviate mechanical allodynia and thermal hyperalgesia	[27, 28]
CCI	Koumine	Downregulate the expression of TNF-α and IL-1β; inhibit microglia and astrocyte activation	[29, 30]
SNI	Ro5-4864	Downregulate the expression of p-ERK1/2 and BDNF in DRG; improve axonal regeneration and functional recovery	[31, 32]
SCI	PK11195	Assess the role of glial activation	[33]
	ZBD-2	Inhibit chronic activation of microglia and astrocytes; alleviate mechanical allodynia and thermal hyperalgesia	[34, 35]
	Progesterone	Reduce spinal expression of proinflammatory enzymes and cytokines	[36, 37]
CIBP	MZL	Inhibit the IL-6/sIL-6R trans-signaling pathway and MAPK ERK pathway; alleviate thermal hyperalgesia	[26, 38] [39, 40]
CFA-induced	TSPO	Downregulate proinflammatory mediator IL-1β expression	[41–43]
Monoarthritic model	Ro5-4864	Alleviate mechanical allodynia and thermal hyperalgesia	[41, 44]

SNL: spinal nerve ligation; CCI: chronic constriction injury; SNI: sciatic nerve injury; SCI: spinal cord injury; CIBP: cancer-induced bone pain; CFA: Complete Freund's adjuvant; TSPO: translocator protein; ZBD-2: N-benzyl-N-ethyl-2-(7,8-dihydro-7-benzyl-8-oxo-2-phenyl-9H-purin-9-yl) acetamide; MZL: midazolam; CXCL1: chemokine CXC motif ligand 1; CXCR2: chemokine CXC motif receptor 2; TNF-α: tumor necrosis factor-α; BDNF: brain-derived neurotrophic factor; DRG: dorsal root ganglion.

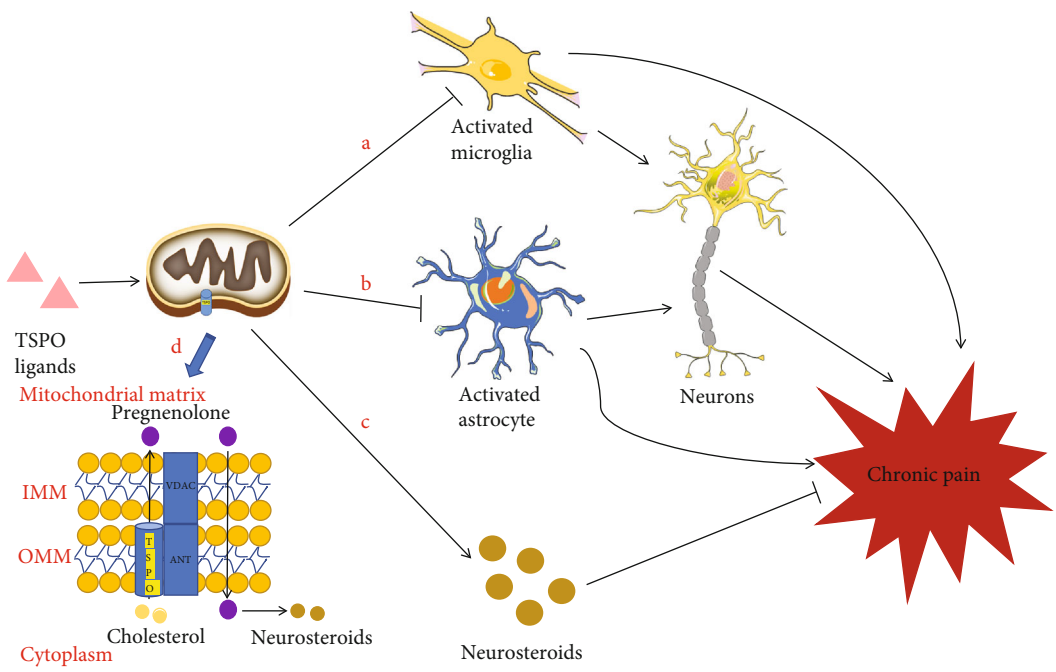

Figure 1: Mechanisms by which TSPO and its ligands inhibit chronic pain. (a, b) TSPO and its ligands inhibit microglial and astrocyte activation, thereby inhibiting activation-mediated central sensitization and chronic pain. (c) TSPO and its ligands inhibit chronic pain by mediating neurosteroid synthesis. (d) TSPO and its ligands promote cholesterol transport from the cytoplasm to the mitochondrial inner membrane, mediating progesterone synthesis and thus promoting neurosteroid synthesis. TSPO: translocator protein; IMM: inner mitochondrial membrane; OMM: outer mitochondrial membrane; VDAC: voltage-dependent anion channel; ANT: adenine nucleotide transporter.

These inflammatory cytokine changes indicate that TSPO ligands can influence inflammation in the peripheral nerve.

In recent years, investigators have focused on the role of neuroinflammation in neuropathic pain induced by PNI, many of whom have evaluated the influence of TSPO-mediated anti-inflammation in this condition. TSPO expression is significantly increased in a L5 SNL rat model [24], and a single intrathecal injection of TSPO agonist Ro5-4864 or FGIN-1-27 alleviates the established mechanical allodynia and thermal hyperalgesia. Subsequently, upregulated TSPO was decreased when neuropathic pain healed naturally followed by administration of these agonists. This phenomenon may explain that TSPO might promote recovery from a neuropathic pain state. Enzyme-linked immunosorbent assay work has revealed that increased TNF-α, a proinflammatory cytokine, in the spinal dorsal horn is suppressed after Ro5-4864 treatment. Further, early upregulation of TSPO in astrocytes of the spinal dorsal horn partly inhibit chemokine CXC motif ligand 1-chemokine CXC motif receptor 2- (CXCL1-CXCR2-) dependent astrocyte-to-neuron signaling and central sensitization, eliciting potent analgesic effects against chronic neuropathic pain induced by SNL [27]. These studies cumulatively suggest that TSPO agonists can inhibit neuroinflammation induced by proinflammatory cytokines or chemokines in a SNL model against chronic neuropathic pain.

Proinflammatory cytokines TNF-α and IL-1β participate in neuropathic pain in a chronic constriction injury (CCI) model [29]. Jin et al. [30] described TSPO's inhibitory effects on increased levels of these two proinflammatory cytokines and CCI-evoked microglial and astrocyte activation, in the spinal cord of a rat CCI model using koumine, a potential agonist. Further, TSPO was activated in neurons of the rat dorsal root ganglion (DRG) after spared nerve injury [31], and a single intrathecal injection of Ro5-4864 exerts remarkable analgesic effect in a SNI model. Western blotting shows that increased levels of phospho-extracellular signal-regulated kinase 1/2 (p-ERK1/2) and brain-derived neurotrophic factor (BDNF) in the DRG are inhibited after Ro5-4864 injection. Activation of the ERK1/2 signaling pathway and its downstream BDNF in DRG neurons also participate in the development of neuropathic pain after PNI via peripheral inflammation [32]. In that study, all increased levels of activated TSPO were suppressed or returned to normal after neuropathic pain healing, indicating that the role of TSPO upregulation may be to induce this recovery. The mechanism of its inhibition effect may be also involved in anti-neuroinflammation in PNI models (Figure 2).

3.1.2. TSPO and Spinal Cord Injury. In addition to primary motor and sensory deficits, patients suffering from SCI may experience other debilitating consequences, including neuropathic pain [62]. Neuropathic pain after SCI (SCI-associated neuropathic pain) remains difficult to treat because its mechanism is yet unclear. Microglia- or astrocyte-mediated neuroinflammation in the dorsal horn participates in the development and maintenance of neuropathic pain after SCI [63]. Many studies have used PET imaging of PK11195, which binds to TSPO, to assess the role of glial activation, including that in neuroinflammatory processes, in neuropathic pain patients [33]. Recent reports suggest that TSPO can improve chronic SCI-induced neuropathic pain [34, 35]. Li et al. found that intragastric administration of ZBD-2 (N-benzyl-N-ethyl-2-(7,8-dihydro-7-benzyl-8-oxo-2-phenyl-9H-purin-9-yl) acetamide), an agonistic TSPO ligand, markedly reduces mechanically induced allodynia and thermal hyperalgesia in a SCI model [35]. Immunohistochemistry and western blot data suggest reversed effects of ZBD-2 on chronic activation of microglia and astrocytes after SCI, further explaining the relation between TSPO and neuroinflammation.

Liu et al. [34] also found an effect of TSPO in SCI through another mechanism: the steroid hormone progesterone. This hormone activated TSPO, downregulating mechanical and thermal allodynia in a SCI model. Progesterone administration can also reduce spinal expression of proinflammatory enzymes and cytokines in chronic neuropathic pain [36, 37], suggesting a potential role of progesterone in TSPO and neuroinflammation. These findings suggest that TSPO and its ligands may be potential targets for the treatment of SCI-associated neuropathic pain.

3.2. TSPO and Cancer Pain. Chronic pain is among the most common, burdensome, and feared cancer complications [64]. Many patients with advanced cancer experience severe pain, for which adequate analgesia strategies, without unacceptable side effects, remain a clinical challenge [65, 66]. Despite concomitant neuropathic and inflammatory pain, cancer pain's additional distinctive characteristics include metastatic cancer-induced bone pain [67]. Increased attention has been paid to investigating the role of neuroinflammation in cancer pain [68]. Herein, we focus on the anti-inflammation effects of TSPO in chronic pain from bone metastasis. TSPO level is increased in both astrocytes and microglia of a rat model for bone cancer pain (BCP) [26]. Further, a single intrathecal administration of midazolam (MZL), an agonistic TSPO ligand [38], can inhibit thermal hyperalgesia in BCP rats via spinal activation of TSPO. Increased expression of the inflammatory cytokine IL-6 is decreased after MZL injection. IL-6 is considered a trigger for the initiation and maintenance of chronic pain [38]. In the BCP model, IL-6 expression increased in the DRG and spinal cord [26, 39]. Remarkably, Fang et al. attenuated bone cancer-induced hyperalgesia in BCP rats by inhibiting the IL-6/sIL-6R trans-signaling pathway, implicating IL-6 in the development of BCP [39]. Increased IL-6 expression was decreased after MZL injection, indicating that TSPO may play a protective role in bone cancer-induced inflammation. Furthermore, the spinal MAPK ERK pathway, which participates in neuroinflammation [40], was inhibited in MZL-attenuated thermal hyperalgesia in BCP rats. These changes in two inflammation mediators indicate that glial TSPO may be a potential target for bone cancer-induced neuroinflammation.

3.3. TSPO and Inflammatory Pain. Inflammatory pain is the most important clinical symptom of inflammatory diseases. It can severely impact the quality of life among patient, suffering from osteoarthritis (OA), rheumatoid arthritis, and other diseases [25]. Prolonged inflammatory pain can lead to

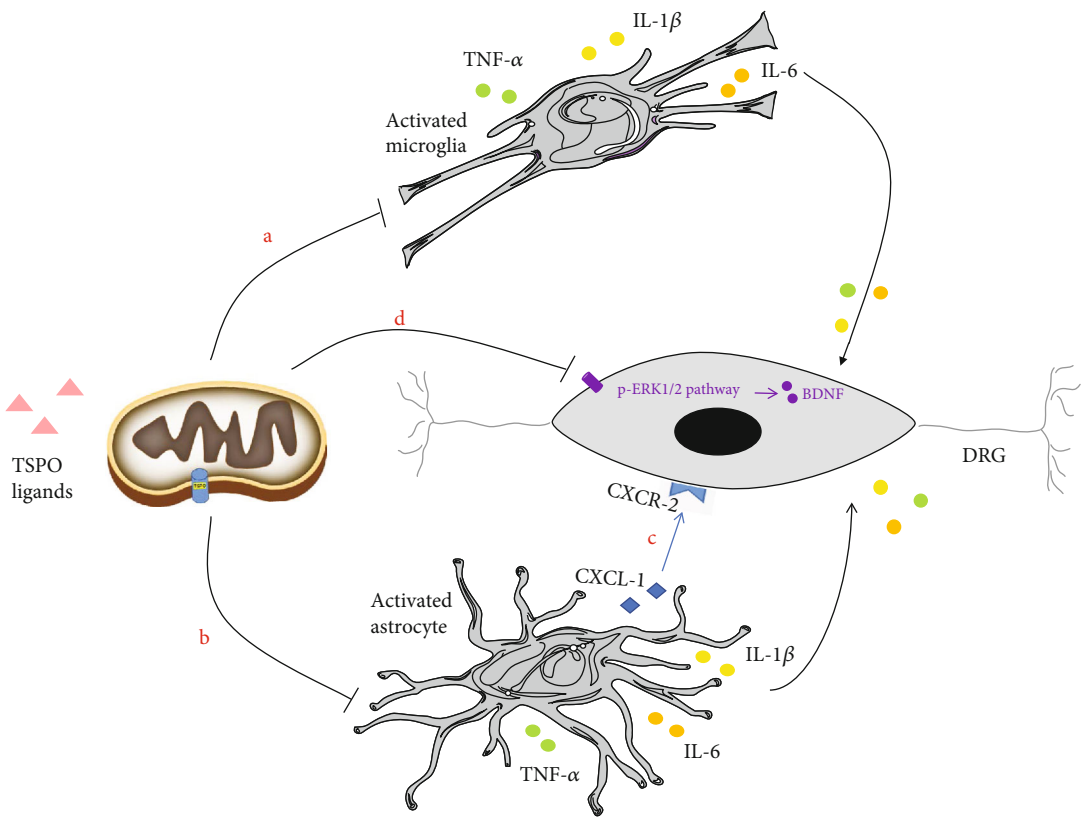

Figure 2: Molecular mechanisms by which TSPO and its ligands inhibit chronic pain induced by peripheral nerve injury. (a, b) TSPO and its ligands inhibit microglia and astrocytes to secrete inflammatory factors TNF-α, IL-1β, and IL-6. These inflammatory factors can cause neuroinflammation leading to chronic pain. (c) TSPO and its ligands inhibit CXCL1-CXCR2-dependent astrocyte-to-neuron signaling and central sensitization. (d) TSPO and its ligands inhibit the expression of the p-ERK1/2 signaling pathway and its downstream BDNF in DRG. BDNF is synthesized in DRG causing chronic pain by regulating neurotransmitter production. TNF-α: tumor necrosis factor-α; IL-1β: interleukin-1β; IL-6: interleukin-6; CXCL1: chemokine CXC motif ligand 1; CXCR2: chemokine CXC motif receptor 2; p-ERK1/2: phospho-extracellular signal-regulated kinase 1/2; BDNF: brain-derived neurotrophic factor; DRG: dorsal root ganglion.

activation of spinal microglia and astrocytes [69]. Investigators have explored whether increased TSPO can serve as a marker of nervous system activation in an OA pain model, for use in predicting development of chronic pain using novel PBR/TSPO imaging agents [70–72]. In recent animal inflammatory pain models, TSPO was identified as playing anti-inflammation and antinociception roles in chronic pain. To build a CFA-induced monoarthritic model, rats were injected with CFA into the right tibiotarsal joint [25]; intra-articular CFA injection reliably induced thermal hyperalgesia and mechanical allodynia, and spinal TSPO expression was increased in neurons, astrocytes, and microglia, implying activated nervous system activity. Furthermore, intrathecal TSPO agonist (Ro5-4864) administration dose-dependently inhibited CFA-induced mechanical allodynia and thermal hyperalgesia. A similar anti-inflammatory effect was detected in formalin-induced chronic pain and ATP-induced NLRP3 inflammasome activation [41, 44]. A previous study also found that treatment with a TSPO ligand can downregulate proinflammatory mediator IL-1β expression and activate the NLRP3 inflammasome [41]. Spinal IL-1β can play an important role in formalin- and CFA-induced inflammatory pain [42, 43]. These cumulative findings suggest that TSPO may play an anti-inflammatory effect by mediating the release of these proinflammation cytokines, exerting part of their antinociceptive effects on inflammatory pain.

4. Conclusions

In this review, we reviewed the relations between TSPO and chronic pain. Cumulative findings have clarified that TSPO plays a vital role in alleviating the initiation and maintenance of chronic pain, including neuropathic pain, inflammatory pain, and cancer pain. Although TSPO expression is increased under inflammatory conditions [73, 74], it acts as a negative regulator of inflammation [75]. In the studies described herein, expression of proinflammation factors like IL-1β, IL-6, and CXCL1 is decreased after overexpression or activation of TSPO, further validating the role of TSPO in the inhibition of the neuroinflammatory response. Although the mechanisms of TSPO's effective role in nerve diseases has been validated through clinical trials [76], the clinical effects of TSPO as an agent for alleviating chronic pain have not yet been explored. However, the preclinical TSPO studies described herein provide novel insight that may facilitate drug development to advance pain therapies. Further clinical trials will now be needed to explore the effects of TSPO treatment for pain alleviation.

Conflicts of Interest

All authors have no competing interests.

Acknowledgments

This work was supported by the Natural Science Foundation of Shandong Province (ZR2017MH066), the Weifang Science and Technology Development Program Project (No. 2019YX005), and the Shandong Medical and Health Technology Development Program (No. 202104020452).

References

[1] R. D. Treede, W. Rief, A. Barke et al., "Chronic pain as a symptom or a disease: the IASP Classification of Chronic Pain for the International Classification of Diseases (ICD-11)," *Pain*, vol. 160, no. 1, pp. 19–27, 2019.

[2] T. Abijo, K. Blum, and M. C. Gondre-Lewis, "Neuropharmacological and neurogenetic correlates of opioid use disorder (OUD) as a function of ethnicity: relevance to precision addiction medicine," *Current Neuropharmacology*, vol. 18, no. 7, pp. 578–595, 2020.

[3] D. Q. Liu, Y. Q. Zhou, and F. Gao, "Targeting cytokines for morphine tolerance: a narrative review," *Current Neuropharmacology*, vol. 17, no. 4, pp. 366–376, 2019.

[4] Y. Q. Zhou, D. Q. Liu, S. P. Chen et al., "Cellular and molecular mechanisms of calcium/calmodulin-dependent protein kinase II in chronic pain," *The Journal of Pharmacology and Experimental Therapeutics*, vol. 363, no. 2, pp. 176–183, 2017.

[5] S. Liu, Y. P. Liu, Y. Lv et al., "IL-18 contributes to bone cancer pain by regulating glia cells and neuron interaction," *The Journal of Pain*, vol. 19, no. 2, pp. 186–195, 2018.

[6] E. Coppi, F. Cherchi, E. Lucarini et al., "Uncovering the mechanisms of adenosine receptor-mediated pain control: focus on the A3 receptor subtype," *International Journal of Molecular Sciences*, vol. 22, no. 15, p. 7952, 2021.

[7] C. Braestrup and R. F. Squires, "Specific benzodiazepine receptors in rat brain characterized by high-affinity (3H) diazepam binding," *Proceedings of the National Academy of Sciences of the United States of America*, vol. 74, no. 9, pp. 3805–3809, 1977.

[8] V. Papadopoulos, M. Baraldi, T. R. Guilarte et al., "Translocator protein (18 kDa): new nomenclature for the peripheral-type benzodiazepine receptor based on its structure and molecular function," *Trends in Pharmacological Sciences*, vol. 27, no. 8, pp. 402–409, 2006.

[9] L. J. Motloch, J. Hu, and F. G. Akar, "The mitochondrial translocator protein and arrhythmogenesis in ischemic heart disease," *Oxidative Medicine and Cellular Longevity*, vol. 2015, Article ID 234104, 8 pages, 2015.

[10] M. W. McEnery, A. M. Snowman, R. R. Trifiletti, and S. H. Snyder, "Isolation of the mitochondrial benzodiazepine receptor: association with the voltage-dependent anion channel and the adenine nucleotide carrier," *Proceedings of the National Academy of Sciences of the United States of America*, vol. 89, no. 8, pp. 3170–3174, 1992.

[11] M. Garnier, A. B. Dimchev, N. Boujrad, J. M. Price, N. A. Musto, and V. Papadopoulos, "In vitro reconstitution of a functional peripheral-type benzodiazepine receptor from mouse Leydig tumor cells," *Molecular Pharmacology*, vol. 45, no. 2, pp. 201–211, 1994.

[12] L. Veenman, Y. Shandalov, and M. Gavish, "VDAC activation by the 18 kDa translocator protein (TSPO), implications for apoptosis," *Journal of Bioenergetics and Biomembranes*, vol. 40, no. 3, pp. 199–205, 2008.

[13] J. Gatliff and M. Campanella, "TSPO: kaleidoscopic 18-kDa amid biochemical pharmacology, control and targeting of mitochondria," *The Biochemical Journal*, vol. 473, no. 2, pp. 107–121, 2016.

[14] A. Batarseh and V. Papadopoulos, "Regulation of translocator protein 18 kDa (TSPO) expression in health and disease states," *Molecular and Cellular Endocrinology*, vol. 327, no. 1-2, pp. 1–12, 2010.

[15] C. Giatzakis and V. Papadopoulos, "Differential utilization of the promoter of peripheral-type benzodiazepine receptor by steroidogenic versus nonsteroidogenic cell lines and the role of Sp1 and Sp3 in the regulation of basal activity," *Endocrinology*, vol. 145, no. 3, pp. 1113–1123, 2004.

[16] D. Morin, J. Musman, S. Pons, A. Berdeaux, and B. Ghaleh, "Mitochondrial translocator protein (TSPO): from physiology to cardioprotection," *Biochemical Pharmacology*, vol. 105, pp. 1–13, 2016.

[17] J. P. Faure, H. Baumert, Z. Han et al., "Evidence for a protective role of trimetazidine during cold ischemia: targeting inflammation and nephron mass," *Biochemical Pharmacology*, vol. 66, no. 11, pp. 2241–2250, 2003.

[18] S. Taketani, H. Kohno, M. Okuda, T. Furukawa, and R. Tokunaga, "Induction of peripheral-type benzodiazepine receptors during differentiation of mouse erythroleukemia cells. A possible involvement of these receptors in heme biosynthesis," *The Journal of Biological Chemistry*, vol. 269, no. 10, pp. 7527–7531, 1994.

[19] S. R. Torres, T. S. Fröde, G. M. Nardi et al., "Anti-inflammatory effects of peripheral benzodiazepine receptor ligands in two mouse models of inflammation," *European Journal of Pharmacology*, vol. 408, no. 2, pp. 199–211, 2000.

[20] A. A. Yeliseev and S. Kaplan, "TspO of *Rhodobacter sphaeroides*," *The Journal of Biological Chemistry*, vol. 275, no. 8, pp. 5657–5667, 2000.

[21] R. Rupprecht, V. Papadopoulos, G. Rammes et al., "Translocator protein (18 kDa) (TSPO) as a therapeutic target for neurological and psychiatric disorders," *Nature Reviews. Drug Discovery*, vol. 9, no. 12, pp. 971–988, 2010.

[22] C. Girard, S. Liu, F. Cadepond et al., "Etifoxine improves peripheral nerve regeneration and functional recovery," *Proceedings of the National Academy of Sciences of the United States of America*, vol. 105, no. 51, pp. 20505–20510, 2008.

[23] J. W. Lee, H. Nam, and S. W. Yu, "Systematic analysis of translocator protein 18 kDa (TSPO) ligands on toll-like receptors-mediated pro-inflammatory responses in microglia and astrocytes," *Experimental Neurobiology*, vol. 25, no. 5, pp. 262–268, 2016.

[24] X. H. Wei, X. Wei, F. Y. Chen et al., "The upregulation of translocator protein (18 kDa) promotes recovery from neuropathic pain in rats," *The Journal of Neuroscience*, vol. 33, no. 4, pp. 1540–1551, 2013.

[25] H. Hernstadt, S. Wang, G. Lim, and J. Mao, "Spinal translocator protein (TSPO) modulates pain behavior in rats with CFA-induced monoarthritis," *Brain Research*, vol. 1286, pp. 42–52, 2009.

[26] C. H. Guo, L. Bai, H. H. Wu et al., "Midazolam and ropivacaine act synergistically to inhibit bone cancer pain with

different mechanisms in rats," *Oncology Reports*, vol. 37, no. 1, pp. 249–258, 2017.

[27] X. Liu, H. Liu, S. Xu et al., "Spinal translocator protein alleviates chronic neuropathic pain behavior and modulates spinal astrocyte-neuronal function in rats with L5 spinal nerve ligation model," *Pain*, vol. 157, no. 1, pp. 103–116, 2016.

[28] C. Mills, M. Makwana, A. Wallace et al., "Ro5-4864 promotes neonatal motor neuron survival and nerve regeneration in adult rats," *The European Journal of Neuroscience*, vol. 27, no. 4, pp. 937–946, 2008.

[29] L. W. Chu, K. I. Cheng, J. Y. Chen et al., "Loganin prevents chronic constriction injury-provoked neuropathic pain by reducing TNF-α/IL-1β-mediated NF-κB activation and Schwann cell demyelination," *Phytomedicine*, vol. 67, article 153166, 2020.

[30] G. L. Jin, S. D. He, S. M. Lin et al., "Koumine attenuates neuroglia activation and inflammatory response to neuropathic pain," *Neural Plasticity*, vol. 2018, Article ID 9347696, 13 pages, 2018.

[31] B. Ma, X. Liu, X. Huang, Y. Ji, T. Jin, and K. Ma, "Translocator protein agonist Ro5-4864 alleviates neuropathic pain and promotes remyelination in the sciatic nerve," *Molecular Pain*, vol. 14, p. 174480691774801, 2018.

[32] K. Obata, H. Yamanaka, Y. Dai et al., "Differential activation of MAPK in injured and uninjured DRG neurons following chronic constriction injury of the sciatic nerve in rats," *The European Journal of Neuroscience*, vol. 20, no. 11, pp. 2881–2895, 2004.

[33] N. Imamoto, S. Momosaki, M. Fujita et al., "[^{11}C]PK11195 PET imaging of spinal glial activation after nerve injury in rats," *NeuroImage*, vol. 79, pp. 121–128, 2013.

[34] M. F. Coronel, M. L. S. Granel, M. C. Raggio et al., "Temporal changes in the expression of the translocator protein TSPO and the steroidogenic enzyme 5α-reductase in the dorsal spinal cord of animals with neuropathic pain: effects of progesterone administration," *Neuroscience Letters*, vol. 624, pp. 23–28, 2016.

[35] X. M. Li, J. Meng, L. T. Li et al., "Effect of ZBD-2 on chronic pain, depressive-like behaviors, and recovery of motor function following spinal cord injury in mice," *Behavioural Brain Research*, vol. 322, pp. 92–99, 2017.

[36] M. F. Coronel, F. Labombarda, A. F. De Nicola, and S. L. Gonzalez, "Progesterone reduces the expression of spinal cyclooxygenase-2 and inducible nitric oxide synthase and prevents allodynia in a rat model of central neuropathic pain," *European Journal of Pain*, vol. 18, no. 3, pp. 348–359, 2014.

[37] M. F. Coronel, M. C. Raggio, N. S. Adler, A. F. De Nicola, F. Labombarda, and S. L. Gonzalez, "Progesterone modulates pro-inflammatory cytokine expression profile after spinal cord injury: implications for neuropathic pain," *Journal of Neuroimmunology*, vol. 292, pp. 85–92, 2016.

[38] K. Tanabe, O. Kozawa, and H. Iida, "Midazolam suppresses interleukin-1β-induced interleukin-6 release from rat glial cells," *Journal of Neuroinflammation*, vol. 8, no. 1, p. 68, 2011.

[39] D. Fang, L. Y. Kong, J. Cai et al., "Interleukin-6-mediated functional upregulation of TRPV1 receptors in dorsal root ganglion neurons through the activation of JAK/PI3K signaling pathway: roles in the development of bone cancer pain in a rat model," *Pain*, vol. 156, no. 6, pp. 1124–1144, 2015.

[40] J. H. Park, Y. H. Seo, J. H. Jang, C. H. Jeong, S. Lee, and B. Park, "Asiatic acid attenuates methamphetamine-induced neuroinflammation and neurotoxicity through blocking of NF-kB/STAT3/ERK and mitochondria-mediated apoptosis pathway," *Journal of Neuroinflammation*, vol. 14, no. 1, p. 240, 2017.

[41] J. W. Lee, L. E. Kim, H. J. Shim et al., "A translocator protein 18 kDa ligand, Ro5-4864, inhibits ATP-induced NLRP3 inflammasome activation," *Biochemical and Biophysical Research Communications*, vol. 474, no. 3, pp. 587–593, 2016.

[42] L. R. Watkins, D. Martin, P. Ulrich, K. J. Tracey, and S. F. Maier, "Evidence for the involvement of spinal cord glia in subcutaneous formalin induced hyperalgesia in the rat," *Pain*, vol. 71, no. 3, pp. 225–235, 1997.

[43] A. Gajtko, E. Bakk, K. Hegedus, L. Ducza, and K. Hollo, "IL-1β induced cytokine expression by spinal astrocytes can play a role in the maintenance of chronic inflammatory pain," *Frontiers in Physiology*, vol. 11, article 543331, 2020.

[44] S. DalBo, G. M. Nardi, P. Ferrara, R. M. Ribeiro-do-Valle, and R. C. Farges, "Antinociceptive effects of peripheral benzodiazepine receptors," *Pharmacology*, vol. 70, no. 4, pp. 188–194, 2004.

[45] B. Becher, S. Spath, and J. Goverman, "Cytokine networks in neuroinflammation," *Nature Reviews. Immunology*, vol. 17, no. 1, pp. 49–59, 2017.

[46] H. Wilms, J. Claasen, C. Röhl, J. Sievers, G. Deuschl, and R. Lucius, "Involvement of benzodiazepine receptors in neuroinflammatory and neurodegenerative diseases: evidence from activated microglial cells in vitro," *Neurobiology of Disease*, vol. 14, no. 3, pp. 417–424, 2003.

[47] T. Bordet, B. Buisson, M. Michaud et al., "Specific antinociceptive activity of cholest-4-en-3-one, oxime (TRO19622) in experimental models of painful diabetic and chemotherapy-induced neuropathy," *The Journal of Pharmacology and Experimental Therapeutics*, vol. 326, no. 2, pp. 623–632, 2008.

[48] V. Papadopoulos and L. Lecanu, "Translocator protein (18 kDa) TSPO: an emerging therapeutic target in neurotrauma," *Experimental Neurology*, vol. 219, no. 1, pp. 53–57, 2009.

[49] E. Kosek, S. Martinsen, B. Gerdle et al., "The translocator protein gene is associated with symptom severity and cerebral pain processing in fibromyalgia," *Brain, Behavior, and Immunity*, vol. 58, pp. 218–227, 2016.

[50] B. Xiong, G. Jin, Y. Xu et al., "Identification of koumine as a translocator protein 18 kDa positive allosteric modulator for the treatment of inflammatory and neuropathic pain," *Frontiers in Pharmacology*, vol. 12, article 692917, 2021.

[51] E. Lloyd-Evans and H. Waller-Evans, "Biosynthesis and signalling functions of central and peripheral nervous system neurosteroids in health and disease," *Essays in Biochemistry*, vol. 64, no. 3, pp. 591–606, 2020.

[52] V. Sheibani, M. A. Rajizadeh, M. A. Bejeshk et al., "The effects of neurosteroid allopregnanolone on synaptic dysfunction in the hippocampus in experimental parkinsonism rats: an electrophysiological and molecular study," *Neuropeptides*, vol. 92, article 102229, 2022.

[53] D. S. Reddy, "Role of anticonvulsant and antiepileptogenic neurosteroids in the pathophysiology and treatment of epilepsy," *Frontiers in Endocrinology*, vol. 2, article 38, 2011.

[54] V. Papadopoulos, J. Liu, and M. Culty, "Is there a mitochondrial signaling complex facilitating cholesterol import?," *Molecular and Cellular Endocrinology*, vol. 265, pp. 59–64, 2007.

[55] D. Matsui, M. Sakari, T. Sato et al., "Transcriptional regulation of the mouse steroid 5alpha-reductase type II gene by

progesterone in brain," *Nucleic Acids Research*, vol. 30, no. 6, pp. 1387–1393, 2002.

[56] M. Zhang, J. Liu, M. M. Zhou et al., "Elevated neurosteroids in the lateral thalamus relieve neuropathic pain in rats with spared nerve injury," *Neuroscience Bulletin*, vol. 32, no. 4, pp. 311–322, 2016.

[57] N. B. Finnerup, R. Kuner, and T. S. Jensen, "Neuropathic pain: from mechanisms to treatment," *Physiological Reviews*, vol. 101, no. 1, pp. 259–301, 2021.

[58] IASP IASP, "Taxonomy," 2019https://www.iasp-pain.org/terminology?navItemNumber=576.

[59] E. Cavalli, S. Mammana, F. Nicoletti, P. Bramanti, and E. Mazzon, "The neuropathic pain: an overview of the current treatment and future therapeutic approaches," *International Journal of Immunopathology and Pharmacology*, vol. 33, article 205873841983838, 2019.

[60] J. N. Campbell and R. A. Meyer, "Mechanisms of neuropathic pain," *Neuron*, vol. 52, no. 1, pp. 77–92, 2006.

[61] Y. Q. Zhou, Z. Liu, Z. H. Liu et al., "Interleukin-6: an emerging regulator of pathological pain," *Journal of Neuroinflammation*, vol. 13, no. 1, pp. 1–9, 2016.

[62] R. Shiao and C. A. Lee-Kubli, "Neuropathic pain after spinal cord injury: challenges and research perspectives," *Neurotherapeutics*, vol. 15, no. 3, pp. 635–653, 2018.

[63] J. Y. Lee, H. Y. Choi, B. G. Ju, and T. Y. Yune, "Estrogen alleviates neuropathic pain induced after spinal cord injury by inhibiting microglia and astrocyte activation," *Biochimica et Biophysica Acta - Molecular Basis of Disease*, vol. 1864, no. 7, pp. 2472–2480, 2018.

[64] G. Deng, "Integrative medicine therapies for pain management in cancer patients," *Cancer Journal*, vol. 25, no. 5, pp. 343–348, 2019.

[65] S. Liu, W. T. Liu, Y. P. Liu et al., "Blocking EphB1 receptor forward signaling in spinal cord relieves bone cancer pain and rescues analgesic effect of morphine treatment in rodents," *Cancer Research*, vol. 71, no. 13, pp. 4392–4402, 2011.

[66] S. A. Schug and C. Chandrasena, "Pain management of the cancer patient," *Expert Opinion on Pharmacotherapy*, vol. 16, no. 1, pp. 5–15, 2015.

[67] R. M. Fink and E. Gallagher, "Cancer pain assessment and measurement," *Seminars in Oncology Nursing*, vol. 35, no. 3, pp. 229–234, 2019.

[68] Y. Q. Zhou, Z. Liu, H. Q. Liu et al., "Targeting glia for bone cancer pain," *Expert Opinion on Therapeutic Targets*, vol. 20, no. 11, pp. 1365–1374, 2016.

[69] F. I. F. Gomes, F. Q. Cunha, and T. M. Cunha, "Peripheral nitric oxide signaling directly blocks inflammatory pain," *Biochemical Pharmacology*, vol. 176, article 113862, 2020.

[70] V. Palada, A. Siddiqah Ahmed, A. Hugo, M. R. Radojcic, C. I. Svensson, and E. Kosek, "Expression of mitochondrial TSPO and FAM173B is associated with inflammation and symptoms in patients with painful knee osteoarthritis," *Rheumatology (Oxford, England)*, vol. 60, no. 4, pp. 1724–1733, 2021.

[71] T. R. Miller, J. B. Wetter, M. F. Jarvis, and R. S. Bitner, "Spinal microglial activation in rat models of neuropathic and osteoarthritic pain: an autoradiographic study using [3H]PK11195," *European Journal of Pain*, vol. 17, no. 5, pp. 692–703, 2013.

[72] Z. Hou, Q. Wang, Z. Guo et al., "Gadolinium-conjugated CB86: a novel TSPO-targeting MRI contrast agent for imaging of rheumatoid arthritis," *Journal of Drug Targeting*, vol. 28, no. 4, pp. 398–407, 2020.

[73] M. K. Chen and T. R. Guilarte, "Translocator protein 18 kDa (TSPO): molecular sensor of brain injury and repair," *Pharmacology & Therapeutics*, vol. 118, no. 1, pp. 1–17, 2008.

[74] Q. Lv, D. Xu, J. Ma et al., "Uric acid drives intestinal barrier dysfunction through TSPO-mediated NLRP3 inflammasome activation," *Inflammation Research*, vol. 70, no. 1, pp. 127–137, 2021.

[75] K. R. Bae, H. J. Shim, D. Balu, S. R. Kim, and S. W. Yu, "Translocator protein 18 kDa negatively regulates inflammation in microglia," *Journal of Neuroimmune Pharmacology*, vol. 9, no. 3, pp. 424–437, 2014.

[76] J. Gong, E. M. Szego, A. Leonov et al., "Translocator protein ligand protects against neurodegeneration in the MPTP mouse model of Parkinsonism," *The Journal of Neuroscience*, vol. 39, no. 19, pp. 3752–3769, 2019.

Hindawi
Neural Plasticity
Volume 2022, Article ID 6131696, 11 pages
https://doi.org/10.1155/2022/6131696

Review Article

The Effectiveness of High-Frequency Repetitive Transcranial Magnetic Stimulation on Patients with Neuropathic Orofacial Pain: A Systematic Review of Randomized Controlled Trials

Yingxiu Diao,[1,2] **Yuhua Xie**,[1,2] **Jiaxin Pan**,[2,3] **Manxia Liao**,[3] **Hao Liu**,[3] **and Linrong Liao**[1]

[1]*Rehabilitation Medicine Center, The First Dongguan Affiliated Hospital, Guangdong Medical University, Dongguan, Guangdong 523710, China*
[2]*School of Rehabilitation Medicine, Gannan Medical University, Ganzhou, Jiangxi 341000, China*
[3]*Department of Rehabilitation, Yixing JORU Rehabilitation Hospital, Wuxi, Jiangsu 214200, China*

Correspondence should be addressed to Hao Liu; liuhao0909@163.com and Linrong Liao; lr-liao@126.com

Received 27 April 2022; Revised 23 June 2022; Accepted 5 August 2022; Published 24 August 2022

Academic Editor: Hao-Yu Hu

Background. Repetitive transcranial magnetic stimulation (rTMS) has been widely used in the treatment of neuropathic orofacial pain (NOP). The consistency of its therapeutic efficacy with the optimal protocol is highly debatable. *Objective*. To assess the effectiveness of rTMS on pain intensity, psychological conditions, and quality of life (QOL) in individuals with NOP based on randomized controlled trials (RCTs). *Methods*. We carefully screened and browsed 5 medical databases from inception to January 1, 2022. The study will be included that use of rTMS as the intervention for patients with NOP. Two researchers independently completed record retrieval, data processing, and evaluation of methodological quality. Quality and evidence were assessed using the PEDro scores and the Grading of Recommendations Assessment, Development, and Evaluation (GRADE) system. *Results*. Six RCTs with 214 participants were included in this systematic review: 2 studies were considered level 1 evidence, and 4 were considered level 2 evidence. Six studies found that high-frequency rTMS had a pain-relieving effect, while 4 studies found no improvement in psychological conditions and QOL. Quality of evidence (GRADE system) ranged from moderate to high. No significant side effects were found. *Conclusions*. There is moderate-to-high evidence to prove that high-frequency rTMS is effective in reducing pain in individuals with NOP, but it has no significant positive effect on psychological conditions and QOL. High-frequency rTMS can be used as an alternative treatment for pain in individuals with NOP, but further studies will be conducted to unify treatment parameters, and the sample size will be expanded to explore its influence on psychological conditions and QOL.

1. Introduction

Neuropathic orofacial pain (NOP) is a specific neurological disorder, usually caused by the somatosensory nervous system or related disorders [1]. NOP mainly affects women over the age of 50 years old [2]. The prevalence varies from 0.03% to 0.5%, depending on the type and characteristics of the disease [3, 4]. The diagnosis of NOP requires the history of peripheral nervous system injury and the distribution of neuroanatomy pain. This disease exists in several specific forms, including pathologies such as atypical facial pain (AFP), burning mouth syndrome (BMS) (also known as glossodynia), trigeminal neuralgia (TN), persistent idiopathic facial pain (PIFP), and postherpetic neuralgia (PHN) [5]. NOP belongs to chronic peripheral neuropathic pain, involving a variety of neurotransmitters and mechanisms. Pain conditions in the mouth and face can interfere with activities of daily living and interfere with communication, eating, and other pleasures of social life, which can result in patients being isolated by society [6]. This kind of disease is relatively common in life, and it not only

brings a great economic burden to the patient's family but also affects the patient's physical and psychological health. NOP can be treated with minimally invasive therapy [7], surgery [8], and adjuvant analgesics [9], but people tend to be more receptive to treatments that are noninvasive and nondrug dependent [10]. In the vast majority of cases, neuropathic pain is not satisfactorily treated with traditional analgesics and is often resistant to opioids, so most patients are reluctant to receive such treatment [11].

With the development of high technology and highly evidence-based medicine, noninvasive and painless neuromodulation techniques have received more attention and research in recent years. Repetitive transcranial magnetic stimulation (rTMS) is a noninvasive neuromodulation technique that delivers focal stimulation to an individual's brain using locally pulsed magnetic fields [12, 13]. rTMS has various output forms and stimulation modes, each with different characteristics and applications [14, 15]. Theta burst stimulation (TBS), as a treatment mode of rTMS, has also been widely used in the treatment of NOP [16–18]. There are many subtypes of NOP, and pain and other uncomfortable symptoms are mainly confined around the mouth and face. rTMS produces analgesic effects through different mechanisms in the treatment [19–22]. Due to the diversity and complexity of NOP patients, the efficacy of rTMS for NOP is still controversial [13, 23, 24] because the stimulation site, frequency, intensity, and course of rTMS treatment of NOP are not standardized and unified. According to previous studies [18, 25], NOP is the disease that benefits most from rTMS treatment in the motor cortex. Although there have been reviews evaluating the efficacy of rTMS for NOP patients, there have been no comprehensive evaluations specifically for NOP.

Since rTMS has been widely used to treat different types of pain, it is urgent to explore whether rTMS is safe and effective in patients with NOP [26]. Therefore, the primary objective of this systematic review was to evaluate the effectiveness of rTMS on pain intensity, psychological conditions, and QOL in individuals with NOP. The secondary objective was to review the selection of rTMS parameters for patients with different types of NOP.

2. Materials and Methods

2.1. Study Design and Registration. This research was performed according to the *Cochrane Handbook* [27]. The protocol for this systematic review was registered at the PROSPERO (CRD42021254738). This systematic review is based on RCTs to measure the effectiveness of rTMS in the treatment of NOP symptoms. The participant, intervention, comparison, and outcome (PICO) [28, 29] principle was adopted in this research. It follows the preferred reporting items for systematic reviews and meta-analyses (PRISMA) [30].

2.2. Research Question. In this systematic review, patients were divided into the real stimulation group and sham stimulation group, and different parameters of rTMS were used. The physical manifestations of patients were compared. Therefore, this systematic review mainly answers the following two questions. Is rTMS in the experimental group more effective than that in the sham stimulation group in improving the pain, psychological conditions, and QOL of patients with NOP? Are there differences in the selection of rTMS parameters and treatment sites among NOP patients with different symptoms?

2.3. Search Strategy. Two researchers (YXD and YHX) independently conducted database searches in PubMed, Embase, Web of Science, Physiotherapy Evidence Database (PEDro), and Cochrane Library to review the titles and abstracts of the retrieved articles to identify articles that meet the criteria and to qualify studies of rTMS in the treatment of NOP from database establishment to publication on January 1, 2022. English language restrictions were applied, and the search terms for each database were slightly modified. Combined medical terms were searched as follows: ("Transcranial Magnetic Stimulation" OR "TMS") AND ("Neuropathic orofacial pain" OR "Facial pain" OR "Face pain" OR "Trigeminal Neuralgia" OR "Burning mouth syndrome" OR "Persistent idiopathic facial pain" OR "postherpetic neuralgia").

2.4. Study Selection. The entire screening process was completed by two reviewers (YXD and YHX). Eligible articles were published in English. Only RCTs of intervening NOP with rTMS were included in this systematic review. In addition, references to related articles were reviewed to facilitate the search for other research studies. All RCTs involved rTMS for patients with different types of NOP: BMS, PIFP, AFP, TN, and PHN. Interventions included rTMS, and control groups included sham rTMS interventions or placebo controls. All existing disagreements were discussed through a meeting, and then a consensus was reached. The effects of rTMS on pain intensity, QOL, and psychological conditions in individuals with NOP were evaluated using the following outcome indicators. The Visual Analogue Scale (VAS) is primarily used to measure pain intensity [31]. Psychological conditions were assessed by the Self-rating Depression Scale (SDS), Beck Anxiety Inventory (BAI), Beck Depression Inventory (BDI), and other scales, and QOL was assessed by sleep quality (SQ), 36-Item Short-Form Health Survey (SF-36), and other tools.

Exclusion criteria were as follows: (1) rTMS in combination with other interventions; (2) incomplete data or inability to obtain full-text literature; (3) conference reviews, meta-analyses, letters, or case reports; (4) animal experiments; and (5) non-English literature.

2.5. Data Extraction. The first author (YXD) analyzed and summarized the characteristics and effects of rTMS on NOP, and then two co-authors (YXD and YHX) further evaluated the accuracy of the extracted data. Differences between the two will be settled by one of the corresponding authors (HL). Relevant information was extracted for each study as follows: article title, authors' names, publication date, number of participants, type of treatment, mean age of participants, inclusion and exclusion criteria of participants, outcome measures, adverse events, study findings, and conclusions.

2.6. Risk-of-Bias Assessment in Included Studies. The selected study was rigorously evaluated using the PEDro scale (PEDro scores of 0–3, 4–5, 6–8, and 9–10 were considered to indicate

"poor," "fair," "good," and "excellent" quality) [32]. The PEDro scale provides a more scientific measure of methodological quality. Studies using a PEDro rating of good or excellent with a sample size of >50 are considered level 1 evidence, and studies of lower quality are considered level 2 evidence (fair or poor by PEDro with a sample size of ≤50). The quality of the evidence was assessed by using the GRADE system [33], which uses the domains of study limitations, indirectness, inconsistency, and imprecision in results, and was assessed as "high," "moderate," "low," or "very low" [34]. The recommendation strength is divided into two levels: strong recommendation and weak recommendation, and symbols for description are provided. It identified five categories of problems affecting the quality of evidence, including risk of bias, inaccuracy, inconsistency, indirectness, and publication bias.

2.7. Data Synthesis and Analysis. The data and characteristics of rTMS on NOP were summarized by the first author (YXD), and the accuracy of the included data was checked by the next two authors (YHX and MXL). Disagreements were resolved by discussion with the principal investigator (LRL) until a consensus was reached. Data on other indicators were also summarized to describe the effects of the intervention. We summarized the relevant data characteristics of rTMS, such as parameters of different frequencies, intensities, and pulse times, as well as different stimulation sites and parameter selection, and summarized the characteristics of rTMS on NOP patients. In this systematic review, patients with BMS, PIFP, AFP, TN, and PHN of different amounts were summarized as NOP, and the effectiveness of rTMS was explored by integrating rTMS data and stimulating sites in patients with different types of NOP. Ultimately, no meta-analysis was performed because the heterogeneity of the studies was too great. Therefore, we present the summarized data as a systematic review.

3. Results

3.1. Study Selection. The retrieval strategy identified a total of 1973 articles and 12 additional records identified through other sources. There were still 1427 articles left after removing duplicate items, and 1373 studies were excluded after screening of study titles and abstracts for the following reasons: evaluation of symptoms involving different pathologies and populations different from NOP, systematic reviews, conference abstracts, non-English literature, animal studies, and publications where full texts and data are not available. Subsequently, by full content screening out of 54 RCTs, after assessing their eligibility, 6 RCTs remained. Figure 1 shows a more detailed description of the literature screening process using the PRISMA flow chart, and six RCTs [18, 25, 35–38] were considered eligible for inclusion in this systematic review.

3.2. Methodological Quality Assessment. We could search the Physiotherapy Evidence Database website for PEDro scores included in the studies, but we found that none were registered on it. Thus, this systematic review was reviewed and scored independently by two researchers (YXD and JXP). The differences between the two were resolved by another researcher (HL). Ultimately, six trials reported concealed allocation: three of the studies [18, 25, 35] were double-blind, two studies [36, 38] were single-blind, and the other study [37] did not specify what type of blindness was used (Table 1). Overall, only two studies [25, 35] were considered level 1 evidence (PEDro score ≥ 6 and sample size > 50) and four [18, 36–38] were considered level 2 evidence due to differences in sample sizes. The grading of evidence for each study is summarized in Table 2, and all studies were rated as medium-to-high quality.

3.3. Study Characteristics. After strict literature screening and scientific quality evaluation processing, 6 RCTs [18, 25, 35–38] were chosen for this systematic review and these studies were published between 2013 and 2019. The characteristics among which patients have NOP are summarized in Table 3, and the main characteristics of rTMS are summarized in Table 4. Three studies [18, 35, 36] of patients with multiple types of NOP were included. Due to the complexity of the patients, they were uniformly summarized as NOP patients. There were two studies in patients with PHN [25, 37] and one in patients with BMS [38]. Their pain lasts for at least six months and up to 30 years. The coil types used in the rTMS were the figure-of-eight coil [36, 38] and round coil [37]. All included rTMS were high-frequency stimulation, and other related parameters are obtained, such as the intertrain interval (ITI), motor threshold (MT), and total number of pulses. The systematic review provided data on 214 patients who were followed multiple times by evaluators. All the patients included had problems of varying degrees, such as pain, depression, and sleep disorders.

3.4. Participants. A total of 214 NOP patients were included in the 6 studies [18, 25, 35–38]. Since the diagnosis types of patients in the 3 studies were not clear [18, 35, 36], the number of each category of NOP patients could not be determined. Ninety-four patients were enrolled in the three studies with orofacial pain duration ranging from one month to 30 years [18, 35, 36]. 100 patients were diagnosed with PHN [25, 37]: 60 in the experimental group and 40 in the nonintervening group, and all patients with PHN had pain lasting more than six months. Among the 16 patients included in the study of Shamseer et al. [28], 4 patients had AFP, 5 patients had BMS, and 7 patients had TN. Most of the patients suffered from intractable pharmacotherapy pain with an average period of pain exceeding six months. The specific number of male and female patients in the experimental group and control group could not be determined, but there were 14 female patients and 2 male patients. Since precise data on the number of gender in the nonintervening group could not be obtained from the study of Cumpston et al. [27], it was impossible to judge the ratio of men and women in the control group. Overall, there were significantly more women in the study than men.

3.5. Interventions. In six studies, rTMS targeted the primary motor cortex (M1) [18, 25, 37], left dorsolateral prefrontal cortex (DLPFC) [38], primary sensory cortex (S1) [36], and secondary somatosensory cortex (S2) [36] in patients with NOP. Six studies included five [25, 35–38] high-

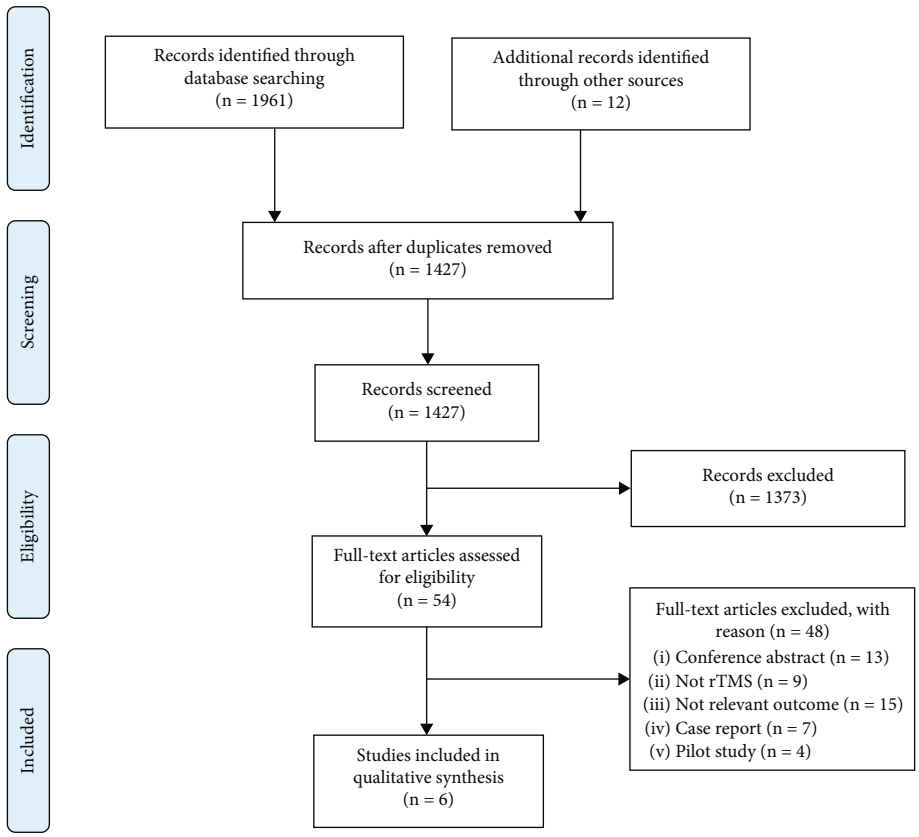

Figure 1: PRISMA flow diagram.

Table 1: Rating of the PEDro scale and level of evidence.

Study criteria	Fricová et al. [35]	Lindholm et al. [36]	Ma et al. [37]	Umezaki et al. [38]	Kohútová et al. [18]	Pei et al. [25]
Eligibility criteria	Yes	Yes	Yes	Yes	Yes	Yes
Random allocation	1	1	1	1	1	1
Concealed allocation	1	1	1	1	1	1
Baseline comparability	1	1	1	1	1	1
Blinded participants	1	0	0	0	1	1
Blinded therapists	1	1	0	1	1	1
Blinded assessors	0	0	0	0	0	0
Adequate follow-up	1	0	1	1	1	0
Intention-to-treat analysis	1	1	1	1	1	1
Between-group comparisons	1	1	1	1	1	1
Point estimates and variability	1	1	1	1	1	1
Total PEDro score	9	7	7	8	9	8
Sample size ≥ 50	Yes	No	No	No	No	Yes
Level of evidence	1	2	2	2	2	1

frequency (5-20 Hz) rTMS treatments and one TBS [18] treatment at 50 Hz, and the control group used sham stimulation or rTMS at different frequencies. Fricová et al. [35] treated NOP patients with 20 Hz and 10 Hz rTMS by stimulating the body part of the contralateral motor cortex that corresponds to the location of the pain and comparing the two parameters at different frequencies to see if symptoms improved. It received five sessions (applications) continuously during working days (days 1-5). Lindholm et al. [36] used a frequency of 10 Hz to intervene in the three targets of patients (M1, S1, and S2) to observe which one could alleviate chronic drug-resistant NOP to the greatest extent and concluded that the right S2 is a promising new target. The stimulation was given in trains of 50 pulses at 10-second intervals and a 15-minute break. The same rTMS parameters were used for PHN in both studies [25, 37] with a frequency

Table 2: Grading of Recommendations Assessment, Development, and Evaluation (GRADE) quality of evidence.

Outcome	Number of studies	Design	Study limitations	Inconsistency	Indirectness	Imprecision	Publication bias	Effect size	GRADE quality	Symbolic expression
Pain intensity: VAS or NRS	6	RCT	0	0	0	0	0	0	High	⨁⨁⨁⨁
Psychological conditions: BDI or SDS	4	RCT	0	0	0	-1*	0	0	Moderate	⨁⨁⨁⊖
Quality of life: QOL or SQ	3	RCT	0	0	0	-1*	0	0	Moderate	⨁⨁⨁⊖
Sensory testing: QST	2	RCT	0	0	0	-1*	0	0	Moderate	⨁⨁⨁⊖

Note: BDI: Beck Depression Inventory; VAS: Visual Analogue Scale; SDS: Self-rating Depression Scale; SQ: sleep quality; QST: quantitative sensory testing; RCT: randomized controlled trial. *Downgraded by levels due to small sample size.

Table 3: Characteristics of participants with NOP in the reviewed studies.

Study	Study design	Duration	NOP condition	Inclusion criteria	Exclusion criteria	Adverse events
Fricová et al. [35]	A double-blind placebo-controlled trial	At least 6 months	Chronic orofacial pain (trigeminal neuralgia, atypical orofacial pain, postherpetic neuralgia, dental pain)	(a) Orofacial pain syndrome, intractable pharmacoresistant pain (b) Stable analgesic medication for at least 1 month before the start of the study and throughout its course and during follow-up evaluation two weeks after completion of rTMS (c) 18-65 years of age	(a) Severe organic brain damage or other serious diseases (b) Which could interfere with rTMS (epilepsy) (c) Any metallic implants in the body (restrictions similar to those for an MRI)	No
Lindholm et al. [36]	A randomized placebo-controlled crossover study	2-30 years	Chronic drug-resistant neuropathic orofacial pain (trigeminal neuropathic pain, atypical facial pain, burning mouth syndrome)	(a) Chronic daily neuropathic pain 4 in severity using NRS of 0 to 10 (b) Patients had no history of seizure, pacemaker implantation, major stroke, or other contraindication for TMS	(a) Multiple ischemic lesions and another after the pain diary follow-up because of average pain less than 4 on the NRS (b) Major depression	Unpleasant temporalis contractions
Ma et al. [37]	A sham stimulation-controlled randomized trial	Longer than 6 months	Postherpetic neuralgia	(a) Patients with chronic pain, moderate to severe in intensity (VAS ≥ 4) despite optimized pharmacological treatment (b) Pain lasting longer than 1 month	(a) Inability to participate in the questionnaires (b) The presence of suicidal ideation and the presence of contraindications for rTMS	Slight dry mouth, headache, neck pain, and dizziness symptoms
Umezaki et al. [38]	A randomized controlled single-blind study	63.42 ± 65.51 months	Burning mouth syndrome	(a) Diagnosed as having BMS daily and deep bilateral burning sensation of the oral mucosa (b) Burning sensation for at least 4-6 months, constant intensity or increasing intensity during the day	(a) Inflammation or autoimmune disease (b) Major depression or major personality disorders or a history of substance abuse (except caffeine or nicotine)	Slight headache
Kohútová et al. [18]	A double-blind sham-controlled parallel-group randomized study	At least 6 months	Chronic orofacial pain	(a) Orofacial pain syndrome in the duration of at least 6 months, intractable pharmacotherapy-resistant pain (b) 18-65 years of age	(a) Severe organic brain damage or other serious diseases	Comprising mild and transient headache symptoms
Pei et al. [25]	A double-blind sham-controlled randomized trial	Lasting for over 1 month	Postherpetic neuralgia	(a) Aged above 50 years old (b) Conforming to the diagnostic criteria of PHN, PHN lasting for over one month. VAS above 4, and having clear consciousness	(a) Personal or family history of epilepsy (b) History of craniocerebral surgery (c) Intracranial implants (d) Cardiac pacemakers (e) Heart, liver, or kidney insufficiency and coagulation disorders	Slight dry mouth, headache, neck pain, and dizziness symptoms

Table 4: The main characteristics of rTMS in the reviewed studies.

Study	Study design	Main diagnosis	EG									CG									Measurement
			n	Female/male (*n*)	Stimulation site	Age (yrs)	Frequency (Hz)	MT	ITI (s)	Coil type	Total pulses	*n*	Female/male (*n*)	Stimulation site	Age (yrs)	Frequency (Hz)	MT	ITI (s)	Coil type	Total pulses	
Fricová et al. [35]	A double-blind placebo-controlled trial	COP	23	16/7	N/A	50.7	20	95% MT	1.9	N/A	720	36	N/A	N/A	33-65 yrs	10/0	95% MT	1.9	N/A	720	VAS QST
Lindholm et al. [36]	A randomized placebo-controlled crossover study	COP	10	N/A	S2	39-74	10	90% RMT	10	Figure-of-eight coil	1000	6	N/A	M1/S1	39-74	10	90% RMT	10	Figure-of-eight coil	1000	NRS BDI QOL SF-36 BPI NePIQoL
Ma et al. [37]	A sham stimulation-controlled randomized trial	PHN	20	9/11	M1	65.4 ± 10.5	10	80% RMT	3	Round coil	1500	20	11/9	M1	67.3 ± 11.9	10	80% RMT	3	Round coil	1500	VAS SF-MPQ QOL SQ PGIC SDS
Umezaki et al. [38]	A randomized controlled single-blind study	BMS	12	N/A	L-DLPFC	63.36 ± 10.78	10	110% RMT	10	Figure-of-eight coil	3000	8	N/A	L-DLPFC	64.42 ± 8.35	10	110% RMT	10	Figure-of-eight coil	3000	VAS SF-MPQ BPI PHQ-9 PGIC CGI
Kohútová et al. [18]	A double-blind sham-controlled parallel-group randomized study	COP	10	6/4	M1	55.5 ± 12.7	50	90% MT	8	N/A	600	9	6/3	M1	59.3 ± 14.9	50	90% MT	10	N/A	600	VAS BDI BAI QST
Pei et al. [25]	A double-blind sham-controlled randomized trial	PHN	40	21/19	M1	65.9 ± 12.3 /65.4 ± 10.5	5/10	80% MT	2.5	N/A	1500	20	9/11	M1	67.3 ± 11.9	0	80% MT	3	N/A	1500	V AS SF-MPQ QOL SQ SDS PGIC

Note: BMS: burning mouth syndrome; BPI: Brief Pain Inventory; BDI: Brief Depression Inventory; CG: control group; COP: chronic orofacial pain; CGI-I: Clinical Global Impression for global improvement scale; EG: experimental group; iTBS: intermittent theta burst stimulation; imTBS: intermediate theta burst stimulation; ITI: intertrain interval; L-DLPFC: left dorsolateral prefrontal cortex; M1/S1/S2: primary motor cortex (M1), primary sensory cortex (S1), and secondary somatosensory cortex (S2); NePIQoL: neuropathic pain impact on quality of life; MT: motor threshold; N/A: not available; NRS: Numerical Rating Scales; PHN: postherpetic neuralgia; PGIC: Patients' Global Impression of Change; PHQ-9: Patient Health Questionnaire; QOL: quality of life; QST: quantitative sensory testing; RMT: resting active motor threshold; SDS: Self-rating Depression Scale; SF-MPQ: Short-Form McGill Pain Questionnaire; SQ: sleep quality; VAS: Visual Analogue Scale.

of 10 Hz, 80% MT, and a total of 1500 pulses. The duration of each stimulus was 0.5 seconds, and the interval between two stimuli was 3 seconds. rTMS was performed once a day for 15 consecutive days. Frequency selection in six studies [18, 25, 35–38] ranged from 5 Hz to 50 Hz, and the intensity of stimulation ranges from 80% resting motor threshold to 110% resting motor threshold with total pulses ranging from 600 to 3000.

3.6. Outcome Measures. The outcome measurements for each RCT are shown in Table 4. The outcomes obtained in this systematic review mainly included three aspects: pain, psychological conditions, and QOL. In all studies, pain was measured by VAS [18, 25, 35, 37, 38], Numerical Rating Scales (NRS) [36], Short-Form McGill Pain Questionnaire (SF-MPQ) [25, 37, 38], and Brief Pain Inventory (BPI) [36, 38]. The assessment of psychological conditions includes BDI [36, 38], Patients' Global Impression of Change (PGIC) [25, 37, 38], SDS [25, 37], Patient Health Questionnaire (PHQ-9) [38], Clinical Global Impression for global improvement scale (CGI-I) [38], and BAI [18]. QOL was assessed by SF-36 [36], BPI [36, 38], neuropathic pain impact on quality of life (NePIQoL) questionnaire [25, 36, 37], and SQ [25, 37].

3.7. Effectiveness

3.7.1. Effect of rTMS on Pain Intensity. The effectiveness of rTMS protocols in patients with NOP is summarized in Table 4. The pain intensity of NOP was evaluated using VAS and NRS in these studies [18, 25, 35–38], and 214 patients were involved in the rTMS group and control groups. Five studies [25, 35–38] have shown that rTMS can significantly improve pain in patients with NOP, but in another study [18], iTBS of M1 can temporarily relieve temporary and moderate subjective pain in NOP patients. In Fricová et al. [35], we found about a 24% reduction in pain values in patients with NOP. In Lindholm et al.'s [36] study, we found a 38% reduction in pain. Umezaki et al. [38] found that patients in the real group reported a 67% decrease in BMS pain intensity, and 75% of the subjects in the real group reported a >50% decrease in BMS pain intensity from baseline to day 60. We found that in Kohútová et al.'s [18] study, patients' pain values decreased by about 15%. Pei et al. [25] found that the pain value of PHN patients decreased by 39.89%. Ma et al. [37] found that the mean VAS reduction in the real rTMS group was 16.89% for the duration of disease longer than 6 months. In summary, all six studies showed that high-frequency rTMS had a positive effect on reducing pain.

3.7.2. Effect of rTMS on Psychological Conditions. Major indicators such as SDS and BDI were used to evaluate the psychological status of patients. Five studies [18, 25, 36–38] analyzed the psychological conditions of patients, but compared with the nonintervening group, patients showed no significant changes in anxiety and depression. Therefore, the above results indicate that rTMS has no obvious advantage in improving patients' psychological conditions, especially anxiety and depression.

3.7.3. Effect of rTMS on Quality of Life. Four studies [25, 36–38] reported on patients' QOL, sleep quality, and so on. Measures of QOL will be combined with patient activities and participation, but there was a slight reduction in the QOL score. In addition, Lindholm et al. [36] showed a slight improvement in patients' QOL, while the other four studies did not have a positive impact on the improvement of QOL, including sleep quality and patients' physical health. Therefore, rTMS does not significantly improve QOL in individuals with NOP.

3.8. Adverse Effects. Minor adverse events associated with rTMS treatment were reported in five studies [18, 25, 36–38], and only one study reported no significant adverse events. Umezaki et al. [38] found that patients had side effects of headache symptoms after rTMS application, but the symptoms were mild and disappeared within 1-2 days. Kohútová et al. [18] noted that TBS was tolerated well with mild side effects, primarily comprising mild and transient headache symptoms. In the two studies of PHN patients [25, 37], there were slight symptoms such as dry mouth, headache, neck pain, and dizziness. Lindholm et al. [36] reported 2 patients who developed unpleasant temporalis contractions. In summary, rTMS in patients with NOP caused only mild discomfort.

4. Discussion

As far as we know, there has been no systematic review for rTMS on pain intensity, psychological conditions, and quality of life in individuals with NOP. Overall, the rTMS intervention is safe and has consistent benefits in reducing pain, but improvements in mental health and QOL are difficult to detect, and long-term treatment can have positive effects on QOL. Different study designs and stimulus patterns affect the stability and reliability of the results. The stability and reliability of rTMS treatment in patients with NOP are influenced by study designs and stimulus regimens.

4.1. The Mechanisms and Parameters of TMS Action on NOP. rTMS may reduce neuropathic pain in NOP patients by regulating the excitatory activation of the pain circuit in the cerebral cortex, inhibiting the transmission of pain signals through the spinothalamic pathway, and also acting on the neural plasticity of brain regions implicated in the modulation of pain [39]. Studies have demonstrated that high-frequency stimulation (≥5 Hz) delivered to M1 of NOP patients (Evidence Level A) has a definite analgesic effect, suggesting it could be used for treating related diseases [13]. For the treatment of patients with neuropathic pain, stimulation of the motor cortex with rTMS at no less than 1000 pulses at 5-20 Hz can reduce pain intensity by about 25-30% [40]. NOP belongs to chronic peripheral neuropathic pain, and high-frequency rTMS of the M1 region has an obvious analgesic effect, confirming that M1 is the classic region for pain treatment. All factors and mechanisms are ultimately manifested in the activation of the pain network and the production of pain sensation, while rTMS can be regulated in both the upstream and downstream directions and affect the change of the whole pain neural circuit, which also provides a feasible scientific theoretical basis for the treatment of NOP.

For all these reasons, the effect of age or pain duration does not appear to be a key factor in treatment effectiveness, so it may be unreasonable to set age or pain duration limits for selecting suitable patients with rTMS. In addition, functional connections between the M1, S1, and S2 and the insular cortex were found to some extent [41]. The effect of S2 stimulation can be explained by its location near the insular cortex, which is important for pain perception. Connections to the S2 are particularly strong during painful stimuli, which may be one reason for mild discomfort [42]. However, stimulation of the S1 was considered to be inefficient or to cause hyperalgesia in some earlier studies [43]. Contrary to the previous view that the best stimulus target may be adjacent areas rather than the corresponding pain "hot spot," S2 stimulation induces better analgesia regardless of the pain level [44]. Thus, the right S2 appears to be a potential target for NOP treatment.

4.2. Effects of rTMS on Psychological Conditions of NOP Patients. NOP will cause different degrees of psychological conditions in patients, and long-term pain will cause them depression, anxiety, and other adverse emotions [45]. The application of rTMS in some brain regions has significant effects on emotional regulation, depression regulation, and other psychological regulations, which may be because the knot structure involved in these regions is intrinsically related. Stimulation of DLPFC targets by rTMS can change the psychological conditions of patients. Conventional rTMS includes high frequency to the left DLPFC and low frequency to the right DLPFC. However, not all depressed patients could benefit from standard rTMS protocols. DLPFC is a key brain region in cognitive and emotional regulation circuits. High-frequency rTMS stimulates the left DLPFC to enhance the activity of neurons in local brain regions, which is a therapeutic principle for rTMS to correct the lateralization of abnormal brain functions. In the study of Umezaki et al. [38], stimulation of the left DLPFC with 10 Hz rTMS did not achieve the expected improvement in psychological conditions. This may be limited by the research protocol. Bares et al. [46] found that stimulation of the right DLPFC region by 1 Hz rTMS was effective in treating refractory depression. Sixty patients with depression who had not previously responded to treatment with one or more antidepressants were randomly assigned to receive 1 Hz rTMS, which showed improvement in depression. The Montgomery-Asberg Depression Rating Scale (MADRS) score improved significantly compared with pretreatment. In the study of Bystritsky et al. [47], it has long been found that stimulation of the right DLPFC by low-frequency rTMS can also reduce generalized anxiety. Ten participants completed six sessions of rTMS over a 3-week period, stereotaxically directed to a previously identified prefrontal location. However, in the study of Umezaki et al. [38], stimulation of the left DLPFC with 10 Hz rTMS did not achieve the expected improvement in psychological conditions. This may be because the choice of stimulus frequency leads to different results. It is also worth exploring whether there is a link with the type of depression.

4.3. Effects of rTMS on QOL of NOP Patients. The improvement of QOL in patients with NOP by rTMS may come from two aspects. The reduction of pain makes patients have a great change in their attitude towards life, which enhances their confidence not only physically but also psychologically. QOL covers many aspects, such as sleep quality, work efficiency, and social interaction. The improvement of sleep quality is also the premise for patients to ensure the above. In two studies on PHN patients [25, 37], high-frequency stimulation of the M1 position also improved the sleep quality of patients in the short term. In the only study of BMS [38], these patients experienced daily and deep bilateral burning of the oral mucosa for 4-6 months with no disturbance to appetite or sleep. Umezaki et al. [38] confirmed in their study that high-frequency stimulation of the DLPFC site had positive effects on BMS in terms of pain, psychology, and QOL. Analysis showed that rTMS did not improve the quality of life of NOP patients in the short term by stimulating the left DLPFC site but could slightly improve the quality of life of NOP patients over time. According to the discussion on pain and psychological conditions, the reason why the left DLPFC can improve the quality of life may be caused by the improvement of patients' pain and psychological conditions. The reasons for the failure to improve quality of life may be influenced by the treatment cycle, and the choice of the left DLPFC site may also be potentially associated with the improvement of quality of life.

4.4. Limitations. This systematic review was based on only 6 articles, which may have publication bias. The biggest limitation of this study is that no large-scale randomized controlled trials were integrated into the meta-analysis. The sample size of this study was small, and the follow-up time for each study may be too short to determine any long-term treatment regimen resulting in a reduction in positive symptoms. There were many differences in the types and severity of disease among the patients included in the study, so there may be some heterogeneity.

4.5. Clinical Application and Prospect. The evidence presented in this review suggests that high-frequency rTMS should be used to improve the clinical symptoms of NOP. NOP, as a common type of neuropathic pain, can be treated clinically with high-frequency rTMS, but the specific site of treatment should also be evaluated based on symptoms. Further research studies should use larger sample sizes and include more patients with NOP-related diseases, such as trigeminal neuralgia. Confirming the parameters and optimal position of coil placement significantly improved the therapeutic effect. This model can be integrated into future studies to standardize rTMS treatment for NOP. Intervention parameters for rTMS should be standardized in addition to blind evaluators, subjects, and therapists. Future emphasis should also be placed on designing RCTs with sufficiently large samples to measure the clinically relevant effects of rTMS on NOP symptoms.

5. Conclusion

In summary, high-frequency rTMS is a very safe intervention and may serve as one of the therapeutic modalities to reduce pain intensity in individuals with NOP. There is moderate-to-high evidence to prove that high-frequency rTMS is

effective in individuals with NOP, but it has no significant positive effect on psychological conditions and QOL. This study was limited by the number of high-quality studies and the nature of the target population, and more recommendations are needed to encourage further validation in large-sample, multicenter, randomized, double-blind trials.

Data Availability

The data used to support the finding of this study are available from the corresponding authors upon request.

Disclosure

The funder had no role during the entire process of this study.

Conflicts of Interest

The authors declare that there are no conflicts of interest regarding the publication of this article.

Authors' Contributions

Yingxiu Diao and Yuhua Xie contributed equally to this work.

Acknowledgments

This study was supported by the Yixing Science and Technology Project (grant no. 2020SF16) and the Talent Development Foundation of the First Dongguan Affiliated Hospital of Guangdong Medical University (grant no. GCC2022004).

References

[1] J. Christoforou, "Neuropathic orofacial pain," *Dental Clinics of North America*, vol. 62, no. 4, pp. 565–584, 2018.

[2] F. J. Rodríguez-Lozano, A. Sanchez-Pérez, M. J. Moya-Villaescusa, A. Rodríguez-Lozano, and M. R. Sáez-Yuguero, "Neuropathic orofacial pain after dental implant placement: review of the literature and case report," *Oral Surgery, Oral Medicine, Oral Pathology, Oral Radiology, and Endodontics*, vol. 109, no. 4, pp. e8–e12, 2010.

[3] A. Berger, E. M. Dukes, and G. Oster, "Clinical characteristics and economic costs of patients with painful neuropathic disorders," *The Journal of Pain*, vol. 5, no. 3, pp. 143–149, 2004.

[4] D. Mueller, M. Obermann, M. S. Yoon et al., "Prevalence of trigeminal neuralgia and persistent idiopathic facial pain: a population-based study," *Cephalalgia*, vol. 31, no. 15, pp. 1542–1548, 2011.

[5] P. McDonough, J. P. McKenna, C. McCreary, and E. J. Downer, "Neuropathic orofacial pain: cannabinoids as a therapeutic avenue," *The International Journal of Biochemistry & Cell Biology*, vol. 55, pp. 72–78, 2014.

[6] S. K. Jääskeläinen, "Differential diagnosis of chronic neuropathic orofacial pain: role of clinical neurophysiology," *Journal of Clinical Neurophysiology*, vol. 36, no. 6, pp. 422–429, 2019.

[7] R. Baron, A. Binder, and G. Wasner, "Neuropathic pain: diagnosis, pathophysiological mechanisms, and treatment," *Lancet Neurology*, vol. 9, no. 8, pp. 807–819, 2010.

[8] L. Bendtsen, J. M. Zakrzewska, T. B. Heinskou et al., "Advances in diagnosis, classification, pathophysiology, and management of trigeminal neuralgia," *Lancet Neurology*, vol. 19, no. 9, pp. 784–796, 2020.

[9] A. Binder and R. Baron, "Postherpetic neuralgia–fighting pain with fire," *Lancet Neurology*, vol. 7, no. 12, pp. 1077-1078, 2008.

[10] D. A. Francis, A. T. Christopher, and B. D. Beasley, "Conservative treatment of peripheral neuropathy and neuropathic pain," *Clinics in Podiatric Medicine and Surgery*, vol. 23, no. 3, pp. 509–530, 2006.

[11] M. Mücke, T. Phillips, L. Radbruch, F. Petzke, and W. Häuser, "Cannabis-based medicines for chronic neuropathic pain in adults," *Cochrane Database of Systematic Reviews*, vol. 3, no. 3, article CD012182, 2020.

[12] M. S. George, Z. Nahas, F. A. Kozel et al., "Mechanisms and state of the art of transcranial magnetic stimulation," *The Journal of ECT*, vol. 18, no. 4, pp. 170–181, 2002.

[13] J. P. Lefaucheur, N. André-Obadia, A. Antal et al., "Evidence-based guidelines on the therapeutic use of repetitive transcranial magnetic stimulation (rTMS)," *Clinical Neurophysiology*, vol. 125, no. 11, pp. 2150–2206, 2014.

[14] S. Groppa, A. Oliviero, A. Eisen et al., "A practical guide to diagnostic transcranial magnetic stimulation: report of an IFCN committee," *Clinical Neurophysiology*, vol. 123, no. 5, pp. 858–882, 2012.

[15] H. J. Lin, P. C. Chen, T. T. Tsai, and S. P. Hsu, "Comparison of nerve conduction study and transcranial magnetic stimulation for early diagnosis and prognosis prediction of idiopathic facial palsy," *Neurological Sciences*, vol. 42, no. 10, pp. 4149–4154, 2021.

[16] K. Hosomi, K. Sugiyama, Y. Nakamura et al., "A randomized controlled trial of 5 daily sessions and continuous trial of 4 weekly sessions of repetitive transcranial magnetic stimulation for neuropathic pain," *Pain*, vol. 161, no. 2, pp. 351–360, 2020.

[17] J. K. Kim, H. S. Park, J. S. Bae, Y. S. Jeong, K. J. Jung, and J. Y. Lim, "Effects of multi-session intermittent theta burst stimulation on central neuropathic pain: a randomized controlled trial," *NeuroRehabilitation*, vol. 46, no. 1, pp. 127–134, 2020.

[18] B. Kohútová, J. Fricová, M. Klírová, T. Novák, and R. Rokyta, "Theta burst stimulation in the treatment of chronic orofacial pain: a randomized controlled trial," *Physiological Research*, vol. 66, no. 6, pp. 1041–1047, 2017.

[19] R. Cavaleri, L. S. Chipchase, S. J. Summers, J. Chalmers, and S. M. Schabrun, "The relationship between corticomotor reorganization and acute pain severity: a randomized, controlled study using rapid transcranial magnetic stimulation mapping," *Pain Medicine*, vol. 22, no. 6, pp. 1312–1323, 2021.

[20] M. Saltychev and K. Laimi, "Effectiveness of repetitive transcranial magnetic stimulation in patients with fibromyalgia: a meta-analysis," *International Journal of Rehabilitation Research*, vol. 40, no. 1, pp. 11–18, 2017.

[21] C. G. Zhao, W. Sun, F. Ju et al., "Analgesic effects of directed repetitive transcranial magnetic stimulation in acute neuropathic pain after spinal cord injury," *Pain Medicine*, vol. 21, no. 6, pp. 1216–1223, 2020.

[22] C. Quesada, B. Pommier, C. Fauchon et al., "New procedure of high-frequency repetitive transcranial magnetic stimulation for central neuropathic pain: a placebo-controlled randomized crossover study," *Pain*, vol. 161, no. 4, pp. 718–728, 2020.

[23] B. Yılmaz, S. Kesikburun, E. Yaşar, and A. K. Tan, "The effect of repetitive transcranial magnetic stimulation on refractory neuropathic pain in spinal cord injury," *The Journal of Spinal Cord Medicine*, vol. 37, no. 4, pp. 397–400, 2014.

[24] G. Cruccu, L. Garcia-Larrea, P. Hansson et al., "EAN guidelines on central neurostimulation therapy in chronic pain conditions," *European Journal of Neurology*, vol. 23, no. 10, pp. 1489–1499, 2016.

[25] Q. Pei, B. Wu, Y. Tang et al., "Repetitive transcranial magnetic stimulation at different frequencies for postherpetic neuralgia: a double-blind, sham-controlled, randomized trial," *Pain Physician*, vol. 22, no. 4, pp. E303–E313, 2019.

[26] M. Jodoin, D. M. Rouleau, A. Bellemare et al., "Moderate to severe acute pain disturbs motor cortex intracortical inhibition and facilitation in orthopedic trauma patients: a TMS study," *PLoS One*, vol. 15, no. 3, article e0226452, 2020.

[27] M. Cumpston, T. Li, M. J. Page et al., "Updated guidance for trusted systematic reviews: a new edition of the Cochrane Handbook for Systematic Reviews of Interventions," *Cochrane Database of Systematic Reviews*, vol. 10, article ED000142, 2019.

[28] L. Shamseer, D. Moher, M. Clarke et al., "Preferred reporting items for systematic review and meta-analysis protocols (PRISMA-P) 2015: elaboration and explanation," *BMJ*, vol. 349, article g7647, 2015.

[29] M. B. Eriksen and T. F. Frandsen, "The impact of patient, intervention, comparison, outcome (PICO) as a search strategy tool on literature search quality: a systematic review," *Journal of the Medical Library Association*, vol. 106, no. 4, pp. 420–431, 2018.

[30] A. Liberati, D. G. Altman, J. Tetzlaff et al., "The PRISMA statement for reporting systematic reviews and meta-analyses of studies that evaluate health care interventions: explanation and elaboration," *PLoS Medicine*, vol. 6, no. 7, article e1000100, 2009.

[31] G. Z. Heller, M. Manuguerra, and R. Chow, "How to analyze the visual analogue scale: myths, truths and clinical relevance," *Scandinavian Journal of Pain*, vol. 13, no. 1, pp. 67–75, 2016.

[32] S. K. Bhogal, R. W. Teasell, N. C. Foley, and M. R. Speechley, "The PEDro scale provides a more comprehensive measure of methodological quality than the Jadad scale in stroke rehabilitation literature," *Journal of Clinical Epidemiology*, vol. 58, no. 7, pp. 668–673, 2005.

[33] M. Mercuri, B. Baigrie, and R. E. G. Upshur, "Going from evidence to recommendations: can GRADE get us there?," *Journal of Evaluation in Clinical Practice*, vol. 24, no. 5, pp. 1232–1239, 2018.

[34] G. Guyatt, A. D. Oxman, E. A. Akl et al., "GRADE guidelines: 1. Introduction–GRADE evidence profiles and summary of findings tables," *Journal of Clinical Epidemiology*, vol. 64, no. 4, pp. 383–394, 2011.

[35] J. Fricová, M. Klírová, V. Masopust, T. Novák, K. Vérebová, and R. Rokyta, "Repetitive transcranial magnetic stimulation in the treatment of chronic orofacial pain," *Physiological Research*, vol. 62, Supplement 1, pp. S125–S134, 2013.

[36] P. Lindholm, S. Lamusuo, T. Taiminen et al., "Right secondary somatosensory cortex-a promising novel target for the treatment of drug-resistant neuropathic orofacial pain with repetitive transcranial magnetic stimulation," *Pain*, vol. 156, no. 7, pp. 1276–1283, 2015.

[37] S. M. Ma, J. X. Ni, X. Y. Li, L. Q. Yang, Y. N. Guo, and Y. Z. Tang, "High-frequency repetitive transcranial magnetic stimulation reduces pain in postherpetic neuralgia," *Pain Medicine*, vol. 16, no. 11, pp. 2162–2170, 2015.

[38] Y. Umezaki, B. W. Badran, W. H. DeVries, J. Moss, T. Gonzales, and M. S. George, "The efficacy of daily prefrontal repetitive transcranial magnetic stimulation (rTMS) for burning mouth syndrome (BMS): a randomized controlled single-blind study," *Brain Stimulation*, vol. 9, no. 2, pp. 234–242, 2016.

[39] M. S. Bak, H. Park, and S. K. Kim, "Neural plasticity in the brain during neuropathic pain," *Biomedicine*, vol. 9, no. 6, p. 624, 2021.

[40] B. S. Kang, H. I. Shin, and M. S. Bang, "Effect of repetitive transcranial magnetic stimulation over the hand motor cortical area on central pain after spinal cord injury," *Archives of Physical Medicine and Rehabilitation*, vol. 90, no. 10, pp. 1766–1771, 2009.

[41] E. Peltz, F. Seifert, R. DeCol, A. Dörfler, S. Schwab, and C. Maihöfner, "Functional connectivity of the human insular cortex during noxious and innocuous thermal stimulation," *NeuroImage*, vol. 54, no. 2, pp. 1324–1335, 2011.

[42] L. K. Case, C. M. Laubacher, E. A. Richards, P. A. Spagnolo, H. Olausson, and M. C. Bushnell, "Inhibitory rTMS of secondary somatosensory cortex reduces intensity but not pleasantness of gentle touch," *Neuroscience Letters*, vol. 653, pp. 84–91, 2017.

[43] M. R. Borich, S. M. Brodie, W. A. Gray, S. Ionta, and L. A. Boyd, "Understanding the role of the primary somatosensory cortex: opportunities for rehabilitation," *Neuropsychologia*, vol. 79, no. Part B, pp. 246–255, 2015.

[44] J. Ojala, J. Vanhanen, H. Harno et al., "A randomized, sham-controlled trial of repetitive transcranial magnetic stimulation targeting M1 and S2 in central poststroke pain: a pilot trial," *Neuromodulation*, vol. 25, no. 4, pp. 538–548, 2022.

[45] C. Penlington, V. Araújo-Soares, and J. Durham, "Predicting persistent orofacial pain: the role of illness perceptions, anxiety, and depression," *JDR Clinical & Translational Research*, vol. 5, no. 1, pp. 40–49, 2020.

[46] M. Bares, M. Kopecek, T. Novak et al., "Low frequency (1-Hz), right prefrontal repetitive transcranial magnetic stimulation (rTMS) compared with venlafaxine ER in the treatment of resistant depression: a double-blind, single-centre, randomized study," *Journal of Affective Disorders*, vol. 118, no. 1-3, pp. 94–100, 2009.

[47] A. Bystritsky, J. T. Kaplan, J. D. Feusner et al., "A preliminary study of fMRI-guided rTMS in the treatment of generalized anxiety disorder," *The Journal of Clinical Psychiatry*, vol. 69, no. 7, pp. 1092–1098, 2008.

Hindawi
Neural Plasticity
Volume 2022, Article ID 4416672, 16 pages
https://doi.org/10.1155/2022/4416672

Research Article

Altered Brain Activity and Effective Connectivity within the Nonsensory Cortex during Stimulation of a Latent Myofascial Trigger Point

Xinglou Li,[1] Meiling Luo,[1] Yan Gong,[2] Ning Xu,[3] Congcong Huo,[4] Hui Xie,[4] Shouwei Yue,[1] Zengyong Li,[5,6] and Yonghui Wang[1]

[1]*Rehabilitation Center, Qilu Hospital of Shandong University, Jinan, Shandong 250012, China*
[2]*Department of Physical Medicine and Rehabilitation, The Affiliated Suzhou Hospital of Nanjing Medical University, Suzhou, Jiangsu 215000, China*
[3]*School of Rehabilitation Medicine of Shandong University of Traditional Chinese Medicine, Jinan, Shandong 250355, China*
[4]*Key Laboratory for Biomechanics and Mechanobiology of Ministry of Education, School of Biological Science and Medical Engineering, Beihang University, Beijing 100086, China*
[5]*Beijing Key Laboratory of Rehabilitation Technical Aids for Old–Age Disability, National Research Center for Rehabilitation Technical Aids, Beijing 100176, China*
[6]*Key Laboratory of Neuro-functional Information and Rehabilitation Engineering of the Ministry of Civil Affairs, Beijing 100176, China*

Correspondence should be addressed to Yonghui Wang; yonghuiw6606@126.com

Received 12 April 2022; Revised 27 May 2022; Accepted 18 July 2022; Published 12 August 2022

Academic Editor: Xue-Qiang Wang

Myofascial trigger point (MTrP), an iconic characteristic of myofascial pain syndrome (MPS), can induce cerebral cortex changes including altered cortical excitability and connectivity. The corresponding characteristically reactive cortex is still ambiguous. Seventeen participants with latent MTrPs underwent functional near-infrared spectroscopy (fNIRS) to collect cerebral oxygenation hemoglobin (Δ[oxy-Hb]) signals. The Δ[oxy-Hb] signals of the left/right prefrontal cortex (L/R PFC), left/right motor cortex (L/R MC), and left/right occipital lobe (L/R OL) of the subjects were measured using functional near-infrared spectroscopy (fNIRS) in the resting state, nonmyofascial trigger point (NMTrP), state and MTrP state. The data investigated the latent MTrP-induced changes in brain activity and effective connectivity (EC) within the nonsensory cortex. The parameter wavelet amplitude (WA) was used to describe cortical activation, EC to show brain network connectivity, and main coupling direction (mCD) to exhibit the dominant connectivity direction in different frequency bands. An increasing trend of WA and a decreasing trend of EC values were observed in the PFC. The interregional mCD was primarily shifted from a unidirectional to bidirectional connection, especially from PFC to MC or OL, when responding to manual stimulation during the MTrP state compared with resting state and NMTrP state in the intervals III, IV, and V. This study demonstrates that the nonsensory cortex PFC, MC, and OL can participate in the cortical reactions induced by stimulation of a latent MTrP. Additionally, the PFC shows nonnegligible higher activation and weakened regulation than other brain regions. Thus, the PFC may be responsible for the central cortical regulation of a latent MTrP. This trial is registered with ChiCTR2100048433.

1. Introduction

Myofascial trigger points (MTrPs) are limited sensitive points and can be found within almost any strained muscle, thus leading to the most extensive neck, shoulder, waist, and leg pain [1]. As the main obstacles to a better myofascial pain syndrome (MPS) clinical outcome [2], MTrPs will induce local pain, local convulsive response, and autonomic nerve phenomena once provoked and can be active and latent. Latent MTrPs commonly exist in healthy people

and patients with musculoskeletal pain, leading to sensory-motor dysfunction. Compared with the active MTrPs, latent MTrPs can also play an essential role in characteristic neuromuscular excitability [3]. Mechanisms involved in MTrP production, including the "integrated hypothesis" and "energy crisis theory," have been generally accepted [4, 5]. After cortical activation, central sensitization also contributes to the emergence of MTrPs [6]. Treatments focusing on the local MTrP, such as dry needling, shock wave therapy, and local block therapy, are the most common strategies [7]. However, there is a lack of specific and effective treatment, with pain easily recurring.

MTrPs can induce a complex multidimensional emotional experience, which relies on the neuronal activity of multiple regions of the cerebral cortex to complete the process of sensory, emotional, and cognitive responses [8]. However, there is no specific central nervous system for pain or nociception within the brain, and the cortical activation patterns can vary with different clinical pain symptoms. Although the somatosensory cortex can reflex pain signals, it is mainly responsible for perceiving pain, especially for identifying the location of pain in the body [9]. The complicated cortical pain processing needs further investigation as specific pain biomarkers and target treatments are lacking.

In recent years, the nonsensory cortex, particularly the prefrontal cortex (PFC), motor cortex (MC), and occipital lobe (OL), has been reported to play increasingly indispensable roles in pain processing. A series of brain imaging studies demonstrated that the PFC participates in neuropathic and musculoskeletal pain production. The PFC is also where pain information (painful and nociceptive stimuli) and others (including memory, emotion, and space) are integrated and processed [10]. Excitability changes in the MC are related to the severity of pain intensity, hyperalgesia, and allodynia [11]. Additionally, activation of the MC can also have an analgesic effect on chronic pain [12]. Thus, the MC has been a common target area for pain research, due to its connection with the nociceptive system and the effect of pain on motor function. Although the OL is not a typical "pain matrix" or salient network member, it can also be involved in the central processing of pain signals. The excitability of the OL, demonstrated by the electrophysiological images in patients with migraine and visual snow syndrome, has proved the loss of pain habituation and a lower pain threshold [13]. One study of 114 subjects has further illustrated that thermal pain stimuli can activate the pain matrix, while OL neuronal activity was observed inhibited [14]. Still, however, the cortical changes in the nonsensory cortical associated with the latent MTrPs are not understood.

Several brain imaging techniques, such as functional magnetic resonance imaging (fMRI) [15], positron emission tomography (PET) [16], and magnetoencephalography (MEG) [17], are the most available devices to collect pain-related cortical neuronal activity data. However, they are not suitable for the clinical rapid and patient-centric brain assessment. In this decade, functional near-infrared spectroscopy (fNIRS), supported by portability, affordability, and resistance to motion artifacts, has been suggested to assess neuronal activity by recording oxygenated and deoxygenated hemoglobin changes in cerebral tissues. As a noninvasive optical imaging technique, fNIRS can be applied in the clinic to monitor the human brain function changes [18]. This study was aimed at investigating the functionality of fNIRS to explore pain-related cortical activity.

The nonsensory cortex can elicit a large amount of information correlated to its role in the pain process. However, this informative resource has not been characterized in MTrP-related pain. This study stimulates the MTrP and NMTrP of recruited participants and was aimed at exploring the latent MTrP-induced changes of activation and network connections within the nonsensory cerebral cortex by an fNIRS.

2. Materials and Methods

2.1. Participants. This study is prospective and observational, involving a single-center, self-control, and single-blinding clinical trial. This project uses right brachioradialis, usually more frequently used and susceptible to lateral epicondylalgia than the left one, to study latent MTrPs [19].

The subjects are screened according to the following inclusion criteria: (1) no mental health diagnoses have been founded; (2) no medicine has been taken this 48 h; (3) age ranged from 20 to 50 years for both genders; (4) minimum primary school education; and (5) a latent MTrP is on the right brachioradialis but absent from the left side (there is no pain sensation in daily life, but pain could be stimulated by pressing or other methods) [20, 21]. The exclusion criteria are as follows: (1) pain resulting from other causes (such as rheumatic diseases, malignant tumors, and other infections); (2) disoriented subjects; (3) and subjects with more severe health comorbidities (such as heart, liver, lung, kidney, and other organs dysfunction). All participants signed a written informed consent before inclusion.

From July to October 2021, 17 participants were identified according to our study protocol. The study cohort consisted of 15 males and two females, with an average age of 25.41 ± 5.14 years. Other fundamental parameter indexes, such as visual analogue scale (VAS), blood pressure (BP), and heart rate (HR), also had been recorded when initially enrolled.

2.2. Experimental Design. Firstly, the examiner pressed the right brachioradialis with bare hands to determine the position of the potential MTrP and then marked it with a marker pen. The latent MTrP could be diagnosed manually if these criteria were present: taut band, hypersensitive spot, and local twitch response during pressing. Symmetrical to the right side, the corresponding position on the left was marked and defined as NMTrP. Figures 1(a) and 1(b) show the distribution of MTrP and NMTrP. A graphical diagram of the experimental setup is shown in Figure 1(c). All participants were asked to relax during the induction of stimulating pain using 25 Newton pressure from the force gauge [22, 23] on MTrPs and NMTrPs, respectively.

An initial resting state session of 8 min was measured using fNIRS for each subject for the whole experiment. During this session, the participants were required to remain as

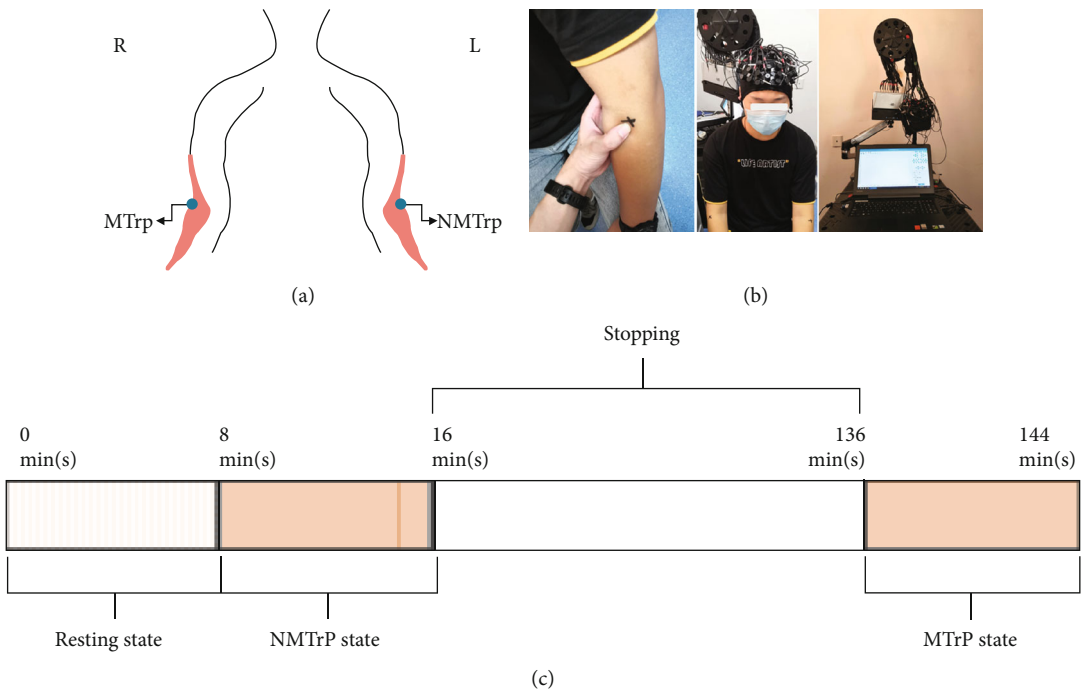

Figure 1: Schematic diagram of the experimental setup. (a) The distribution of MTrP and NMTrP: the marked blue regions of the bilateral brachioradialis muscle are the corresponding MTrP and NMTrP. (b) Experimental illustration. (c) Experimental schedule. NMTrP: nonmyofascial trigger point; MTrP: myofascial trigger point. Abbreviations: min(s), minute(s).

motionless as possible with their eyes closed and minds relaxed. Secondly, pain stimulation was induced by a force gauge on the position of NMTrP for 8 min. This session was defined as an NMTrP state, and fNIRS signals were collected simultaneously. The subjects were then asked to stop (but not sleep) and take off the fNIRS head cap for 2 h, helping subjects restore to their resting state. Lastly, pain stimulation was induced on the position of the latent MTrP for 8 min.

2.3. Data Acquisition. In this study, a continuous-wave fNIRS system (Nirsmart, Danyang Huichuang Medical Equipment Co., Ltd., China) was utilized, using light at 760 and 850 nm wavelengths to measure the changes in the concentrations of oxygenated hemoglobin (Δ[oxy-Hb]) with a sampling rate of 10 Hz. A total of 52 channels, set up as 24 source optodes and 16 detector optodes, were symmetrically positioned over the L/R PFC, L/R MC, and L/R OL regions. The channel configuration and regions of interest areas are illustrated in Figure 2. Using the calibration function of the instrument and the corresponding template, the channels were determined to precisely fill the corresponding of the 10/10 electrode positions with different head sizes of the participants [24].

2.4. Data Preprocessing and Analysis. Firstly, we removed the channel with invalid horizontal line signals of the collected fNIRS signals by visual inspection for each subject. Then, the fNIRS signals were filtered by a Butterworth filter with a cutoff frequency 0.005-2 Hz. The motion artifacts in fNIRS signals were detected and removed by moving the standard deviation and spline interpolation [25]. Then, the fluctuation signals of Δ[oxy-Hb] were deduced using the modified Beer-Lambert law [26]. Wavelet transform was adopted to obtain the phase dynamic information of the oscillation signals [27]. The phase dynamic information identified the effective network model among the 52 channels of the fNIRS measurement, which was established based on the coupling function [28]. The parameters describing the coupling model were inferred by dynamic Bayesian inference, which reveals the functional rules of interaction in the brain dynamical system [29]. The coupling relationships (including coupling strength and direction) between every two channels were described quantitatively by the model parameters. The instantaneous phases and their possible relationships with wavelet phase coherence were identified.

Collected fNIRS signals can be divided into evoked/nonevoked neurovascular coupling and systematic physiological interference. Therefore, mechanisms such as endothelial-derived nitric oxide, vascular myogenic response, and sympathetic nervous system could overlap and affect wavelet signals. The wavelet amplitude (WA), coupling strength (CS), and main coupling direction (mCD) were calculated in five intervals [30, 31]: I: cardiac activity (0.6–2 Hz), II: respiratory activity (0.145–0.6 Hz), III: myogenic activity (0.052–0.145 Hz), IV: neurogenic activity (0.021–0.052 Hz), and V: endothelial cell metabolism (0.0095-0.021 Hz), to describe the frequency-specific cortical activities and EC network, and intervals III, IV, and V were exhibited to reveal different relationships [32, 33].

2.5. Statistical Analysis. The Kolmogorov-Smirnov and Levene tests were applied to test the data's variance, normality, and homogeneity at the group level. Statistical analyses

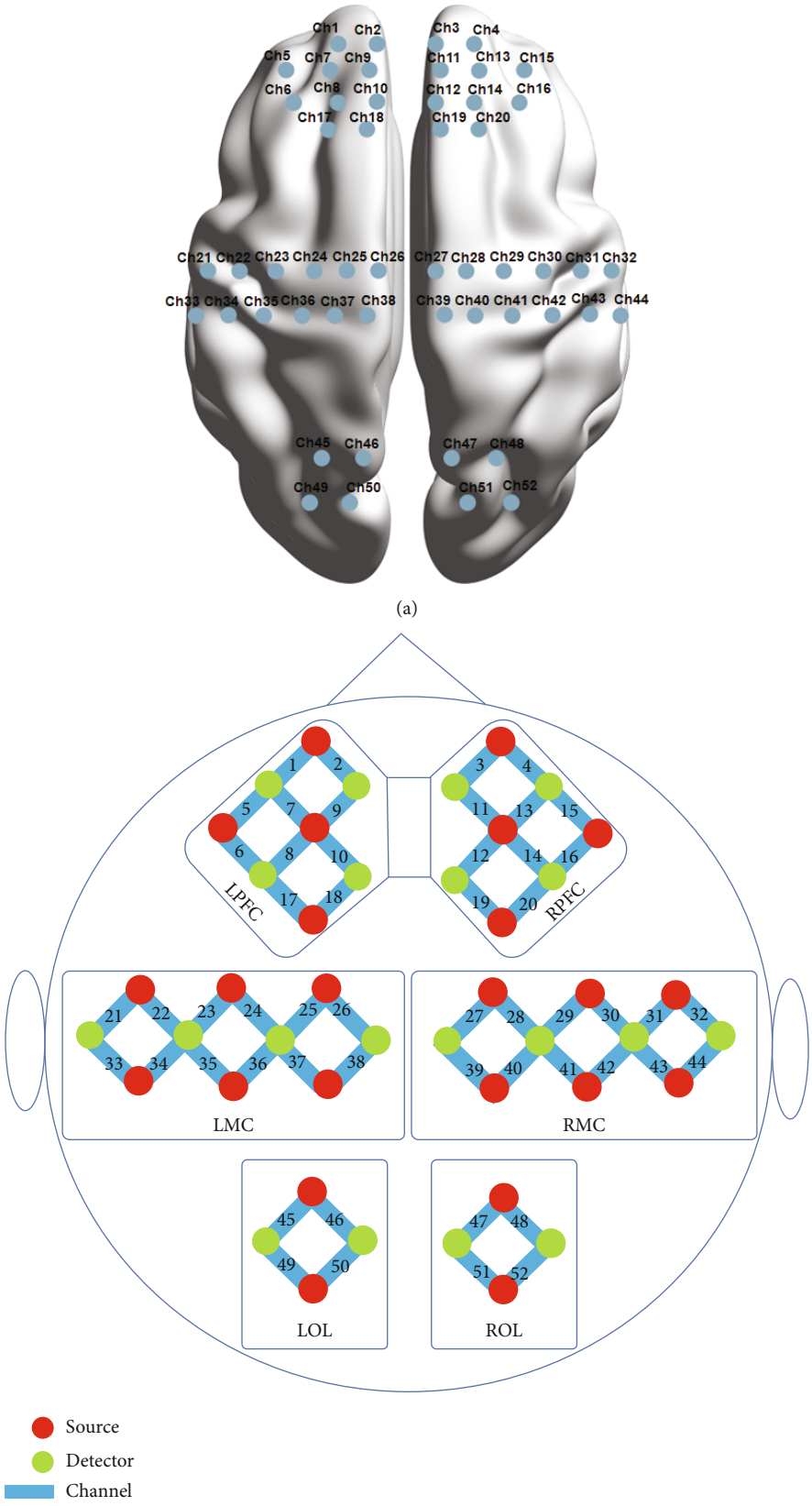

Figure 2: (a) Superior view 3D topography of optode positions in PFC-, MC-, and OL-related regions. (b) Configuration of 52 channels corresponding to the 10/10 electrode positions. Ch: channel; L: left; R: right; PFC: prefrontal cortex; MC: motor cortex; OL: occipital lobe.

Table 1: Fundamental information of experimental subjects in the latent MTrP before and during stimuli.

Parameter	VAS	BP (mmHg)		HR (times/min)
		SBP	DBP	
Before stimuli	0	119.00 ± 15.95	70.88 ± 8.13	73.13 ± 7.95
During stimuli	7.53 ± 0.72***	120.00 ± 16.46	71.50 ± 8.16	72.38 ± 9.12

VAS: visual analogue scale; BP: blood pressure; SBP: systolic blood pressure; DBP: diastolic blood pressure: HR: heart rate; MTrP: myofascial trigger point; min: minute. ***: $p \leq 0.001$. Error bars are mean ± s.e.m.

for the wavelet amplitude (WA), effective connectivity (EC), and main coupling direction (mCD) were evaluated using a one-way ANOVA in IBM SPSS (V 26.0). An α level of 0.05 and 95% confidence intervals were assumed to be statistically significant for all analyses, except comparison of EC among three states in three different intervals where the α value was adjusted as 0.0167 (0.05/3).

3. Results

3.1. Basic Parameters' Changes. The latent MTrP characteristics of the subjects are presented in Table 1. There was no statistical difference in BP and HR, but the participants' pain degree changed apparently in VAS results before and during stimuli of the latent MTrP.

3.2. Wavelet Amplitude Analysis. Wavelet amplitude (WA) reflects the fluctuation magnitude of the original signal in a specific frequency, so it serves as an index of power that describes the activity intensity of the cortical region [34]. The following graphs depict the changes in WA for the III, IV, and V intervals.

Figure 3 shows the WA in interval III (myogenic activity (0.052–0.145 Hz)). Within LPFC, there were five channels (1, 2, 5, 6, and 9) with statistical differences between resting state and MTrP state, two channels (5 and 6) between resting state and NMTrP state, and only one channel (9) between the NMTrP state and MTrP state. Within RPFC, significant differences have been found in six channels (3, 11, 13, 14, 15, and 16) between the resting state and MTrP state, only one channel (15) between the resting state and NMTrP state, and two channels (14 and 16) between NMTrP state and MTrP state. Within LMC, two channels (22 and 33) showed statistical differences between the resting state and MTrP state; no statistical differences were found between the resting state and NMTrP state or NMTrP state and MTrP state. Within RMC, only one channel (32) showed a significant difference between the resting state and MTrP state; only one channel (32) illustrated a statistically significant difference between resting state and NMTrP state and no statistical differences between NMTrP state and MTrP state. Within LOL and ROL, no statistical differences were ascertained.

Figure 4 illustrates data for WA in the interval IV (neurogenic activity (0.021–0.052 Hz)). Within LPFC, four channels (2, 5, 6, and 9) yielded statistical differences between the resting state and MTrP state; no statistical differences were observed for resting state vs. NMTrP state and NMTrP state vs. MTrP state. Within RPFC, six channels (3, 11, 13, 14, 15, and 16) yielded significant differences between resting state and MTrP state. When comparing the resting state with NMTrP state, no channel showed significant differences, while two channels (14 and16) showed significant differences between the NMTrP state and MTrP state. Within LMC, only one channel (22) exhibited a significant difference between the resting state and MTrP state. No statistical difference was found comparing the resting state vs. NMTrP state, or NMTrP state vs. MTrP state. Within RMC, only one channel (32) exhibited significant differences between the resting state and MTrP state. Only one channel (32) yielded significant differences between the resting state vs. NMTrP state, and no channel recorded a statistical difference between the NMTrP state and MTrP state. Within LOL and ROL, there were no statistical differences detected.

Figure 5 shows the WA in interval V (endothelial cell metabolism (0.0095-0.021 Hz)). Within LPFC, no existing statistical differences were recorded. Within RPFC, no channel recorded a statistical difference between the resting state vs. MTrP state, resting state vs. NMTrP state, and NMTrP state vs. MTrP state. Within LMC, no channel yielded a statistical difference when comparing the resting state with the MTrP state, resting state with the NMTrP state, and the NMTrP state with MTrP state. Within RMC, only one channel (32) significantly differed between the resting state and MTrP state. One channel (32) was significantly different between the resting state and NMTrP state. No channel was statistically different between the NMTrP and MTrP states. Within LOL and ROL, no statistical differences were found.

The results demonstrated that WA increased in the LPFC, RPFC, LMC, and RMC channels in intervals III and IV and only one RMC channel in the interval V (Figures 3–5) in the MTrP state compared to that in the resting state. In the NMTrP state, the WA in the RMC channel of interval III (Figure 3) was significantly higher than that in the resting state. Although an increasing trend was observed between the MTrP state and NMTrP state, it was not statistically significant. Thus, there seems to be an increasing trend of WA values in the MTrP and NMTrP states, compared with the resting state in the intervals III, IV, and V.

3.3. Effective Connectivity Analysis. To further investigate the neurovascular coupling interaction among these cortexes, the effective connectivity (EC), which refers explicitly to the influence that one neural system exerted over another to help describe the causality of interactions among brain regions, was adopted [35]. EC is assessed by coupling strengths.

Figure 6 shows the significant changes in EC values between two states in three different intervals, individually.

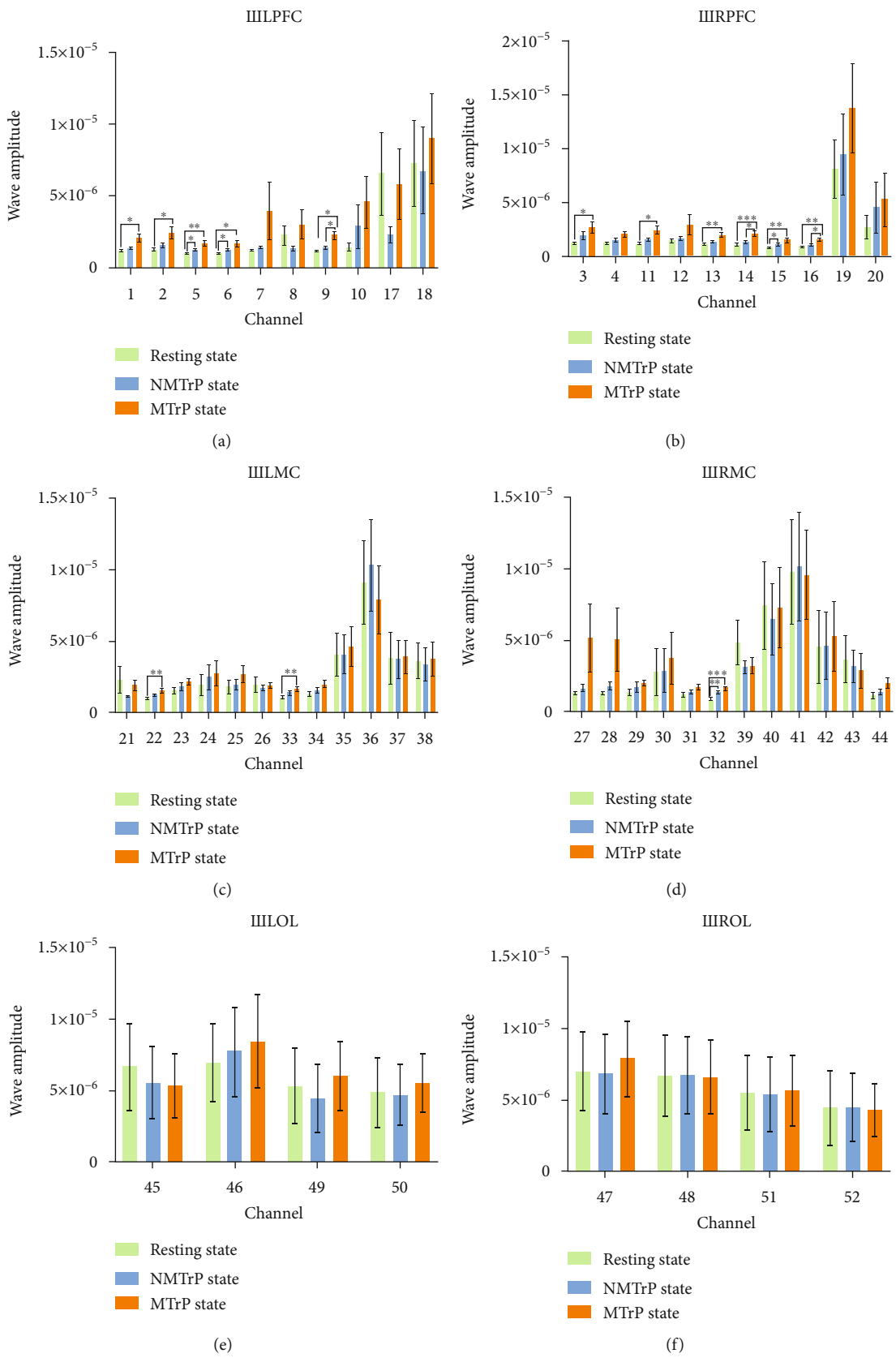

Figure 3: Comparison of wavelet amplitude (WA) changes among three stages in the frequency interval III: PFC (a and b), MC (c and d), and OL (e and f). Error bars are mean ± s.e.m. ∗: $p < 0.05$; ∗∗: $p < 0.01$; ∗∗∗: $p < 0.001$. MTrP: myofascial trigger point; NMTrP: nonmyofascial trigger point; L: left; R: right; PFC: prefrontal cortex; MC: motor cortex; OL: occipital lobe.

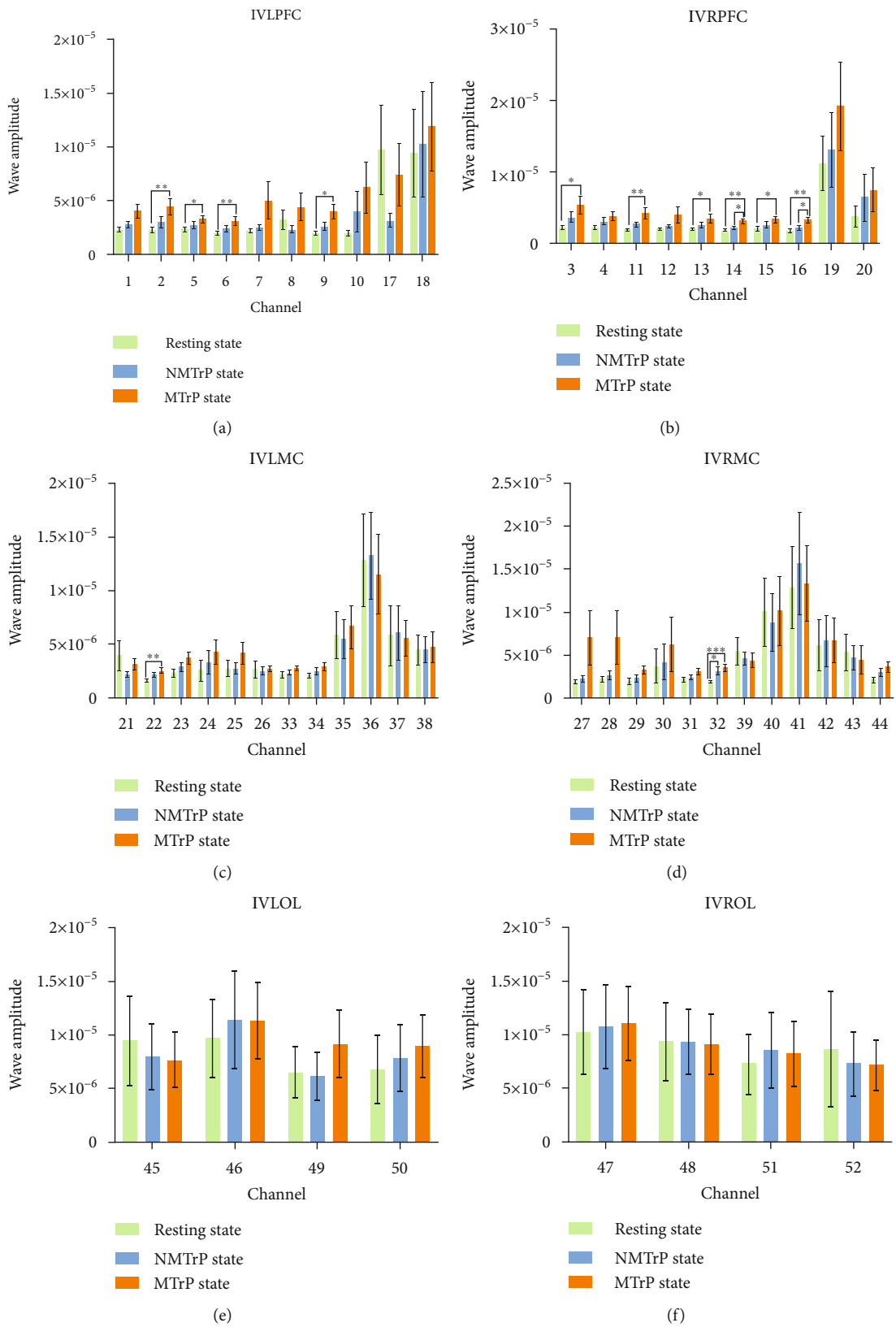

Figure 4: Comparison of wavelet amplitude (WA) changes among three stages in the frequency interval IV: PFC (a and b), MC (c and d), and OL (e and f). Error bars are mean ± s.e.m. ∗: $p < 0.05$; ∗∗: $p < 0.01$; ∗∗∗: $p < 0.001$. MTrP: myofascial trigger point; NMTrP: nonmyofascial trigger point; L: left; R: right; PFC: prefrontal cortex; MC: motor cortex; OL: occipital lobe.

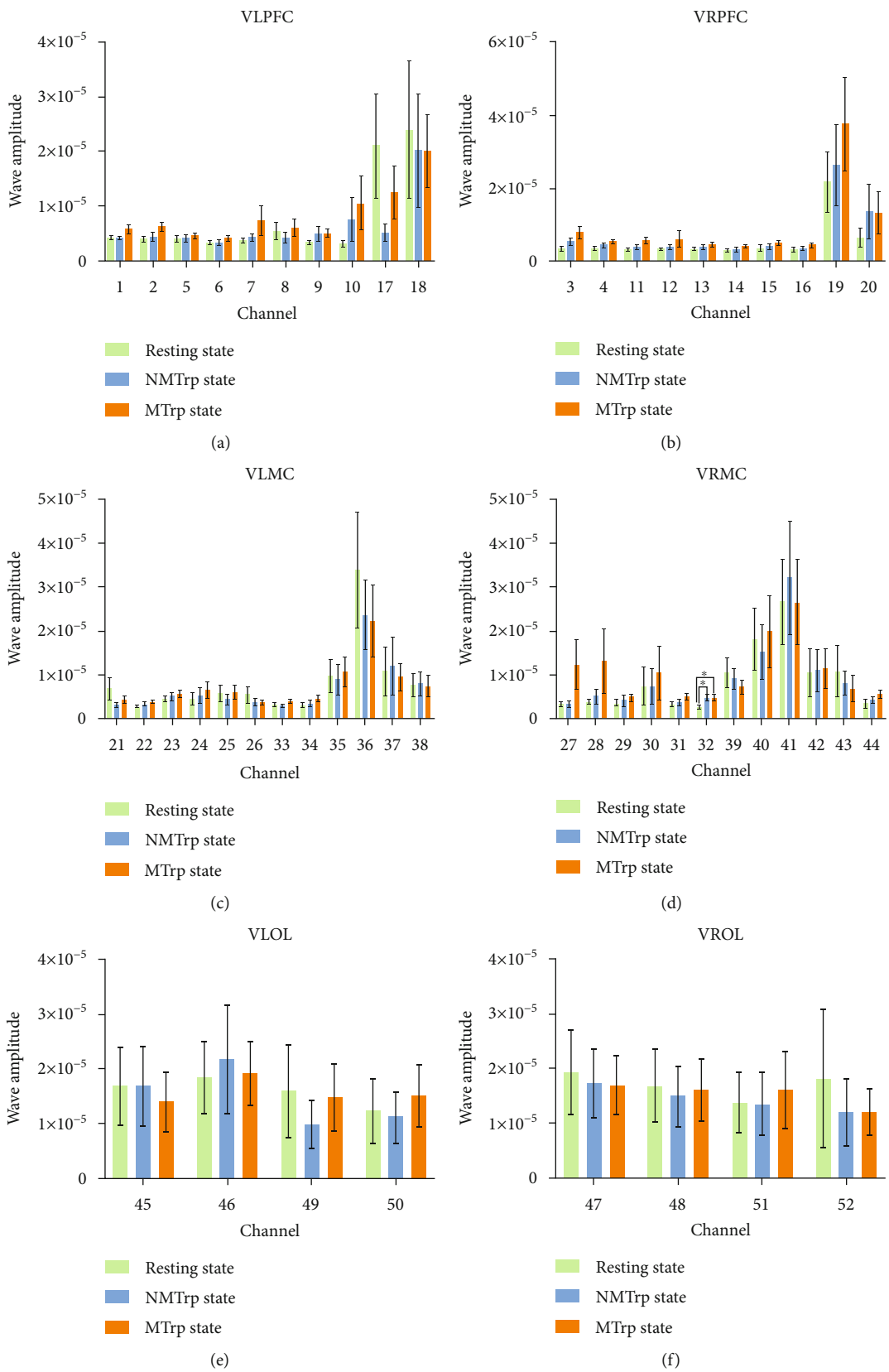

Figure 5: Comparison of wavelet amplitude (WA) changes among three stages in frequency interval V: PFC (a and b), MC (c and d), and OL (e and f). Error bars are mean ± s.e.m.∗: $p < 0.05$; ∗∗: $p < 0.01$; ∗∗∗: $p < 0.001$. MTrP: myofascial trigger point; NMTrP: nonmyofascial trigger point; L: left; R: right; PFC: prefrontal cortex; MC: motor cortex; OL: occipital lobe.

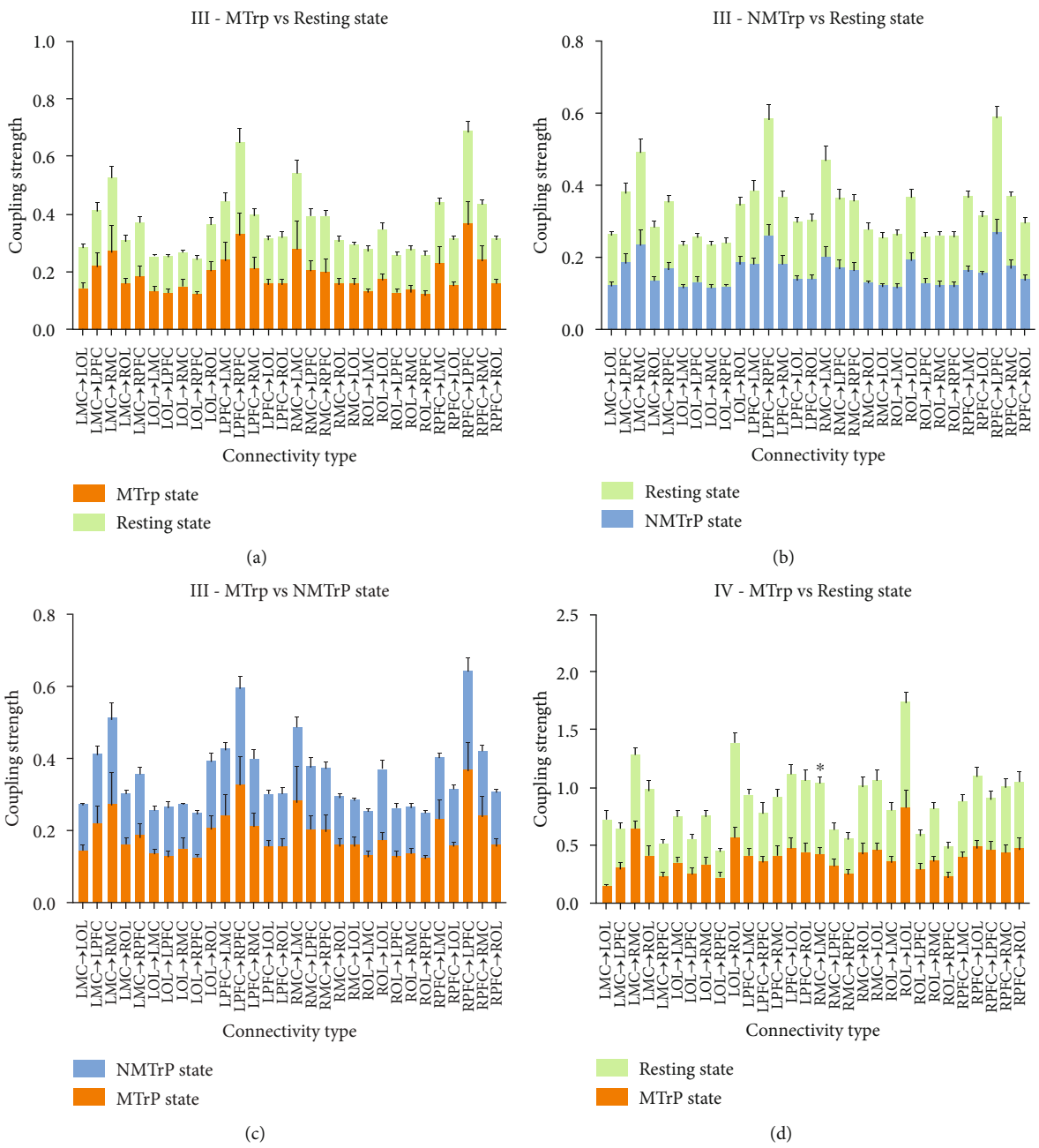

Figure 6: Continued.

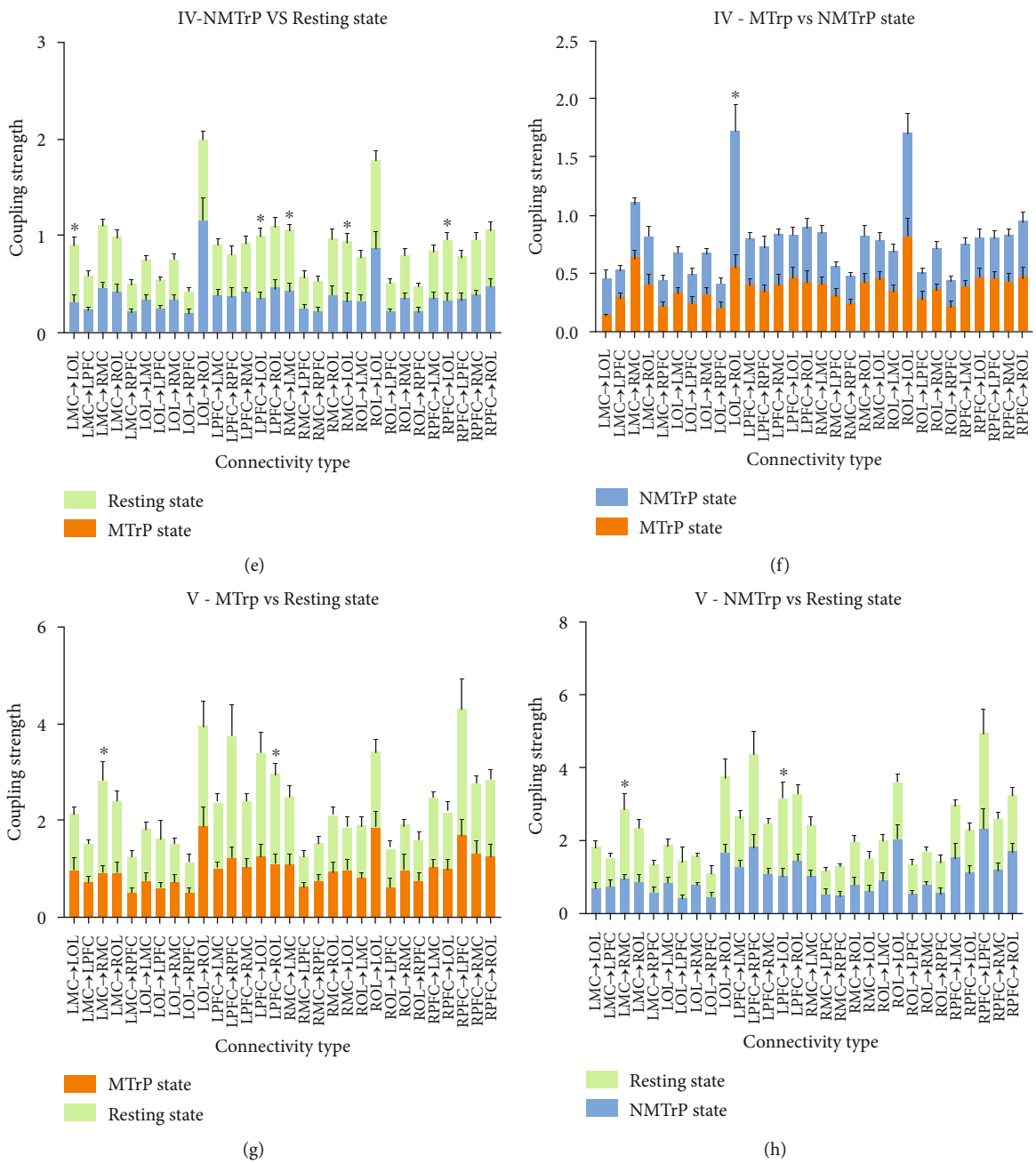

Figure 6: Continued.

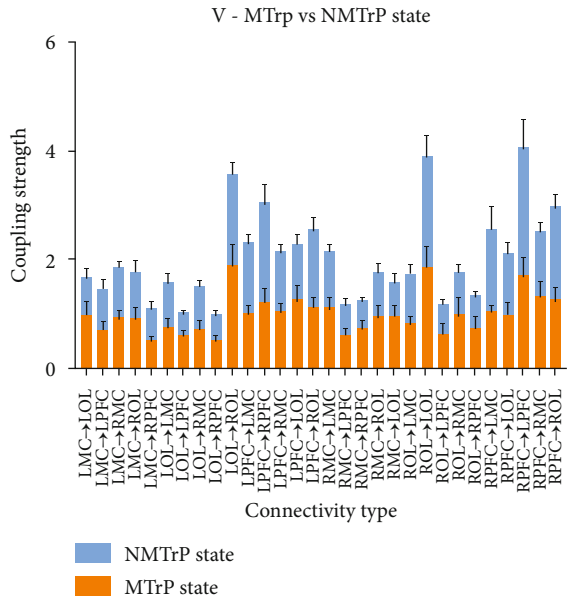

(i)

Figure 6: Comparison of region-wise EC among three states in three different intervals: interval III (a–c), interval IV (d–f), and interval V (g–i). Error bars are mean ± s.e.m. No significant difference ($p > 0.0167$); ∗: $p < 0.0167$. MTrP: myofascial trigger point; NMTrP: nonmyofascial trigger point; L: left; R: right; PFC: prefrontal cortex; MC: motor cortex; OL: occipital lobe.

No significant differences were recorded in interval III (Figures 6(a)–6(c)). In interval IV (Figures 6(d)–6(f)), comparing the MTrP and resting states, the connectivity of RMC→LMC showed a statistical difference. Considering NMTrP state vs. resting state, five significant differences in LPFC→LOL, RPFC→LOL, LMC→LOL, RMC→LMC, and RMC→LOL were found. Only the connectivity of LOL→-ROL is statistically different when comparing the NMTrP and MTrP states. In the frequency interval V (Figures 6(g)–6(i)), significant differences were detected between the MTrP state and the resting state in the two connections (LPFC→ROL and LMC→RMC). Considering NMTrP state vs. resting state also yielded statistical differences in the two conditions (LPFC→LOL and LMC→RMC). A decreasing trend of EC values in the MTrP and NMTrP states was apparent, compared with the resting state in the intervals III, IV, and V.

3.4. Main Coupling Direction Analysis. Main coupling direction (mCD) calculations were undertaken to investigate how every significant interaction of all possible pair channels between 2 brain regions can exhibit different dominant functions. When the oscillator value of $CS_{i\to j}$ exceeded $CS_{j\to i}$, it would be defined $i\to j$ as the main coupling direction (mCD) of the interaction between channel i and channel j, for the coupling parameters of each channel pair. Significant differences can demonstrate interregional mCD, suggesting that a predominant coupling function between the two regions is possible. Otherwise, it would be considered bidirectional coupling [36]. The frequency-specific interregional coupling directions among the six brain regions in the resting state, NMTrP state, and MTrP state, respectively, are displayed below (in Tables 2 and 3 and Figure 7).

Table 2: Statistical results of mCDs among 6 brain regions in Interval IV.

mCD	Resting state	NMTrP state	MTrP state
LPFC→RPFC	p = 0.869	p = 0.732	p = 0.165
LPFC→LMC	p = 0.020*	p = 0.013*	p = 0.090
LPFC→RMC	p = 0.035*	p = 0.004**	p = 0.297
LPFC→LOL	p ≤ 0.001***	p = 0.135	p = 0.021*
LPFC→ROL	p = 0.002**	p = 0.005**	p = 0.174
RPFC→LMC	p = 0.003**	p = 0.022*	p = 0.005**
RPFC→RMC	p = 0.001**	p =0.002**	p =0.016*
RPFC→LOL	p ≤ 0.001***	p = 0.079	p = 0.015*
RPFC→ROL	p = 0.001**	p = 0.003**	p = 0.016*
LMC→RMC	p = 0.788	p = 0.675	p = 0.823
LMC→LOL	p = 0.052	p = 0.805	p = 0.138
LMC→ROL	p = 0.227	p = 0.429	p = 0.563
RMC→LOL	p = 0.05	p = 0.883	p = 0.146
RMC→ROL	p = 0.201	p = 0.657	p = 0.486
LOL→ROL	p = 0.526	p = 0.307	p = 0.133

mCD: main coupling direction; L: left; R: right; PFC: prefrontal cortex; MC: motor cortex; OL: occipital lobe. $p > 0.05$, no statistic difference existed; ∗: significant difference; ∗: $p < 0.05$; ∗∗: $p < 0.01$; ∗∗∗: $p \le 0.001$.

In interval III, in the resting state, two mCDs were detected, LPFC→LOL ($p = 0.009$) and RPFC→LOL ($p = 0.004$). In the MTrP state, two mCDs were detected, including RPFC→LOL ($p = 0.03$) and RPFC→ROL ($p = 0.037$). These mCDs are illustrated in Figure 7(a).

Table 3: Statistical results of mCDs among six brain regions in Interval V.

mCD	Resting state	NMTrP state	MTrP state
LPFC→RPFC	p = 0.951	p = 0.394	p = 0.205
LPFC→LMC	p = 0.005**	p = 0.013*	p = 0.095
LPFC→RMC	p ≤ 0.001***	p = 0.002**	p = 0.035*
LPFC→LOL	p = 0.052	p = 0.002**	p = 0.023*
LPFC→ROL	p ≤ 0.001***	p ≤ 0.001***	p = 0.057
RPFC→LMC	p = 0.001**	p = 0.022*	p ≤ 0.001***
RPFC→RMC	p = 0.002**	p ≤ 0.001***	p = 0.039*
RPFC→LOL	p = 0.040*	p = 0.004**	p = 0.047*
RPFC→ROL	p = 0.007**	p ≤ 0.001***	p = 0.083
LMC→RMC	p = 0.264	p = 0.471	p = 0.432
LMC→LOL	p = 0.684	p = 0.532	p = 0.374
LMC→ROL	p = 0.100	p = 0.835	p = 0.674
RMC→LOL	p = 0.599	p = 0.284	p = 0.344
RMC→ROL	p = 0.191	p = 0.983	p = 0.942
LOL→ROL	p = 0.382	p = 0.428	p = 0.949

mCD: main coupling direction; L: left; R: right; PFC: prefrontal cortex; MC: motor cortex; OL: occipital lobe. $p > 0.05$, no statistic difference existed; ∗: significant difference. ∗: $p < 0.05$; ∗∗: $p < 0.01$; ∗∗∗: $p \leq 0.001$.

In interval IV, resting state yielded four mCDs dominant in LPFC and RPFC and no mCD from either MC or OL. In the NMTrP state, there were three mCDs from LPFC, three mCDs from RPFC, and no mCD from either MC or OL. In the MTrP state, only one mCDs from LPFC, four mCDs from RPFC, and no mCD from either MC or OL were found (Table 2 and Figure 7(b)).

In interval V, in the resting state, three mCDs were dominant in LPFC, four mCDs in RPFC, and no mCD from either MC or OL. In the NMTrP state, there were four mCDs from LPFC, four mCDs from RPFC, and no mCD from either MC or OL. In the MTrP state, two mCDs from LPFC, three mCDs from RPFC, and no mCD from either MC or OL were detected (Table 3 and Figure 7(c)).

In the NMTrP state, the interregional mCD was primarily observed in intervals IV and V from LPFC to LMC, RMC, and ROL; from RPFC to LMC, RMC, and ROL; and from LPFC to LOL and RPFC to LOL in the interval V. In the MTrP state, the interregional mCD was primarily found in intervals IV and V from RPFC to LMC and RMC, LPFC, to LOL, in the intervals III, IV, and V from RPFC to LOL, in intervals III and IV from RPFC to ROL, and in interval V from LPFC to RMC. Thus, the interregional mCD tends to be from LPFC and RPFC in intervals III, IV, and V.

4. Discussion

This study investigated the nonsensory cortical reactions, including changes in cortex neuronal activity and brain effective connectivity induced by a latent MTrP with fNIRS. WA has been used to describe cortical activity intensity, and EC refers to the interactional directional connectivity among regions. We observed an increasing trend of WA and a decreasing trend of EC values in the MTrP and NMTrP states, compared with the resting state in intervals III, IV, and V. Notably, the interregional mCD preferred to be from LPFC and RPFC in intervals III, IV, and V.

Previous studies have found that pain activates a wide range of cortical and subcortical areas, not only from one region. Except for the primary and secondary somatosensory areas, it includes the motor-related cortex, anterior cingulate cortex, and prefrontal cortex [37]. Moreover, this study further found that the nonsensory cortex including PFC, MC, and OL was activated when latent MTrPs were stimulated in MPS patients, and during which processes, complex mechanisms can be activated [30, 38, 39].

The present study shows that the MC can be activated either for the MTrP or NMTrP state, but the PFC has been activated only for the MTrP state (Figures 3–5). Previous studies also show that the PFC experiences an abnormal increase in activity during chronic pain [40, 41], contributing to the PFC's role in the transition between resting and task-processing states [29]. All these findings indicate that activation of the MC occurs within the cerebral cortex when various pain occurs, but PFC activation occurs specifically in MTrP-related changes. In contrast to the NMTrP state, some channels of LPFC and RPFC were significantly activated in the intervals III and IV in the MTrP state. Such activation may be related to the increased sensitivity, decrease of the pain threshold, and possibly the increase of the receptive field of the MTrP state correlated with peripheral and central sensitization [32, 42].

In addition, the connectivity between coupling cortexes also varied (Figure 6). The term connectivity can refer to different and interrelated aspects of brain organization. A fundamental distinction is between structural, functional, and effective connectivity. Among them, functional and effective connectivity refers to the functional connection between brain regions, based on a particular cognitive process [43]. The EC is a directional connectivity that depends on interactions among regions. In this study, its value in the connectivity of LOL→ROL in the MTrP state decreased in interval IV compared with the NMTrP state, suggesting that OL may play a role in the regulation of MTrP and may relate to specialized cells or groups of cells existing in the occipital cortex that can recognize the spatial location of pain [44]. Notably, the interregional mCD (Figure 7) was primarily shifted from unidirectional to bidirectional connection in responding to the MTrP state compared with the NMTrP state [36, 45]. These changes suggest that the PFC regulation on other brain regions was weakened, while the feedback regulation of other brain regions on the PFC was enhanced during the MTrP state rather than in the NMTrP state.

Previous studies also found that the PFC is an essential node in brain connectivity, which can play a higher cognitive role in pain processing, and regulates pain awareness and pain response through the redistribution of attention

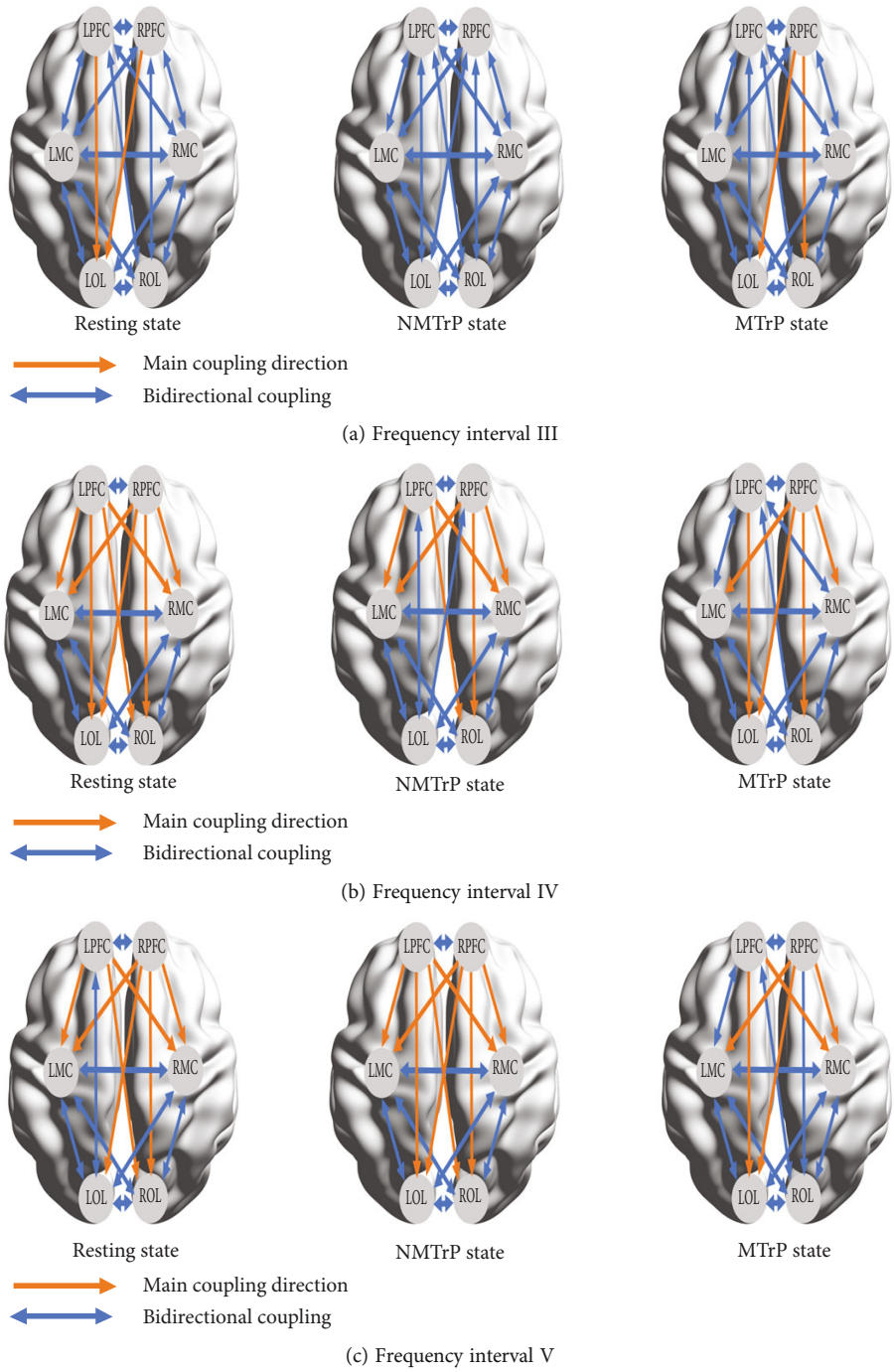

Figure 7: Illustration of frequency-specific interregional main coupling directions (mCD) (resting state, NMTrP state, and MTrP state) among the six brain regions in frequency intervals III (a), IV (b), and V (c), respectively. MTrP: myofascial trigger point; NMTrP: nonmyofascial trigger point; L: left; R: right; PFC: prefrontal cortex; MC: motor cortex; OL: occipital lobe.

[46, 47]. The PFC was not only related to other parts of the frontal lobe but also to other brain areas through such structures as the frontooccipital tracts [48, 49], which may be the basis of PFC regulation of network connections in other brain areas.

Further evidence further suggests that chronic pain is associated with structural and functional changes in M1 and affects the motor reflex arc (inputs and outputs) [50, 51]. Consequently, these changes may correlate with the increased regulation of the prefrontal cortex by motor areas that plan the avoidance response to pain. In a recent report, it has been demonstrated that long-term noxious stimulation can lead to changes in brain structure and function and dysfunction of neurovascular coupling [52]. It can also provide a possible explanation for cortical changes related to the latent MTrP.

5. Limitations

Firstly, the sample size is relatively small and needs to be expanded in future studies. Secondly, longitudinal experiments are needed to characterize further cortical changes induced by the latent and active MTrPs.

6. Conclusions

This study suggests that the nonsensory cortex, including the PFC, MC, and OL, can be involved in the reaction after stimulation of the latent MTrP. Additionally, high activation of the PFC and its weakened regulation in other brain regions were also characterized. The PFC shows high relevance and responsibility for regulating latent MTrP. However, further studies are needed to understand the MPS clinical outcomes regarding the findings of this study.

Data Availability

Data is available on request from the corresponding author (e-mail: yonghuiw6606@126.com).

Ethical Approval

The experimental procedure was approved by the Ethics Committee of Qilu Hospital, Cheeloo College of Medicine, Shandong University, and in accordance with the ethical standards specified by the Helsinki Declaration of 1975 (revised in 2008). (Registry Name: Application of functional near-infrared spectroscopy (fNIRS) in rehabilitation efficacy evaluation and rehabilitation program formulation Registration Number: ChiCTR2100048433)

Conflicts of Interest

The authors declare no competing financial interests.

Authors' Contributions

Yan Gong, Zengyong Li, and Yonghui Wang were responsible for the Conceptualization. Xinglou Li, Congcong Huo, and Hui Xie were responsible for the data curation. Ning Xu was responsible for the formal analysis. Yonghui Wang was responsible for the funding acquisition. Xinglou Li and Meiling Luo were responsible for the investigation. Zengyong Li and Yonghui Wang were responsible for the methodology. Yonghui Wang was responsible for the project administration. Yan Gong and Zengyong Li were responsible for the resources. Congcong Huo and Hui Xie were responsible for the software. Shouwei Yue and Yonghui Wang were responsible for the supervision. Xinglou Li and Hui Xie were responsible for the validation. Xinglou Li was responsible for the visualization. Xinglou Li and Meiling Luo wrote the original draft. Meiling Luo and Yonghui Wang wrote, reviewed, and edited the manuscript. All authors reviewed the manuscript. Xinglou Li and Meiling Luo contributed equally to this work.

Acknowledgments

This study was supported by the National Natural Science Foundation of China (NSFC Numbers 81672249, 81972154, and 31771071).

References

[1] H. R. Norman, "Muscle pain syndromes," *American Journal of Physical Medicine & Rehabilitation*, vol. 86, 1 Suppl, pp. S47–S58, 2007.

[2] J. Fleckenstein, D. Zaps, L. J. Rüger et al., "Discrepancy between prevalence and perceived effectiveness of treatment methods in myofascial pain syndrome: results of a cross-sectional, nationwide survey," *BMC Musculoskeletal Disorders*, vol. 11, no. 1, p. 32, 2010.

[3] H. Y. Ge and L. Arendt-Nielsen, "Latent myofascial trigger points," *Current Pain and Headache Reports*, vol. 15, no. 5, pp. 386–392, 2011.

[4] D. G. Simons, "New views of myofascial trigger points: etiology and diagnosis," *The Archives of Physical Medicine and Rehabilitation*, vol. 89, no. 1, pp. 157–159, 2008.

[5] E. D. Lavelle, W. Lavelle, and H. S. Smith, "Myofascial trigger points," *Medical Clinics of North America*, vol. 91, no. 2, pp. 229–239, 2007.

[6] D. M. Niddam, S. H. Lee, Y. T. Su, and R. C. Chan, "Brain structural changes in patients with chronic myofascial pain," *European Journal of Pain*, vol. 21, no. 1, pp. 148–158, 2017.

[7] T. Aydin, B. Dernek, T. Sentürk Ege, A. Karan, and C. Aksoy, "The effectiveness of dry needling and exercise therapy in patients with dizziness caused by cervical myofascial pain syndrome; prospective randomized clinical study," *Pain Medicine*, vol. 20, no. 1, pp. 153–160, 2019.

[8] T. V. Salomons, G. D. Iannetti, M. Liang, and J. N. Wood, "The "pain matrix" in pain-free individuals," *JAMA Neurology*, vol. 73, no. 6, pp. 755-756, 2016.

[9] W. Kim, S. K. Kim, and J. Nabekura, "Functional and structural plasticity in the primary somatosensory cortex associated with chronic pain," *Journal of Neurochemistry*, vol. 141, no. 4, pp. 499–506, 2017.

[10] W. Y. Ong, C. S. Stohler, and D. R. Herr, "Role of the prefrontal cortex in pain processing," *Molecular Neurobiology*, vol. 56, no. 2, pp. 1137–1166, 2019.

[11] P. Schwenkreis, A. Scherens, A. K. Rönnau, O. Höffken, M. Tegenthoff, and C. Maier, "Cortical disinhibition occurs in chronic neuropathic, but not in chronic nociceptive pain," *BMC Neuroscience*, vol. 11, no. 1, p. 73, 2010.

[12] E. Gentile, A. Brunetti, K. Ricci, M. Delussi, V. Bevilacqua, and M. de Tommaso, "Mutual interaction between motor cortex activation and pain in fibromyalgia: EEG-fNIRS study," *PLoS One*, vol. 15, no. 1, article e0228158, 2020.

[13] F. G. Yildiz, U. Turkyilmaz, and I. Unal-Cevik, "The clinical characteristics and neurophysiological assessments of the occipital cortex in visual snow syndrome with or without migraine," *Headache*, vol. 59, no. 4, pp. 484–494, 2019.

[14] T. D. Wager, L. Y. Atlas, M. A. Lindquist, M. Roy, C. W. Woo, and E. Kross, "An fMRI-based neurologic signature of physical pain," *The New England Journal of Medicine*, vol. 368, no. 15, pp. 1388–1397, 2013.

[15] L. R. Becerra, H. C. Breiter, M. Stojanovic et al., "Human brain activation under controlled thermal stimulation and

habituation to noxious heat: an fMRI study," *Magnetic Resonance in Medicine*, vol. 41, no. 5, pp. 1044–1057, 1999.

[16] K. L. Casey, T. J. Morrow, J. Lorenz, and S. Minoshima, "Temporal and spatial dynamics of human forebrain activity during heat pain: analysis by positron emission tomography," *The Journal of Neurophysiology*, vol. 85, no. 2, pp. 951–959, 2001.

[17] J. Ren, J. Xiang, Y. Chen, F. Li, T. Wu, and J. Shi, "Abnormal functional connectivity under somatosensory stimulation in migraine: a multi-frequency magnetoencephalography study," *The Journal of Headache and Pain*, vol. 20, no. 1, p. 3, 2019.

[18] P. W. Dans, S. D. Foglia, and A. J. Nelson, "Data processing in functional near-infrared spectroscopy (fNIRS) motor control research," *Brain Science*, vol. 11, no. 5, p. 606, 2021.

[19] J. Fernández-Carnero, C. Fernández-de-Las-Peñas, A. I. de la Llave-Rincón, H. Y. Ge, and L. Arendt-Nielsen, "Prevalence of and referred pain from myofascial trigger points in the forearm muscles in patients with lateral epicondylalgia," *The Clinical Journal of Pain*, vol. 23, no. 4, pp. 353–360, 2007.

[20] C. Fernández-de-Las-Peñas and J. Dommerholt, "International consensus on diagnostic criteria and clinical considerations of myofascial trigger points: a Delphi study," *Pain Medicine*, vol. 19, no. 1, pp. 142–150, 2018.

[21] M. J. Kao, T. I. Han, T. S. Kuan, Y. L. Hsieh, B. H. Su, and C. Z. Hong, "Myofascial trigger points in early life," *The Archives of Physical Medicine and Rehabilitation*, vol. 88, no. 2, pp. 251–254, 2007.

[22] H. Gemmell and A. Allen, "Relative immediate effect of ischaemic compression and activator trigger point therapy on active upper trapezius trigger points: a randomised trial," *Clinical Chiropractic*, vol. 11, no. 4, pp. 175–181, 2008.

[23] C. T. Tsai, L. F. Hsieh, T. S. Kuan, M. J. Kao, L. W. Chou, and C. Z. Hong, "Remote effects of dry needling on the irritability of the myofascial trigger point in the upper trapezius muscle," *American Journal of Physical Medicine & Rehabilitation*, vol. 89, no. 2, pp. 133–140, 2010.

[24] V. Jurcak, D. Tsuzuki, and I. Dan, "10/20, 10/10, and 10/5 systems revisited: their validity as relative head-surface-based positioning systems," *NeuroImage*, vol. 34, no. 4, pp. 1600–1611, 2007.

[25] F. Scholkmann, S. Spichtig, T. Muehlemann, and M. Wolf, "How to detect and reduce movement artifacts in near-infrared imaging using moving standard deviation and spline interpolation," *Physiological Measurement*, vol. 31, no. 5, pp. 649–662, 2010.

[26] K. Sakatani, D. Yamashita, T. Yamanaka et al., "Changes of cerebral blood oxygenation and optical pathlength during activation and deactivation in the prefrontal cortex measured by time-resolved near infrared spectroscopy," *Life Sciences*, vol. 78, no. 23, pp. 2734–2741, 2006.

[27] Y. Shiogai, A. Stefanovska, and P. V. McClintock, "Nonlinear dynamics of cardiovascular ageing," *Physics Reports*, vol. 488, no. 2-3, pp. 51–110, 2010.

[28] C. Huo, G. Xu, Z. Li et al., "Limb linkage rehabilitation training-related changes in cortical activation and effective connectivity after stroke: a functional near-infrared spectroscopy study," *Scientific Reports*, vol. 9, no. 1, p. 6226, 2019.

[29] T. Stankovski, T. Pereira, P. V. McClintock, and A. Stefanovska, "Coupling functions: universal insights into dynamical interaction mechanisms," *Reviews of Modern Physics*, vol. 89, no. 4, article 45001, 2017.

[30] A. Stefanovska, "Physics of the human cardiovascular system," *Contemporary Physics*, vol. 40, no. 1, pp. 31–55, 1999.

[31] A. Stefanovska, M. Bracic, and H. D. Kvernmo, "Wavelet analysis of oscillations in the peripheral blood circulation measured by laser Doppler technique," *IEEE Transactions on Biomedical Engineering*, vol. 46, no. 10, pp. 1230–1239, 1999.

[32] G. Xu, M. Zhang, Y. Wang et al., "Functional connectivity analysis of distracted drivers based on the wavelet phase coherence of functional near-infrared spectroscopy signals," *PLoS One*, vol. 12, no. 11, article e0188329, 2017.

[33] L. Bu, C. Huo, G. Xu et al., "Alteration in brain functional and effective connectivity in subjects with hypertension," *Frontiers in Physiology*, vol. 9, p. 669, 2018.

[34] M. Liang, Q. Su, A. Mouraux, and G. D. Iannetti, "Spatial patterns of brain activity preferentially reflecting transient pain and stimulus intensity," *Cerebral Cortex*, vol. 29, no. 5, pp. 2211–2227, 2019.

[35] K. J. Friston, "Functional and effective connectivity: a review," *Brain Connectivity*, vol. 1, no. 1, pp. 13–36, 2011.

[36] C. Huo, X. Li, J. Jing et al., "Median nerve electrical stimulation-induced changes in effective connectivity in patients with stroke as assessed with functional near-infrared spectroscopy," *Neurorehabilitation & Neural Repair*, vol. 33, no. 12, pp. 1008–1017, 2019.

[37] I. Tracey and P. W. Mantyh, "The cerebral signature for pain perception and its modulation," *Neuron*, vol. 55, no. 3, pp. 377–391, 2007.

[38] I. K. Martikainen, J. Hirvonen, U. Pesonen et al., "Differential associations between brain 5-HT(1A) receptor binding and response to pain versus touch," *Journal of Neural Transmission*, vol. 116, no. 7, pp. 821–830, 2009.

[39] M. Geisler, A. Ritter, M. Herbsleb, K. J. Bär, and T. Weiss, "Neural mechanisms of pain processing differ between endurance athletes and nonathletes: a functional connectivity magnetic resonance imaging study," *Human Brain Mapping*, vol. 42, no. 18, pp. 5927–5942, 2021.

[40] D. A. Seminowicz and M. Moayedi, "The dorsolateral prefrontal cortex in acute and chronic pain," *Journal of Pain*, vol. 18, no. 9, pp. 1027–1035, 2017.

[41] D. Pang and L. Liao, "Abnormal functional connectivity within the prefrontal cortex in interstitial cystitis/bladder pain syndrome (IC/BPS): a pilot study using resting state functional near-infrared spectroscopy (rs-fNIRS)," *Neurourology and Urodynamics*, vol. 40, no. 6, pp. 1634–1642, 2021.

[42] M. Zhang, F. Jin, Y. Zhu, and F. Qi, "Peripheral FGFR1 regulates myofascial pain in rats via the PI3K/AKT pathway," *Neuroscience*, vol. 436, pp. 1–10, 2020.

[43] K. J. Friston, "Functional and effective connectivity in neuroimaging: a synthesis," *Human Brain Mapping*, vol. 2, no. 2, pp. 56–78, 1994.

[44] H. Komatsu, A. Nishio, N. Ichinohe, and N. Goda, "Structure and function of neural circuit related to gloss perception in the macaque inferior temporal cortex: a case report," *Brain Structure & Function*, vol. 226, no. 9, pp. 3023–3030, 2021.

[45] S. H. Lee, S. H. Jin, and J. An, "Distinction of directional coupling in sensorimotor networks between active and passive finger movements using fNIRS," *Biomedical Optics Express*, vol. 9, no. 6, pp. 2859–2870, 2018.

[46] K. D. Karunakaran, K. Peng, D. Berry et al., "NIRS measures in pain and analgesia: fundamentals, features, and function,"

Neuroscience & Biobehavioral Reviews, vol. 120, pp. 335–353, 2021.

[47] A. D. Vittersø, G. Buckingham, A. F. Ten Brink, M. Halicka, M. J. Proulx, and J. H. Bultitude, "Characterising sensorimotor adaptation in complex regional pain syndrome," *Cortex*, vol. 140, pp. 157–178, 2021.

[48] J. M. Orr, H. R. Smolker, and M. T. Banich, "Organization of the human frontal pole revealed by large-scale DTI-based connectivity: implications for control of behavior," *PLoS One*, vol. 10, no. 5, article e0124797, 2015.

[49] Y. Wu, D. Sun, Y. Wang, and Y. Wang, "Subcomponents and connectivity of the inferior fronto-occipital fasciculus revealed by diffusion spectrum imaging fiber tracking," *Frontiers in Neuroanatomy*, vol. 10, p. 88, 2016.

[50] W. J. Chang, N. E. O'Connell, E. Burns, L. S. Chipchase, M. B. Liston, and S. M. Schabrun, "Organisation and function of the primary motor cortex in chronic pain: protocol for a systematic review and meta-analysis," *BMJ Open*, vol. 5, no. 11, article e008540, 2015.

[51] W. J. Chang, N. E. O'Connell, P. R. Beckenkamp, G. Alhassani, M. B. Liston, and S. M. Schabrun, "Altered primary motor cortex structure, organization, and function in chronic pain: a systematic review and meta-analysis," *Journal of Pain*, vol. 19, no. 4, pp. 341–359, 2018.

[52] B. Hu, Y. Yu, Y. J. Dai et al., "Multi-modal MRI reveals the neurovascular coupling dysfunction in chronic migraine," *Neuroscience*, vol. 419, pp. 72–82, 2019.

Hindawi
Neural Plasticity
Volume 2022, Article ID 2036736, 19 pages
https://doi.org/10.1155/2022/2036736

Review Article

Repetitive Transcranial Magnetic Stimulation for Neuropathic Pain and Neuropsychiatric Symptoms in Traumatic Brain Injury: A Systematic Review and Meta-Analysis

Xin Li,[1,2] Tijiang Lu,[1] Hong Yu,[1] Jie Shen,[3] Zhengquan Chen,[1] Xiaoyan Yang,[1] Zefan Huang,[1] Yuqi Yang,[4] Yufei Feng,[2] Xuan Zhou,[1] and Qing Du[1,5]

[1]*Department of Rehabilitation, Xinhua Hospital, Shanghai Jiao Tong University School of Medicine, Shanghai 200092, China*
[2]*School of Kinesiology, Shanghai University of Sport, Shanghai 200438, China*
[3]*Rehabilitation Medical Center, Jiaxing Second Hospital, Jiaxing, Zhejiang 314000, China*
[4]*College of Global Public Health, New York University, New York, NY 10003, USA*
[5]*Chongming Branch of Xinhua Hospital, School of Medicine, Shanghai Jiao Tong University, Shanghai 202150, China*

Correspondence should be addressed to Xuan Zhou; zhouxuan@xinhuamed.com.cn and Qing Du; duqing@xinhuamed.com.cn

Received 23 April 2022; Revised 5 June 2022; Accepted 6 July 2022; Published 30 July 2022

Academic Editor: Yazhuo Kong

Neuropathic pain and neuropsychiatric symptoms are common complications reported by the traumatic brain injury (TBI) population. Although a growing body of research has indicated the effectiveness of repetitive transcranial magnetic stimulation (rTMS) for the management of neurological and psychiatric disorders, little evidence has been presented to support the effects of rTMS on neuropathic pain and neuropsychiatric symptoms in patients with TBI in all age groups. In addition, a better understanding of the potential factors that might influence the therapeutic effect of rTMS is necessary. The objective of this preregistered systematic review and meta-analysis was to quantify the effects of rTMS on physical and psychological symptoms in individuals with TBI. We systematically searched six databases for randomized controlled trials (RCTs) of rTMS in TBI patients reporting pain and neuropsychiatric outcomes published until March 20, 2022. The mean difference (MD) with 95% confidence intervals (CIs) was estimated separately for outcomes to understand the mean effect size. Twelve RCTs with 276 TBI patients were ultimately selected from 1605 records for systematic review, and 11 of the studies were included in the meta-analysis. Overall, five of the included studies showed a low risk of bias. The effects of rTMS on neuropathic pain were statistically significant (MD = −1.00, 95% CI -1.76 to -0.25, $P = 0.009$), with high heterogeneity ($I^2 = 76\%$). A significant advantage of 1 Hz rTMS over the right dorsolateral prefrontal cortex (DLPFC) in improving depression (MD = −6.52, 95% CI -11.58 to -1.46, $P = 0.01$) was shown, and a significant improvement was noted in the Rivermead Post-Concussion Symptoms Questionnaire-13 (RPQ-13) scores of mild TBI patients after rTMS (MD = −5.87, 95% CI -10.63 to -1.11, $P = 0.02$). However, no significance was found in cognition measurement. No major adverse events related to rTMS were reported. Moderate evidence suggests that rTMS can effectively and safely improve neuropathic pain, while its effectiveness on depression, postconcussion symptoms, and cognition is limited. More trials with a larger number of participants are needed to draw firm conclusions. This trial is registered with PROSPERO (PROSPERO registration number: CRD42021242364.

1. Introduction

Traumatic brain injury (TBI) is caused by a violent bump, blow, or jolt to the head or a penetrating head injury with substantial neurological disabilities and mental distress. It remains a global health problem, with an annual incidence of 200-1967 cases/100,000 individuals [1]. Approximately half of TBI patients do not reach the preinjury functional level within 1 year, and more than 50% of moderate/severe TBI patients are unable to return to work at 2 and 5 years postinjury [2, 3], which presents a substantial economic burden to victims, their families, and society. Some promising

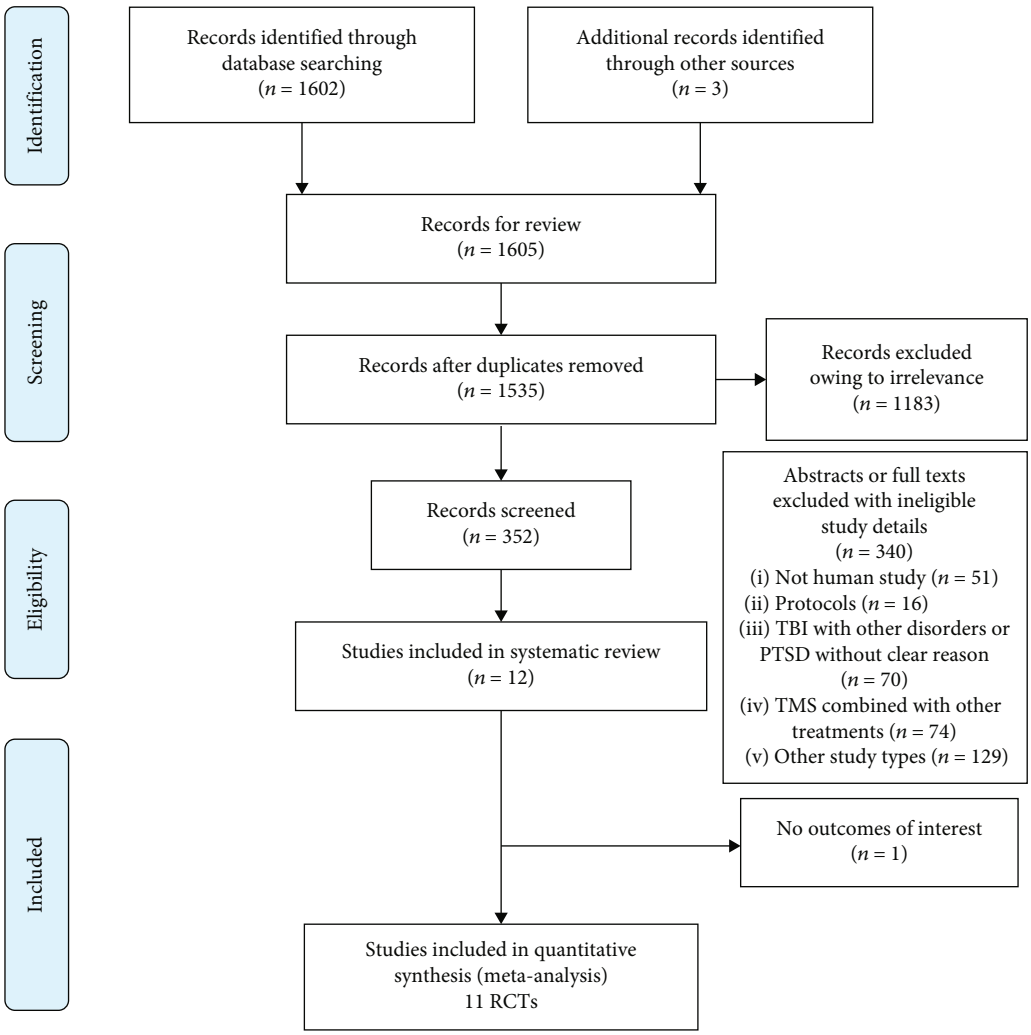

Figure 1: Flow diagram of the selection process.

noninvasive-based approaches have emerged to relieve pain and to improve neural connectivity in people with TBI. Transcranial magnetic stimulation (TMS) is a noninvasive, painless interventional method that induces nerve cell activity in superficial areas of the sensory-motor circuits and facilitates plastic changes in neural networks [4, 5]. Repeated application of TMS at regular intervals, also called repetitive TMS (rTMS), is a tool to enhance clinical recovery in both mild [6, 7] and more severe TBI patients [8–10]. rTMS treatment acts through an electromagnetic field created by a coil placed on the scalp [11], generating a superficial cortical current that is capable of changing neuron activity, even in brain regions that are distant from the stimulation site.

The categorization of TBI into severe, moderate, and mild by scores on the Glasgow coma scale (GCS) is based on clinical grounds (including responses assessed in the visual, motor, and verbal domains) and standard brain imaging. Patients with mild TBI have GCS scores of 13–15 with full neurological recovery, those with moderate TBI have GCS scores of 9–12 with a decreased level of consciousness, and those with severe TBI have GCS scores of 3–8 with coma [12]. Corrigan and Hammond reported that nearly 60% of patients surviving moderate to severe TBI complained of cognitive deficits and behavioral changes [13], which present major barriers to positive social outcomes, such as community reintegration and employment, among post-TBI patients and generate a major socioeconomic impact [14].

Neuropathic pain is another common complication reported by 57.8% of the TBI population, and the cumulative incidence of headache was almost 91% 1 year after mild TBI [15, 16]. Moreover, central pain, which is caused by a lesion or dysfunction of the somatosensory nervous system within the central nervous system and presents as neuropathic pain (such as headache) [17], has been reported to have a similar prevalence across brain trauma severity levels, potentially making it the most prevalent form of chronic pain associated with moderate-to-severe TBI [18]. Patients with central pain usually experience sensations of tingling, chills, itching, and numbness, in addition to pain, as well as abnormal sensations that feel like electrical shocks or burns, especially when numb areas are touched [19], leading to limited functional recovery, impairment in activities of daily living, and poor quality of life.

Table 1: Characteristics of included studies.

Author, year	No. of participants (% men)	Age (y), range/ mean (SD)	Duration since TBI/ concussion (yrs)	Severity of TBI (mild/ moderate/ severe/ unconfirmed)	Medications used	Outcome measures	Time points
Stilling et al., 2020	20 TBI with persistent PTH and PPCS (10%)	18-65; overall: 36.0 (11.4); G1: 40.3 (11.2); G2: 31.6 (10.4)	G1: 2.4(1.2); G2: 3.0(1.0)	G1: 10/0/0/0; G2: 10/0/0/0	OnabotulinumtoxinA: G1: 3, G2: 7; preventative headache medication: (1) Amitriptyline: G1: 3; G2: 1 (2) Topiramate: G1: 1; G2: 1 (3) Duloxetine: G1: 2; G2: 0 (4) Venlafaxine: G1: 1; G2: 0	(1) Headache: NRS (2) Cognition: MoCA, BCPSI, RPSQ (3) Function: HIT-6 (4) Depression: PHQ-9 (5) Anxiety: GAD-7 (6) Posttraumatic stress disorder: PTSD, PCL-5 (7) Quality of life: QOLIBRI	Baseline; midtreatment; posttreatment; 4 weeks/ 12 weeks/24 weeks posttreatment
Rao et al., 2019	30 TBI and anxiety G1: 13; G2:17 Men: 53.3%	Overall: 40 (14.4); G1: 40.2 (14.6); G2: 39.8 (14.2)	Not mentioned	G1: 15/2/0/0 G2: 13/0/0/0	Not mentioned	(1) Depression: HRSD (2) Clinical global impression-severity (CGI-S) scale (3) Clinical global impression-improvement (CGI-I) scale (4) The Beck scale for suicide ideation (BSSI) (5) Cognition: MoCA, RPSQ, BCPSI	Baseline; posttreatment; 4 weeks/8 weeks/12 weeks posttreatment
Moussavi et al., 2019	18 mild TBI; G1: 9; G2: 9; men: 50%	49.5 (12.4)	G1: <1.0; G2: >1.2	Not mentioned	Lamictal, zeldox, Zoloft, clonazapam, trazadone, amitriptyline, amitriptyline	(1) Symptom: RPSQ (2) Depression: MADRS	Baseline; posttreatment; 4 weeks/12 weeks posttreatment
Neville et al., 2019	30 TBI with chronic DAI; G1: 17; G2: 13; men: 90%	18-60; G1: 29.0 (10.35); G2: 32.62 (12.81)	>1.0	Not mentioned	No plans to change during the 90-day study period	(1) Cognition: TMT, COWAT, Stroop test, FPT, DST, SDT (2) Memory: HVLT and BVMT (3) Motor function: GPT	Baseline; posttreatment; 12 weeks posttreatment

Table 1: Continued.

Author, year	No. of participants (% men)	Age (y), range/ mean (SD)	Duration since TBI/ concussion (yrs)	Severity of TBI (mild/ moderate/ severe/ unconfirmed)	Medications used	Outcome measures	Time points
Hoy et al., 2019	21 closed TBI; G1: 11; G2: 10; men: 47.6%	25-78; 46.29 (12.65)	Not mentioned	G1: 7/2/2/0; G2: 5/2/2/1	Antidepressant medication (yes/no): G1: 10/1; G2: 5/5; Mood stabiliser medication (yes/no): G1: 1/10; G2: 0/10; Benzodiazepine medication (yes regular/yes as needed/ no): G1: 0/2/9; G2: 1/1/8; Antipsychotic medication (yes/no): G1: 1/10; G2:1/9;	(1) Depression: MADRS, IDS-CR, IDS-SR (3) Cognition: DST, TMT, arithmetic, RVALT, BVSMT, verbal fluency, Stroop test	Baseline; midtreatment; posttreatment
Siddiqi et al., 2019	15 mild TBI; G1: 9; G2: 5; men: 73.3%	G1: 43.0 (13.0); G2: 50.0 (18.0)	G1: 8.4 (8.2); G2: 8.1 (11.3)	Not mentioned	Not mentioned	(1) Depression: MADRS, DSM-5 (2) Personality: TCI, EB-SRMS, CB-CT, SRHLS, HIT-6	Baseline; midtreatment; posttreatment; 1 week/12 weeks/24 weeks posttreatment
Choi, et al., 2018	12 consecutive patients with mild TBI G1: 6; G2:6 Men: 50%	30-56; overall: 42.6 (8.7) G1: 43.2 (9.7) G2: 42 (8.4)	G1: 17.0 (7.5) G2: 14.3 (7.2)	G1: 6/0/0/0 G2: 6/0/0/0	Not mentioned	(1) Central pain: NPRS (2) Life quality: SF-36	Baseline; midtreatment; posttreatment; 1 week/2 weeks/4 weeks posttreatment
Lee et al., 2018	13 TBI; G1: 7; G2: 6; men: 69.2%	G1: 42.4 (11.3); G2: 41.3 (11.0)	G1: 3.9 (1.7); G2: 3.9 (1.9)	Not mentioned	Not mentioned	(1) Depression: MADRS (2) Cognition: TMT, SCWT	Baseline; posttreatment
Leung et al., 2018	29 mild TBI; G1: 14; G2: 15; men: 79.3%	G1: 33.0 (8.0); G2: 35.0 (8.0)	G1: 7.9 (6.9); G2: 8.3 (4.8)	Not mentioned	Maintain their existing medications	(1) Attention: CPT-II (2) Headache: NPRS, BPI (3) Cognition: WAIS-IV, Stroop test (4) Verbal: HVLT (5) Depression: HRSD (6) PTSD: CAPS	Baseline; 1 week/4 weeks posttreatment
Leung et al., 2016	24 mild TBI; G1: 12; G2: 12; men: 91.7%	G1: 41.2 (14.0); G2: 41.4 (11.6)	G1: 14.8 (14.7); G2: 13.6 (11.8)	Not mentioned	Medications	(1) Headache: NPRS (2) Attention: CPT-II (3) Depression: HRSD (4) PTSD: M-PTSD (5) Pain: BPI	Baseline; 1 week/4 weeks posttreatment

Table 1: Continued.

Author, year	No. of participants (% men)	Age (y), range/ mean (SD)	Duration since TBI/ concussion (yrs)	Severity of TBI (mild/ moderate/ severe/ unconfirmed)	Medications used	Outcome measures	Time points
Franke et al., 2022	28 mild-to-moderate TBI; men: 85.7; G1 (active first): 13/14; G2 (sham first): 11/14	Overall: 45.6 (10.1); G1: 45.1 (11.3); G2: 46.0 (9.0)	Overall: 12.04 (6.8); G1: 11.43 (3.5); G2: 12.64 (9.1)	Mild or moderate	Not mentioned	(1) Depression: CAPS; PHQ-9 (2) Pain: McGill pain questionnaire (3) EEG (4) GSE; PSQI; TBI-QOL	Baseline; posttreatment for first condition (active or sham); pretreatment for second condition; posttreatment for second condition; 2 weeks posttreatment
Rodrigues et al., 2020	36 TBI and anxiety symptoms; G1: 18; G2: 18; men: 88.6%	18-65; G1: 32.8 (13.3); G2: 31.6 (11.3)	Not mentioned	Not mentioned	Not mentioned	(1) STAI-state (2) BDI-I (3) EF index	Baseline; midtreatment; posttreatment; 0 weeks posttreatment; 3 months

BCPSI: British Columbia Postconcussion Symptom Inventory; BDI-II: Beck Depression Inventory-II; BI: Barthel Index; BPI: Brief Pain Inventory; BSSI: Beck Scale for Suicide Ideation; BVMT: Brief Visuospatial Memory Test; BVSMT: brief visual spatial memory test; CAPS: Clinician-Administered PTSD Scale; CB-CT: Cognitive Testing-Cognitive Battery; CGI-I/CGI-S: Clinical Global Improvement-Severity/Improvement Scale Score; CMCT: Central Motor Conduction Time; COWAT: Controlled Oral Word Association Test; CPT-II: Conner's Continuous Performance Test II; DAI: Diffuse Axonal Injury; DSM-5: Diagnostic and Statistical Manual of Mental Disorders; DST: Digit Span Test; EB-SRMS: Emotion Battery-Self-Report Mood Scale; EEG: Electroencephalogram; EF index: Executive Function Index; FMA: Fugl-Meyer Assessment; FPT: Five-Point Test; G1: TMS group; G2: sham group; GAD-7: Generalized Anxiety Disorder Scale-7; GPT: Grooved Pegboard Test; GSE: General Self-Efficacy Scale; HAM-D: Hamilton Rating Scale for Depression; HIT-6: Headache Impact Test 6; HRSA/HRSD: Hamilton Rating Scale for Anxiety/Depression; HVLT: Verbal Hopkins Verbal Learning Test; IDS-CR/IDS-SR: Inventory of Depressive Symptomatology-Clinician Rated Version/Self-Rated Version; M1: primary motor cortex; MADRS: Montgomery-Asberg Depression Rating Scale; MEP: Motor Evoked Potential; MoCA: Montreal Cognitive Assessment; M-PTSD: Mississippi Scale for PTSD; NIHSS: National Institutes of Health Stroke Scale; NPRS: numeric pain rating scale; PCL-5: PTSD Checklist for DSM-5; PCL-M: PTSD Checklist-Military Version; PHQ-9: Patient Health Questionnaire-9; PPCS: persistent postconcussion symptoms; PSQI: Pittsburgh Sleep Quality Index; PTH: Posttraumatic Headache; PTSD: Posttraumatic Stress Disorder; QOLIBRI: Quality of Life after Brain Injury Questionnaire; RPQ: Rivermead Post-Concussion Symptoms Questionnaire; RPSQ-3: Rivermead Post-Concussion Symptoms Questionnaire-3; RVALT: Rey Verbal Auditory Learning Test; SCID: Structured Clinical Interview for DSM-IV Axes I & II; SCWT: Stroop Color-Word Test; SDT: symbol digit test; SF-36: MOS 36-Item Short-Form Health Survey; SRHLS: Self-Report Headache Likert Scores; SSRIs: Selective Serotonin Reuptake Inhibitors; STAI: State-Trait Anxiety Inventory; TBI: traumatic brain injury; TBI-QOL: traumatic brain injury quality of life; TCI: Temperament and Character Inventory; TMS: transcranial magnetic stimulation; TMT: Trail Making Test; WAIS-IV: Wechsler Adult Intelligence Scale; WMFT: Wolf Motor Function Test.

Previous brain stimulation techniques, including rTMS, were recommended in cognitive rehabilitation, with working memory seeming particularly amenable to enhancement [20]. Studies have shown that low-frequency rTMS at 1 Hz decreases cortical excitability, whereas high-frequency rTMS at ≥5 Hz increases the excitability of the cerebral cortex [21, 22]. More specifically, dorsolateral prefrontal cortex (DLPFC) stimulation has been related to improvements in trauma-related conditions [23], such as neurobehavioral gains, cognitive enhancement, and depression reduction [24, 25].

In addition, rTMS has been recommended by the International Federation of Clinical Neurophysiology for the management of neurological and psychiatric disorders [26], and evidence is now quickly increasing, highlighting that DLPFC-rTMS should relieve pain in patients with chronic pain conditions, including migraine [27], spinal cord injury [26], and fibromyalgia syndrome [28]. Actually, a recent meta-analysis found that high-frequency DLPFC stimulation is able to induce an analgesic effect in patients with chronic pain [29], but at present, the overwhelming majority of systematic reviews and meta-analyses on health-related consequences after TBI have focused on depression, memory, selective attention, and postconcussion syndrome [30–32], with far less attention given to neuropathic pain. Therefore, the present systematic review and meta-analysis was aimed at examining the evidence supporting the effectiveness of an rTMS intervention program for neuropathic pain and neuropsychiatric measurements of patients with TBI.

2. Methods

2.1. Study Design. This systematic review and meta-analysis was conducted in accordance with the Preferred Reporting Items for Systematic Reviews and Meta-Analysis (PRISMA) guidelines, and the protocol was registered in the PROSPERO database (No. CRD42021242364).

2.2. Search Strategy. A comprehensive search was conducted in the PubMed, Embase, Cochrane Library, Cumulative Index of Nursing and Allied Health Literature (CINAHL), and Web of Science databases until March 20, 2022. Key terms were used, including "traumatic brain injury," "TBI," "posttraumatic stress disorder," "PTSD," "transcranial magnetic stimulation," and "TMS," to identify articles on the effect of rTMS on TBI. The search strategies are shown in Appendix S1.

Table 2: TMS treatment and control group interventions in the included parallel group trials.

Author, year	TMS treatment group intervention						Sham control group intervention	Study duration	Adverse events
	Coil	Target brain region	Intensity	Frequency	Protocol frequency (sessions∗period)	Stimulation pulse/train			
Stilling et al., 2020	F8	Left DLPFC	70% RMT	10 Hz	1 session/d × 10 d	600/10	A sham air-film coil; the same protocol as TMS group	2 weeks	rTMS group: mild aggravation of headache; scalp discomfort; toothache; dizziness
Rao et al., 2019	A focal double 70 mm air-cooled coil	Right DLPFC	110% RMT	1 Hz	1 sessions/w × 4 w	1200/4	An identically appearing coil that produces the same sound and is the same weight as the active coil, but has negligible magnetic field strength	4 weeks	rTMS group: Headache: 5 Dizziness: 1 Blurred vision: 1 Tiredness: 1 Discomfort: 1 Eye twitching: 1 Sleep problem: 1 Depression: 1 Anxiety: 1 Puffy face: 1 Sham group: Headache: 12 Dizziness: 2 Discomfort: 1 Face twitching: 2 Sleep problem:4 Depression:1 Anxiety:3
Moussavi et al., 2019	F8	Left DLPFC	100% RMT	20 Hz	5 sessions/w × 2 w + 3 sessions/w × 1 w	750/25	The same protocol as TMS group	3 weeks	None
Neville et al., 2019	F8	Left DLPFC	110% RMT	10 Hz	1 session/d × 10 d	2000/40	A similar shape, color, and sound coil as TMS coil	12 weeks	Frequency of mild adverse events rTMS group vs. sham group (70.6% vs. 46.2%)
Hoy et al., 2019	F8	Bilateral DLPFC(right and then to left)	110% RMT	Right: 1 Hz Left: 10 Hz	5 sessions/w × 4 w	Right: 900/1 Left: 1500/30	The same protocol as TMS group; coil angled at 45° off the head	4 weeks	None
	F8	Bilateral DLPFC (right	120% RMT	Right: 1 Hz	1 session/d × 20 d		An alpha sham coil	5 weeks	Transient twitching and

Table 2: Continued.

Author, year	Coil	Target brain region	TMS treatment group intervention			Stimulation pulse/train	Sham control group intervention	Study duration	Adverse events
			Intensity	Frequency	Protocol frequency (sessions∗period)				
		and then to left)		Left: 10 Hz					discomfort in the facial muscles: 7 in rTMS group; Worsening headaches: 1 in rTMS group and 1 in sham group; Presyncopal episode: 1 in rTMS group
Siddiqi et al., 2019						Right: 1000/1 Left: 4000/5			
Choi et al., 2018	F8	M1	90% RMT	10 Hz	5 sessions/w × 2 w	1000/20	The same protocol as TMS group	2 weeks	None
Lee et al., 2018	F8	Right DLPFC	100% RMT	1 Hz	5 sessions/w × 2 w	2000/50	A same size and shape coil as TMS coil	2 weeks	None
Leung et al., 2018	F8	Left DLPFC	80% RMT	10 Hz	4 sessions/w × 1 w	2000/20	180° away from the scalp after the RMT and with the coil side facing the scalp shielded with a molded cover containing two layers of Giron magnetic shielding film	1 week	Not mentioned
Leung et al., 2016	F8	Left MC	80% RMT	10 Hz	3 sessions/w × 1 w	2000/20	Visualize the movement of coil and treatment beam over their own cortices on the monitor, and heard the sound and felt the vibration of the stimulation just like the patients receiving the active treatment	1 week	None
Franke et al., 2022	F8	Right DLPFC	80% RMT for day1 and 100% RMT thereafter	10 Hz	1 sessions/d × 5 d	—	Stimulation set at 25% RMT with the coil tilted 90 degrees from the scalp	5 days	Not mentioned

F8: figure of 8 coil; ABP: abductor pollicis brevis; RMT: resting motor threshold; DLPFC: dorsolateral prefrontal cortex; M1: primary motor cortex area, MT: motor threshold; MC: motor cortex.

Table 3: The Cochrane tool of assessing risk of bias for methodological assessment (RoB 2.0 tool).

Article, year	Randomization process	Deviations from intended interventions	Missing outcome data	Measurement of the outcome	Selection of the reported	Overall
Stilling et al., 2020	Low	Low	Low	Unclear	Low	Unclear
Moussavi et al., 2019	Low	High	Low	High	Low	High
Neville et al., 2019	Low	Low	Low	Unclear	Low	Unclear
Hoy et al., 2019	Low	Low	Low	Low	Low	Low
Siddiqi et al., 2019	Unclear	Low	Low	Low	Low	Unclear
Choi et al., 2018	Low	Low	Low	Low	Low	Low
Lee et al., 2018	Low	Low	Low	High	Low	High
Leung et al., 2018	Low	Low	Low	Low	Low	Low
Leung et al., 2016	Low	Low	Low	Low	Low	Low
Rao et al., 2019	Low	Low	Low	Low	Low	Low
Franke et al., 2022	Unclear	Low	Low	Low	Low	Unclear

RoB: risk of bias.

Two reviewers (Xin Li and Xiaoyan Yang) independently assessed the eligibility of the literature. The preliminary screening was based on the titles and abstracts. The selected articles were then evaluated in their entirety. If there was a disagreement, the full text of the article was checked and discussed, if necessary, with third-party adjudication (Yuqi Yang).

2.3. Eligibility Criteria and Selection Process. Studies were considered eligible if they met the following criteria: (1) *population*: patients who were diagnosed with TBI, with no restrictions on sex, age, or ethnicity; (2) *intervention*: rTMS; medication was allowed during rTMS; (3) *comparisons*: sham stimulation or any conventional TBI treatment (e.g., pharmacological therapy or nonpharmacological therapy); (4) *outcomes*: neuropathic pain (including central pain and headache) and neuropsychiatric symptoms (including postconcussive symptoms, depression, or cognitive function); and (5) *study design*: randomized controlled trials (RCTs) published in peer-reviewed English journals.

2.4. Outcome Measurements and Data Extraction. Change in neuropathic pain was the primary outcome for extraction. Self-reported neuropathic pain was assessed by the numeric pain rating scale (NPRS), an 11-point scale with scores ranging from 0 to 10, where "0" indicates no pain and "10" suggests the most severe pain imaginable. When reported, changes in depression severity evaluated by the Montgomery-Asberg Depression Rating Scale (MADRS), Hamilton Rating Scale for Depression (HRSD), Inventory of Depressive Symptomatology (IDS), or Patient Health Questionnaire-9 (PHQ-9) were extracted, with high scores representing severe depression. Data on postconcussive symptoms and cognition were also extracted as the secondary outcomes, and an MD was calculated from pre- to postintervention.

Two reviewers (Hong Yu and Xuan Zhou) independently extracted data from the included studies. If the opinions were inconsistent, a third reviewer reevaluated the articles and discussed them with the two reviewers to reach an agreement. They extracted the following data using a data extraction form: study design, number of participants, age, duration since TBI/concussion, severity of TBI, medication used, outcome assessed, interventions, comparators, relevant statistical data, and adverse events. The intervention protocols of the rTMS group and control group were extracted and included the following details: coil, intensity, frequency, stimulation pulse/train, target brain region, sessions, study duration, and adverse events.

The mean, standard deviation (SD), and sample size were extracted for the outcome measures in each group (i.e., active and sham) for the pooled analysis. Published protocols were referenced, and the corresponding authors were contacted for additional data when data were not directly available in the article.

2.5. Risk of Bias Assessment. Reviewers (Tijiang Lu, Jie Shen, and Zefan Huang) independently assessed the methodological quality of the included studies using the revised Cochrane risk-of-bias assessment tool (RoB 2.0) for RCTs [33]. There are five domains in RoB 2.0: the randomization process, deviations from the intended intervention, missing outcome data, the measurement of the outcome, and selection of the reported outcomes. For missing outcome data in individual studies, we stipulated a low risk of bias for a loss to follow-up of less than 10% and a difference of less

Study or subgroup	TMS Mean	TMS SD	TMS Total	Sham Mean	Sham SD	Sham Total	Weight	Mean difference IV, Random, 95% CI
1.1.1 mid-treatment								
Choi, G. S. 2018	−1.13	0.69	6	0.2	0.77	6	11.3%	−1.33 [−2.16, −0.50]
Stilling, J. 2020	−1.7	9.62	10	−1.3	13	10	0.5%	−0.40 [−10.42, 9.62]
Subtotal (95% CI)			16			16	11.8%	−1.32 [−2.15, −0.50]
Heterogeneity: $\tau^2 = 0.00$; $\chi^2 = 0.03$, df = 1 ($P = 0.86$); $I^2 = 0\%$								
Test for overall effect: $Z = 3.15$ ($P = 0.002$)								
1.1.2 post-treatment								
Choi, G. S. 2018	−1.97	0.72	6	0.04	0.72	6	11.3%	−2.01 [−2.82, −1.20]
Stilling, J. 2020	−3.7	11.11	10	−2.5	13.27	10	0.5%	−1.20 [−11.93, 9.53]
Subtotal (95% CI)			16			16	11.8%	−2.01 [−2.82, −1.19]
Heterogeneity: $\tau^2 = 0.00$; $\chi^2 = 0.02$, df = 1 ($P = 0.88$); $I^2 = 0\%$								
Test for overall effect: $Z = 4.84$ ($P < 0.00001$)								
1.1.3 post-treatment 1 week								
Choi, G. S. 2018	−2.63	0.72	6	0.36	0.72	6	0.0%	−2.99 [−3.80, −2.18]
Leung, A. 2016	−3.56	2.41	12	−1.09	1.77	12	7.9%	−2.47 [−4.16, −0.78]
Leung, A. 2018	−1.38	−1.88	14	0	1.51	15	9.6%	−1.38 [−2.63, −0.13]
Subtotal (95% CI)			26			27	17.5%	−1.77 [−2.79, −0.75]
Heterogeneity: $\tau^2 = 0.02$; $\chi^2 = 1.03$, df = 1 ($P = 0.31$); $I^2 = 3\%$								
Test for overall effect: $Z = 3.39$ ($P = 0.0007$)								
1.1.4 post-treatment 4 weeks								
Choi, G. S. 2018	−2.47	0.74	6	0.03	0.72	6	11.3%	−2.50 [−3.33, −1.67]
Leung, A. 2016	−2.5	2.64	12	−2.36	2.02	12	7.2%	−0.14 [−2.02, 1.74]
Leung, A. 2018	−1.3	−1.88	14	−0.09	1.56	15	9.5%	−1.21 [−2.47, 0.05]
Stilling, J. 2020	−0.21	1.47	10	−0.41	1.01	10	10.2%	0.20 [−0.91, 1.31]
Subtotal (95% CI)			42			43	38.2%	−0.99 [−2.40, 0.42]
Heterogeneity: $\tau^2 = 1.64$; $\chi^2 = 16.63$, df = 3 ($P = 0.0008$); $I^2 = 82\%$								
Test for overall effect: $Z = 1.38$ ($P = 0.17$)								
1.1.5 post-treatment 12 weeks								
Stilling, J. 2020	−0.47	1.44	10	−0.42	1.14	10	10.0%	−0.05 [−1.19, 1.09]
Subtotal (95% CI)			10			10	10.0%	−0.05 [−1.19, 1.09]
Heterogeneity: Not applicable								
Test for overall effect: $Z = 0.09$ ($P = 0.93$)								
1.1.6 post-treatment 24 weeks								
Stilling, J. 2020	0.25	1.22	10	−0.66	0.93	10	10.8%	0.91 [−0.04, 1.86]
Subtotal (95% CI)			10			10	10.8%	0.91 [−0.04, 1.86]
Heterogeneity: Not applicable								
Test for overall effect: $Z = 1.88$ ($P = 0.06$)								
Total (95% CI)			120			122	100.0%	−1.00 [−1.76, −0.25]
Heterogeneity: $\tau^2 = 1.14$; $\chi^2 = 45.63$, df = 11 ($P < 0.00001$); $I^2 = 76\%$								
Test for overall effect: $Z = 2.61$ ($P = 0.009$)								
Test for subgroup differences: $\chi^2 = 26.81$. df = 5 ($P < 0.0001$). $I^2 = 81.4\%$								

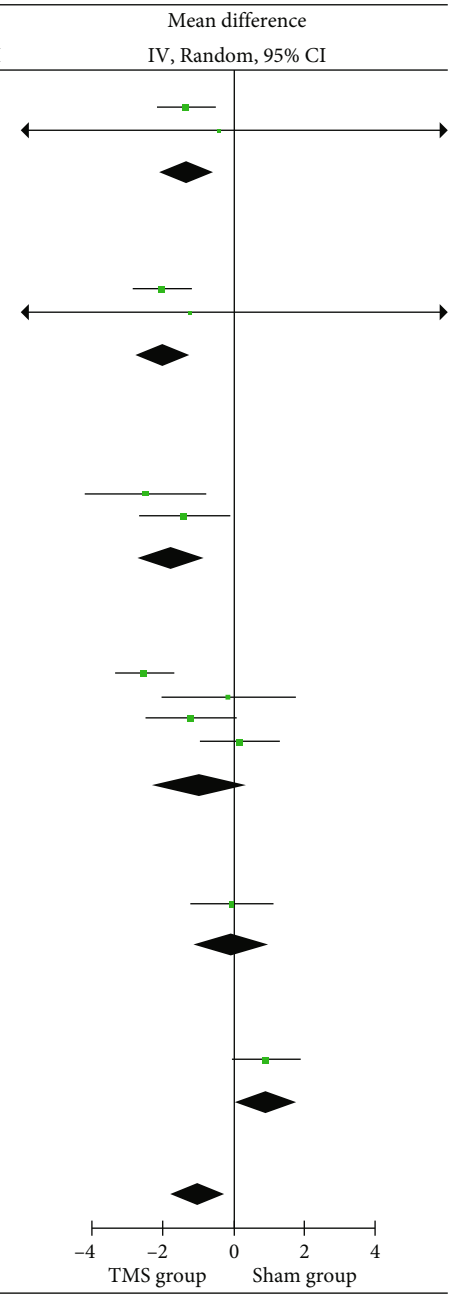

Figure 2: Forest plots of the different-term effects of rTMS on self-reported neuropathic pain in TBI.

than 5% in missing data between intervention and control groups. Publication bias was assessed through visual inspection of funnel plots for each outcome in which 10 or more eligible studies were identified.

2.6. Meta-Analysis and Subgroup Analyses. Review Manager Software version 5.3 (Cochrane Collaboration, Oxford, England) was used to analyze the data in this meta-analysis (Xin Li and Qing Du). The effect of rTMS was expressed as the mean difference (MD) with 95% confidence intervals (CIs). The heterogeneity was estimated by using the I^2 test. If the I^2 value was less than 50%, the fixed-effect model was used; otherwise, a random-effect model was used. A statistically significant P value was set at 0.05. Moreover, meta-analysis was performed on outcome measures of different postintervention time points according to the included studies. As provoked depression studies evaluated by MADRS reported stimulation over the bilateral, left, or right DLPFC, subgroup analyses were further conducted based on the target brain region.

2.7. Certainty of Evidence. We summarized the evidence and assessed its certainty separately for bodies of evidence from RCTs. Two reviewers (Zhengquan Chen and Yufei Feng) used the Grading of Recommendations Assessment, Development and Evaluation (GRADE) methodology to rate the certainty of the evidence for each outcome as high, moderate, low, or very low. Detailed GRADE guidance was used

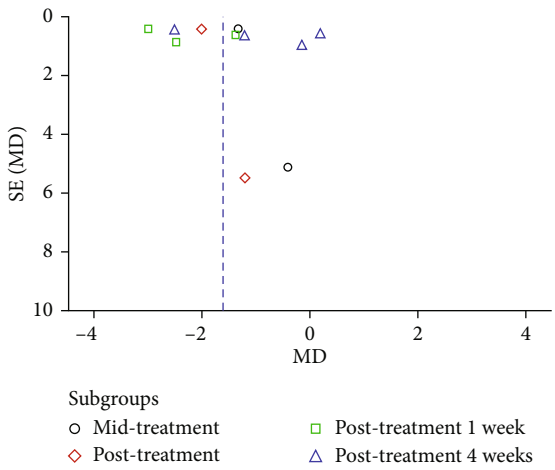

Figure 3: Funnel plot regarding self-reported neuropathic pain in the rTMS group compared with the control group.

to assess the overall risk of bias, imprecision, inconsistency, indirectness, and publication bias and to summarize the results [34].

3. Results

3.1. Study Selection. Twelve RCTs were ultimately selected for systematic review from 1605 records with a total of 276 TBI patients [7, 10, 35–45], and 11 of them with 236 patients were included in the meta-analysis [7, 35–43, 45], as shown in Figure 1.

The baseline demographic and clinical characteristics of the included studies are shown in Table 1. The age of the included patients was between 14 and 65 years. The included studies reported neuropathic pain (including posttraumatic headache), posttraumatic stress disorder (PTSD) symptoms, or mental health issues, such as declines in cognitive function and depression. In most of the studies, the intervention groups were treated with both rTMS and drugs. All patients were in subacute and chronic stages, from 3 weeks to over 20 years after their injuries. The follow-up time was up to 24 weeks after rTMS treatment.

Four included studies stimulated the left DLPFC with 10-20 Hz high-frequency rTMS [35–37, 42], while others applied rTMS over the right DLPFC ($n = 3$) [41, 43, 45], the bilateral DLPFC ($n = 2$) [38, 39], or the motor cortex ($n = 2$) [7, 40] with stimulation of 1 Hz or 10 Hz. Four studies used 70%-90% resting motor threshold (RMT) subthreshold stimulation [7, 35, 40, 42], and 7 studies used 100% RMT to 120% RMT suprathreshold stimulation [36–39, 41, 43, 45]. The intervention duration ranged from 5 days to 4 weeks, with frequencies ranging from 3 sessions per week to 20 sessions per day. Table 2 summarizes the detailed intervention protocols of the rTMS interventions and sham interventions in the 11 articles.

The risk of bias measured by the RoB 2.0 tool in the 11 studies included for meta-analysis is presented in Table 3. Overall, five studies showed a low risk of bias. Ten RCTs generated an adequately randomized sequence, and eight of them were conducted using a blinded method for the outcome measurement. Ratings using the GRADE methodology for all outcome measurements were inconsistent and ranged from moderate to very low quality (see Appendix S2); therefore, most studies were classified as fair.

3.2. Primary Outcome

3.2.1. Neuropathic Pain. Three studies investigated the effect of rTMS on chronic posttraumatic headache (over 3 months) [7, 35, 42], whereas one study included patients with central pain (consisting of shooting pain, burning pain, etc.) lasting for 6 months [40]. In the three studies examining headache, the duration of treatment was from 1 week to 2 weeks (3 sessions to 10 sessions), whereas in the study of central pain, the intervention frequency was 5 sessions per week, lasting for 2 weeks. When the data from four randomized controlled studies were pooled, significant improvement in pain was found to be associated with rTMS in TBI patients (MD = −1.00, 95% CI -1.76 to -0.25, $P = 0.009$). However, there was strong evidence of heterogeneity ($I^2 = 76\%$) (Figure 2), which might be due to the inconsistent distinct targeted brain regions and diversified follow-up durations.

The four studies had an intervention duration of 1 to 2 weeks, and the outcome measures were collected at baseline and posttreatment (or 1 week posttreatment), with at least 4 weeks of observation after the intervention. The pooled results showed midtreatment and posttreatment effects, as a significant analgesic effect was found in the rTMS group (MD = −1.32, 95% CI -2.15 to -0.50, $P = 0.002$ and MD = −2.01, 95% CI -2.82 to -1.19, $P < 0.0001$, respectively) [35, 40]. The pooled data of three studies showed that a significant change in pain in the rTMS group was found at the 1-week follow-up after treatment (MD = −1.77, 95% CI -2.79 to -0.75, $P < 0.001$, $I^2 = 3\%$) [7, 40, 42]. After four weeks of follow-up, no significant differences were found between the rTMS and sham control groups (MD = −0.99, 95% CI -2.40 to 0.42, $P = 0.17$) with high heterogeneity ($I^2 = 82\%$), which seemed to be associated with the small number of rTMS sessions reported in the study of Leung et al. [7, 42]. Only Stilling et al. reported the mean changes in headache severity at 3 months and 6 months postintervention, but no significant difference was revealed ($P = 0.93$ and $P = 0.06$, respectively) (Figure 2) [35]. In addition, the funnel plot showed an asymmetrical distribution regarding central pain or headache, suggesting a high risk of publication bias (Figure 3).

3.3. Secondary Outcomes

3.3.1. Depression. Nine of the included studies evaluated the effect of rTMS on depression [7, 35, 36, 38, 39, 41–43, 45], and the Montgomery-Asberg Depression Rating Scale (MADRS), Hamilton Rating Scale for Depression (HRSD), Inventory of Depressive Symptomatology (IDS), or Patient Health Questionnaire-9 (PHQ-9) was used to rate depression, with high scores representing severe depression. The interventional protocol in the nine studies also varied from 3 sessions of 80% RMT intensity to 20 sessions of 120%

Study or subgroup	TMS Mean	TMS SD	TMS Total	Sham Mean	Sham SD	Sham Total	Weight	Mean difference IV, Random, 95% CI
1.3.1 mid treatment								
Siddigi, S. H. 2019	−10.29	10.76	9	−8.11	7.79	9	12.9%	−2.18 [−10.86, 6.50]
Subtotal (95% CI)			9			9	12.9%	−2.18 [−10.86, 6.50]
Heterogeneity: Not applicable								
Test for overall effect: $Z = 0.49$ ($P = 0.62$)								
1.3.2 post treatment								
Hoy, K. E. 2019	−6.54	10.45	11	−10.27	10	10	12.7%	3.73 [−5.02, 12.48]
Lee, S. A. 2018	−6.86	5.28	7	−0.34	4.02	6	28.9%	−6.52 [−11.58, −1.46]
Moussavi, Z. 2019	−3.2	5.65	9	−2.3	11.39	9	13.8%	−0.90 [−9.21, 7.41]
Siddiqi, S. H. 2019	−17.91	12.71	9	−4.3	14.23	5	4.8%	−13.61 [−28.59, 1.37]
Subtotal (95% CI)			36			30	60.2%	−3.42 [−9.41, 2.56]
Heterogeneity: $\tau^2 = 18.15$; $\chi^2 = 6.06$, df = 3 ($P = 0.11$); $I^2 = 51\%$								
Test for overall effect: $Z = 1.12$ ($P = 0.26$)								
1.3.3 post-treatment 4 weeks								
Moussavi, Z. 2019	−3.5	7.5	9	−4.2	9.71	9	14.7%	0.70 [−7.32, 8.72]
Subtotal (95% CI)			9			9	14.7%	0.70 [−7.32, 8.72]
Heterogeneity: Not applicable								
Test for overall effect: $Z = 0.17$ ($P = 0.86$)								
1.3.4 post-treatment 12 weeks								
Moussavi, Z. 2019	−3.5	9.23	9	−2.2	10.1	9	12.2%	−1.30 [−10.24, 7.64]
Subtotal (95% CI)			9			9	12.2%	−1.30 [−10.24, 7.64]
Heterogeneity: Not applicable								
Test for overall effect: $Z = 0.29$ ($P = 0.78$)								
Total (95% CI)			63			57	100.0%	−2.53 [−5.92, 0.86]
Heterogeneity: $\tau^2 = 3.68$; $\chi^2 = 7.27$, df = 6 ($P = 0.30$); $I^2 = 18\%$								
Test for overall effect: $Z = 1.46$ ($P = 0.14$)								
Test for subgroup differences: $\chi^2 = 0.67$. df = 3 ($P = 0.88$). $I^2 = 0\%$								

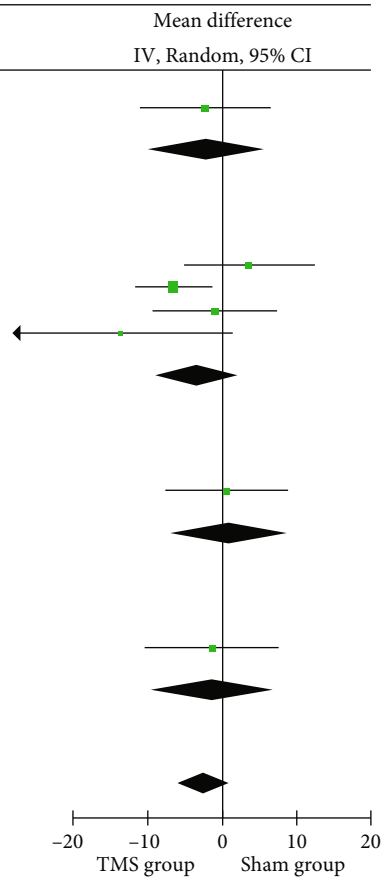

(a)

Study or subgroup	TMS Mean	TMS SD	TMS Total	Sham Mean	Sham SD	Sham Total	Weight	Mean difference IV, Random, 95% CI
1.4.1 Bilateral DLPFC								
Hoy, K. E. 2019	−6.54	10.45	11	−10.27	10	10	24.5%	3.73 [−5.02, 12.48]
Siddiqi, S. H. 2019	−17.91	12.71	9	−4.3	14.23	5	12.2%	−13.61 [−28.59, 1.37]
Subtotal (95% CI)			20			15	36.6%	−3.83 [−20.68, 13.02]
Heterogeneity: $\tau^2 = 111.15$; $\chi^2 = 3.84$, df = 1 ($P = 0.05$); $I^2 = 74\%$								
Test for overall effect: $Z = 0.45$ ($P = 0.66$)								
1.4.2 Right DLPFC								
Lee, S. A. 2018	−6.86	5.28	7	−0.34	4.02	6	37.5%	−6.52 [−11.58, −1.46]
Subtotal (95% CI)			7			6	37.5%	−6.52 [−11.58, 1.46]
Heterogeneity: Not applicable								
Test for overall effect: $Z = 2.52$ ($P = 0.01$)								
1.4.3 Left DLPFC								
Moussavi, Z. 2019	−3.2	5.65	9	−2.3	11.39	9	25.8%	−0.90 [−9.21, 7.41]
Subtotal (95% CI)			9			9	25.8%	−0.90 [−9.21, 7.41]
Heterogeneity: Not applicable								
Test for overall effect: $Z = 0.21$ ($P = 0.83$)								
Total (95% CI)			36			30	100.0%	−3.42 [−9.41, 2.56]
Heterogeneity: $\tau^2 = 18.15$; $\chi^2 = 6.06$, df = 3 ($P = 0.11$); $I^2 = 51\%$								
Test for overall effect: $Z = 1.12$ ($P = 0.26$)								
Test for subgroup differences: $\chi^2 = 1.30$. df = 2 ($P = 0.52$). $I^2 = 0\%$								

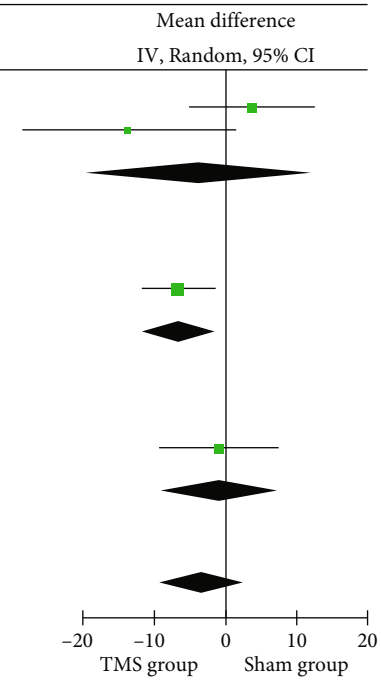

(b)

Figure 4: Forest plots of the effect of rTMS on depression measured by the MADRS in TBI patients. (a) Total analysis; (b) subgroup analysis of posttreatment effectiveness. DLPFC: dorsolateral prefrontal cortex; MADRS: Montgomery-Asberg Depression Rating Scale.

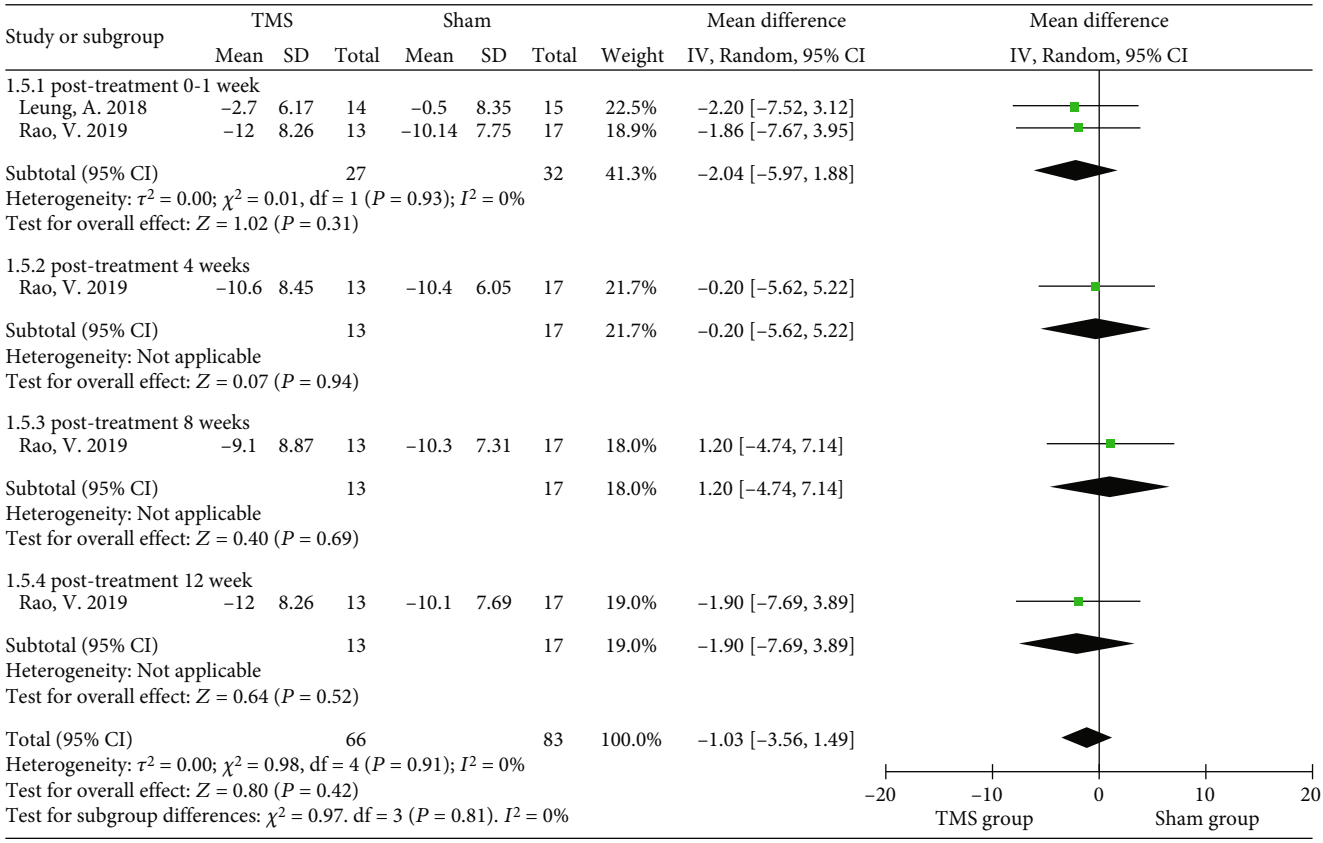

Figure 5: Forest plots of the effect of rTMS on depression measured by the HRSD in TBI patients. HRSD: Hamilton Rating Scale for Depression.

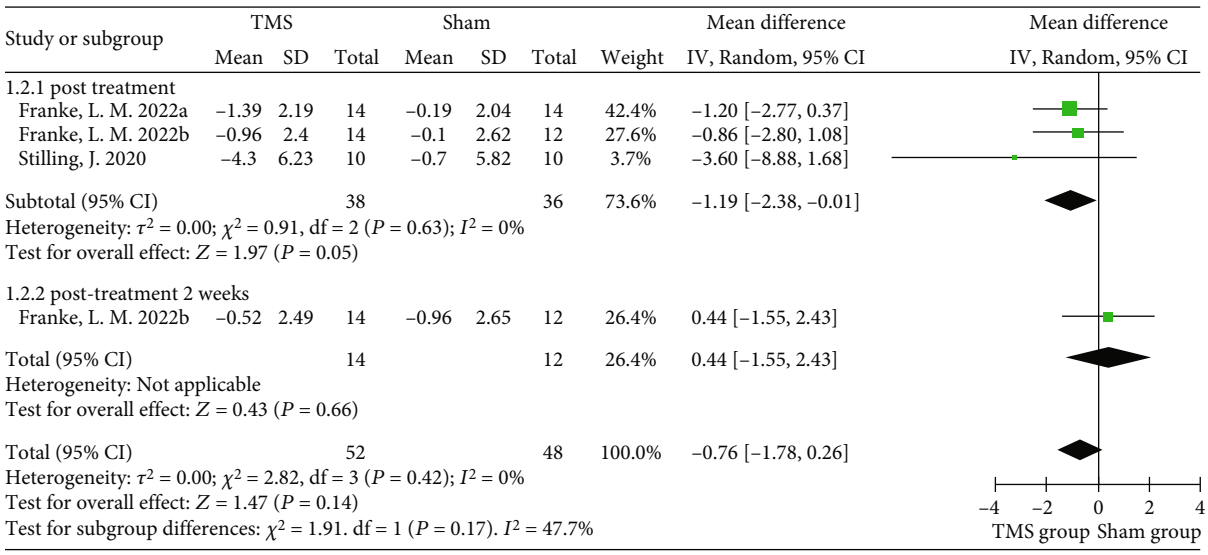

Figure 6: Forest plots of different-term effects of rTMS on depression measured by the PHQ-9 in TBI patients. PHQ-9: Patient Health Questionnaire-9.

RMT intensity. No significant improvement in depression was found after rTMS intervention (MD = −2.53, 95% CI -5.92 to 0.86, $P = 0.14$, $I^2 = 18\%$) when the MADRS data from four randomized controlled studies were pooled (Figure 4(a)). Subgroup analysis of MADRS data showed no significant difference between groups of patients receiving either bilateral ($P = 0.66$) or left rTMS ($P = 0.83$) on DLPFC areas immediately posttreatment, while Lee and Kim introduced a significant advantage of 1 Hz right DLPFC-rTMS in improving depression (MD = −6.52, 95%

Study or subgroup	TMS Mean	TMS SD	TMS Total	Sham Mean	Sham SD	Sham Total	Weight	Mean difference IV, Random, 95% CI
1.8.1 post-treatment								
Rao, V. 2019	−14.94	8.73	13	−11.36	12.51	17	28.3%	−3.58 [−11.19, 4.03]
Subtotal (95% CI)			13			17	28.3%	−3.58 [−11.19, 4.03]
Heterogeneity: Not applicable								
Test for overall effect: $Z = 0.92$ ($P = 0.36$)								
1.8.2 post-treatment 4 weeks								
Rao, V. 2019	−12.6	10.57	13	−12.13	12.32	17	24.4%	−0.47 [−8.67, 7.73]
Subtotal (95% CI)			13			17	24.4%	−0.47 [−8.67, 7.73]
Heterogeneity: Not applicable								
Test for overall effect: $Z = 0.11$ ($P = 0.91$)								
1.8.3 post-treatment 8 weeks								
Rao, V. 2019	−14.02	10.74	13	−11.27	12.71	17	23.2%	−2.75 [−11.15, 5.65]
Subtotal (95% CI)			13			17	23.2%	−2.75 [−11.15, 5.65]
Heterogeneity: Not applicable								
Test for overall effect: $Z = 0.64$ ($P = 0.52$)								
1.8.4 post-treatment 12 weeks								
Rao, V. 2019	−16.23	8.31	13	−8.84	14.55	17	24.0%	−7.39 [−15.65, 0.87]
Subtotal (95% CI)			13			17	24.0%	−7.39 [−15.65, 0.87]
Heterogeneity: Not applicable								
Test for overall effect: $Z = 1.75$ ($P = 0.08$)								
Total (95% CI)			52			68	100.0%	−3.55 [−7.60, 0.51]
Heterogeneity: $\tau^2 = 0.00$; $\chi^2 = 1.41$, df = 3 ($P = 0.70$); $I^2 = 0\%$								
Test for overall effect: $Z = 1.72$ ($P = 0.09$)								
Test for subgroup differences: $\chi^2 = 1.41$. df = 3 ($P = 0.70$). $I^2 = 0\%$								

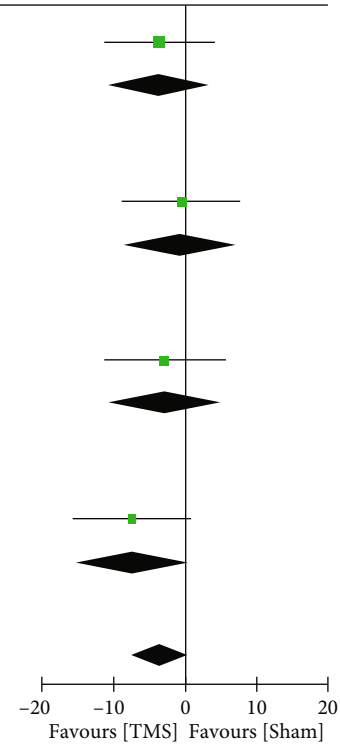

(a)

Study or subgroup	TMS Mean	TMS SD	TMS Total	Sham Mean	Sham SD	Sham Total	Weight	Mean difference IV, Random, 95% CI
1.10.1 post treatment								
Moussavi, Z. 2019	−4	10.19	9	−1.6	10.57	9	24.6%	−2.40 [−11.99, 7.19]
Subtotal (95% CI)			9			9	24.6%	−2.40 [−11.99, 7.19]
Heterogeneity: Not applicable								
Test for overall effect: $Z = 0.49$ ($P = 0.62$)								
1.10.2 post-treatment 4 weeks								
Moussavo, Z. 2019	−11	10.51	9	−1.4	10.05	9	25.1%	−9.60 [−19.10, −0.10]
Stilling, J. 2020	−7.1	11.58	10	−2.8	7.6	10	30.7%	−4.30 [−12.88, 4.28]
Subtotal (95% CI)			19			19	55.8%	−6.68 [−13.05, −0.31]
Heterogeneity: $\tau^2 = 0.00$; $\chi^2 = 0.66$, df = 1 ($P = 0.42$); $I^2 = 0\%$								
Test for overall effect: $Z = 2.06$ ($P = 0.04$)								
1.10.3 post-treatment 8 weeks								
Moussavi, Z. 2019	−10.2	11.01	9	−2.3	12.19	9	19.6%	−7.90 [−18.63, 2.83]
Subtotal (95% CI)			9			9	19.6%	−7.90 [−18.63, 2.83]
Heterogeneity: Not applicable								
Test for overall effect: $Z = 1.44$ ($P = 0.15$)								
Total (95% CI)			37			37	100.0%	−5.87 [−10.63, −1.11]
Heterogeneity: $\tau^2 = 0.00$; $\chi^2 = 1.36$, df = 3 ($P = 0.71$); $I^2 = 0\%$								
Test for overall effect: $Z = 2.42$ ($P = 0.02$)								
Test for subgroup differences: $\chi^2 = 0.70$. df = 2 ($P = 0.70$). $I^2 = 0\%$								

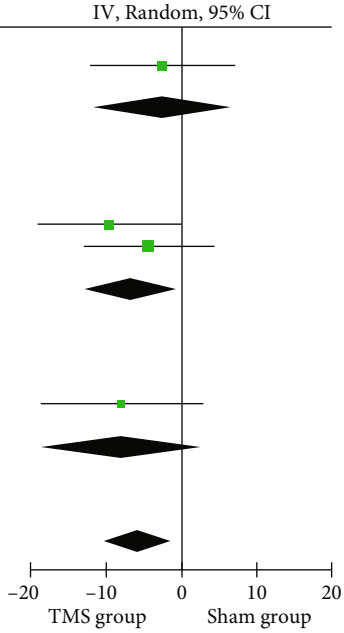

(b)

Figure 7: Continued.

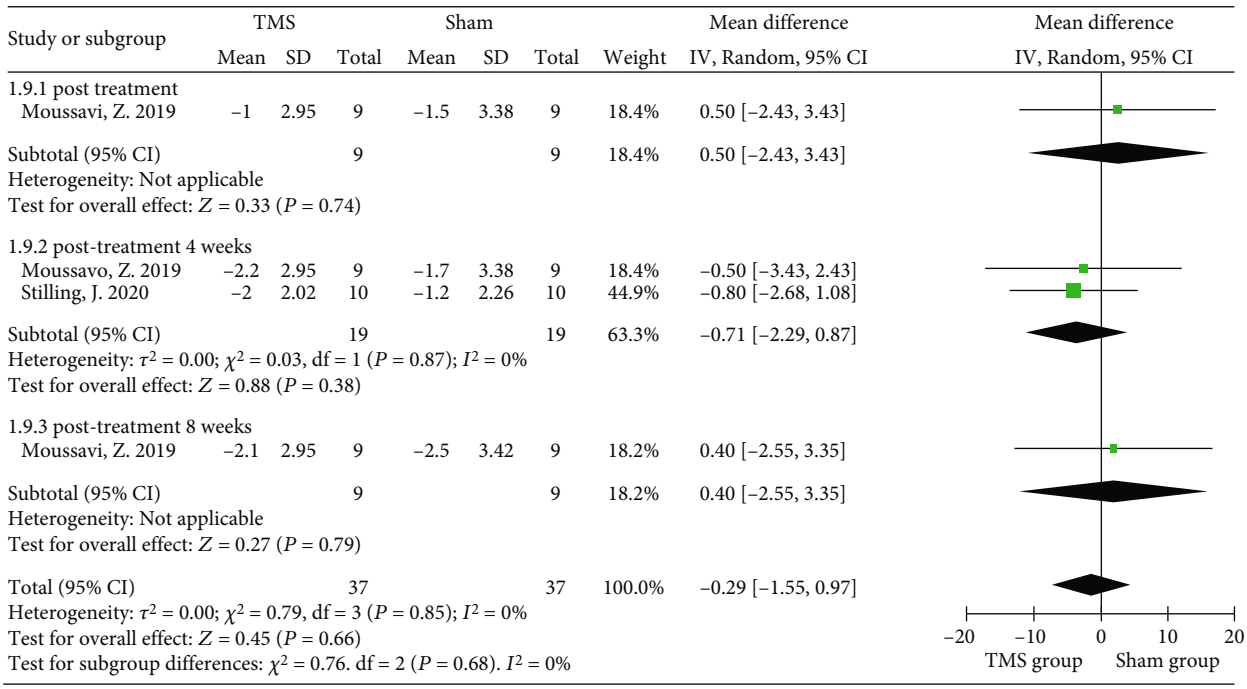

(c)

Figure 7: Forest plots of different parts of rTMS on the severity of different symptoms measured by the RPQ in TBI patients: (a) the RPQ; (b) the RPQ-13; (c) the RPQ-3. RPQ: Rivermead Post-Concussion Questionnaire.

CI -11.58 to -1.46, $P = 0.01$) (Figure 4(b)) [41]. Similarly, no significant improvement in depressive symptoms was found using HRSD scores (MD = −1.03, 95% CI -3.56 to 1.49, $P = 0.42$, $I^2 = 0\%$) (Figure 5). The PHQ-9 was used in 2 studies, and no significant result was found (MD = −0.76, 95% CI -1.78 to 0.26, $P = 0.14$, $I^2 = 47.7\%$) (Figure 6).

3.3.2. Postconcussive Symptoms. The Rivermead Post-Concussion Symptoms Questionnaire (RPQ) is a self-reported and reliable measure of PCS. Scores from the 16 RPQ questions can range from 0 to 64, as symptoms are rated on a 4-point Likert scale, ranging from "not experienced at all" to "a severe problem" [46]. In the meta-analysis, the 16 questions making up the RPQ were only used in one RCT [43], and the pooled data among varied follow-up durations showed no significant difference (MD = −3.55, 95% CI -7.60 to 0.51, $P = 0.09$) (Figure 7(a)). Otherwise, the RPQ could be broken into the RPQ-13 (cognitive and emotional) and the RPQ-3 (headaches, dizziness, and nausea) to form a unidimensional construct [47]. The subgroup analysis showed that rTMS over the left DLPFC could generate a significant and sustained improvement, especially at 4 weeks of follow-up, as measured by the RPQ-13 scores (MD = −5.87, 95% CI -10.63 to -1.11, $P = 0.02$, $I^2 = 0\%$) (Figure 7(b)). However, no significant changes were found in the RPQ-3 scores of mild TBI patients between the rTMS and sham groups after intervention ($P = 0.66$, Figure 7(c)). In addition, postconcussive symptoms were not explored in the included studies that recruited moderate and severe TBI patients.

3.3.3. Cognition. A large variety of questionnaires and cognitive tests were used in the included studies, such as the Wechsler Adult Intelligence Scale (WAIS) and Montreal Cognitive Assessment (MoCA). Due to the insufficient number of studies using the WAIS, data pooling could not be executed. However, the Trailmaking Test (TMT) [37, 38, 43] and Stroop Color-Word Test (SCWT) [38, 41, 43] were used in three included studies. The TMT is a psychological test scoring the time spent connecting numbered circles in sequential order, with the TMT-A and TMT-B representing two subtests by connecting numbered circles in specific order. A meta-analysis revealed insignificant changes in TMT-A (MD = −0.87, 95% CI −6.51 to 4.76, $P = 0.76$, $I^2 = 9\%$) and TMT-B (MD = −5.15, 95% CI −20.19 to 9.89, $P = 0.5$, $I^2 = 0\%$) scores after rTMS intervention (Figure 8). Three RCTs used the SCWT to assess the ability to inhibit cognitive interference; two of the RCTs recorded the number of words (word task), number of bar colors (color task), and number of color words (color-word task) spoken within a specified time, while the other RCT analyzed the accumulated time for completing the 3 tasks [41]. No significant difference was revealed from the pooled analysis (MD = 0.66, 95% CI -6.52 to 7.84, $P = 0.86$, $I^2 = 0\%$) (Figure 9).

3.3.4. Adverse Events. The included RCTs did not report major adverse events, such as vomiting or syncope, during the rTMS interventions, although several mild side effects were reported, including headache, scalp discomfort, toothache, transient twitching, or neck discomfort (Table 2). In one study, the rate of side effects was up to 70.6% during the rTMS intervention.

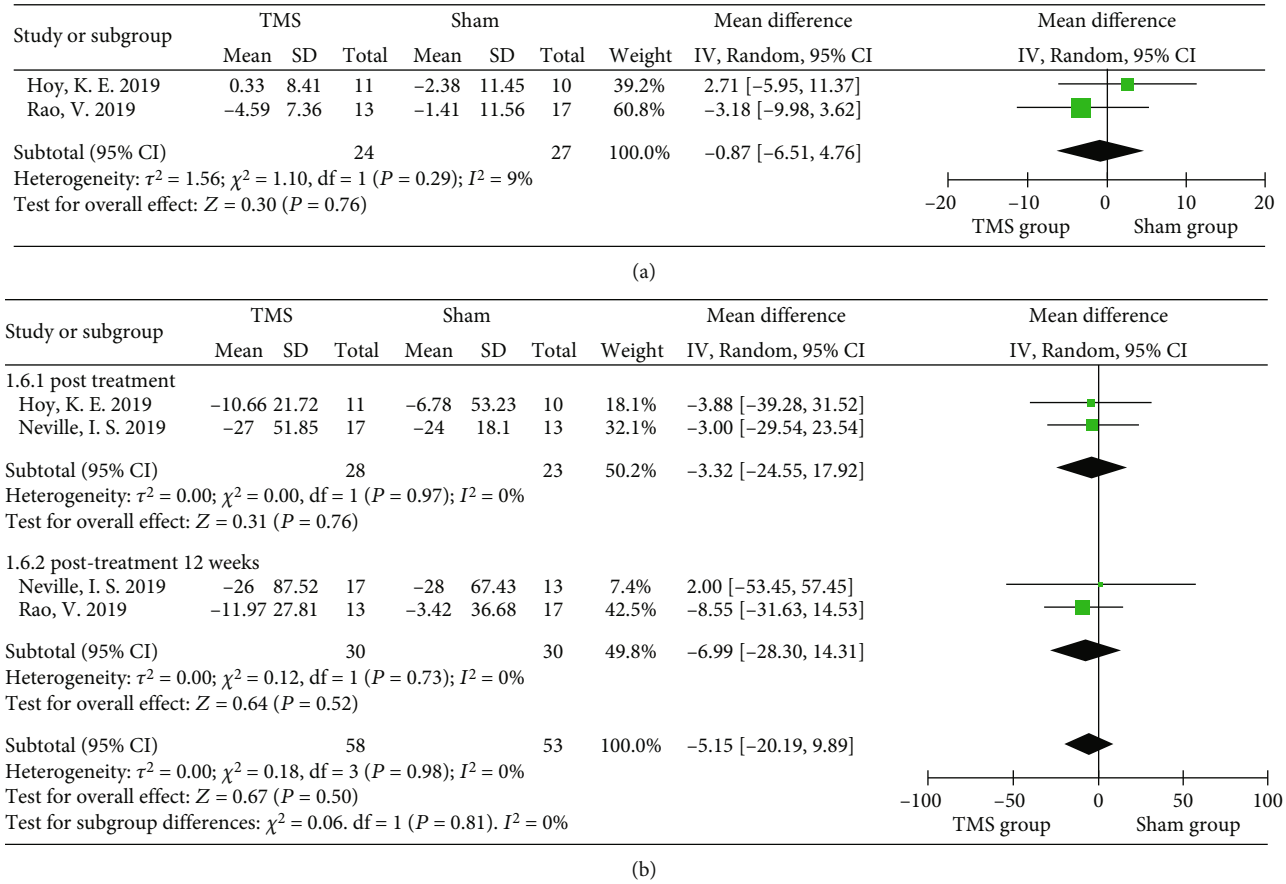

Figure 8: Forest plots of different parts of rTMS on cognition measured by the TMT-A and TMT-B in TBI patients: (a) the TMT-A; (b) the TMT-B. TMT: Trail Making Test.

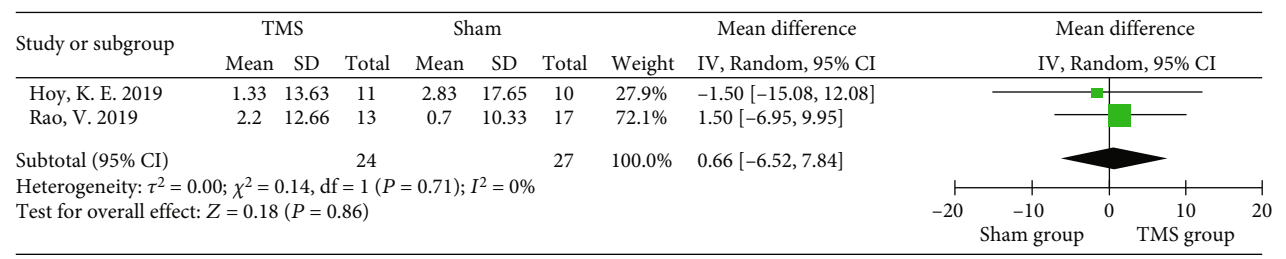

Figure 9: Forest plots of different parts of rTMS on cognition measured by the SCWT in TBI patients. SCWT: Stroop Color-Word Test.

4. Discussion

The aims of the present systematic review and meta-analysis were to clarify the effects of rTMS on neuropathic pain and neuropsychiatric functional measurements in patients with TBI. The results of the meta-analysis including 11 studies indicated that rTMS could induce significant analgesic effects, especially for headaches, although there was large heterogeneity in the rTMS interventional protocols that were followed. Compared to the sham control groups, the rTMS groups showed significant changes in postconcussive symptoms (measured by the RPQ-13). However, rTMS did not seem to improve depression and cognitive function, as the changes did not reach statistical significance.

Although headache or central pain gradually decreased with recovery from TBI, significant improvement in pain was found in the rTMS group. The ability of motor cortex rTMS to interfere with the processing of acute provoked pain was demonstrated by Lefaucheur et al., even if there was underlying chronic neuropathic pain [48]. In the quantitative analysis of neuropathic pain, the stimulated regions, including the left or right DLPFC, the bilateral DLPFC, the primary motor cortex (M1), and the left motor cortex, were selected, while quantitative assessment of the changes between the stimulation locations was limited due to the small number of included studies.

The roles of the M1 and DLPFC in pain modulation have long been established. A previous meta-analysis of high-frequency rTMS of M1 for neuropathic pain calculated

effect sizes corresponding to a pain reduction of 12% and 13.7% on a visual analog scale [49, 50], and the analgesic effects were shown to be associated with changes in intracortical modulation, which depends on both the GABAergic and glutamatergic pathways [51–53]. On the other hand, a quantitative synthesis suggested that high-frequency rTMS over the DLPFC, an area of the cortex involved in pain perception and mood, should be considered as an alternative target in the management of neuropathic pain [29]; the mechanism was noted to be due to its connections with the limbic system and brainstem structures involved in descending modulation [54]. Moreover, several functional neuroimaging studies in humans have confirmed that, like M1 stimulation, rTMS of the DLPFC induces changes in the activity of a network of structures involved in the integration and modulation of pain signals, including the thalamus, brainstem, insular, and cingulate cortices [55–58]. Similar to our results, a recent study by Gatzinsky et al. also reported relief of persistent pain after DLPFC magnetic stimulation and at a 1-week follow-up, compared to baseline [59].

Nevertheless, we evaluated the 4- to 24-week follow-up effects of rTMS and found no significant pain reduction at either the mid- or long-term follow-up, which is not entirely consistent with Mhalla et al.'s opinion that the analgesic effects of repeated daily stimulations could last for 2-3 weeks after the last stimulation [60]. Current evidence indicates that the magnitude of diffuse analgesic effects induced by rTMS of the M1 and DLPFC, which can last several days after a single stimulation session and are reinforced by the repetition of sessions, depends both on the stimulation parameters (frequency, intensity, and pattern) and orientation of the coil [61]. The number of pulses per session in these included studies was lower than that in most previous studies (600-2000 pulses vs. 1000-2000 pulses) [62, 63], and the total number of pulses per treatment was also relatively small compared with other studies (6000-10,000 pulses vs. 10,000-20,000 pulses) [64]. Moreover, the average intervention duration was 7-14 days, and the negative results may be associated with the overall short treatment durations (average of 9.5 days with 3-10 treatment sessions). These treatment durations would be considered short relative to psychological or behavioral therapies for chronic pain [65].

The effects of rTMS were associated with some potential physiological mechanisms, as rTMS over the DLPFC could decrease amygdala activation-threatening stimuli [47]. The results showed that rTMS could generate a significant and sustained improvement in postconcussive symptoms in mild TBI, which is in accordance with the findings of Baeken et al. [66]. Moreover, rTMS has some superiority in that it can directly influence the brain, including regulating the prefrontal cortex, amygdala, and hippocampus [67], as well as expanding the cerebral blood vessels, thus improving microcirculation and cerebral blood flow [68]. As a result, the recovery of nerve function could be promoted, which could guide magnetoencephalogram activities to be normal and well organized [69].

Significant improvement in depression was observed only when TBI patients received 1 Hz right DLPFC rTMS. However, Cao et al. demonstrated that both high-frequency rTMS over the left DLPFC and low-frequency rTMS over the right DLPFC have similar therapeutic efficacy for the treatment of patients with major depressive disorder [70]. In addition, positive effects of rTMS on depression were confirmed by some clinical controlled studies and expert consensus [71], and the optimal stimulation dose was recommended as double 900 pulses on the right side or double 1500 pulses on the left side to maximize the antidepressant effect [4]. Although strong evidence suggests the effectiveness of rTMS on refractory depression, few studies have explored whether rTMS improves depression in TBI patients. A controlled study performed by Hoy and colleagues did not find an improvement in post-TBI depression [38]. To enhance the implication of rTMS on TBI patients with depression, unilateral or bilateral rTMS approaches need to be further investigated.

Moreover, the insignificance in cognition could be explained by the complexity of cognition modulation. The trials excluded patients with cognitive disorders, and the baseline cognitive function of patients in the included studies was normal, which represents an obstacle to detecting significant but small changes in cognition tests. Therefore, in light of the limitations above, some improvements in cognition following active treatment are encouraging, and well-designed RCTs with larger sample sizes should be conducted to determine the effect of rTMS on cognition.

4.1. Clinical Implications and Limitations. There are some strengths in this study. We presented the latest evidence-based quantitative review of the potential effects of rTMS on neuropathic pain and neuropsychiatric symptoms. The reviewed studies showed that rTMS can be conducted safely without major adverse events in TBI patients aged from 14 to 65 years old. This is a noteworthy result since it enables future research in the field, such as the exploration of unilateral or bilateral DLPF-rTMS techniques, which may have distinct effectiveness for ameliorating neuropathic pain, depression, and postconcussion symptoms but appear to have questionable efficacy for cognition in this population.

As shown in the funnel plot, there was some chance of publication bias. Furthermore, we cannot exclude the possibility of bias in our meta-analysis because of the small sample sizes and short intervention periods of the included studies. The length of follow-up in the included RCTs ranged from 1 to 24 weeks, and it is unknown whether the changes would persist beyond this time point. There were 5 studies showing a low risk of bias, while not all included RCTs generated an adequately randomized sequence or used a blinded method for the outcome measurement. The high risk of bias of the included studies may influence the reliability of the results. Due to the lack of included studies, it is difficult to execute further analysis on the effect of different timings and protocols of rTMS on TBI patients. Moreover, there is no evidence to support the efficacy and safety of rTMS for symptom improvement in children with TBI who are younger than 14 years old. The heterogeneity of outcome measures also limits the clinical implications.

5. Conclusions

Due to the small sample sizes and a lack of methodological quality, we can only make a fair recommendation that rTMS is a safe and effective tool to improve pain and postconcussive symptoms after TBI. More strict evaluation standards and high-quality RCT designs are necessary to further explore the effects of rTMS on TBI.

Data Availability

The data used to support the findings of this study are available from the corresponding authors upon request.

Conflicts of Interest

The authors declare that there are no conflicts of interest regarding the publication of this paper.

Authors' Contributions

All authors contributed to the writing and redrafting of the manuscript. Xin Li and Qing Du had the original idea. Xin Li, Xiaoyan Yang, and Yuqi Yang performed the literature search; Tijiang Lu, Jie Shen, and Zefan Huang assessed the risk of bias; Zhengquan Chen and Yufei Feng rated the certainty of the evidence for each outcome; and Hong Yu and Xuan Zhou undertook the data collection. The results were analyzed, interpreted, and discussed by Xin Li and Qing Du. Xin Li, Tijiang Lu, and Hong Yu contributed equally to this study.

Acknowledgments

The authors thank Juping Liang for providing support and advice. The authors disclose receipt of the following financial support for the research, authorship, and/or publication of this article. This work was supported by the Action Plan for Sustainable Development of Science and Technology Innovation in Chongming District, Shanghai (CKY2021-50); Advanced and Appropriate Technology Promotion Projects of the Shanghai Municipal Health Commission (2019SY021); and Chongming District Medical Key Specialty Project.

Supplementary Materials

Supplementary 1. search strategies for all databases shown in (Appendix S1).

Supplementary 2. summary of findings table: GRADE levels of evidence for studies of TMS (Appendix S2).

References

[1] M. C. Dewan, A. Rattani, S. Gupta et al., "Estimating the global incidence of traumatic brain injury," *Journal of Neurosurgery*, vol. 130, no. 4, pp. 1080–1097, 2018.

[2] L. D. Nelson, N. R. Temkin, S. Dikmen et al., "Recovery after mild traumatic brain injury in patients presenting to US level I trauma centers: a Transforming Research and Clinical Knowledge in Traumatic Brain Injury (TRACK-TBI) study," *JAMA Neurology*, vol. 76, no. 9, pp. 1049–1059, 2019.

[3] D. DiSanto, R. G. Kumar, S. B. Juengst et al., "Employment stability in the first 5 years after moderate-to-severe traumatic brain injury," *Archives of Physical Medicine and Rehabilitation*, vol. 100, no. 3, pp. 412–421, 2019.

[4] P. B. Fitzgerald, K. E. Hoy, D. Elliot, R. N. Susan McQueen, L. E. Wambeek, and Z. J. Daskalakis, "Accelerated repetitive transcranial magnetic stimulation in the treatment of depression," *Neuropsychopharmacology*, vol. 43, no. 7, pp. 1565–1572, 2018.

[5] S. Rossi, M. Hallett, P. M. Rossini, A. Pascual-Leone, and Safety of TMS Consensus Group, "Safety, ethical considerations, and application guidelines for the use of transcranial magnetic stimulation in clinical practice and research," *Clinical Neurophysiology: Official Journal of the International Federation of Clinical Neurophysiology*, vol. 120, no. 12, pp. 2008–2039, 2009.

[6] E. Paxman, J. Stilling, L. Mercier, and C. T. Debert, "Repetitive transcranial magnetic stimulation (rTMS) as a treatment for chronic dizziness following mild traumatic brain injury," *BMJ Case Reports*, vol. 2018, 2018.

[7] A. Leung, S. Shukla, A. Fallah et al., "Repetitive transcranial magnetic stimulation in managing mild traumatic brain injury-related headaches," *Neuromodulation: Journal of the International Neuromodulation Society*, vol. 19, no. 2, pp. 133–141, 2016.

[8] C. A. Tassinari, M. Cincotta, G. Zaccara, and R. Michelucci, "Transcranial magnetic stimulation and epilepsy," *Clinical Neurophysiology: Official Journal of the International Federation of Clinical Neurophysiology*, vol. 114, no. 5, pp. 777–798, 2003.

[9] S. Li, A. L. Zaninotto, I. S. Neville, W. S. Paiva, D. Nunn, and F. Fregni, "Clinical utility of brain stimulation modalities following traumatic brain injury: current evidence," *Neuropsychiatric Disease and Treatment*, vol. 11, pp. 1573–1586, 2015.

[10] P. A. Rodrigues, A. L. Zaninotto, H. M. Ventresca et al., "The effects of repetitive transcranial magnetic stimulation on anxiety in patients with moderate to severe traumatic brain injury: a post-hoc analysis of a randomized clinical trial," *Frontiers in Neurology*, vol. 11, article 564940, 2020.

[11] I. Filipčić, I. Šimunović Filipčić, Ž. Milovac et al., "Efficacy of repetitive transcranial magnetic stimulation using a figure-8-coil or an H1-coil in treatment of major depressive disorder; a randomized clinical trial," *Journal of Psychiatric Research*, vol. 114, pp. 113–119, 2019.

[12] D. Pavlovic, S. Pekic, M. Stojanovic, and V. Popovic, "Traumatic brain injury: neuropathological, neurocognitive and neurobehavioral sequelae," *Pituitary*, vol. 22, no. 3, pp. 270–282, 2019.

[13] J. D. Corrigan and F. M. Hammond, "Traumatic brain injury as a chronic health condition," *Archives of Physical Medicine and Rehabilitation*, vol. 94, no. 6, pp. 1199–1201, 2013.

[14] J. Styrke, B. M. Stålnacke, P. Sojka, and U. Björnstig, "Traumatic brain injuries in a well-defined population: epidemiological aspects and severity," *Journal of Neurotrauma*, vol. 24, no. 9, pp. 1425–1436, 2007.

[15] A. M. Andersen, H. Ashina, A. Iljazi et al., "Risk factors for the development of post-traumatic headache attributed to traumatic brain injury: a systematic review," *Headache*, vol. 60, no. 6, pp. 1066–1075, 2020.

[16] D. E. Nampiaparampil, "Prevalence of chronic pain after traumatic brain injury," *JAMA*, vol. 300, no. 6, pp. 711–719, 2008.

[17] A. Leung, S. Shukla, E. Yang et al., "Diminished supraspinal pain modulation in patients with mild traumatic brain injury," *Molecular Pain*, vol. 12, p. 174480691666266, 2016.

[18] S. Lahz and R. A. Bryant, "Incidence of chronic pain following traumatic brain injury," *Archives of Physical Medicine and Rehabilitation*, vol. 77, no. 9, pp. 889–891, 1996.

[19] C. J. Woolf and R. J. Mannion, "Neuropathic pain: aetiology, symptoms, mechanisms, and management," *Lancet (London, England)*, vol. 353, no. 9168, pp. 1959–1964, 1999.

[20] F. T. Kashiwagi, R. El Dib, H. Gomaa et al., "Noninvasive brain stimulations for unilateral spatial neglect after stroke: a systematic review and meta-analysis of randomized and nonrandomized controlled trials," *Neural Plasticity*, vol. 2018, Article ID 1638763, 25 pages, 2018.

[21] A. Peinemann, B. Reimer, C. Löer et al., "Long-lasting increase in corticospinal excitability after 1800 pulses of subthreshold 5 Hz repetitive TMS to the primary motor cortex," *Clinical Neurophysiology: Official Journal of the International Federation of Clinical Neurophysiology*, vol. 115, no. 7, pp. 1519–1526, 2004.

[22] C. G. Mansur, F. Fregni, P. S. Boggio et al., "A sham stimulation-controlled trial of rTMS of the unaffected hemisphere in stroke patients," *Neurology*, vol. 64, no. 10, pp. 1802–1804, 2005.

[23] C. Solé-Padullés, D. Bartrés-Faz, C. Junqué et al., "Repetitive transcranial magnetic stimulation effects on brain function and cognition among elders with memory dysfunction. A randomized sham-controlled study," *Cerebral Cortex*, vol. 16, no. 10, pp. 1487–1493, 2006.

[24] T. Louise-Bender Pape, J. Rosenow, G. Lewis et al., "Repetitive transcranial magnetic stimulation-associated neurobehavioral gains during coma recovery," *Brain Stimulation*, vol. 2, no. 1, pp. 22–35, 2009.

[25] P. B. Fitzgerald, K. E. Hoy, J. J. Maller et al., "Transcranial magnetic stimulation for depression after a traumatic brain injury," *The Journal of ECT*, vol. 27, no. 1, pp. 38–40, 2011.

[26] C. Saleh, T. S. Ilia, P. Jaszczuk, M. Hund-Georgiadis, and A. Walter, "Is transcranial magnetic stimulation as treatment for neuropathic pain in patients with spinal cord injury efficient? A systematic review," *Neurological Sciences*, vol. 43, no. 5, pp. 3007–3018, 2022.

[27] M. Saltychev and J. Juhola, "Effectiveness of high-frequency repetitive transcranial magnetic stimulation (rTMS) in migraine - a systematic review and meta-analysis," *American Journal of Physical Medicine & Rehabilitation*, vol. Publish Ahead of Print, 2022.

[28] B. Forogh, H. Haqiqatshenas, T. Ahadi, S. Ebadi, V. Alishahi, and S. Sajadi, "Repetitive transcranial magnetic stimulation (rTMS) versus transcranial direct current stimulation (tDCS) in the management of patients with fibromyalgia: a randomized controlled trial," *Clinical Neurophysiology*, vol. 51, no. 4, pp. 339–347, 2021.

[29] X. Che, R. F. H. Cash, X. Luo et al., "High-frequency rTMS over the dorsolateral prefrontal cortex on chronic and provoked pain: a systematic review and meta-analysis," *Brain Stimulation*, vol. 14, no. 5, pp. 1135–1146, 2021.

[30] P. Y. Tsai, Y. C. Chen, J. Y. Wang, K. H. Chung, and C. H. Lai, "Effect of repetitive transcranial magnetic stimulation on depression and cognition in individuals with traumatic brain injury: a systematic review and meta-analysis," *Scientific Reports*, vol. 11, no. 1, p. 16940, 2021.

[31] D. K. Ahorsu, E. S. Adjaottor, and B. Y. H. Lam, "Intervention effect of non-invasive brain stimulation on cognitive functions among people with traumatic brain injury: a systematic review and meta-analysis: a systematic review and meta-analysis," *Brain Sciences*, vol. 11, no. 7, article 840, 2021.

[32] W. Beedham, A. Belli, S. Ingaralingam, S. Haque, and R. Upthegrove, "The management of depression following traumatic brain injury: a systematic review with meta-analysis," *Brain Injury*, vol. 34, no. 10, pp. 1287–1304, 2020.

[33] J. A. C. Sterne, J. Savović, M. J. Page et al., "RoB 2: a revised tool for assessing risk of bias in randomised trials," *BMJ*, vol. 366, article l4898, 2019.

[34] D. Atkins, D. Best, P. A. Briss et al., "Grading quality of evidence and strength of recommendations," *BMJ*, vol. 328, no. 7454, article 1490, 2004.

[35] J. Stilling, E. Paxman, L. Mercier et al., "Treatment of persistent post-traumatic headache and post-concussion symptoms using repetitive transcranial magnetic stimulation: a pilot, double-blind, randomized controlled trial," *Journal of Neurotrauma*, vol. 37, no. 2, pp. 312–323, 2020.

[36] Z. Moussavi, A. Suleiman, G. Rutherford et al., "A pilot randomised double-blind study of the tolerability and efficacy of repetitive transcranial magnetic stimulation on persistent post-concussion syndrome," *Scientific Reports*, vol. 9, no. 1, pp. 1–15, 2019.

[37] I. S. Neville, A. L. Zaninotto, C. Y. Hayashi et al., "Repetitive TMS does not improve cognition in patients with TBI: a randomized double-blind trial," *Neurology*, vol. 93, no. 2, pp. e190–e199, 2019.

[38] K. E. Hoy, S. McQueen, D. Elliot, S. E. Herring, J. J. Maller, and P. B. Fitzgerald, "A pilot investigation of repetitive transcranial magnetic stimulation for post-traumatic brain injury depression: safety, tolerability, and efficacy," *Journal of Neurotrauma*, vol. 36, no. 13, pp. 2092–2098, 2019.

[39] S. H. Siddiqi, N. T. Trapp, C. D. Hacker et al., "Repetitive transcranial magnetic stimulation with resting-state network targeting for treatment-resistant depression in traumatic brain injury: a randomized, controlled, double-blinded pilot study," *Journal of Neurotrauma*, vol. 36, no. 8, pp. 1361–1374, 2019.

[40] G. S. Choi, S. G. Kwak, H. D. Lee, and M. C. Chang, "Effect of high-frequency repetitive transcranial magnetic stimulation on chronic central pain after mild traumatic brain injury: a pilot study," *Journal of Rehabilitation Medicine*, vol. 50, no. 3, pp. 246–252, 2018.

[41] S. A. Lee and M. K. Kim, "Effect of low frequency repetitive transcranial magnetic stimulation on depression and cognition of patients with traumatic brain injury: a randomized controlled trial," *Medical Science Monitor: International Medical Journal of Experimental and Clinical Research*, vol. 24, pp. 8789–8794, 2018.

[42] A. Leung, V. Metzger-Smith, Y. He et al., "Left dorsolateral prefrontal cortex rTMS in alleviating MTBI related headaches and depressive symptoms," *Neuromodulation: Journal of the International Neuromodulation Society*, vol. 21, no. 4, pp. 390–401, 2018.

[43] V. Rao, K. Bechtold, U. McCann et al., "Low-frequency right repetitive transcranial magnetic stimulation for the treatment of depression after traumatic brain injury: a randomized sham-controlled pilot study," *The Journal of Neuropsychiatry and Clinical Neurosciences*, vol. 31, no. 4, pp. 306–318, 2019.

[44] P. Liu, J. Gao, S. Pan et al., "Effects of high-frequency repetitive transcranial magnetic stimulation on cerebral hemodynamics in patients with disorders of consciousness: a sham-controlled study," *European Neurology*, vol. 76, no. 1-2, pp. 1–7, 2016.

[45] L. M. Franke, G. T. Gitchel, R. A. Perera, R. L. Hadimani, K. L. Holloway, and W. C. Walker, "Randomized trial of rTMS in traumatic brain injury: improved subjective neurobehavioral symptoms and increases in EEG delta activity," *Brain Injury*, vol. 36, no. 5, pp. 683–692, 2022.

[46] N. S. King, S. Crawford, F. J. Wenden, N. E. Moss, and D. T. Wade, "The Rivermead Post Concussion Symptoms Questionnaire: a measure of symptoms commonly experienced after head injury and its reliability," *Journal of Neurology*, vol. 242, no. 9, pp. 587–592, 1995.

[47] S. Eyres, A. Carey, G. Gilworth, V. Neumann, and A. Tennant, "Construct validity and reliability of the Rivermead Post-Concussion Symptoms Questionnaire," *Clinical Rehabilitation*, vol. 19, no. 8, pp. 878–887, 2005.

[48] J. P. Lefaucheur, G. Jarry, X. Drouot, I. Ménard-Lefaucheur, Y. Keravel, and J. P. Nguyen, "Motor cortex rTMS reduces acute pain provoked by laser stimulation in patients with chronic neuropathic pain," *Clinical Neurophysiology: Official Journal of the International Federation of Clinical Neurophysiology*, vol. 121, no. 6, pp. 895–901, 2010.

[49] A. Leung, M. Donohue, R. Xu et al., "rTMS for suppressing neuropathic pain: a meta-analysis," *The Journal of Pain*, vol. 10, no. 12, pp. 1205–1216, 2009.

[50] N. E. O'Connell, L. Marston, S. Spencer, L. H. DeSouza, and B. M. Wand, "Non-invasive brain stimulation techniques for chronic pain," *Cochrane Database of Systematic Reviews*, vol. 3, article Cd008208, 2018.

[51] J. P. Lefaucheur, N. André-Obadia, A. Antal et al., "Evidence-based guidelines on the therapeutic use of repetitive transcranial magnetic stimulation (rTMS)," *Clinical Neurophysiology: Official Journal of the International Federation of Clinical Neurophysiology*, vol. 125, no. 11, pp. 2150–2206, 2014.

[52] J. P. Lefaucheur, X. Drouot, I. Ménard-Lefaucheur, Y. Keravel, and J. P. Nguyen, "Motor cortex rTMS restores defective intracortical inhibition in chronic neuropathic pain," *Neurology*, vol. 67, no. 9, pp. 1568–1574, 2006.

[53] D. Kapogiannis and E. M. Wassermann, "Transcranial magnetic stimulation in clinical pharmacology," *Central Nervous System Agents in Medicinal Chemistry*, vol. 8, no. 4, pp. 234–240, 2008.

[54] P. T. Ohara, J. P. Vit, and L. Jasmin, "Cortical modulation of pain," *Cellular and Molecular Life Sciences: CMLS*, vol. 62, no. 1, pp. 44–52, 2005.

[55] J. Barrett, V. Della-Maggiore, P. A. Chouinard, and T. Paus, "Mechanisms of action underlying the effect of repetitive transcranial magnetic stimulation on mood: behavioral and brain imaging studies," *Neuropsychopharmacology: Official Publication of the American College of Neuropsychopharmacology*, vol. 29, no. 6, pp. 1172–1189, 2004.

[56] X. Li, Z. Nahas, F. A. Kozel, B. Anderson, D. E. Bohning, and M. S. George, "Acute left prefrontal transcranial magnetic stimulation in depressed patients is associated with immediately increased activity in prefrontal cortical as well as subcortical regions," *Biological Psychiatry*, vol. 55, no. 9, pp. 882–890, 2004.

[57] T. Ohnishi, H. Matsuda, E. Imabayashi et al., "Chapter 76 rCBF changes elicited by rTMS over DLPFC in humans," *Supplements to Clinical Neurophysiology*, vol. 57, pp. 715–720, 2004.

[58] T. Paus, M. A. Castro-Alamancos, and M. Petrides, "Cortico-cortical connectivity of the human mid-dorsolateral frontal cortex and its modulation by repetitive transcranial magnetic stimulation," *The European Journal of Neuroscience*, vol. 14, no. 8, pp. 1405–1411, 2001.

[59] K. Gatzinsky, C. Bergh, A. Liljegren et al., "Repetitive transcranial magnetic stimulation of the primary motor cortex in management of chronic neuropathic pain: a systematic review," *Scandinavian Journal of Pain*, vol. 21, no. 1, pp. 8–21, 2021.

[60] A. Mhalla, S. Baudic, D. C. de Andrade et al., "Long-term maintenance of the analgesic effects of transcranial magnetic stimulation in fibromyalgia," *Pain*, vol. 152, no. 7, pp. 1478–1485, 2011.

[61] X. Moisset, D. C. de Andrade, and D. Bouhassira, "From pulses to pain relief: an update on the mechanisms of rTMS-induced analgesic effects," *European Journal of Pain*, vol. 20, no. 5, pp. 689–700, 2016.

[62] N. André-Obadia, P. Mertens, A. Gueguen, R. Peyron, and L. Garcia-Larrea, "Pain relief by rTMS: differential effect of current flow but no specific action on pain subtypes," *Neurology*, vol. 71, no. 11, pp. 833–840, 2008.

[63] A. Passard, N. Attal, R. Benadhira et al., "Effects of unilateral repetitive transcranial magnetic stimulation of the motor cortex on chronic widespread pain in fibromyalgia," *Brain: A Journal of Neurology*, vol. 130, no. 10, pp. 2661–2670, 2007.

[64] E. M. Khedr, H. Kotb, N. F. Kamel, M. A. Ahmed, R. Sadek, and J. C. Rothwell, "Longlasting antalgic effects of daily sessions of repetitive transcranial magnetic stimulation in central and peripheral neuropathic pain," *Journal of Neurology, Neurosurgery, and Psychiatry*, vol. 76, no. 6, pp. 833–838, 2005.

[65] S. Morley, C. Eccleston, and A. Williams, "Systematic review and meta-analysis of randomized controlled trials of cognitive behaviour therapy and behaviour therapy for chronic pain in adults, excluding headache," *Pain*, vol. 80, no. 1, pp. 1–13, 1999.

[66] C. Baeken, R. De Raedt, P. Van Schuerbeek et al., "Right prefrontal HF-rTMS attenuates right amygdala processing of negatively valenced emotional stimuli in healthy females," *Behavioural Brain Research*, vol. 214, no. 2, pp. 450–455, 2010.

[67] T. Raij, A. Nummenmaa, M. F. Marin et al., "Prefrontal cortex stimulation enhances fear extinction memory in humans," *Biological Psychiatry*, vol. 84, no. 2, pp. 129–137, 2018.

[68] X. Zong, Y. Li, C. Liu et al., "Theta-burst transcranial magnetic stimulation promotes stroke recovery by vascular protection and neovascularization," *Theranostics*, vol. 10, no. 26, pp. 12090–12110, 2020.

[69] J. Kamins, E. Bigler, T. Covassin et al., "What is the physiological time to recovery after concussion? A systematic review," *British Journal of Sports Medicine*, vol. 51, no. 12, pp. 935–940, 2017.

[70] X. Cao, C. Deng, X. Su, and Y. Guo, "Response and remission rates following high-frequency vs. low-frequency repetitive transcranial magnetic stimulation (rTMS) over right DLPFC for treating major depressive disorder (MDD): a meta-analysis of randomized, double-blind trials," *Frontiers in Psychiatry*, vol. 9, p. 413, 2018.

[71] S. M. McClintock, I. M. Reti, L. L. Carpenter et al., "Consensus recommendations for the clinical application of repetitive transcranial magnetic stimulation (rTMS) in the treatment of depression," *The Journal of Clinical Psychiatry*, vol. 79, no. 1, pp. 35–48, 2018.

Hindawi
Neural Plasticity
Volume 2022, Article ID 6472475, 11 pages
https://doi.org/10.1155/2022/6472475

Research Article

Low-Intensity Focused Ultrasound Alleviates Chronic Neuropathic Pain-Induced Allodynia by Inhibiting Neuroplasticity in the Anterior Cingulate Cortex

Bin Wang, Mo-Xian Chen, Shao-Chun Chen, Xiang-Jun Feng, Ye-Hui Liao, Yun-Xin Zhao, Jin-Shan Tie, Yao Liu, and Li-Juan Ao

School of Rehabilitation, Kunming Medical University, Kunming, 650500 Yunnan Province, China

Correspondence should be addressed to Yao Liu; liuyao@kmmu.edu.cn and Li-Juan Ao; aolijuan@kmmu.edu.cn

Received 19 February 2022; Revised 13 June 2022; Accepted 7 July 2022; Published 23 July 2022

Academic Editor: Yazhuo Kong

Low-intensity focused ultrasound (LIFU) is a potential noninvasive method to alleviate allodynia by modulating the central nervous system. However, the underlying analgesic mechanisms remain unexplored. Here, we assessed how LIFU at the anterior cingulate cortex (ACC) affects behavior response and central plasticity resulting from chronic constrictive injury (CCI). The safety of LIFU stimulation was assessed by hematoxylin and eosin (H&E) and Fluoro-Jade C (FJC) staining. A 21-day ultrasound exposure therapy was conducted from day 91 after CCI surgery in mice. We assessed the 50% mechanical withdrawal threshold (MWT_{50}) using Von Frey filaments (VFFs). The expression levels of microtubule-associated protein 2 (MAP2), growth-associated protein 43 (GAP43), and tau were determined via western blotting (WB) and immunofluorescence (IF) staining to evaluate the central plasticity in ACC. The regions of ACC were activated effectively and safely by LIFU stimulation, which significantly increased the number of c-fos-positive cells ($P < 0.05$) with no bleeding, coagulative necrosis, and neuronal loss. Under chronic neuropathic pain- (CNP-) induced allodynia, MWT_{50} decreased significantly ($P < 0.05$), and overexpression of MAP2, GAP43, and tau was also observed. After 3 weeks of treatment, significant increases in MWT_{50} were found in the CCI+LIFU group compared with the CCI group ($P < 0.05$). WB and IF staining both demonstrated a significant reduction in the expression levels of MAP2, GAP43, and tau ($P < 0.05$). LIFU treatment on ACC can effectively attenuate CNP-evoked mechanical sensitivity to pain and reverse aberrant central plasticity.

1. Introduction

Neuropathic pain (NP) is caused by injury or disease of the somatosensory system [1]. Spontaneous pain, persistent or paralysis pain, induction pain, paresthesia, and pinprick sensation are clinical symptoms of NP. Approximately 6.9%–10% of patients worldwide suffer from chronic pain [2], which exerts a negative impact on their quality of life [3, 4]. Recent integrative neuroscience studies have found that chronic pain and acute pain operate through different central mechanisms, and central sensitization (CS) is the most important mechanism for chronic pain maintenance [5]. CS is an enhancement in the function of neurons and circuits in nociceptive pathways caused by the increases in membrane excitability and synaptic efficacy as well as by reduced inhibition. It is a manifestation of the remarkable plasticity of the somatosensory nervous system in response to activity, inflammation, and neural injury [6]. Pharmacotherapy for neuropathic pain is nonspecific and often insufficiently effective, and CS implies poor functioning of endogenous analgesia; thus, analgesic drugs are ineffective in controlling chronic pain with CS [6, 7]. In addition, drugs have many side effects after long-term use [8, 9]. Consequently, CS has revealed the role of the development of chronic pain in the central nervous system.

CS encompasses various related dysfunctions within the central nervous system, including altered sensory processing in the brain with a disrupted resting state functional connectivity in the default mode and salience networks and increased brain activity in areas known to be involved in

acute pain sensations, including the anterior cingulate cortex (ACC). ACC is an important cortical area in sensory and cognitive research. In animal studies, cumulative evidence has revealed that the generation and maintenance of chronic pain and pain-related emotions are accompanied by long-term plastic changes within the ACC after peripheral injury [10–14]. It has been shown that central synaptic plasticity contributes to CS in chronic pain. In a spinal nerve ligation (SNL) rat pain model, maladaptive plasticity in the ACC brain region has been detected along with the progression of the pain response in rats. Furthermore, it has been found that the inhibition of the neural remodeling of the ACC brain region at both structural and functional levels by the CDK5/microtubule-associated protein 2 (MAP2) and CDK5/tau-NMDA2B pathways provides an analgesic effect [15]. In addition, many studies have reported that inhibiting synaptic plasticity or synaptic enhancement in the ACC region of mice can significantly alleviate the pain sensitivity response caused by peripheral nerve damage [16]. Consequently, plasticity of ACC strongly correlates with chronic neuropathic pain (CNP); it may be considered an important target for CNP drug intervention.

As a means of noninvasive neuromodulation, ultrasound can effectively regulate the activity of neurons in the central nervous system. In vitro experiments have shown that ultrasound stimulation activates neuronal activity and local potentials generated by neuronal charge. In animal experiments, ultrasound stimulation of the central nervous system has been used to treat diseases such as epilepsy, NP, Alzheimer's disease (AD), and Parkinson's disease (PD) by inhibiting the activity of neurons or charge and regulating synaptic plasticity [17–20]. In human trials, this neuromodulation technology has a direct effect on the primary somatosensory cortex, increasing brain activity in this area and improving sensory discrimination but also transiently and reversibly changing the activity of neurons in the subcortical and deep cortical areas [21, 22]. Therefore, the use of ultrasound for the treatment of related neurological disorders is becoming increasingly attractive.

Previous research has shown that low-intensity focused ultrasound (LIFU) has a significant analgesic effect on CNP mice due to central ACC regulation; however, the mechanisms underlying the alleviation of allodynia remain unknown. We used a CCI approach to create a mouse model of CNP and regulated the ACC region by LIFU to investigate the analgesic effect on allodynia and the probable underlying mechanism.

2. Materials and Methods

2.1. Laboratory Animals. Animal care and treatment protocols followed the *Guidelines for the Care and Use of Laboratory Animals* [23]. A total of 42 healthy male C57BL/6J mice (age, 8 weeks; weight, 20–25 g) were used in these experiments. To investigate the safety and effects of LIFU on neurons, we randomly allocated normal C57BL/6J mice to a LIFU(-) group and a LIFU(+) group ($n = 6$ mice/group). For the LIFU neuromodulation experiment, 30 healthy male mice were randomly divided into the following three groups: the sham, CCI, and CCI+LIFU groups ($n = 10$ mice/group). The mice were provided by the Department of Experimental Animals, Kunming Medical University. They were maintained in a standard animal room with a light/dark cycle of 12 h/12 h and were provided free access to food and water. The temperature of the animal room was 22 ± 2°C, and the relative humidity was 50%–70%. The experimental protocol was approved by the Experimental Animal Ethics Committee of Kunming Medical University (No. KMMU2021345).

2.2. Grouping and CNP Model. Prior to the study, the mice were adapted to the maintenance environment for 1 week. Thirty mice were then divided into the sham group, the model group, and the LIFU treatment group, with 10 mice in each group. Then, we used the CCI surgical method [24] to establish CNP models. Specifically, the sciatic nerve in the CCI group and the treatment group was ligated for 90 days. The mice were anesthetized with isoflurane (Sigma-Aldrich, St. Louis, Missouri, USA) and laid on a heating pad. In the prone position, the surgical site was prepared by shaving the posterolateral side of the right hind limb, and then, three applications of 75% ethanol were applied to the site. An incision (1 cm) was then made proximal to the right hind limb. The nerve was then uncovered using a splitting approach on the bicep femoris, and three ligatures (gut ligatures 6.0, Jinhuang, Shanghai, China) were tied at 1 mm long intervals. The deep and superficial muscles were reapproximated by applying an interrupted stitching technique using 4.0 chromic gut (Stoelting Co, Wood Dale, IL). The skin was closed using 4.0 silk sutures (Ethicon, Somerville, NJ). For the sham group, the right sciatic nerve was exposed using the same methods, but the nerve was not ligated. After surgery, the mice were returned to their original cages to continue feeding.

2.3. Ultrasound Treatment Protocol. The mice commenced LIFU stimulation on day 91 after CCI modeling. The treatment group underwent LIFU stimulation under anesthesia with isoflurane via a nose cone. We used an electric shaver and depilatory cream to remove the hair on the skin of the head without damaging the integrity of the skin or skull. We calculated the focal length to prepare the collimator of the LIFU transducer, which was placed directly in the area of the ACC (the Bregma point). A waveform signal was generated by a waveform generator (DG4202, RIGOL, China) and was amplified with a 50 W power amplifier (Dahan Radio Studio, China). The amplified signal then activated the ultrasound transducer (Figure 1(b)). An ultrasonic coupling agent (Aquasonic; Parker Laboratories, Fairfield, NJ, USA) was filled between the ultrasound transducer and the skin of the head to evacuate air bubbles. For LIFU stimulation, we used a focused transducer (4 MHz), with an acoustic intensity of 0.95 MPa, a duty cycle (DC) of 10%, and a pulse repetition frequency (PRF) of 1.5 kHz [25]. LIFU stimulation was administered for 15 min/day for 21 days (Figure 1(a)). We measured the acoustic intensity of the beam by using a hydrophone (HNR 0500; Onda, Sunnyvale, CA, USA). Mice in the model group received the same LIFU stimulation as those in the treatment group under anesthesia; however, LIFU was turned off during the treatment. Animals in the

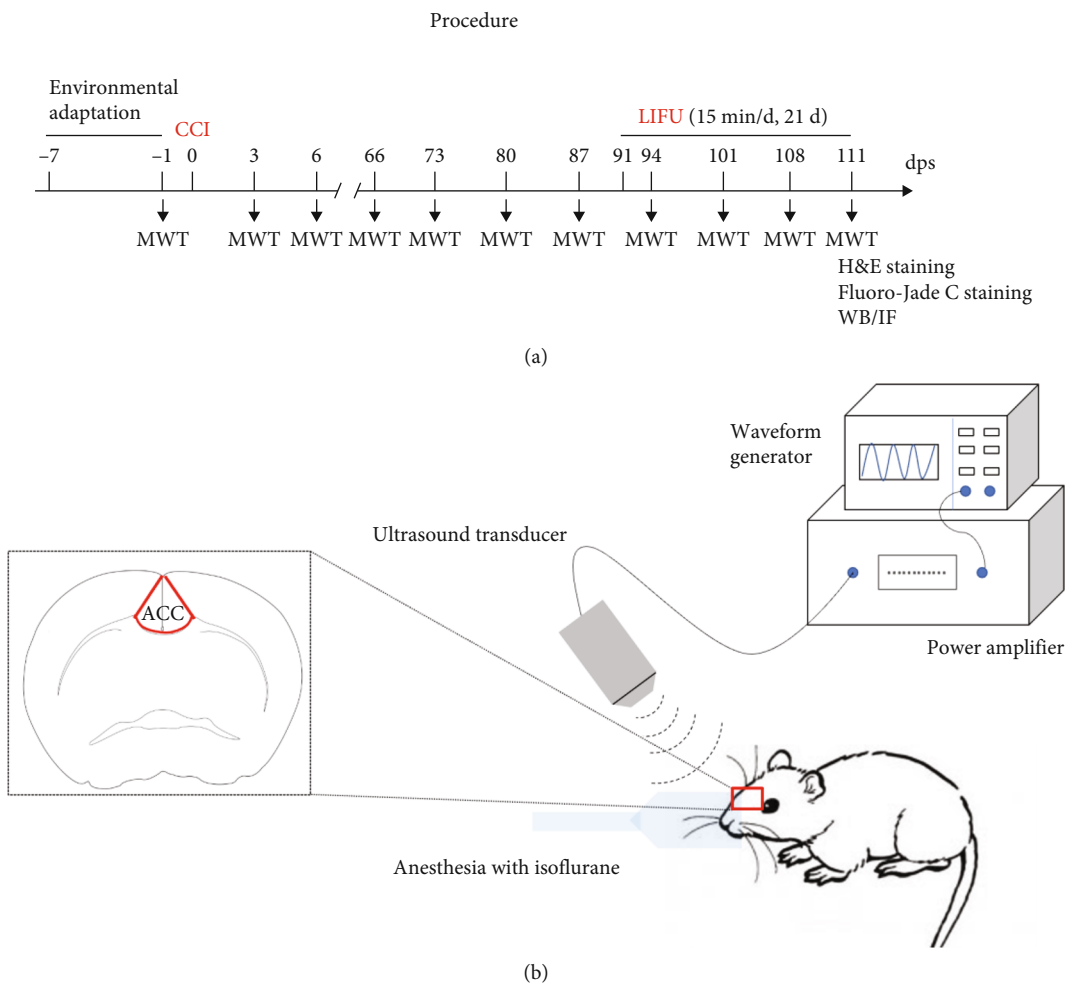

Figure 1: (a) Procedure used for our experiments. Dps: days postsurgery. (b) Schematic diagram of low-intensity focused ultrasound (LIFU) stimulation.

sham group received isoflurane anesthesia for 15 min and were then returned to their original cages.

2.4. Evaluation of Mechanical Withdrawal Threshold. The mice were placed in a $5 \times 5 \times 8\,\text{cm}^3$ plexiglass grid and were allowed to adapt to the testing environment for 10 min prior to experimentation. In accordance with methods described previously [26], we used the "up-down" method to evaluate the 50% mechanical withdrawal threshold (MWT_{50}) of mechanical allodynia in mice. Von Frey filaments (VFFs) (Stoelting, Wood Dale, IL, USA) with ascending degrees of stiffness (0.02, 0.04, 0.07, 0.16, 0.4, 0.6, 1.0, 1.4, and 2 g) were used to stimulate the bottom of the right paw in each mouse. The stimulus intensity started at 0.6 g, and an appropriate external force was applied to make the VFFs bend 90°; this was maintained for 5 s. A positive reaction was defined as cases wherein a test mouse was seen to lick, raise, or retract its paws. Then, we selected larger or smaller VFFs for stimulation based on the response of each mouse. When a reaction different from the previously described one was observed, we repeated the VFFs four more times to end the MWT_{50} test. If the force was >2.0 g or <0.02 g, it was recorded as 2.0 g or 0.02 g, respectively. Then, we calculated the pain threshold as follows:

$$\text{MWT}_{50} = \frac{\left(10^{[xf+k\delta]}\right)}{10000}\Bigg), \tag{1}$$

where xf, k, and δ represent the mean intensity, stimulus coefficient, and log value of the adjacent stimulus, respectively, and xf and K can be obtained from statistical tables; in this study, δ was 0.24.

2.5. Histological Analysis. The mice were anesthetized with an intraperitoneal injection of 1% pentobarbital sodium, followed by cardiac perfusion with 0.9% normal saline and 4% paraformaldehyde. Fresh brain tissues were fixed in a fixative solution for 48 h and then dehydrated in various concentrations of absolute ethanol (75%, 85%, 90%, 95%, and 100%) and different concentrations of xylene. Wax-soaked brain tissues were then embedded in an embedding cassette, and tissue sections with a thickness of 5 μm were cut on a paraffin slicer. For hematoxylin and eosin (H&E) staining, the sections were first dewaxed in xylene I (10 min) and xylene II (10 min), followed by absolute ethanol I, anhydrous ethanol II, 95% alcohol, 90% alcohol, 80% alcohol, and 70% alcohol for 5 min each. The sections were then rinsed in

double-distilled water for 5 min and stained in hematoxylin for 5 min. Next, they were rinsed in double-distilled water, differentiated in 1% hydrochloric acid alcohol for a few seconds, rewashed in double-distilled water, incubated in 0.6% ammonia water (back to blue), and then rinsed in double-distilled water before staining in eosin for 3 min. Finally, the sections were washed with 95% alcohol I, 95% alcohol II, absolute ethanol I, absolute ethanol II, xylene I, and xylene II for 5 min each time. The slides were sealed with neutral gum sealing tablets, and pathological changes in the sections were investigated under a light microscope (Olympus Corporation, Tokyo, Japan).

For Fluoro-Jade C (FJC) staining, entire mouse brains were acquired as described earlier. However, the brains were fixed in 4% paraformaldehyde for 48 h and dehydrated for 24 h in various concentrations of sucrose solution (10%, 20%, and 30%) before being embedded at optimal cutting temperature (OCT). Then, the frozen tissues were cut into sections with a thickness of 10 μm using a frozen microtome. For FJC staining, we used a commercial kit (Biosensis, Adelaide, Australia), and the sectioned tissues were immersed in a mixture of solution A and 80% ethanol for 10 min. This was then incubated in a 70% ethanol solution for 2 min and then in a mixture of solution B and double-distilled water for 10 min. Next, the mixture was incubated with solution C and double-distilled water for 10 min, washed with double-distilled water three times (1 min each time), and dried on a heater at 50°C–60°C for 5 min. Finally, the sections were cleared by xylene treatment for 2 min. DPX mounting medium was added dropwise, and the sections were covered with cover glass. Then, we observed the sections via fluorescence microscopy (Olympus Corporation, Tokyo, Japan).

2.6. Western Blotting (WB). Following the last behavioral test, the mice were anesthetized with an intraperitoneal injection of excessive sodium pentobarbital, followed by cardiac perfusion with 0.9% normal saline. The ACC brain tissues were then dissected, lysed with radioimmunoprecipitation assay (RIPA) buffer on ice for 30 min, and homogenized with an ultrasonic cell crusher. The lysate was then centrifuged at 12000 rpm at 4°C for 30 min. The supernatant was taken, and the total protein concentration was determined with a bicinchoninic acid (BCA) assay kit (Biomed, Beijing, China). Sodium dodecyl sulfate polyacrylamide gel electrophoresis (SDS-PAGE) was then used to separate proteins, which were then transferred to polyvinylidene difluoride (PVDF) membranes (Millipore-Sigma, Burlington, MA, USA). The membranes were then blocked with 5% skimmed milk and incubated overnight at 4°C with primary antibodies against MAP2 (1 : 1000; Cell Signaling Technology (CST), Danvers, MA, USA), GAP43 (1 : 1000; CST), tau (1 : 1000; Proteintech, USA), and β-tubulin (1 : 2000; Abcam, Cambridge, UK). The next day, the membranes were washed three times with tris-buffered saline with 0.1% Tween® 20 (TBST) (15 min per wash) and then incubated with horseradish peroxidase- (HRP-) labeled goat anti-rabbit/anti-mouse IgG (1 : 5000) HRP-linked antibody (1 : 2000; CST) at room temperature (RT) for 2 h. Then, the membranes were washed three times with TBST (15 min per wash). Finally, the chemiluminescence (ECL; Tanon, Shanghai, China) imaging method was used to reveal protein bands, and ImageJ (US National Institutes of Health (NIH), Bethesda, MD, USA) was used to analyze the gray level of each protein band.

2.7. Immunofluorescence (IF). The mice were anesthetized with an overdose of sodium pentobarbital intraperitoneally; they were then perfused (via the heart) with 0.9% normal saline and fixed with 4% paraformaldehyde. The brains were then removed, fixed for 48 h in 4% paraformaldehyde, and dehydrated for 24 h with a gradient of 10%, 20%, and 30% sucrose concentrations. The tissues were then embedded at OCT, and 10 μm thick frozen sections were cut with a microtome. For analysis, the sections were warmed to RT, washed in phosphate-buffered saline (PBS) for 10 min, blocked with 10% goat serum for 2 h, and then incubated at 4°C overnight with primary antibodies against c-fos (1 : 300; Proteintech, USA), MAP2 (1 : 200; CST), GAP43 (1 : 200; CST), tau (1 : 200; CST), and NeuN (1 : 500; Abcam). The next day, the sections were warmed to RT, washed with PBST for 15 min, and then incubated with secondary antibody (anti-rabbit IgG (heavy+light (H+L) chain), F [ab′]2 fragment (Alexa Fluor 488 conjugate); anti-mouse IgG (H +L chain), F [ab′]2 fragment (Alexa Fluor 594 conjugate)) at RT and in the dark for 1.5 h. Next, the sections were washed with PBST for 15 min and incubated with 4′,6-diamidino-2-phenylindole (DAPI; Sigma, USA) for 20 min. Finally, we observed the sections and acquired photographs with a fluorescence microscope (Olympus Corp, Tokyo, Japan). ImageJ software (US National Institutes of Health (NIH), Bethesda, MD, USA) was used to analyze the optical density of the positive area.

2.8. Statistical Analysis. Statistical analysis was performed using SPSS 25.0 software (IBM Corp, Armonk, NY, USA). GraphPad Prism software version 8.0 (GraphPad Software, Inc., San Diego, CA, USA) was used to generate graphs. The raw data obtained were all expressed as means ± standard error of mean (SME). WB bands and IF were analyzed using one-way analysis of variance (ANOVA) with Tukey's post hoc test. Comparisons of two groups were performed by a two-tailed unpaired *t*-test, while behavioral data were analyzed by two-way repeated-measures ANOVA, followed by Bonferroni's test for post hoc comparisons. Two-tailed P values < 0.05 were considered statistically significant.

3. Results

3.1. LIFU Stimulates the ACC in Each Group of Mice in a Safe Manner. H&E staining of the ACC brain tissues (Figure 2(a), ×400) in the LIFU(-) and LIFU(+) groups showed that there was no definitive bleeding, nerve cell swelling, pyknosis, coagulative necrosis, or emptying. We also stained brain tissues with FJC, a marker of neuronal degeneration. There were no significant differences in the number of FJC-positive cells after stimulation between the LIFU(-) and LIFU(+) groups (Figures 2(b) and 2(c)). This

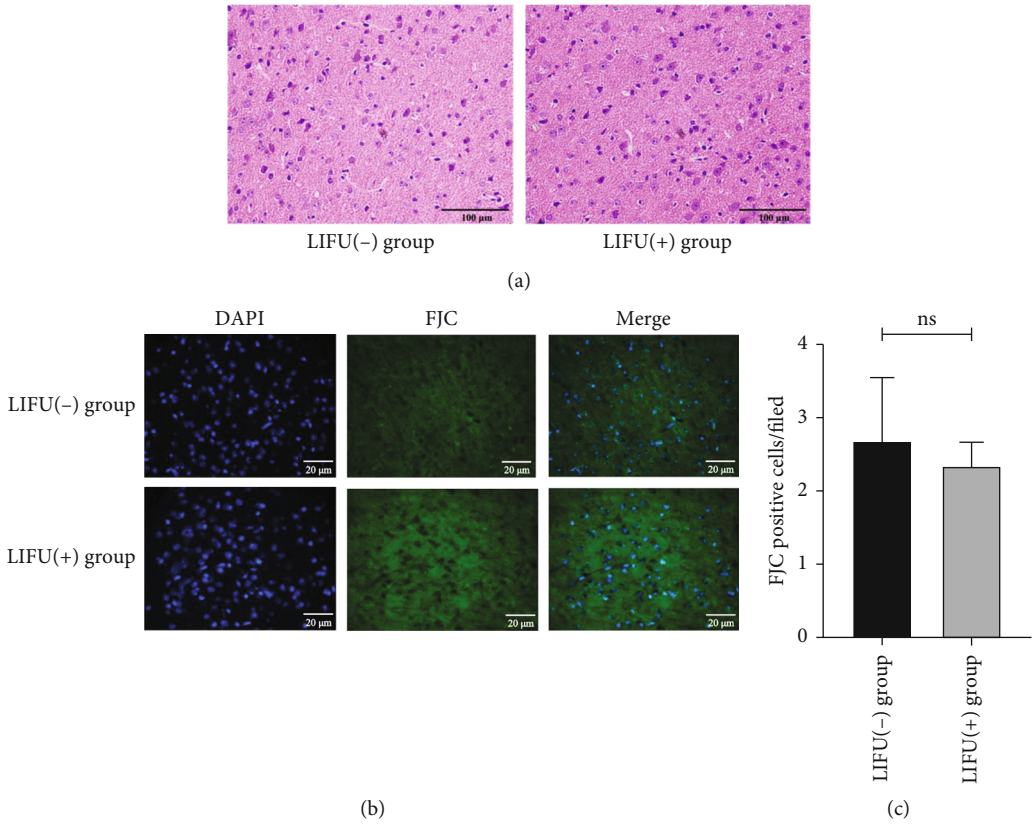

Figure 2: Safety evaluation of LIFU stimulation (×400). Scale bars, 100 μm and 20 μm. (a) Hematoxylin and eosin (H&E) staining showed no evidence of edema, hemorrhage, or cell necrosis; $n = 3$ per group. (b, c) Fluoro-Jade C (FJC) staining showed that there was no significant difference in the number of FJC-positive cells between the LIFU(-) and LIFU(+) groups. Each symbol represents the mean ± SEM; independent-sample t-tests; $n = 3$ mice per assay.

suggests that LIFU stimulates the ACC brain area in a safe manner.

3.2. LIFU Significantly Activates Neurons in the ACC Region. To determine the effects of LIFU on neurons, c-fos expression was examined in the stimulation region. Compared with the LIFU(-) group, we found an increased fluorescence of c-fos in most neurons after LIFU stimulation ($P < 0.05$) (Figures 3(a) and 3(b)), indicating that LIFU significantly activated neurons.

3.3. LIFU Significantly Alleviates Allodynia in CNP Mice. Compared with the sham group, the MWT_{50}s in the CCI and CCI+LIFU groups decreased after surgery on the third day and dropped to the lowest levels on the sixth day; the MWT_{50}s values were 0.18 ± 0.03 g and 0.16 ± 0.03 g, respectively ($P < 0.05$). The reduction of MWT_{50} in the CCI group was sustained until the end of the LIFU stimulation period. Following LIFU stimulation, the MWT_{50} gradually increased, eventually becoming significantly higher in the CCI+LIFU group (0.90 ± 0.10 g) than in the CCI group (0.06 ± 0.01 g) after 10 days of LIFU stimulation ($P < 0.05$); the MWT_{50} then remained stable until the end of LIFU stimulation. However, the MWT_{50} in the CCI+LIFU group was significantly still lower than that in the sham group ($P < 0.05$; Figure 4). These results show that LIFU can alleviate mechanical hyperalgesia caused by CCI in CNP mice.

3.4. LIFU Stimulation Significantly Reduces the Expression of MAP2, GAP43, and Tau Proteins in the ACC. CS is an important mechanism of chronic pain that manifests as neuroplasticity. Neuroplasticity-related proteins include MAP2, GAP43, and tau. In this study, WB showed that the expression levels of MAP2, GAP43, and tau increased significantly in the CCI group ($P < 0.05$) (Figures 5(a)–5(f)). The expression levels of MAP2, GAP43, and tau decreased significantly after 21 days of LIFU treatment when compared to the CCI group ($P < 0.05$; Figures 5(b), 5(d), and 5(f)). IF also showed that the expression levels of MAP2, GAP43, and tau increased significantly in the CCI group ($P < 0.05$) (Figures 6(a)–6(f)). MAP2, GAP43, and tau levels decreased significantly after 21 days of LIFU stimulation when compared to the CCI group ($P < 0.05$; Figures 6(b), 6(d), and 6(f)).

4. Discussion

In this study, we used CCI to create a CNP mouse model as this is a simple technique that is easy to replicate. The CNP model developed by CCI is comprehensive, and the mechanical and heat pain sensitivity thresholds of the afflicted limbs of the animals are significantly lower than that in the sham

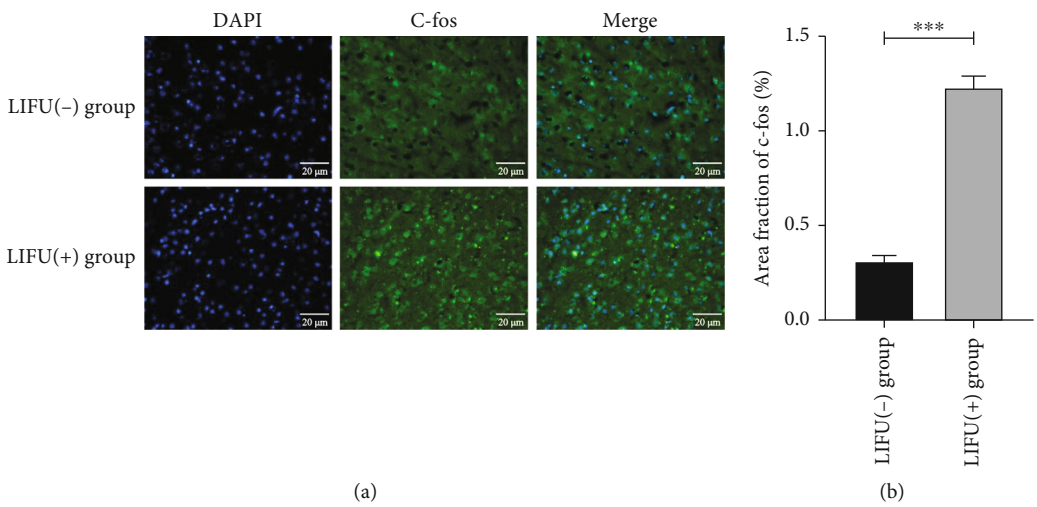

Figure 3: Expression of c-fos (a, b) in the anterior cingulate cortex (ACC) after low-intensity focused ultrasound (LIFU) stimulation. LIFU activated neurons in the ACC (immunofluorescence (IF), ×400). Scale bar, 20 μm. $^{***}P < 0.0001$. Each symbol represents the mean ± SEM; unpaired t -tests; $n = 3$ rats per assay.

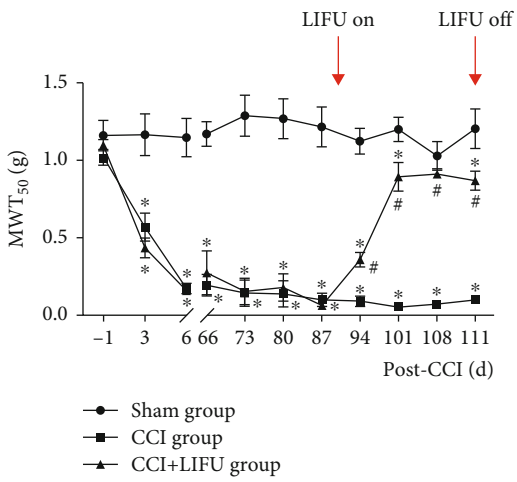

Figure 4: Effects of LIFU stimulation on the ACC in chronic neuropathic pain (CNP) model mice. 50% mechanical withdrawal threshold (MWT_{50}) significantly decreased in the CCI and CCI +LIFU groups after CCI surgery when compared with the sham group until the end of the study. After 21 days of LIFU treatment, the MWT_{50} increased when compared with the CCI group. Each symbol represents the mean ± SEM; $^{\#}P < 0.05$ compared with the CCI and CCI+LIFU groups; $^{*}P < 0.05$ compared with the sham group. Two-way repeated-measures ANOVA, followed by the Bonferroni test; $n = 10$ per group.

group after surgery [27]. The long-term experimental protocol of 21 days of LIFU treatment from day 91 in the current study was based on the results from a previous report of our team [25]. In Feng et al.'s study, in the short-term experiment (21 days of LIFU treatment on ACC from day 6 after CCI injury), the focused ultrasound- (FUS-) induced mechanical analgesic effects appeared at 2 weeks following the surgery. However, an earlier appearance of FUS effects in the long-term experiment (21 days of LIFU treatment from day 91 after CCI) was observed on day 94 after CCI. In a rodent NP model, CS may be indicated by pain-induced generation and maturation of the potentiation of synaptic responses in the ACC and the development of allodynia at 1–4 weeks following nerve injury, as well as by the development of anxiodepressive-like behaviors at 5–8 weeks after injury [28]. This may explain the difference in the time of onset of FUS effects between the short- and long-term experiments and indicate that the ACC or CS may be the optimal target for pain improvement in the long-term experiments rather than in the short-term experimental design.

Therapeutic ultrasound has been widely used in clinical and scientific research due to its unique biological advantages and satisfactory efficacy in the treatment process [29, 30]. FUS is a noninvasive targeting therapy that uses a novel concave head to concentrate ultrasound energy into a range of millimeter diameters [31]. Unlike the thermal effects of high-intensity focused ultrasound (HIFU) [32], the biological effects of LIFU with regard to neuromodulation are primarily mechanical and can activate or inhibit neuronal activity by altering the state of mechanically sensitive ion channels embedded in cell membranes [33, 34]. Over the past decade, ultrasound stimulation of neurons has shown numerous advantages over electrical stimulation. In order to observe the changes in the functional state of neurons, most studies have detected the expression of c-fos in neurons as a marker of neuronal activity [35]. Qi et al. [36] selected low-intensity ultrasound to stimulate auditory neurons in vitro; they found that irrespective of whether low-frequency or high-frequency ultrasound was used, action potentials were produced in the cultured neurons. Furthermore, the expression levels of c-fos protein increased, as indicated by fluorescence staining, and neurons were significantly activated, as indicated by ultrasound. In addition, we showed that LIFU stimulation on ACC of normal mice increased the number of c-fos-positive cells in this region compared with non-LIFU controls by IF staining (Figure 3). The limitation is that we only examined the changes between LIFU and sham stimulation in normal

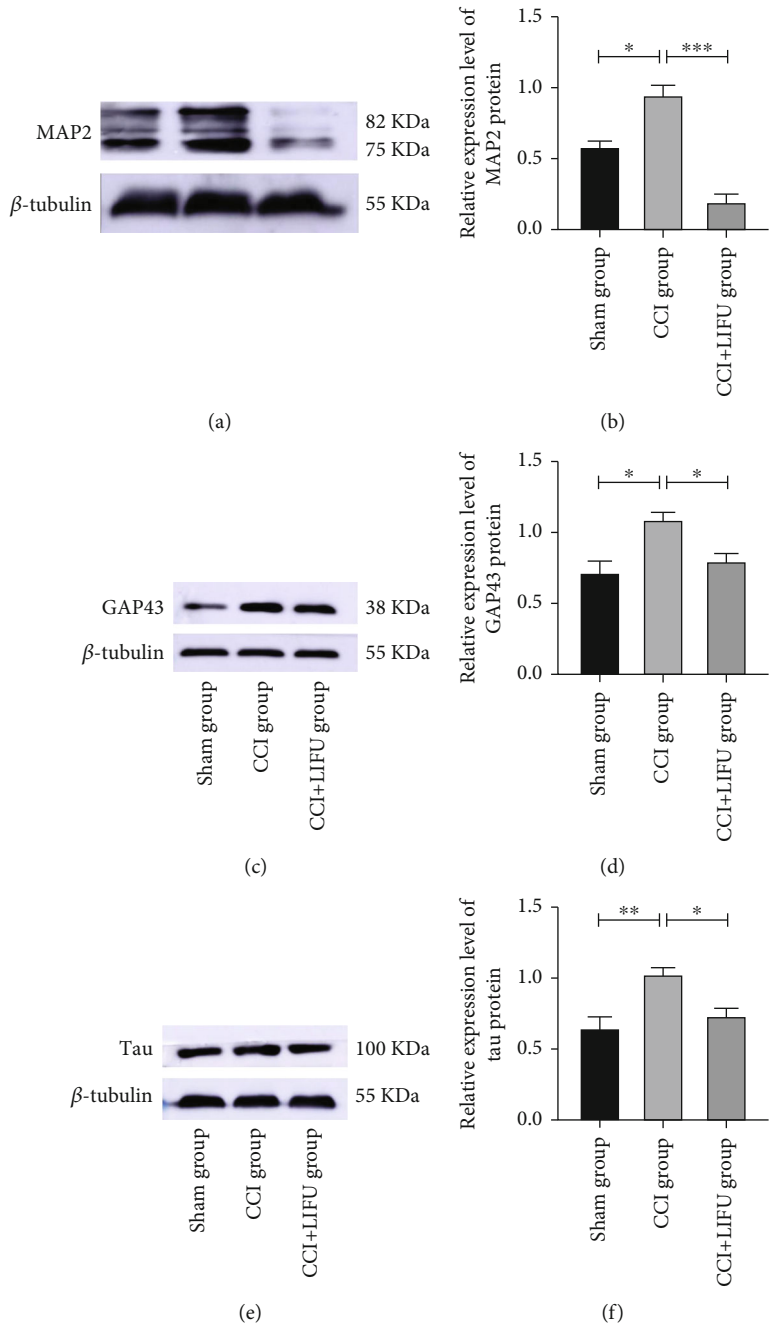

Figure 5: Western blotting (WB) analysis of microtubule-associated protein 2 (MAP2) (a, b), growth-associated protein 43 (GAP43) (c, d), and tau (e, f) expression in the ACC in different groups after 21 days post-LIFU treatment. Values were normalized to β-tubulin. Each symbol represents the mean ± SEM; $^{*}P < 0.05$, $^{**}P < 0.01$, and $^{***}P < 0.001$. One-way ANOVA; $n = 5$ rats per assay.

mice but not in the CCI model. A previous study conducted by our team also showed that the numbers of c-fos-positive cells and GAD65-positive cells (a marker of synaptic activity) increased, respectively, after 0.5 MPa and 1.5 MPa LIFU stimulation compared with that after stimulation with 0 MPa (negative stimulation) in the lumbar region of the spinal cord, producing a similar result that LIFU activates neurons significantly. These findings demonstrate that LIFU may activate the neuronal cells and GABAergic terminals in the brain or spinal cord. In addition, LIFU can be used as a new alternative treatment strategy; its safety profile and practicality are very attractive [37]. Liao et al. [38] investigated spinal cord tissues from both normal rats and a rat model of pain and found that LIFU did not cause edema, bleeding, or the activation of glial cells. There is also evidence that LIFU stimulation does not cause significant damage to the cortex or hippocampus, immune cell infiltration, or changes in the number and morphology of glial cells [39]. In the present study, we investigated the safety of LIFU stimulation in the target brain area and found that there was

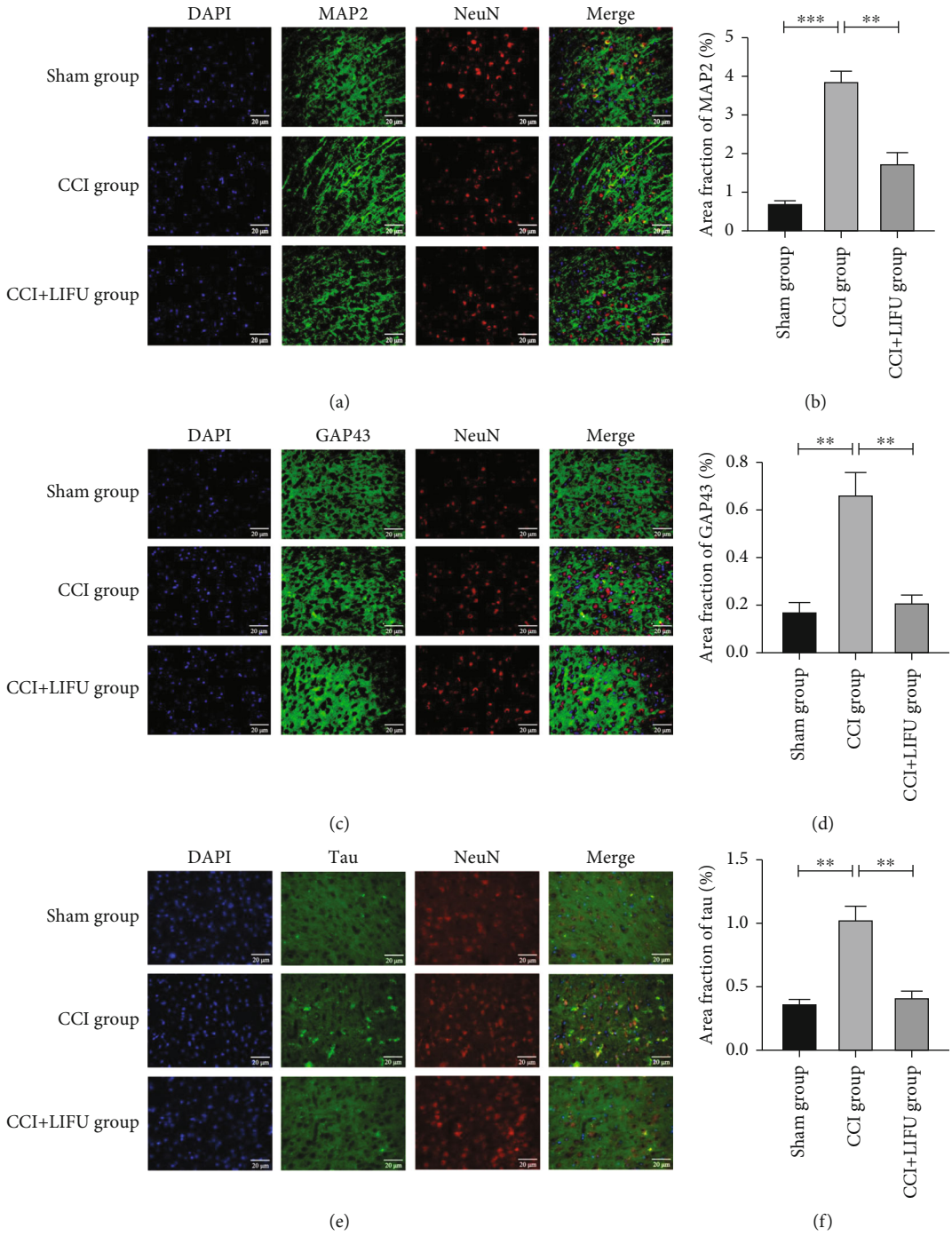

Figure 6: Expression of MAP2 (a), GAP43 (c), and tau (e) in the ACC of mice in different groups (immunofluorescence (IF), ×400). Scale bar, 20 μm. The expression of MAP2 (b), GAP43 (d), and tau (f) in the ACC of mice in different groups after 21 days of LIFU treatment, as detected by IF. Each symbol represents the mean ± SEM; $^{*}P < 0.05$, $^{**}P < 0.01$, and $^{***}P < 0.001$. One-way ANOVA; $n = 5$ rats per assay.

no obvious swelling or apoptosis in the neuronal cells, as demonstrated by H&E and FJC staining. This also confirmed the safety of LIFU in the neuromodulation process and showed that this technique can safely stimulate the ACC area.

Central mechanisms are attracting a lot of attention as research progresses because they play an important role in preventing and developing pain. The ACC, located at the front of the corpus callosum, is involved in the limbic system and the prefrontal cortex (PFC) [40]. This area of the brain is not only associated with the formation of memories, emotional responses, motor control, and cognitive behavior but also involved in encoding nociceptor receptor stimulation, as seen in several rodent models of chronic pain in which chemical or electrolytic stimulation of the ACC effectively attenuated pain-related behavioral responses [40, 41]. Moon

et al. [42] implanted an optical cable in the ACC region of rats with trigeminal neuralgia by using an adenovirus and found that the mechanical pain sensitivity threshold and cold pain sensitivity threshold scores of the rats increased after light stimulation; in addition, there was obvious pain relief, which confirmed the important role of ACC in analgesia. Recently, Feng et al. [25] discovered that LIFU regulated the ACC, as it was possible to effectively reduce the effect of MWT_{50} in the long-term experiment, but there were no significant changes in the thermal withdrawal threshold of the bilateral sides of the CNP model induced by CCI after 21 days of LIFU treatment on ACC. These findings suggest that the ACC brain region plays an important role in CNP, and its regulation may be a viable method to alleviate CNP allodynia. In our study, mechanical pain sensitivity symptoms were observed after surgery in CNP mice and were maintained until treatment was completed. The mechanical pain sensitivity of CNP mice improved significantly after LIFU treatment, thereby confirming the analgesic effect of LIFU on CNP-induced allodynia.

More detailed cell and molecular experiments with rodent models have revealed changes in neuronal and synapse remodeling in many areas of the brain involved in pain management, including the dorsal horns of the spinal cord and the cortical structures [43–45]. These advanced centers of the brain focus broadly on neural and synaptic remodeling of the ACC. At the synaptic level, potentiation of excitatory transmission caused by injuries may be mediated by the enhancement of glutamate release from presynaptic terminals and potentiated postsynaptic responses of AMPA receptors [9]. After long-term research, Lu et al. [46, 47] have found that chronic pain can cause changes in synaptic remodeling in the cerebral cortex and is closely related to pain perception and anxiety behavior, while the long-term potentiation (LTP) of synaptic transmission in the ACC region of the cerebral cortex is an important molecular mechanism for chronic pain. Furthermore, their team has recently discovered that increasing oxytocin content in ACC can selectively reduce chronic pain and eliminate pre-LTP that causes anxious behaviors and anxiety-related behaviors in mice with chronic pain associated with common peroneal nerve (CPN) ligation, confirming the effect of improving chronic pain by modulating central nervous system remodeling [48]. Um et al. [49] found that optical imaging techniques revealed a considerable increase in the neuronal response to peripheral stimulation in the ACC brain region of a rat model of CCI-induced chronic pain; when rapamycin inhibitors were injected into this brain area, the mechanical pain sensitivity response was significantly improved, confirming that the mechanism for relieving chronic pain may be to suppress synaptic plasticity induced by neuropathic pain by downregulating the mTOR signaling pathway, which could be a new strategy for treating chronic pain. Wang et al. [50] confirmed that the number of functional glutamatergic synapses increased along with new neural circuit formation and strengthening of the projection from the medial thalamus to the ACC. Structural remodeling was detected in the ACC, manifested by an increase in dendritic spine density and the number of synapses in a rat model of CCI-induced pain, thereby mediating the occurrence of pain. Furthermore, recent research has found that the enhancement of neural remodeling in the ACC caused by injecting trinitrobenzenesulfonic acid into the pancreatic duct is involved in the development and maintenance of visceral pain sensitivity and anxiety in rats, which supports a strong link between ACC neuroplasticity and chronic pain [51]. In our present study, WB and IF staining both demonstrated that the expression levels of neuroplasticity-related proteins (MAP2, GAP43, and tau) decreased significantly. This finding suggests that LIFU treatment on ACC can effectively attenuate CNP-evoked mechanical sensitivity to pain and reverse the aberrant central plasticity. The results of this study provide further research directions for the treatment of CNP by LIFU.

Overall, we demonstrated that (1) LIFU can be used to safely stimulate the ACC, (2) LIFU significantly improves mechanical pain sensitivity symptoms of the affected side in mouse models of CNP by stimulating the ACC region, (3) LIFU affects the expression levels of MAP2, GAP43, and tau proteins in the ACC area, and (4) the mechanism by which LIFU alleviates the CNP-induced allodynia may be achieved by reversing aberrant central remodeling.

5. Limitations

There are some limitations that need to be considered. First, we only measured MWT_{50}, but the thermal allodynia thresholds and emotional and cognitive behaviors were not tested in mice. Second, this study only examined the morphology of neural remodeling but did not detect changes in neuronal function. The long-term effects of LIFU on neural cells were not studied further. Finally, we found that LIFU can influence the expression levels of MAP2, GAP43, and tau; however, we did not investigate the molecular mechanisms by which LIFU influences neuroplasticity. Thus, further experiments are needed.

6. Conclusions

We found that LIFU can be used safely to stimulate the ACC and alleviate CNP-induced allodynia. Moreover, LIFU analgesia may be related to the suppression of neuroplasticity.

Abbreviations

ACC: Anterior cingulate cortex
AD: Alzheimer's disease
CNP: Chronic neuropathic pain
CS: Central sensitization
CCI: Chronic constrictive injury
CPN: Common peroneal nerve
DC: Duty cycle
FJC: Fluoro-Jade C
GAP43: Growth-associated protein 43
HIFU: High-intensity focused ultrasound
LIFU: Low-intensity focused ultrasound
MWT_{50}: 50% mechanical withdrawal threshold
MAP2: Microtubule-associated protein 2

NP: Neuropathic pain
PD: Parkinson's disease
PFC: Prefrontal cortex
SNL: Spinal nerve ligation
VFFs: Von Frey filaments.

Data Availability

The data used to support the findings of this study are available from the corresponding authors upon request.

Conflicts of Interest

The authors declare that they have no conflicts of interest.

Acknowledgments

This study was supported by the National Natural Science Foundation of China (No. 81960421 and No. 82060421) and the Basic Research Program of Yunnan Provincial Science and Technology Department (No. 202101AT070255).

References

[1] R. D. Treede, W. Rief, A. Barke et al., "Chronic pain as a symptom or a disease: the IASP Classification of Chronic Pain for the International Classification of Diseases (ICD-11)," *Pain*, vol. 160, no. 1, pp. 19–27, 2019.

[2] A. S. C. Rice, B. H. Smith, and F. M. Blyth, "Pain and the global burden of disease," *Pain*, vol. 157, no. 4, pp. 791–796, 2016.

[3] H. Breivik, B. Collett, V. Ventafridda, R. Cohen, and D. Gallacher, "Survey of chronic pain in Europe: prevalence, impact on daily life, and treatment," *European Journal of Pain*, vol. 10, no. 4, pp. 287–333, 2006.

[4] Ó. A. Steingrímsdóttir, T. Landmark, G. J. Macfarlane, and C. S. Nielsen, "Defining chronic pain in epidemiological studies: a systematic review and meta-analysis," *Pain*, vol. 158, no. 11, pp. 2092–2107, 2017.

[5] M. Zhuo, "Long-term potentiation in the anterior cingulate cortex and chronic pain," *Philosophical Transactions of the Royal Society B: Biological Sciences*, vol. 369, no. 1633, p. 3843878, 2014.

[6] A. Latremoliere and C. J. Woolf, "Central sensitization: a generator of pain hypersensitivity by central neural plasticity," *The Journal of Pain*, vol. 10, no. 9, pp. 895–926, 2009.

[7] K. Meacham, A. Shepherd, D. P. Mohapatra, and S. Haroutounian, "Neuropathic pain: central vs. peripheral mechanisms," *Current Pain and Headache Reports*, vol. 21, no. 6, p. 28, 2017.

[8] D. P. Kuffler, "Mechanisms for reducing neuropathic pain," *Molecular Neurobiology*, vol. 57, no. 1, pp. 67–87, 2020.

[9] M. Zhuo, "Cortical plasticity as synaptic mechanism for chronic pain," *Journal of Neural Transmission (Vienna)*, vol. 127, no. 4, pp. 567–573, 2020.

[10] Q. Y. Chen, X. H. Li, and M. Zhuo, "NMDA receptors and synaptic plasticity in the anterior cingulate cortex," *Neuropharmacology*, vol. 197, p. 108749, 2021.

[11] M. A. Apps, M. F. Rushworth, and S. W. Chang, "The anterior cingulate gyrus and social cognition: tracking the motivation of others," *Neuron*, vol. 90, no. 4, pp. 692–707, 2016.

[12] M. T. Tseng, M. C. Chiang, C. C. Chao, W. Y. I. Tseng, and S. T. Hsieh, "fMRI evidence of degeneration-induced neuropathic pain in diabetes: enhanced limbic and striatal activations," *Human Brain Mapping*, vol. 34, no. 10, pp. 2733–2746, 2013.

[13] M. L. Smith, N. Asada, and R. C. Malenka, "Anterior cingulate inputs to nucleus accumbens control the social transfer of pain and analgesia," *Science*, vol. 371, no. 6525, pp. 153–159, 2021.

[14] K. Koga, S. Shimoyama, A. Yamada et al., "Chronic inflammatory pain induced GABAergic synaptic plasticity in the adult mouse anterior cingulate cortex," *Molecular Pain*, vol. 14, p. 6096674, 2018.

[15] Y. Wang, C. M. Li, R. Han et al., "PCC0208009, an indirect IDO1 inhibitor, alleviates neuropathic pain and co- morbidities by regulating synaptic plasticity of ACC and amygdala," *Biochemical Pharmacology*, vol. 177, p. 113926, 2020.

[16] X. Y. Li, H. G. Ko, T. Chen et al., "Alleviating neuropathic pain hypersensitivity by inhibiting PKMzeta in the anterior cingulate cortex," *Science*, vol. 330, no. 6009, pp. 1400–1404, 2010.

[17] P. Ghanouni, K. B. Pauly, W. J. Elias et al., "Transcranial MRI-guided focused ultrasound: a review of the technologic and neurologic applications," *AJR. American Journal of Roentgenology*, vol. 205, no. 1, pp. 150–159, 2015.

[18] V. Krishna, F. Sammartino, and A. Rezai, "A review of the current therapies, challenges, and future directions of transcranial focused ultrasound technology," *JAMA Neurology*, vol. 75, no. 2, pp. 246–254, 2018.

[19] M. Ranjan, A. Boutet, S. Bhatia et al., "Neuromodulation beyond neurostimulation for epilepsy: scope for focused ultrasound," *Expert Review of Neurotherapeutics*, vol. 19, no. 10, pp. 937–943, 2019.

[20] Y. Wang, K. Luo, J. Li et al., "Focused ultrasound promotes the delivery of gastrodin and enhances the protective effect on dopaminergic neurons in a mouse model of Parkinson's disease," *Frontiers in Cellular Neuroscience*, vol. 16, p. 884788, 2022.

[21] W. Legon, T. F. Sato, A. Opitz et al., "Transcranial focused ultrasound modulates the activity of primary somatosensory cortex in humans," *Nature Neuroscience*, vol. 17, no. 2, pp. 322–329, 2014.

[22] D. Folloni, L. Verhagen, R. B. Mars et al., "Manipulation of subcortical and deep cortical activity in the primate brain using transcranial focused ultrasound stimulation," *Neuron*, vol. 101, no. 6, pp. 1109–1116, 2019.

[23] Council, *National Research Guide for the Care and Use of Laboratory Animals.*, National Academies Press, Washington D.C., 2011.

[24] P. Medeiros, R. L. de Freitas, S. Boccella et al., "Characterization of the sensory, affective, cognitive, biochemical, and neuronal alterations in a modified chronic constriction injury model of neuropathic pain in mice," *Journal of Neuroscience Research*, vol. 98, no. 2, pp. 338–352, 2020.

[25] X. Feng, L. Niu, M. Long et al., "Transcranial ultrasound stimulation of the anterior cingulate cortex reduces neuropathic pain in mice," *Evidence-Based Complementary and Alternative Medicinevol*, vol. 2021, article 6510383, 14 pages, 2021.

[26] S. R. Chaplan, F. W. Bach, J. W. Pogrel, J. M. Chung, and T. L. Yaksh, "Quantitative assessment of tactile allodynia in the rat paw," *Journal of Neuroscience Methods*, vol. 53, no. 1, pp. 55–63, 1994.

[27] S. R. Challa, "Surgical animal models of neuropathic pain: pros and cons," *The International Journal of Neuroscience*, vol. 125, no. 3, pp. 170–174, 2015.

[28] F. Barthas, M. Humo, R. Gilsbach et al., "Cingulate overexpression of mitogen-activated protein kinase phosphatase-1 as a key factor for depression," *Biological Psychiatry*, vol. 82, no. 5, pp. 370–379, 2017.

[29] R. Souza, I. C. S. da Silva, A. B. T. Delgado, P. H. V. Silva, and V. R. X. Costa, "Focused ultrasound and Alzheimer's disease a systematic review," *Dementia & Neuropsychologia*, vol. 12, no. 4, pp. 353–359, 2018.

[30] R. Martínez-Fernández, J. U. Máñez-Miró, R. Rodríguez-Rojas et al., "Randomized trial of focused ultrasound subthalamotomy for Parkinson's disease," *The New England Journal of Medicine*, vol. 383, no. 26, pp. 2501–2513, 2020.

[31] E. J. Lee, A. Fomenko, and A. M. Lozano, "Magnetic resonance-guided focused ultrasound : current status and future perspectives in thermal ablation and blood-brain barrier opening," *Journal of Korean Neurosurgical Association*, vol. 62, no. 1, pp. 10–26, 2019.

[32] R. Zhang, J. Y. Chen, L. Zhang et al., "The safety and ablation efficacy of ultrasound-guided high-intensity focused ultrasound ablation for desmoid tumors," *International Journal of Hyperthermia*, vol. 38, no. 2, pp. 89–95, 2021.

[33] A. Hellman, T. Maietta, A. Clum et al., "Pilot study on the effects of low intensity focused ultrasound in a swine model of neuropathic pain," *Journal of Neurosurgery*, vol. 16, pp. 1–8, 2021.

[34] J. Kubanek, J. Shi, J. Marsh, D. Chen, C. Deng, and J. Cui, "Ultrasound modulates ion channel currents," *Scientific Reports*, vol. 6, p. 4845013, 2016.

[35] W. H. Zhang, W. Z. Liu, Y. He et al., "Chronic stress causes projection-specific adaptation of amygdala neurons via small-conductance calcium-activated potassium channel downregulation," *Biological Psychiatry*, vol. 85, no. 10, pp. 812–828, 2019.

[36] X. Qi, K. Lyu, L. Meng et al., "Low-intensity ultrasound causes direct excitation of auditory cortical neurons," *Neural Plasticity*, vol. 2021, Article ID 8855055, 10 pages, 2021.

[37] A. Hellman, T. Maietta, K. Byraju et al., "Low intensity focused ultrasound modulation of vincristine induced neuropathy," *Neuroscience*, vol. 430, pp. 82–93, 2020.

[38] Y. H. Liao, B. Wang, M. X. Chen, Y. Liu, and L. J. Ao, "LIFU alleviates neuropathic pain by improving the KCC(2) expression and inhibiting the CaMKIV-KCC(2) pathway in the L4-L5 section of the spinal cord6659668," *Neural Plasticity*, vol. 2021, 10 pages, 2021.

[39] S. G. Chen, C. H. Tsai, C. J. Lin et al., "Transcranial focused ultrasound pulsation suppresses pentylenetetrazol induced epilepsy in vivo," *Brain Stimulation*, vol. 13, no. 1, pp. 35–46, 2020.

[40] J. P. Ramirez-Mahaluf, J. Perramon, B. Otal, P. Villoslada, and A. Compte, "Subgenual anterior cingulate cortex controls sadness-induced modulations of cognitive and emotional network hubs," *Scientific Reports*, vol. 8, no. 1, p. 8566, 2018.

[41] J. P. Johansen and H. L. Fields, "Glutamatergic activation of anterior cingulate cortex produces an aversive teaching signal," *Nature Neuroscience*, vol. 7, no. 4, pp. 398–403, 2004.

[42] H. C. Moon, W. I. Heo, Y. J. Kim et al., "Optical inactivation of the anterior cingulate cortex modulate descending pain pathway in a rat model of trigeminal neuropathic pain created via chronic constriction injury of the infraorbital nerve," *Journal of Pain Research*, vol. 10, pp. 2355–2364, 2017.

[43] T. V. Bliss, G. L. Collingridge, B. K. Kaang, and M. Zhuo, "Synaptic plasticity in the anterior cingulate cortex in acute and chronic pain," *Nature Reviews. Neuroscience*, vol. 17, no. 8, pp. 485–496, 2016.

[44] M. Zhuo, "A synaptic model for pain: long-term potentiation in the anterior cingulate cortex," *Molecules and Cells*, vol. 23, no. 3, pp. 259–271, 2007.

[45] M. Zhuo, "Long-term cortical synaptic changes contribute to chronic pain and emotional disorders," *Neuroscience Letters*, vol. 702, pp. 66–70, 2019.

[46] J. S. Lu, Q. Y. Chen, X. Chen et al., "Cellular and synaptic mechanisms for Parkinson's disease-related chronic pain," *Molecular Pain*, vol. 17, p. 174480692199902, 2021.

[47] X. H. Li, Q. Y. Chen, and M. Zhuo, "Neuronal adenylyl cyclase targeting central plasticity for the treatment of chronic pain," *Neurotherapeutics*, vol. 17, no. 3, pp. 861–873, 2020.

[48] X. H. Li, T. Matsuura, M. Xue et al., "Oxytocin in the anterior cingulate cortex attenuates neuropathic pain and emotional anxiety by inhibiting presynaptic long-term potentiation," *Cell Reports*, vol. 36, no. 3, p. 109411, 2021.

[49] S. W. Um, M. J. Kim, J. W. Leem, S. J. Bai, and B. H. Lee, "Pain-relieving effects of mTOR inhibitor in the anterior cingulate cortex of neuropathic rats," *Molecular Neurobiology*, vol. 56, no. 4, pp. 2482–2494, 2019.

[50] Y. Q. Wang, J. Wang, S. H. Xia et al., "Neuropathic pain generates silent synapses in thalamic projection to anterior cingulate cortex," *Pain*, vol. 162, no. 5, pp. 1322–1333, 2021.

[51] D. Ren, J. N. Li, X. T. Qiu et al., "Anterior cingulate cortex mediates hyperalgesia and anxiety induced by chronic pancreatitis in rats," *Neuroscience Bulletin*, vol. 38, no. 4, p. 342, 2022.

Hindawi
Neural Plasticity
Volume 2022, Article ID 1489841, 15 pages
https://doi.org/10.1155/2022/1489841

Research Article

Electroacupuncture Alleviates Neuropathic Pain through Regulating miR-206-3p Targeting BDNF after CCI

Wenzhan Tu,[1,2,3] Jingjing Yue,[1] Xuqing Li,[1] Qiaoyun Wu,[1] Guanhu Yang,[1] Shengcun Li,[1] Qiangsan Sun,[2,3] and Songhe Jiang[1]

[1]*Rehabilitation Medicine Center, The Second Affiliated Hospital of Wenzhou Medical University, Wenzhou, Zhejiang, China 325027*
[2]*Shandong University, 27 Shanda Nanlu, Jinan, Shandong, China 250100*
[3]*Department of Rehabilitation Medicine, The Second Hospital, Cheeloo College of Medicine, Shandong University, 247 Beiyuanda Street, Jinan, Shandong, China 250033*

Correspondence should be addressed to Shengcun Li; lishengcun@wmu.edu.cn, Qiangsan Sun; sunqsan@126.com, and Songhe Jiang; jiangsonghe@wmu.edu.cn

Received 28 December 2021; Accepted 27 April 2022; Published 9 June 2022

Academic Editor: Hao-Yu Hu

Background. Electroacupuncture (EA) has benefits for neuropathic pain. However, the underlying mechanisms are still unknown. The current study explores the underlying mechanisms of EA in neuropathic pain of chronic constriction injury (CCI) rats. *Material/Methods*. Overall, 126 Sprague-Dawley (200-250 g) rats were divided into nine groups randomly: the sham-operated, CCI, CCI+EA, CCI+sham EA, CCI+NS, CCI+AAV-NC, CCI+AAV-miR-206-3p, CCI+EA+NS, and CCI+EA+AAV-miR-206-3p groups. The animals were sacrificed 14 days postsurgery. Mechanical withdrawal threshold (MWT) and thermal withdrawal latency (TWL) tests were used to determine differences in neurobehavioral manifestations. qPCR, western blotting, and immunofluorescence (IF) were carried out to detect the expression levels of miR-206-3p, BDNF, BAX/Bcl-2, TNF-α, and IL-6. Nissl staining was measured to observe morphological changes in neurons. Transmission electron microscopy (TEM) was employed to evaluate microscopic changes in dorsal horn synapses. *Results*. Hyperalgesia was reduced markedly by EA in the CCI model. The expression level of miR-206-3p was elevated, whereas the expression levels of BDNF, BAX/Bcl-2, TNF-α, and IL-6 were decreased in EA-treated CCI rats. However, a miR-206-3p inhibitor partially abrogated the analgesic effect of EA and resulted in poor behavioral performance and the BDNF, BAX/Bcl-2, TNF-α, and IL-6 expression was elevated as well. *Conclusions*. EA can relieve neuropathic pain by regulating the miR-206-3p/BDNF pathway, thus exerting anti-inflammatory and antiapoptotic effect.

1. Introduction

It is well recognized that injury or disease of the somatosensory system is responsible for the occurrence of neuropathic pain, presenting with allodynia, hyperalgesia, and abnormal pain [1]. It has become a public health problem worldwide due to the long course of the disease, its high incidence, and its tendency to markedly reduce patients' quality of life [2]. However, there are currently no satisfactory treatments for neuropathic pain [3]. Thus, exploring the mechanism of neuropathic pain to provide novel insight into and a basis for the treatment of pain is of importance. Electroacupuncture (EA), as an acupuncture technique that combines modern electrical stimulation with traditional acupuncture, is popular in clinical practice [4–6]. It is well recognized that EA is effective in ameliorating neuropathic pain, causing few side effects exerting and long-lasting analgesic effects, but the underlying mechanism remains to be further explored [5, 6].

Recently, the function of noncoding RNAs in neuropathic pain has become a hot topic, and noncoding RNAs are speculated to be a new therapeutic target [2, 7]. Research suggests that many microRNAs (miRNAs) participate in the regulatory effect of acupuncture on ischaemic stroke, spinal

cord injury, depression, and other conditions [8–11]. However, the effect of EA on miRNA-dependent modulators in neuropathic pain is largely undefined [12, 13].

Brain-derived neurotrophic factor (BDNF), as a member of the neurotrophic factor (NTF) family, is a key neuromodulator of the transmission of pain in the peripheral nervous system and central nervous system (CNS) [14, 15]. Some data suggest that BDNF is connected with the regulatory process by which EA relieves neuropathic pain [16]. Furthermore, as a potential target gene, BDNF is negatively regulated by a variety of miRNAs such as miR-30a, miR-206, and miR-1B [13, 17].

miRNAs are endogenous, noncoding RNA with approximately 22 nucleotides in length that are found widely in eukaryotes and prevent mRNA translation and/or promote protein degradation by complementarily binding to specific sites in the $3'$-untranslated regions ($3'$-UTRs) of target genes [4]. Some studies have demonstrated that miRNAs are related to the process of chronic pain (Qiang [3, 18]) and that EA might enhance the repair of peripheral nerve injury (PNI) through regulating miRNAs [13]. Evidence has suggested that an increase in miR-206 expression aids the recovery from neuropathic pain [15]. miR-206-3p has attracted increasing attention, and BDNF is regulated by miR-206-3p via a conserved binding site in its $3'$-UTR [15].

It has been well proved that inflammation, apoptosis, and autophagy are associated with the development of neuropathic pain [19–21]. As a key pathological mechanism, neuroinflammation is connected to the activation of glial cells (such as microglia and astrocytes) accompanied by the secretion of proinflammatory cytokines [22, 23]. Some scholars have suggested that EA alleviates neuropathic pain by exerting antiapoptotic and anti-inflammatory effects [24, 25].

Therefore, the current study will further reveal the potential mechanism related to EA treatment in neuropathic pain from the perspective of a gene regulation network with miRNAs as the core. We hypothesized that EA may improve neuropathic pain through the miR-206-3p/BDNF pathway, which is consistent with the secretion of neuroinflammatory cytokines and neuronal apoptosis in spinal dorsal horn. The rats were used to evoke neuropathic pain by establishing a chronic constriction injury (CCI) model and treated with EA. We used the adeno-associated viral (AAV) vectors to determine the function of miR-206-3p in the EA-mediated alleviation of neuropathic pain and further confirmed the existence of a tight correlation between the analgesia effect of EA and the miR-206-3p/BDNF pathway.

2. Material and Methods

2.1. Animals and Experimental Design. All animal protocols were approved by the Animal Research Committee of Wenzhou Medical University and performed following the guidelines of the Guide for the Care and Use of Laboratory Animals published by the US National Institutes of Health (NIH Publication No. 85-23, revised 1996). In total, 126 adult male Sprague-Dawley rats (200–250 g) were purchased from the Laboratory Animal Center of Wenzhou Medical University. The rats were housed at a constant temperature (22°C–24°C) under a norma12 h light-dark cycle, with free access to food and water.

The rats were randomly allocated to the following nine groups ($n = 14$ each): S group (sham-operated), M group (CCI modelling), ME group (CCI+EA treatment), MSE group (CCI+sham EA), M+NS group (CCI+normal saline), M+AAV-NC group (CCI+negative control virus), M +AAV-miR-206-3p group (CCI+AAV-miR-206-3p), ME +NS group (CCI+normal saline+EA), and ME+AAV-miR-206-3p group (CCI+AAV-miR-206-3p+EA).

2.2. CCI Model. Rats were anaesthetized by 2% sodium pentobarbital (30 *mg/kg, i.p.*) and subjected to CCI based on previous methods with modifications [26]. The left sciatic nerve was carefully exposed and tied with four knots loosely. The distance between ligatures was approximately 1 mm, and all ligatures were of the same tightness. Finally, the nerve was returned to its original location after ligation, and the muscle and skin layers were sutured. The sciatic nerve was exposed but not ligated in the sham-operated group.

2.3. Mechanical Withdrawal Threshold (MWT). Mechanical sensitivity was evaluated with Von Frey's method (IITC Life Sciences, California, USA) between 15:00 and −18:00. Briefly, rats were kept in the testing environment for 15 min to allow them to acclimate and become calm. Von Frey stimuli were given to the plantar surface of the rat paw, and the force that elicited paw withdrawal was recorded. The test was repeated 5 times with 5 min interval, and then, the average value was obtained.

2.4. Thermal Withdrawal Latency (TWL). To evaluate thermal hypersensitivity, an A37370 plantar test apparatus (Ugo-Basile, Milan, Italy) was applied. Briefly, the rats were allowed to adapt to the transparent box for 20 min before the test. The plantar surface of the rat paw was irradiated with infrared light generated by an instrument, and the radiant heat source was automatically stopped when the rat lifted its hindpaws. Each test was conducted 5 times at an interval of 5 min for each paw, and the average value was obtained.

2.5. EA Treatment. The acupoints applied in the present study are Zusanli (ST-36) and Yanglingquan (GB-34). Rats were fixed with a rat fixator (similar to a fixed vest, which is self-made and patented by our subject). After training for 2-3 days, the rats can lie down stably and receive electroacupuncture stimulation. Rats in the ME and ME+AAV-miR-206-3 groups were treated with EA intervention every 24 h from the 8th day after CCI, for a total of 7 days. The acupuncture needle stimulated electrically lasting for 30 min using a device at a frequency of 2/100 Hz (1.5 mA) (Hans200e, Jisheng Medical Device) and was inserted 2-3 mm deep. Needles were inserted into the same acupoint at a depth of 0.5 mm, but electrical stimulation was not applied in the MSE group.

2.6. Virus Construction and Intrathecal (i.t.) Injection. A recombinant adeno-associated virus (rAAV2/8), pAKD-CMVbGlobin-enhanced green fluorescent protein (eGFP)-H1-rno-miR-206-3p blocking (AAV-miR-206-3p)

Table 1: Primers for rno-miR-206-3p and BDNF.

Gene	Primers
2003rno-miR-206-3p	
Forward	GCGCGTGGAATGTAAGGAAGT
Reverse	AGTGCAGGGTCCGAGGTATT
RT primer	GTCGTATCCAGTGCAGGGTCCGAGGTATTCGCACTGGATACGACCCACAC
U6	
Forward	AGAGAAGATTAGCATGGCCCCTG
Reverse	ATCCAGTGCAGGGTCCGAGG
BDNF	
Forward	GGTTATTTCATACTTCGGTTGC
Reverse	CCCATTCACGCTCTCCAG
GAPDH	
Forward	GACATGCCGCCTGGAAC
Reverse	AGCCCAGGATGCCCTTTAGT

($1.57E+13\,\mu$g/ml), was produced by Obio Biotechnology Co., Ltd. (Shanghai, China). As a negative control, recombinant AAV-pAKD-CMVbGlobin-eGFP-H1-shRNA (AAV-NC) ($1.11E+13\,\mu$g/ml) was constructed. The AAVs were fluorescence labeled with eGFP. Because adeno-associated virus generally needs more than 2 weeks to replicate and stably express, two weeks before CCI, 8 μl AAV-miR-206-3p or AAV-NC was injected intraspinally into the dorsal L5 spinal cord of the rats using a microinjection syringe (33 G, 10 mm) in situ. The rats in the M+NS group were intrathecally injected with an equal volume of saline as a control.

2.7. Quantitative Real-Time PCR. Using TRIzol reagent, total RNA was extracted from tissues. 1000 ng of total RNA from each sample was applied to synthesize cDNA of miRNAs and mRNAs with an RT Reagent Kit (RR037A, TaKaRa). Afterwards, the cDNA was diluted with ddH_2O and prepared for qPCR using the LightCycler 480 system (Roche, Germany) according to instructions of the TB Green Kit (RR820A, TaKaRa). The $2^{-\Delta\Delta CT}$ method was performed to calculate the relative expression of miR-206-3p and BDNF. The primer sequences used are shown in Table 1 ($5'$-$3'$).

2.8. Nissl Staining. Spinal cord tissues were fixed with 4% paraformaldehyde (PA) and embedded with paraffin. Paraffin slices were dewaxed, immersed in Nissl staining solution, and dehydrated with ethanol. The slices were then placed in xylene and sealed with neutral gum. Then, the sections were analyzed under a brightfield microscope (Olympus, Tokyo, Japan).

2.9. Immunofluorescence (IF). After the rats were sacrificed with saline perfusion followed by 4% PA, spinal cord tissues were obtained and postfixed in PA lasting 24 h. Next, the tissues were dehydrated in sucrose solutions, embedded in OCT freezing medium, and cut to 5 μm frozen sections. Afterwards, the sections were rewarmed for 30 min, washed with 0.01 M PBS, and blocked with 0.3% Triton X-100. The incubation of rabbit anti-BDNF (1 : 200, DF6387) was performed at 4°C overnight. Subsequently, the sections were thoroughly rinsing in PBS and incubated with secondary antibodies at room temperature for 1 h. DAPI staining was added for 10 min, and a fluorescence microscope was applied to observe and collect the images (Olympus, Tokyo, Japan).

2.10. Western Blot Analysis. On postoperative day 14, the lumbar enlargements of spinal cords were obtained and prepared for total protein extraction. The protein was electrophoretically separated with SDS-polyacrylamide gels and transferred onto PVDF membrane. Following a block with 5% skim milk for 2 h, membrane was incubated with primary antibodies for 16-24 h at 4°C. The membrane was rinsed and then incubated with second antibody for 2 h at room temperature. Subsequently, the membrane was imaged, and ImageJ software was used for quantitative analysis. The primary antibodies were as follows: rabbit anti-BDNF (1 : 1000, ab108319), rabbit anti-Bax (1 : 500, AF0120), rabbit anti-Bcl-2 (1 : 500, AF6139), rabbit anti-TNF-α (1 : 500, AF7014), rabbit anti-IL-6 (1 : 500, DF6087), and mouse anti-tubulin (1 : 1000, AF7011).

2.11. Transmission Electron Microscopy (TEM). After the rats were anaesthetized, fresh spinal cord tissues were immediately obtained and fixed overnight with 2.5% glutaraldehyde. After washing, the specimens were placed in 1% osmic acid for 1 h and then stained for 2 h (1% uranium acetate) at room temperature. Dehydration of the samples was performed with gradient acetone followed by embedding. Semithin slices and toluidine blue staining were performed for localization analysis, and ultrathin sections were imaged by TEM (Hitachi, Tokyo, Japan).

2.12. Statistical Analysis. All data were shown as the mean ± SD. One-way ANOVA and Dunnett's test were applied for multigroup comparisons. Student's t-test was applied for evaluation between two experimental groups. The analysis of TWL and MWT was assessed with two-way ANOVA and Bonferroni's post hoc test. SPSS 25.0 statistical software

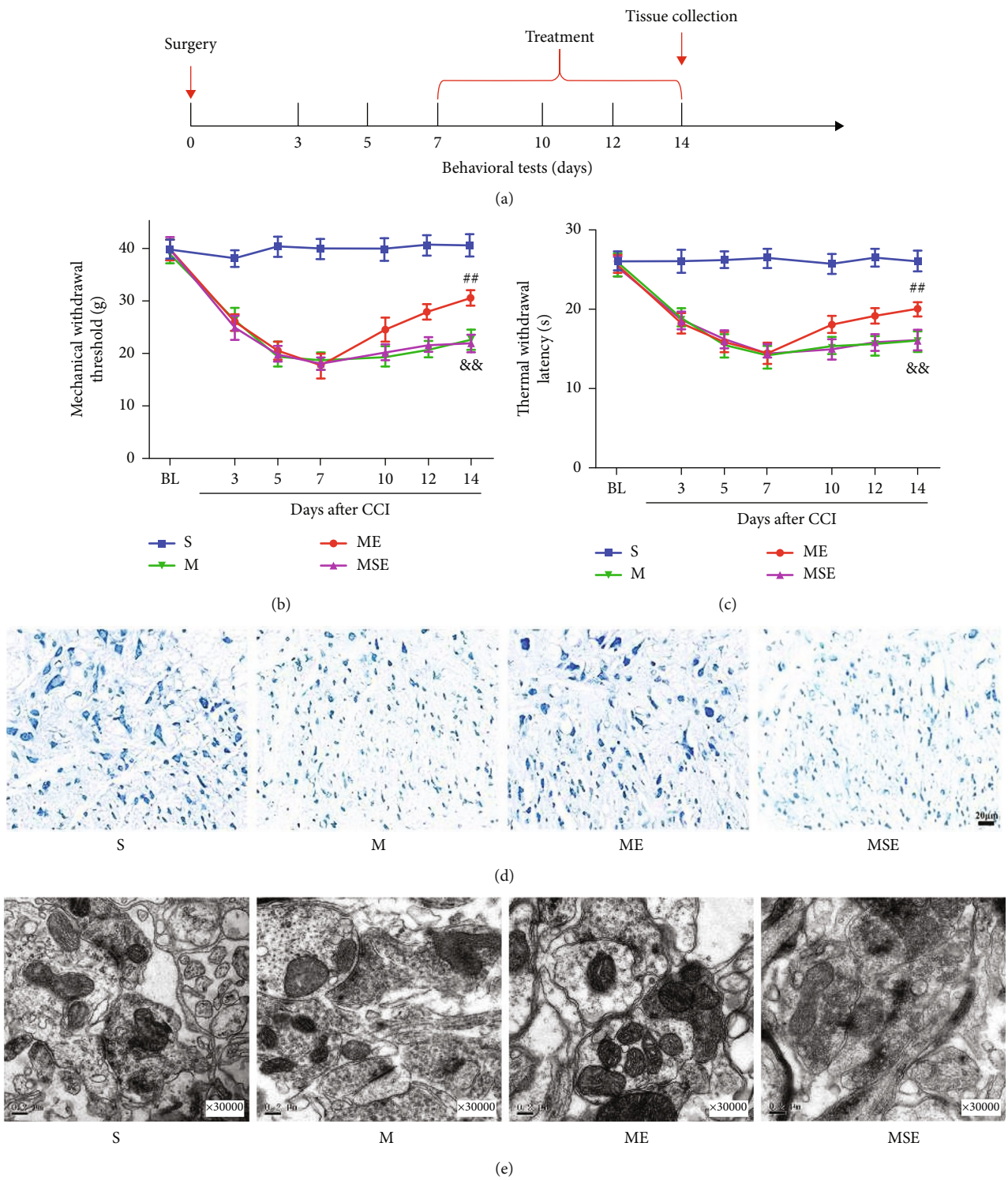

Figure 1: EA treatment alleviated hyperalgesia, reduced nerve damage, and improved synaptic plasticity in CCI rats. (a) Experimental design and timeline. (b, c) Changes in neurobehavioral MWT and TWL values of rats in each group ($n = 14$). (d) Nissl staining to observe the neuron morphology of the spinal dorsal horn (scale bars: 20 μm, 50x). (e) TEM to observe the ultrastructural changes at dorsal horn synapses (0.2 μm, 30000x). $^{\&\&}p < 0.01$ versus S group; $^{\#\#}p < 0.01$ versus M group.

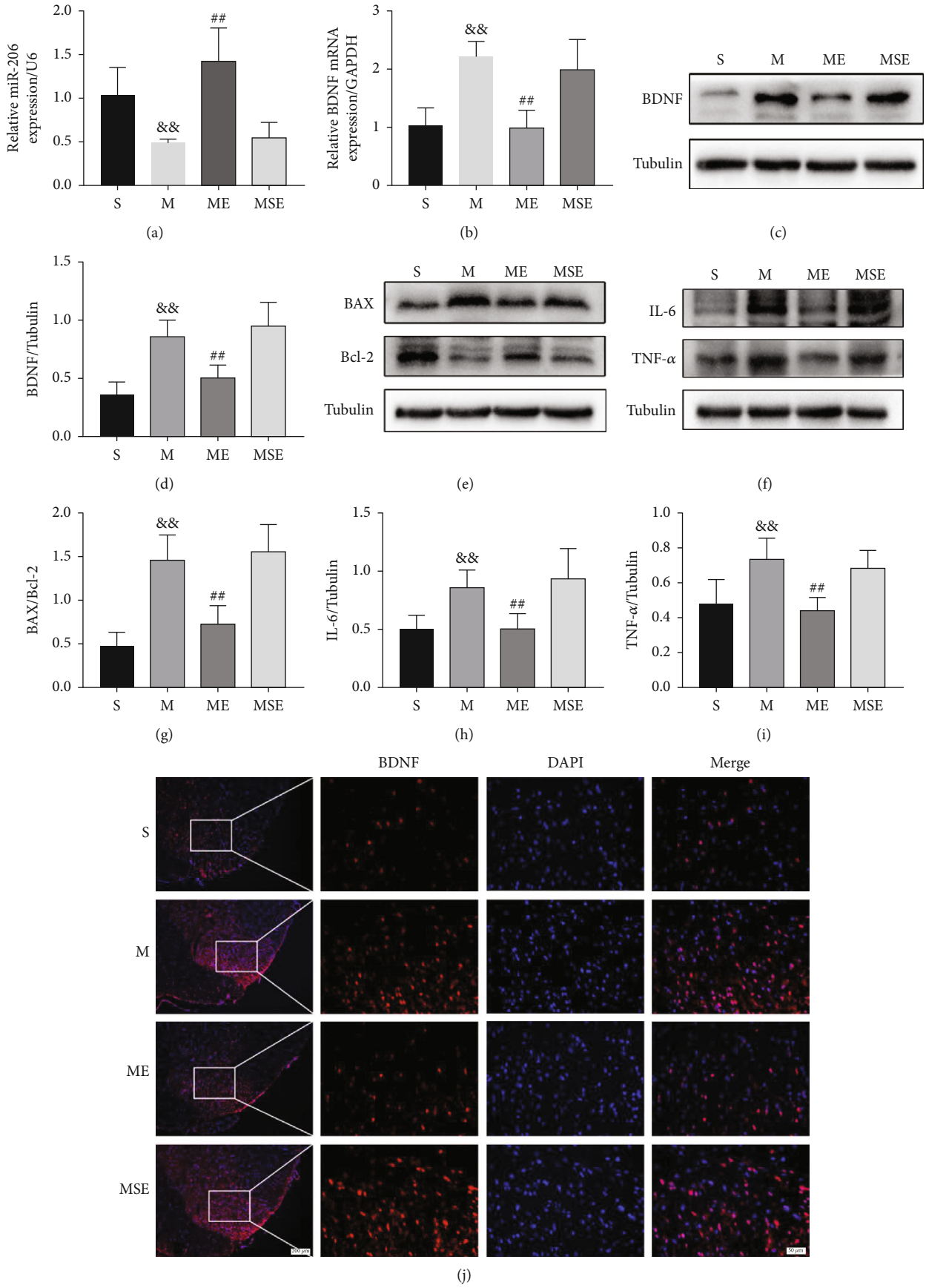

Figure 2: Continued.

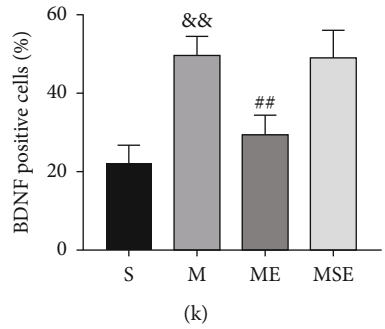

Figure 2: EA upregulated the expression of miR-206-3p and inhibited the expression of the target gene BDNF, while decreasing the expression of BAX/Bcl-2, IL-6, and TNF-α after CCI. (a, b) The expression of miR-206-3p and BDNF mRNA ($n = 5$). (c, d) Representative western blots and quantification data of BDNF/GAPDH ($n = 5$). (e–i) Representative western blots and quantification data of BAX/Bcl-2, IL-6/GAPDH, and TNF-α/GAPDH ($n = 5$). (j, k) Staining for BDNF-positive (red) cells from the spinal dorsal horn (scale bars: 100 μm 100x; 20 μm, 400x) ($n = 5$). Bars indicate the mean ± SD. $^{\&\&}p < 0.01$ versus the S group; $^{\#\#}p < 0.01$ versus the M group.

was employed for analysis, and $p < 0.05$ was considered statistically significant.

3. Results

3.1. EA Treatment Alleviated Hyperalgesia, Reduced Nerve Damage, and Improved Synaptic Plasticity in CCI Rats. Both TWL and MWT data (Figures 1(b) and 1(c)) were collected before surgery and 3, 5, 7, 10, 12, and 14 days after surgery. The behavioral value of the rats remarkably decreased after the surgery, except for that in the S group. Both TWL and MWT of the M group were dramatically decreased ($p < 0.01$) as compared with those of the S group at 14 days after CCI. Both TWL and MWT of the ME group were higher than those of the M group ($p < 0.01$). The pain thresholds of the rats in the M and MSE groups were not significantly different ($p > 0.05$).

Nissl staining (Figure 1(d)) indicated that Nissl bodies showed severe injury in the M group, and that this damage was alleviated after EA. TEM (Figure 1(e)) revealed changes in synapses in each group. Notably, the M group revealed abnormal synaptic structures with more synaptic vesicles and narrower synaptic gap than the S group. In addition, the synaptic structure of the ME group was improved, as this group showed the number of synaptic vesicles is fewer and width of synaptic gaps is larger than the M group.

3.2. EA Upregulated the Expression of miR-206-3p and Inhibited the Expression of the Target Gene BDNF While Decreasing the Expression of BAX/Bcl-2, IL-6, and TNF-α after CCI. To identify whether miR-206-3p was abnormally expressed in the spinal dorsal horn of CCI rats, the expression levels of miR-206-3p were measured using qPCR. The results of qPCR (Figures 2(a) and 2(b)) showed that the expression level of miR-206-3p in the M group was dramatically reduced ($p < 0.01$), and the expression levels of BDNF mRNA in the M group were dramatically increased ($p < 0.01$), compared with those in the S group. In the ME group, the expression level of miR-206-3p was dramatically higher ($p < 0.01$) and BDNF mRNA was dramatically lower than that in the M group ($p < 0.01$) after 1 week of EA.

The BDNF expression levels were also confirmed by western blotting and IF (Figures 2(c), 2(d), 2(j), and 2(k)), and the results were in line with the mRNA expression levels. Western blot analysis (Figures 2(e)–2(h)) revealed that the expression of BAX/Bcl-2, IL-6, and TNF-α in the M group was remarkably increased as compared with that in the S group (BAX/Bcl-2, $p < 0.01$; IL-6, $p < 0.01$; TNF-α, $p < 0.01$), whereas the expression of BAX/Bcl-2, IL-6, and TNF-α was significantly decreased in the ME group (BAX/Bcl-2, $p < 0.01$; IL-6, $p < 0.01$; TNF-α, $p < 0.01$).

3.3. A miR-206-3p Inhibitor Aggravated Hyperalgesia in CCI Rats and Damage to Spinal Dorsal Horn Neurons. To examine the function of miR-206-3p, rats were intrathecally injected with AAV to inhibit miR-206-3p in the lumbar spinal cord 14 days before CCI. The TWL and MWT were measured before surgery (−14 and 0 days) and 3, 5, 7, 10, 12, and 14 days after surgery. Figures 3(b) and 3(c) show that the pain threshold (TWL and MWT) was significantly reduced in all three groups. Both TWL and MWT of the M+AAV-miR-206-3p group were markedly increased on the 14th day after CCI as compared with those of the M +NS group ($p < 0.01$). These data suggested that mechanical and thermal pain hypersensitivity was aggravated by a miR-206-3p inhibitor in CCI rats.

Nissl staining (Figure 3(d)) revealed that neuronal damage was aggravated in the M+AAVmiR-206-3p group than the M+NS group, and vacuole-like changes were observed. TEM (Figure 3(e)) demonstrated that the synapses of neurons in the M+AAV-miR-206-3p group contained more synaptic vesicles and were narrower than those in the M+NS group.

3.4. A miR-206-3p Inhibitor Increased the Expression of BDNF, BAX/Bcl-2, IL-6, and TNF-α after CCI. IF (Figure 4 (i)) showed that, 14 days after injection of eGFP-labelled AAV, the rat lumbar spinal cord was transfected with GFP-AAV-miR-206-3p and GFP-AAV-NC. qPCR and western blot analysis (Figures 4(a)–4(c)) exhibited that the mRNA and protein expression levels of BDNF in the M +AAV-miR-206-3p group were dramatically increased as compared with those in the M+NS group ($p < 0.01$).

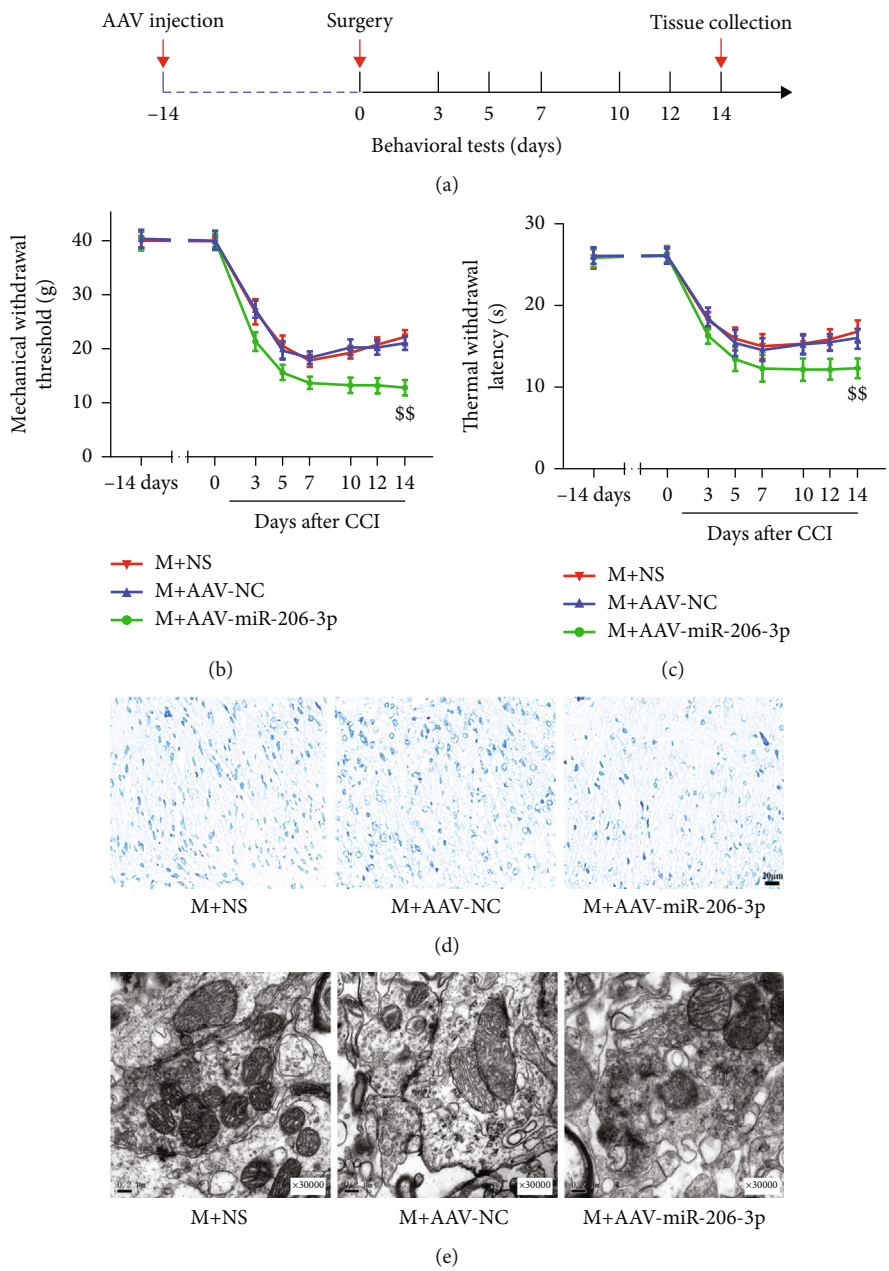

Figure 3: A miR-206-3p inhibitor aggravates hyperalgesia in CCI rats and damage to spinal dorsal horn neurons. (a) Experimental design and timeline. (b, c) MWT and TWL in each group ($n = 14$). (d) Nissl staining images (scale bars: 20 μm, 50x). (e) The ultrastructural changes of synapses in each group (0.2 μm, 30000x). $^{\$\$}$ $p < 0.01$ versus the M+NS group.

IF (Figures 4(j) and 4(k)) again verified that the fluorescence intensity of BDNF in the M+AAV-miR-206-3p group was stronger than that in the M+NS group. Western blot analysis (Figures 4(d)–4(g)) showed that the expression of BAX/Bcl-2, IL-6, and TNF-α was dramatically increased in the M+AAV-miR-206-3p group than the M+NS group (BAX/Bcl-2, $p < 0.01$; IL-6, $p < 0.01$; TNF-α, $p < 0.05$).

3.5. A miR-206-3p Inhibitor Blocked the Therapeutic Effect of EA and Did Not Alleviate Hyperalgesia. To assess the role miR-206-3p in the effect of EA, we treated CCI rats with EA following AAV injection. The TWL and MWT were both measured before surgery (−14 and 0 days) and 3, 5, 7, 10, 12, and 14 days after surgery. As shown in Figures 5(b) and 5(c), the MWT and TWL of rats in both groups were significantly reduced following surgery. After 1 week of EA, the behavioral scores of the ME+AAV-miR-206-3p group were significantly lower compared with those of the ME+NS group ($p < 0.01$).

Nissl staining (Figure 5(d)) showed that the neurons in the ME+AAV-miR-206-3p group were smaller and shown a more irregular morphology than those in the ME+NS group. TEM (Figure 5(e)) showed that the rats in the ME +AAV-miR-206-3p group had abnormal synapses with

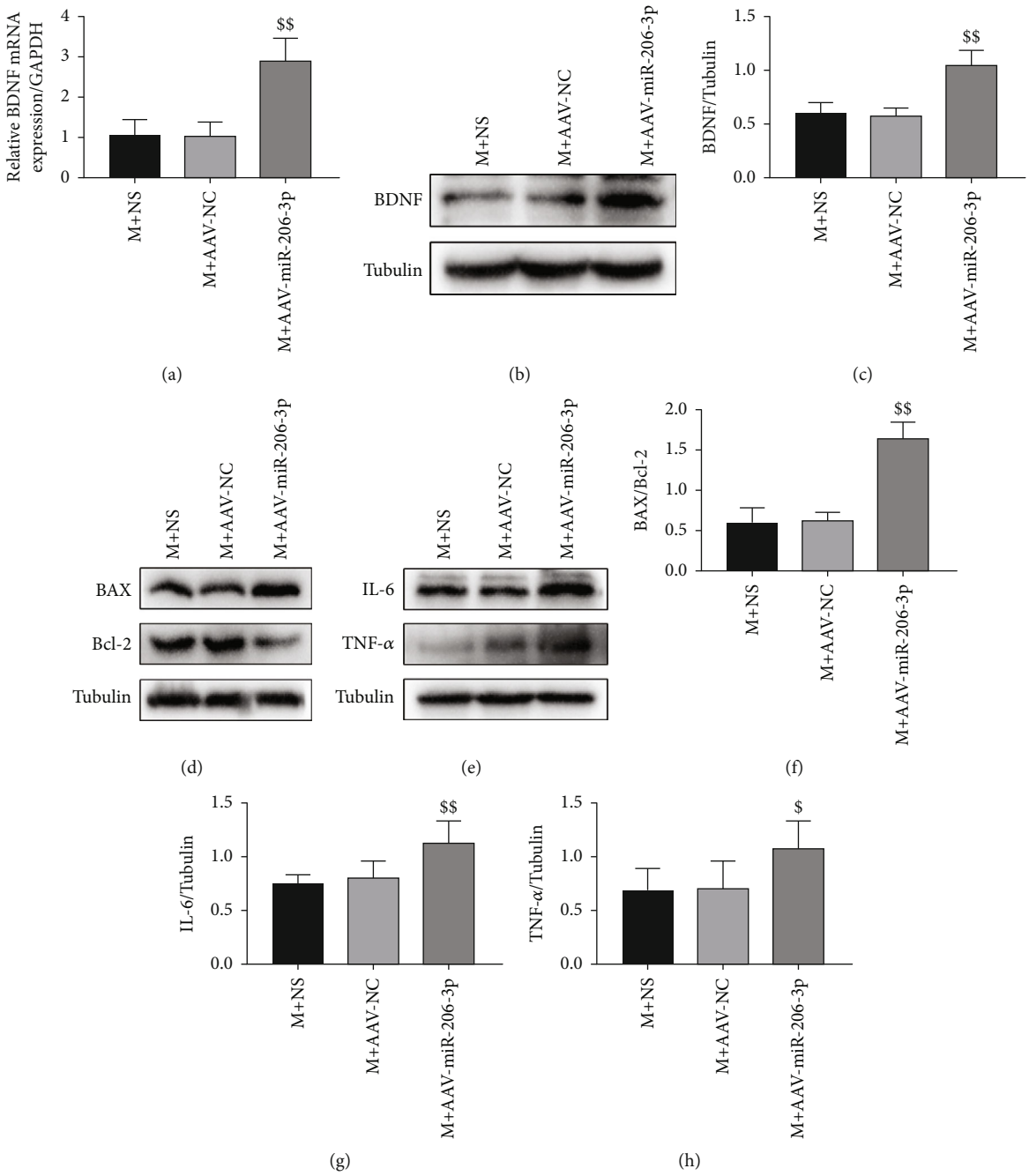

Figure 4: Continued.

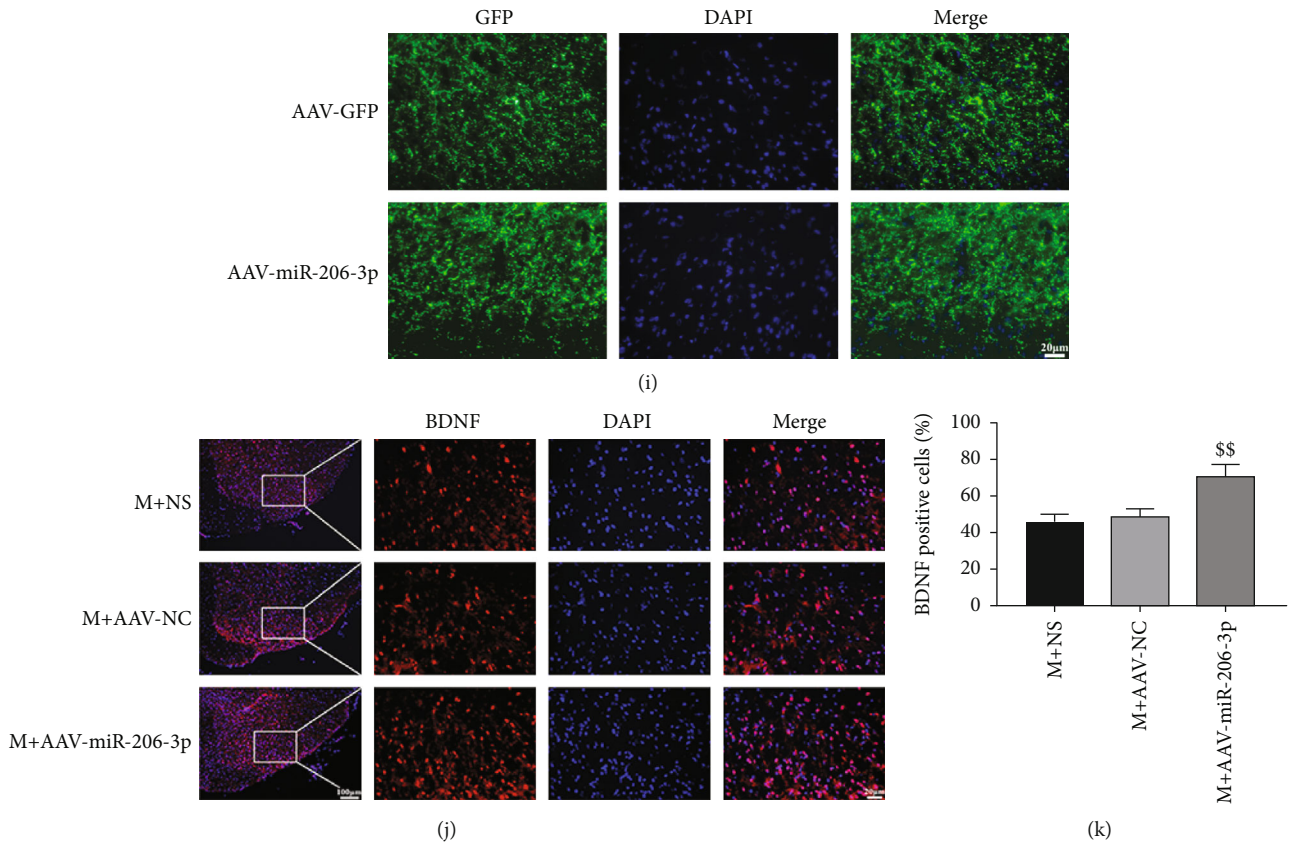

Figure 4: A miR-206-3p inhibitor increased the expression of BDNF, BAX/Bcl-2, IL-6, and TNF-α after CCI. (i) Staining for green fluorescent protein- (GFP-) positive cells (scale bars: 20 μm, 400x). (a–c) The mRNA and protein expression of BDNF/GAPDH ($n = 5$). (j, k) Staining for BDNF-positive (red) cells (scale bars: 100 μm, 100x; 20 μm, 400x) ($n = 5$). (d–g) Representative western blots and quantification data of BAX/Bcl-2, IL-6/GAPDH, and TNF-α/GAPDH ($n = 5$). Bars indicate the mean ± SD. $\$p < 0.05$ and $^{\$\$}$ $p < 0.01$ versus M+NS group.

narrower synaptic spaces and more synaptic vesicles, while the rats in the ME+NS group had synapses with larger synaptic clefts and fewer synaptic vesicles.

3.6. EA Treatment following Injection of a miR-206-3p Inhibitor Did Not Decrease the Expression of BDNF, BAX/Bcl-2, IL-6, and TNF-α after CCI. The results of qPCR and western blot analysis (Figures 6(a)–6(c)) revealed that the mRNA and protein expression levels of BDNF in the ME+AAV-miR-206-3p group were significantly decreased than those in the ME+NS group ($p < 0.01$). IF (Figures 6 (i) and 6(j)) again verified that the fluorescence intensity of BDNF in the ME+AAV-miR-206-3p group was stronger than that in the ME+NS group. Western blot analysis (Figures 6(d)–6(h)) showed that the expression of BAX/Bcl-2, IL-6, and TNF-α was dramatically increased in the ME+AAV-miR-206-3p group than the ME+NS group (BAX/Bcl-2, $p < 0.01$; IL-6, $p < 0.01$; TNF-α, $p < 0.01$).

4. Discussion

Currently, drugs used to relieve neuropathic pain, including opioids and tricyclic antidepressants, do not meet the clinical needs and commonly induce drug resistance [3, 27]. EA, a simple and efficacious treatment method that is usually used to improve neuropathic pain, has long been the focus of researchers [19, 28]. There are studies indicating that the mechanism underlying the analgesic effect of EA involves a variety of processes, such as peripheral and central nervous-humoural regulation [4]. Many studies have demonstrated that the analgesic effect of EA is associated with the frequency of EA stimulation [29]. In our study, the frequency of EA was 2/100 Hz, which can cause enkephalin, endorphins, and dynorphins to be released simultaneously to achieve better analgesia [4, 29]. Clinically, EA treatment is commonly administered at the Zusanli (ST-36) and Yanglingquan (GB-40) acupoints in patients with lower limb neuropathic pain; and the "Segmental Domination Law" is one of the important clinical acupuncture laws, which is widely used in EA for cervical and lumbar spondylosis [30]. Thus, these two acupoints were selected in this study (Figure 7).

The CCI model used in this study was successfully established by Bennett for the first time, and it was the first model used to evaluate neuropathic pain behavior by the mechanical and thermal pain threshold [26]. This model has been widely used because it is easy to construct and induces long-term and stable pain that is highly similar to neuropathic pain observed in the clinic [3, 31]. Our data indicated that the pain thresholds (TWL and MWT) of rats in each

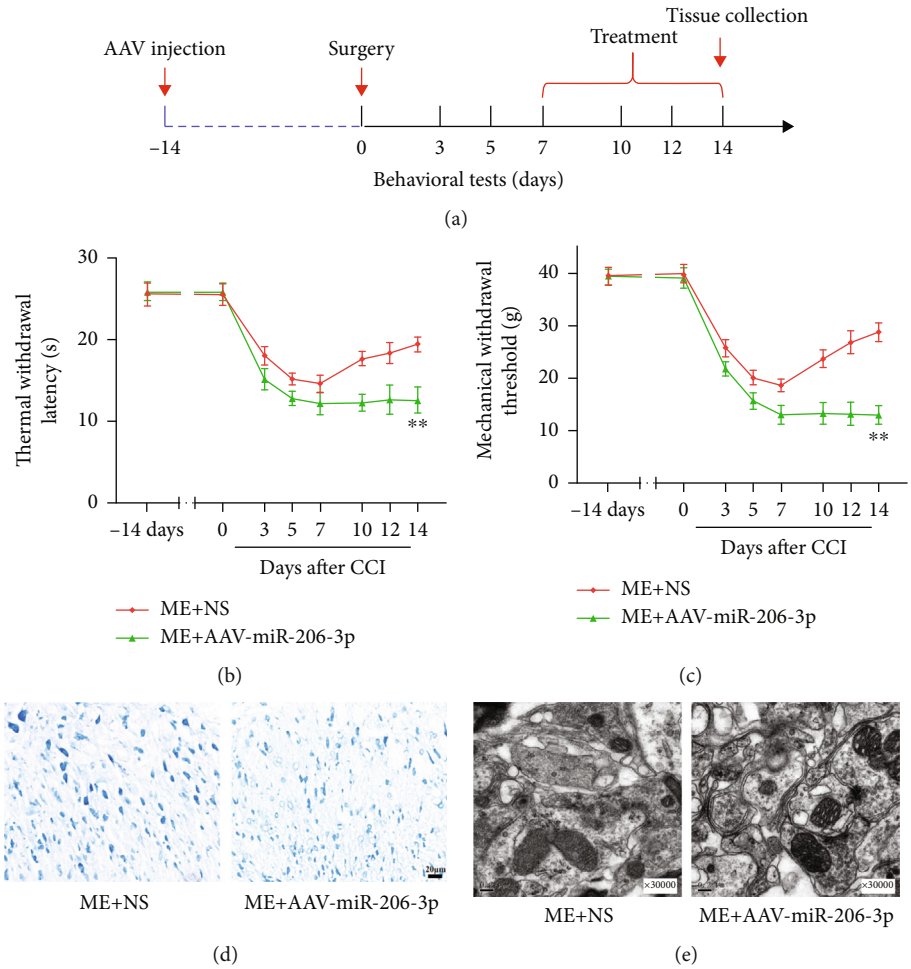

Figure 5: A miR-206-3p inhibitor blocked the therapeutic effect of EA and did not alleviate hyperalgesia. (a) Experimental design and timeline. (b, c) MWT and TWL in each group ($n = 14$). (d) Nissl staining images (scale bars: 20 μm, 50x). (e) The ultrastructural changes of synapses in each group (0.2 μm, 30000x). $^{**}p < 0.01$ versus ME+NS group.

group were significantly decreased after CCI modelling and EA increased these values (Figures 1(b) and 1(c)); this finding is consistent with previous studies.

Neuropathic pain is known to be associated with central sensitization, a process by which the nociceptive signals of neurons at different levels (the spinal dorsal horn, thalamus, and cortex) are gradually enhanced [1, 32]. The spinal dorsal horn plays a central role in pain information transfer and integration, so abnormal excitability and structural remodelling of dorsal horn neurons are crucial for the development of chronic pain [33]. Long-term potentiation (LTP) in the spinal cord is a type of long-term synaptic plasticity and is involved in the central sensitization of pain [23]. Several studies have demonstrated that, after PNI, the release of excitatory neurotransmitters, especially glutamate (Glu), is increased in the spinal dorsal horn, synaptic LTP occurs, and synaptic efficiency is increased [1]. The synapses in the dorsal horn of the spinal cord are key aspects of the connections between neurons, and the increase in their number helps to transmit pain signals between neurons, which may lead to hyperaesthesia during neuropathic pain [23, 34]. The results of TEM indicated that EA alleviated the abnormalities in synapses and that the miR-206-3p inhibitor blocked this effect, by resulting in a smaller synaptic gap and more synaptic vesicles.

During the process of acupuncture-induced analgesia, signals are transferred from acupoints to the CNS, resulting in the spinal cord and brain to release neurotransmitters and neuromodulators (such as opioids, serotonin, and norepinephrine) to suppress pain [4, 35]. Some studies revealed that EA can ameliorate neuropathic pain by inhibiting the activation of microglia and upregulating of BDNF expression in the CCI model [9, 36], which is similar to the results of this study. Moreover, BDNF participates in the formation of spinal cord central sensitization by mediating LTP [33] and is related to synaptic remodelling [13, 15]. miRNAs, as major regulators of gene expression, are known to be associated with the regulation of pain-related networks [2, 37]. Zhao and collaborators confirmed the mechanism by which miRNAs are related to pain in 2010, indicating the importance of miRNAs in inflammatory pain models [28]. Some scholars demonstrated that miRNA-124 and miRNA-146a

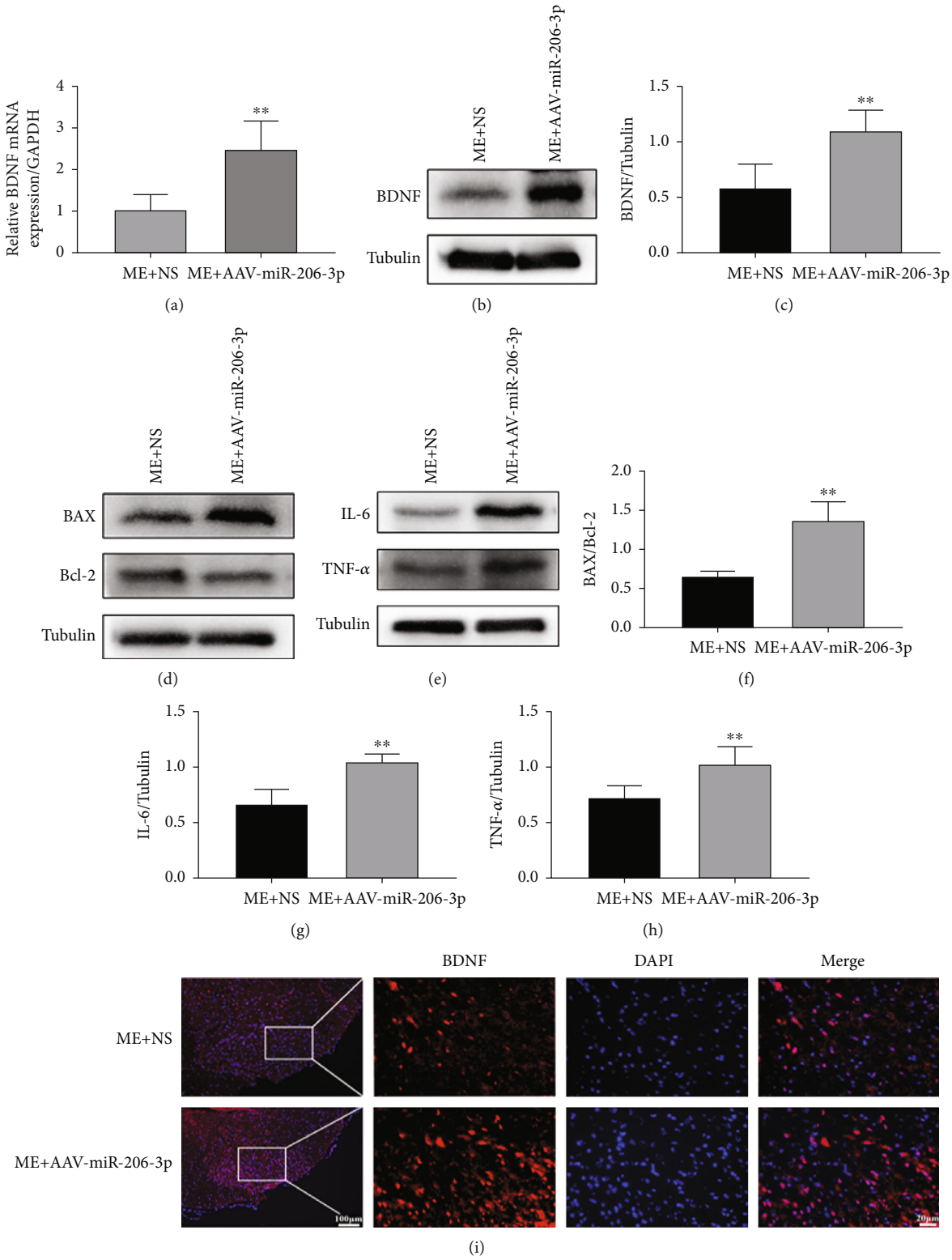

Figure 6: Continued.

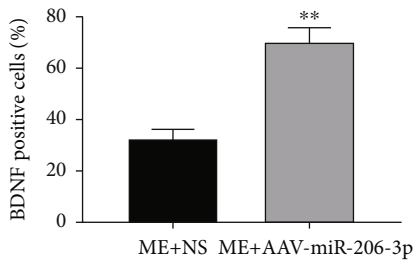

(j)

Figure 6: EA treatment following injection of a miR-206-3p inhibitor did not increase the expression of BDNF, BAX/Bcl-2, IL-6, and TNF-α after CCI. (a–c) The mRNA and protein expression of BDNF/GAPDH ($n = 5$). (i, j) Staining for BDNF-positive (red) cells (scale bars: 100 μm, 100x; 20 μm, 400x) ($n = 5$). (d–h) Representative western blots and quantification data of BAX/Bcl-2, IL-6/GAPDH, and TNF-α/GAPDH ($n = 5$). Bars indicate the mean ± SD. $^{**}p < 0.01$ versus ME+NS group.

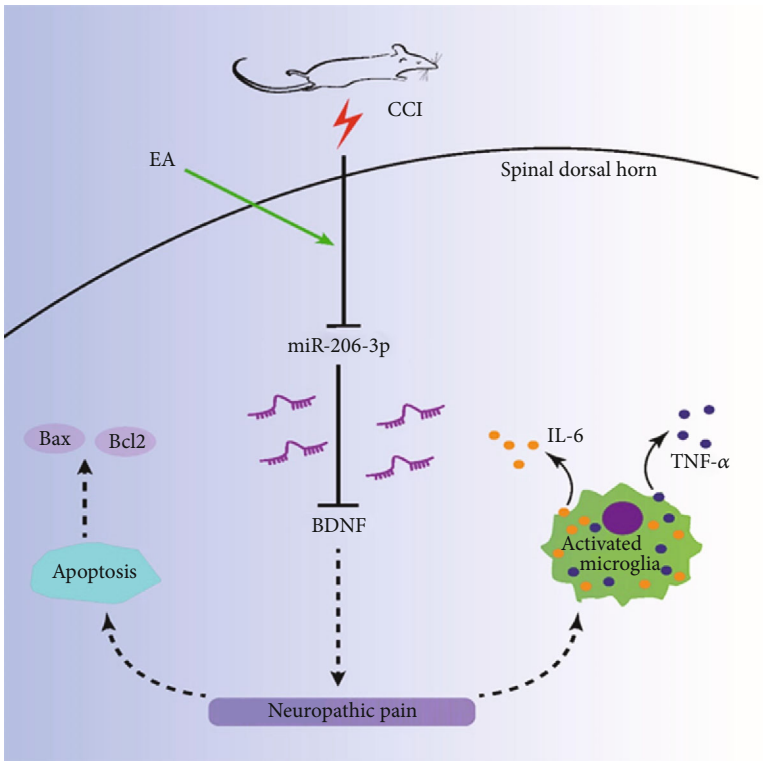

Figure 7: The summary figure for this study. Electroacupuncture exerts analgesic effect by activating miR-206-3P and inhibiting BDNF.

ameliorate continuous neuropathic pain caused by morphine by targeting Toll-like receptor signalling [38]. As a miRNA with a length of 21 nucleotides, miR-206 has two mature isoforms, namely, miR-206-3p and miR-206-5p [31]. Reports have shown that miR-206 has the capacity to modulate nerve and muscle regeneration [39, 40]. In addition, miR-206 promotes neural remodelling by increasing sympathetic and parasympathetic densities [41]. Moreover, miR-206 regulates the target gene BDNF, which participates in neuropathic pain after PNI [15].

Recently, many findings have linked the effect of acupuncture to miRNA function [4]. Extensive evidence has revealed that acupuncture modulates miRNA-BDNF networks, and notably, the complex features of miRNA-BDNF regulatory networks are consistent with the comprehensive multilevel, multitarget, and multilevel modulatory effects of acupuncture [13]. Studies of depression have shown that EA can target BDNF through miR-206 and miR-155 [13]. In this study, BDNF levels were elevated and miR-206-3p levels were decreased in CCI rats. Moreover, BDNF levels were decreased and miR-206-3p levels were markedly higher after EA treatment. Moreover, the miR-206-3p inhibitor led to the upregulation of BDNF expression in the spinal cord dorsal. Consequently, CCI-induced neuropathic pain was alleviated via EA treatment, which was probably the result of an increase in miR-206-3p expression.

Extensive evidence has indicated that the functions of neurons and surrounding glial cells (including astrocytes and microglia) are often mutually regulated, and the complex communication between them promotes peripheral

and central sensitization [22, 42]. The proinflammatory factors (such as IL-6, TNF-α, and IL-1β) are released by spinal microgliosis and that induces the maintenance of neuropathic pain caused by PNI [43, 44]. The major contribution of IL-6 to nociceptive signalling and central sensitization is well established, and TNF-α has been shown to be involved in modulating multiple signalling pathways [22, 45, 46]. Additionally, studies have reported that apoptosis is one programmed form of cell death and is related to the maintenance and occurrence of neuropathic pain [29, 47, 48], and Nissl staining showed that more damaged neurons in the M group were observed than in the S group, which is in accordance with behavioral studies. Furthermore, the BAX gene belongs to the Bcl-2 gene family, which promotes apoptosis, and overexpression of BAX can inhibit the antiapoptotic effect of Bcl-2 and cause cell death [22]. The present study showed that EA treatment led to the low expression of apoptosis-related genes (BAX/Bcl-2) and neuroinflammation markers (IL-6 and TNF-α), while a miR-206-3p inhibitor blocked this effect.

Methods such as interference, overexpression, and inhibition have been widely used in the study of miRNA functions [2, 49]. For instance, some scholars have shown that intrathecal injection of a miR-155 inhibitor can decrease the value of mechanical allodynia and thermal hyperalgesia as well as the expression of proinflammatory cytokines (including IL-1β, IL-6, and TNF-α) in the CCI model remarkably [50]. Viral vectors are commonly applied to control miRNA expression in the nervous system of animal models [2], and AAV vectors are ideal vectors for miRNA research [51]. For instance, Deng and colleagues showed that injecting AAV-SOX10-EGFP into the spinal cord to induce SOX10 overexpression produces mechanical allodynia [52].

In addition, to further clarify whether EA reduces BDNF, BAX/Bcl-2, TNF-α, and IL-6 levels in the CCI model by upregulating miR-206-3p expression, we chose to use AAV to inhibit miR-206-3p expression in lumbar enlargement of the spinal cords in CCI rats. We performed studies at day 14 after virus intrathecal injection, and we used IF to demonstrate that the virus was successfully transfected and evenly distributed in cells in the lumbar spinal cord. In contrast to the beneficial effects of EA therapy, the miR-206-3p inhibitor aggravated the neurobehavioral manifestations and changes in neuronal structure and synaptic plasticity in CCI rats, as well as the increased expression levels of BDNF, BAX/Bcl-2, TNF-α, and IL-6. It was demonstrated that miR-206-3p expression plays an important role in the analgesic effect of EA in CCI rats and that miR-206-3p may be a potential new target for clinical treatment of neuropathic pain following PNI.

However, in our current study, we were unable to construct a miR-206-3p overexpression AAV vector, which is a limitation of our research. Furthermore, our future work will pay more attention to other miRNAs related to the mechanism underlying the effect of EA as well as other noncoding RNAs. Another limitation of our study is that spinal cord specimens from CCI rats were assessed after only 1 week of EA treatment; thus, we did not assess changes at different time points after EA treatment. More research is needed at different time points to address this limitation in the future. Furthermore, only male rats were used in the current study; thus, the possible impact of sex was ignored.

As shown above, EA therapy at the GB-40 and ST-36 acupoints significantly improved the neurobehavioral manifestations and changes in neuronal structure and synaptic plasticity in CCI rats. Furthermore, EA markedly increased miR-206-3p levels, and this effect was accompanied by decreases in BDNF, BAX/Bcl-2, TNF-α, and IL-6 levels in the spinal cord dorsal horn, which were partly blocked by a miR-206-3p inhibitor. Taken together, the current findings suggest that EA has analgesic effects in CCI-induced neuropathic pain, at least partly via miR-206-3p/BDNF regulation.

5. Conclusions

In summary, we found that EA alleviates CCI-induced neuropathic pain by promoting miR-206-3p expression and inhibiting BDNF overexpression in the spinal dorsal horn. Besides, we confirmed the role of apoptosis and neuroinflammation in neuropathic pain.

Data Availability

All datasets generated for this study are available on request to the corresponding author.

Conflicts of Interest

I would like to declare on behalf of my coauthors that no conflict of interest exists in the submission of this manuscript, and the manuscript is approved by all authors for publication.

Authors' Contributions

Tu Wenzhan and Yue Jingjing performed the experiments; Li Xuqing, Wu Qiaoyun, and Yang Guanhu analyzed the data; Shengcun li, Jiang Songhe, and Sun Qiangsan approved the final version of the manuscript. Wenzhan Tu and Jingjing Yue contributed equally to this work. Wenzhan Tu, Jingjing Yue, Xuqing Li are co-first author

Acknowledgments

We thank Wenzhou Medical University for its abundant research platform. This work was supported by the National Natural Science Foundation of China (grant numbers 81873376 and 81574074), the Basic Research Program of Wenzhou City (Y20190200).

References

[1] K. Meacham, A. Shepherd, D. P. Mohapatra, and S. Haroutounian, "Neuropathic pain: central vs. peripheral mechanisms," *Current Pain and Headache Reports*, vol. 21, pp. 21–28, 2017.

[2] M. J. Lopez-Gonzalez, M. Landry, and A. Favereaux, "Micro RNA and chronic pain: from mechanisms to therapeutic

potential," *Pharmacology & Therapeutics*, vol. 180, pp. 1–15, 2017.

[3] Y. Shen, Z. Ding, S. Ma et al., "Targeting aurora kinase B alleviates spinal microgliosis and neuropathic pain in a rat model of peripheral nerve injury," *Journal of Neurochemistry*, vol. 152, pp. 72–91, 2020.

[4] L. Cui, Y. Ding, Y. Feng et al., "MiRNAs are involved in chronic electroacupuncture tolerance in the rat hypothalamus," *Molecular Neurobiology*, vol. 54, pp. 1429–1439, 2017.

[5] J. Wang, Y. Gao, S. Chen et al., "The effect of repeated electroacupuncture analgesia on neurotrophic and cytokine factors in neuropathic pain rats," *Evidence-Based Complementary and Alternative Medicine*, vol. 2016, Article ID 8403064, 11 pages, 2016.

[6] R. Zhang, L. Lao, K. Ren, and B. M. Berman, "Mechanisms of acupuncture–electroacupuncture on persistent pain," *Anesthesiology*, vol. 120, pp. 482–503, 2014.

[7] J. Du, J. Fang, X. Xiang et al., "Effects of low- and high-frequency electroacupuncture on protein expression and distribution of TRPV1 and P2X3 in rats with peripheral nerve injury," *Acupuncture in Medicine*, vol. 39, no. 5, pp. 478–490, 2020.

[8] J. Liu and Y. Wu, "Electro-acupuncture-modulated miR-214 prevents neuronal apoptosis by targeting Bax and inhibits sodium channel Nav 1.3 expression in rats after spinal cord injury," *Biomedicine & Pharmacotherapy*, vol. 89, pp. 1125–1135, 2017.

[9] Y. P. Liu, Z. R. Luo, C. Wang et al., "Electroacupuncture promoted nerve repair after peripheral nerve injury by regulating miR-1b and its target brain-derived neurotrophic factor," *Frontiers in Neuroscience*, vol. 14, 2020.

[10] R. Sha, B. Zhang, X. Han et al., "Electroacupuncture alleviates ischemic brain injury by inhibiting the miR-223/NLRP3 pathway," *Medical Science Monitor*, vol. 25, pp. 4723–4733, 2019.

[11] J. Zhao, H. Tian, H. Song et al., "Effect of electroacupuncture on reuptake of serotonin via miRNA-16 expression in a rat model of depression," *Evidence-Based Complementary and Alternative Medicine*, vol. 2019, Article ID 7124318, 16 pages, 2019.

[12] J. H. Ko and S. N. Kim, "Micro RNA in acupuncture studies: does small RNA shed light on the biological mechanism of acupuncture?," *Evidence-Based Complementary and Alternative Medicine*, vol. 2019, Article ID 3051472, 8 pages, 2019.

[13] X. Li, J. Zhao, Z. Li, L. Zhang, and Z. Huo, "Applications of acupuncture therapy in modulating the plasticity of neurodegenerative disease and depression: do micro RNA and neurotrophin BDNF shed light on the underlying mechanism?," *Neural Plasticity*, vol. 2020, Article ID 8850653, 17 pages, 2020.

[14] N. Cappoli, E. Tabolacci, P. Aceto, and C. Dello Russo, "The emerging role of the BDNF-Trk B signaling pathway in the modulation of pain perception," *Journal of Neuroimmunology*, vol. 349, article 577406, 2020.

[15] W. Sun, L. Zhang, and R. Li, "Overexpression of miR-206 ameliorates chronic constriction injury-induced neuropathic pain in rats via the MEK/ERK pathway by targeting brain-derived neurotrophic factor," *Neuroscience Letters*, vol. 646, pp. 68–74, 2017.

[16] W. Z. Tu, S. S. Li, X. Jiang et al., "Effect of electro-acupuncture on the BDNF-Trk B pathway in the spinal cord of CCI rats," *International Journal of Molecular Medicine*, vol. 41, pp. 3307–3315, 2018.

[17] M. Tan, L. Shen, and Y. Hou, "Epigenetic modification of BDNF mediates neuropathic pain via miR-30a-3p/EP300 axis in CCI rats," *Bioscience Reports*, vol. 40, 2020.

[18] Q. Yang, Z. Liu, and Y. Chang, "Downregulation of miR-206 contributes to neuropathic pain in rats by enhancing RASA1 expression," *International Journal of Clinical and Experimental Medicine*, vol. 9, pp. 3146–3152, 2016.

[19] Z. Wang, T. Yi, M. Long, F. Ding, L. Ouyang, and Z. Chen, "Involvement of the negative feedback of IL-33 signaling in the anti-inflammatory effect of electro-acupuncture on allergic contact dermatitis via targeting micro RNA-155 in mast cells," *Inflammation*, vol. 41, pp. 859–869, 2018.

[20] C. C. Yu, Y. J. Du, S. Q. Wang et al., "Experimental evidence of the benefits of acupuncture for Alzheimer's disease: an updated review," *Frontiers in Neuroscience*, vol. 14, article 549772, 2020.

[21] J. Zhu, Z. Chen, Z. Meng et al., "Electroacupuncture alleviates surgical trauma-induced hypothalamus pituitary adrenal axis hyperactivity via micro RNA-142," *Frontiers in Molecular Neuroscience*, vol. 10, pp. 1–14, 2017.

[22] G.-L. Jin, R.-C. Yue, S.-D. He, L.-M. Hong, Y. Xu, and C.-X. Yu, "Koumine decreases astrocyte-mediated neuroinflammation and enhances autophagy, contributing to neuropathic pain from chronic constriction injury in rats," *Frontiers in Pharmacology*, vol. 9, 2018.

[23] Y. Zheng, Y. Zhou, Q. Wu et al., "Effect of electroacupuncture on the expression of P 2 x 4, GABAA gamma 2 and long-term potentiation in spinal cord of rats with neuropathic pain," *Brain Research Bulletin*, vol. 162, pp. 1–10, 2020.

[24] U. Ali, E. Apryani, H. Y. Wu, X. F. Mao, H. Liu, and Y. X. Wang, "Low frequency electroacupuncture alleviates neuropathic pain by activation of spinal microglial IL-10/β-endorphin pathway," *Biomed Pharmacother*, vol. 125, article 109898, 2020.

[25] Y. Wang, Y.-Y. Xia, M. Xue, Q. Jiang, Z. Huang, and C. Huang, "Electroacupuncture ameliorates mechanical hypersensitivity by down-regulating spinal Janus kinase 2/signal transducer and activation of transcription 3 and interleukin 6 in rats with spared nerve injury," *Acupuncture in Medicine*, vol. 39, no. 4, pp. 358–366, 2020.

[26] J. Bennett Gary and Y.-K. Xie, "A peripheral mononeuropathy in rat that produces disorders of pain sensation like those seen in man," *Pain*, vol. 33, no. 1, pp. 87–107, 1988.

[27] J. Wan, S. Nan, J. Liu et al., "Synaptotagmin 1 is involved in neuropathic pain and electroacupuncture-mediated analgesic effect," *International Journal of Molecular Sciences*, vol. 21, p. 968, 2020.

[28] J. Zhao, M. C. Lee, A. Momin et al., "Small RNAs control sodium channel expression, nociceptor excitability, and pain thresholds," *Journal of Neuroscience*, vol. 30, pp. 10860–10871, 2010.

[29] D. Qi, S. Wu, Y. Zhang, and W. Li, "Electroacupuncture analgesia with different frequencies is mediated via different opioid pathways in acute visceral hyperalgesia rats," *Life Sciences*, vol. 160, pp. 64–71, 2016.

[30] W. Z. Tu, X. F. Lou, S. H. Jiang et al., "Effect of electroacupuncture of local plus distal acupoints in the same segments of spinal cord on spinal substance P expression in rats with chronic radicular pain," *Acupuncture Research*, vol. 33, pp. 7–12, 2008.

[31] J. Wen, T. He, F. Qi, and C. Hongping, "MiR-206-3p alleviates chronic constriction injury-induced 2 neuropathic pain

through targeting HDAC4," *Experimental Animals*, vol. 68, pp. 213–220, 2018.

[32] Z. Dai, H. Chu, J. Ma, Y. Yan, X. Zhang, and Y. Liang, "The regulatory mechanisms and therapeutic potential of micro RNAs: from chronic pain to morphine tolerance," *Frontiers in Molecular Neuroscience*, vol. 11, 2018.

[33] Y. Wang, Y. Zhao, X. Ma, J. Li, J. Hou, and X. Lv, "Beneficial effects of electroacupuncture on neuropathic pain evoked by spinal cord injury and involvement of PI3K-mTOR mechanisms," *Biological Research for Nursing*, vol. 21, pp. 5–13, 2018.

[34] M. Cai, J.-H. Lee, and E. J. Yang, "Electroacupuncture attenuates cognition impairment via anti-neuroinflammation in an Alzheimer's disease animal model," *Journal of Neuroinflammation*, vol. 16, p. 264, 2019.

[35] Y. Gong, N. Li, Z. Lv et al., "The neuro-immune microenvironment of acupoints-initiation of acupuncture effectiveness," *Journal of Leukocyte Biology*, vol. 108, pp. 189–198, 2020.

[36] M. Xue, Y. L. Sun, Y. Y. Xia, Z. H. Huang, C. Huang, and G. G. Xing, "Electroacupuncture modulates spinal BDNF/Trkappa B signaling pathway and ameliorates the sensitization of dorsal horn WDR neurons in spared nerve injury rats," *International Journal of Molecular Sciences*, vol. 21, 2020.

[37] L.-L. Chang, H.-C. Wang, K.-Y. Tseng et al., "Upregulation of miR-133a-3p in the sciatic nerve contributes to neuropathic pain development," *Molecular Neurobiology*, vol. 57, pp. 3931–3942, 2020.

[38] P. M. Grace, K. A. Strand, E. L. Galer, S. F. Maier, and L. R. Watkins, "Micro RNA-124 and micro RNA-146a both attenuate persistent neuropathic pain induced by morphine in male rats," *Brain Research*, vol. 1692, pp. 9–11, 2018.

[39] N. Liu, A. H. Williams, J. M. Maxeiner et al., "Micro RNA-206 promotes skeletal muscle regeneration and delays progression of Duchenne muscular dystrophy in mice," *Journal of Clinical Investigation*, vol. 122, pp. 2054–2065, 2012.

[40] A. H. Williams, G. Valdez, V. Moresi et al., "Micro RNA-206 delays ALS progression and promotes regeneration of neuromuscular synapses in mice," *Science*, vol. 326, pp. 1549–1554, 2009.

[41] Y. Zhang, S. Zheng, Y. Geng et al., "Micro RNA profiling of atrial fibrillation in canines: miR-206 modulates intrinsic cardiac autonomic nerve remodeling by regulating SOD1," *PLoS One*, vol. 10, article e0122674, 2015.

[42] G. Yang, Q. Tan, Z. Li et al., "The AMPK pathway triggers autophagy during CSF1-induced microglial activation and may be implicated in inducing neuropathic pain," *Journal of Neuroimmunology*, vol. 345, 2020.

[43] J. Shi, K. Jiang, and Z. Li, "MiR-145 ameliorates neuropathic pain via inhibiting inflammatory responses and mTOR signaling pathway by targeting Akt 3 in a rat model," *Neuroscience Research*, vol. 134, pp. 10–17, 2017.

[44] Y. Wang, Y. Shi, Y. Huang et al., "Resveratrol mediates mechanical allodynia through modulating inflammatory response via the TREM2-autophagy axis in SNI rat model," *Journal of Neuroinflammation*, vol. 17, no. 1, p. 311, 2020.

[45] Y. Gao, L. Bai, W. Zhou et al., "PARP-1-regulated TNF-alpha expression in the dorsal root ganglia and spinal dorsal horn contributes to the pathogenesis of neuropathic pain in rats," *Brain, Behavior, and Immunity*, vol. 88, pp. 482–496, 2020.

[46] Y.-X. Liang, N.-N. Wang, Z.-Y. Zhang, Z.-D. Juan, and C. Zhang, "Necrostatin-1 ameliorates peripheral nerve injury-induced neuropathic pain by inhibiting the RIP1/RIP3 pathway," *Frontiers in Cellular Neuroscience*, vol. 13, pp. 1–11, 2019.

[47] P. Inquimbert, M. Moll, A. Latremoliere et al., "NMDA receptor activation underlies the loss of spinal dorsal horn neurons and the transition to persistent pain after peripheral nerve injury," *Cell Reports*, vol. 23, pp. 2678–2689, 2018.

[48] S. Kittelmann and A. P. McGregor, "Modulation and evolution of animal development through micro RNA regulation of gene expression," *Genes (Basel)*, vol. 10, 2019.

[49] M. Qu, J. Pan, L. Wang et al., "Micro RNA-126 regulates angiogenesis and neurogenesis in a mouse model of focal cerebral ischemia," *Molecular Therapy-Nucleic Acids*, vol. 16, pp. 15–25, 2019.

[50] Y. Tan, J. Yang, K. Xiang, Q. Tan, and Q. Guo, "Suppression of micro RNA-155 attenuates neuropathic pain by regulating SOCS1 signalling pathway," *Neurochemical Research*, vol. 40, pp. 550–560, 2014.

[51] K. Haenraets, G. W. Albisetti, E. Foster, and H. Wildner, "Adeno-associated virus-mediated transgene expression in genetically defined neurons of the spinal cord," *JoVE (Journal of Visualized Experiments)*, vol. 135, article e57382, 2018.

[52] J. Deng, H. H. Ding, J. L. Long et al., "Oxaliplatin-induced neuropathic pain involves HOXA6 via a TET1-dependent demethylation of the SOX10 promoter," *International Journal of Cancer*, vol. 147, pp. 2503–2514, 2020.

Hindawi
Neural Plasticity
Volume 2022, Article ID 7055697, 8 pages
https://doi.org/10.1155/2022/7055697

Research Article

Short-Term Spinal Cord Stimulation or Pulsed Radiofrequency for Elderly Patients with Postherpetic Neuralgia: A Prospective Randomized Controlled Trial

Lei Sheng,[1] Zihao Liu,[2] Wang Zhou,[1] Xiaojun Li,[1] Xin Wang,[1] and Qingjuan Gong[3]

[1]*Center for Rehabilitation Medicine, Department of Anesthesiology, Zhejiang Provincial People's Hospital (Affiliated People's Hospital, Hangzhou Medical College), Hangzhou, Zhejiang, China*
[2]*Department of Anesthesiology, The First Affiliated Hospital of Guangzhou Medical University, Guangzhou, China*
[3]*Department of Pain Management, The State Key Clinical Specialty in Pain Medicine, The Second Affiliated Hospital, Guangzhou Medical University, Guangzhou, China*

Correspondence should be addressed to Qingjuan Gong; 13093788016@163.com

Received 10 February 2022; Revised 20 March 2022; Accepted 24 March 2022; Published 27 April 2022

Academic Editor: Xue-Qiang Wang

Background. Postherpetic neuralgia (PHN) is the most common and severe complication after varicella-zoster infection, especially in elderly patients. PHN is always refractory to treatment. Both pulsed radiofrequency (PRF) and short-term spinal cord stimulation (stSCS) have been used as effective analgesia methods in clinic. However, which technique could provide better pain relief remains unknown. *Objectives*. This study is aimed at evaluating the efficacy and safety of PRF and stSCS in elderly patients with PHN. *Study Design*. A prospective, randomized-controlled study. *Setting*. Department of Pain Management, the Second Affiliated Hospital of Guangzhou Medical University. *Methods*. A total of 70 elderly patients with PHN were equally randomized to the PRF group or stSCS group. Patients in the PRF group received PRF treatment, while patients in the stSCS group received stSCS treatment. The primary outcome was the effective rate. The secondary outcomes included the Visual Analogue Scale (VAS), the 36-Item Short Form Health Survey Questionnaire (SF-36), and the pregabalin dosage. All outcomes were evaluated at baseline and at different postoperative time points. *Results*. At 12 months after surgery, the effective rate reached 79.3% in stSCS group, while 42.1% in PRF group. The effective rate was significantly higher in the stSCS group than in the PRF group at 3, 6, and 12 months after surgery. VAS scores decreased significantly at each postoperative time point in both groups ($P < 0.001$). The VAS scores were significantly lower in the stSCS group than in the PRF group at 3, 6, and 12 months after surgery. SF-36 scores (bodily pain and the physical role) were significantly improved at each postoperative time point in both groups ($P < 0.001$). The SF-36 scores were significantly higher in the stSCS group than in the PRF group at some postoperative time points. The pregabalin dosage was significantly lower in the stSCS group than in the PRF group at 3, 6, and 12 months after surgery. *Limitations*. A single-center study with a relatively small sample size. *Conclusions*. Both PRF and stSCS are effective and safe neuromodulation techniques for elderly patients with PHN. However, stSCS could provide better and longer-lasting analgesic effect compared to PRF.

1. Introduction

Postherpetic neuralgia (PHN) is one of the most severe complications after infection of herpes zoster (HZ) [1]. The typical symptom of PHN is neuropathic pain distributed over the dermatomal innervation of the affected nerve for more than 3 months [2, 3]. It is estimated that more than 15% of the population worldwide will experience HZ infection in their lifetime, and the incidence will be significantly increasing among people aged over 50 years [4, 5]. Among these elderly HZ patients, complications will occur in almost half of them, especially PHN which has a high occurrence rate of 12.5% [2, 6]. After decades of research on PHZ, its exact neuropathological mechanisms are still not well understood [3]. Currently, effective treatments for PHZ mainly include oral analgesics, pulsed radiofrequency (PRF), and

spinal cord stimulation (SCS) [1, 7–9]. For elderly patients with intractable PHN, oral drugs always fail to achieve complete pain relief and produce side effects as the drugs dose increases. Besides, the clinical efficacy of drugs is uncertain due to individual differences [1]. Hence, invasive therapies are always required for patients who are unresponsive to oral drugs.

PRF is commonly used as a neuromodulation technique in the field of chronic pain therapy [10]. PRF uses short pulsed current to create a high-voltage electric field around the target nerve, which can cause transient edema of the target nerve and further interfere with pain transmission. The effectiveness of PRF in treatment of PHN has been reported in lots of clinical studies [11–13]. SCS has been proven to be an effective interventional technique for patients with pain, especially for those with chronic and intractable neuropathic pain [8, 14]. By implanting electrodes in the epidural space of the appropriate spinal segment and further stimulating it, patients can feel paresthesia in specific area, which can reduce or cover their pain. Since introduced in 1967, SCS has been applied for chronic pain treatment in various diseases [15, 16]. In recent clinical studies, short-term spinal cord stimulation (stSCS) was used in PHZ patients, which produced definite therapeutic effect [17, 18]. Currently, both PRF and stSCS are clinically used for PHZ treatment, yet relevant clinical studies on the comparison between these two techniques are less, especially in elderly patient with intractable pain.

In the present study, we designed a prospective, randomized controlled trial to verify which therapy method is better for PHN patients aged over 50 years old.

2. Methods

2.1. Patients and Study Design. This study was a prospective, randomized, parallel group and controlled trial. It was conducted from January 1, 2015, to January 1, 2018, at the Department of Pain Management, the Second Affiliated Hospital of Guangzhou Medical University, Guangdong, China. This trial was carried out in accordance with the Declaration of Helsinki and approved by the Ethics Committee of the Second Affiliated Hospital of Guangzhou Medical University. All patients were informed the potential risks and complications of the trial and signed the written informed consent before therapy.

2.2. Inclusion and Exclusion Criteria. The inclusion criteria were as follows: (1) patients who were diagnosed with PHN according to the clinical diagnostic criteria [5]; (2) age ≥ 50 years old; (3) typical symptoms of PHN less than one year, such as pricking pain, burning pain, paresthesia, and pruritus; (4) the spinal nerves that were involved, including cervical, thoracic, and lumbar nerves; (5) Visual Analog Scale (VAS) score ≥ 4 points; and (6) pain refractory to conventional pharmacological (such as opiate analgesics, tricyclic antidepressants, anticonvulsants, and topical analgesics) or physical (such as percutaneous electrical nerve stimulation and acupuncture) therapies.

The exclusion criteria were as follows: (1) severe organ dysfunction, including brain, heart, lung, kidney, and liver diseases; (2) severe coagulation disorder or recent use of anticoagulant drugs; and (3) patients who had intellectual problems and were unable to complete self-evaluations, including VAS and 36-Item Short Form Health Survey Questionnaire (SF-36) [19].

2.3. Grouping and Sample Size. One hundred and forty-seven patients with PHN were recruited in this study. Among them, 77 patients were excluded (61 patients did not meet the inclusion criteria; 10 patients refused surgical therapies; 4 patients declined to participate; and 2 patients refused to follow-up), and the remaining 70 patients were randomly assigned to the PRF group ($n = 40$) or the stSCS group ($n = 30$) by using the sealed envelope method (each patient randomly chooses one of the two envelopes containing the PRF group and the stSCS group, respectively) (Figure 1).

According to our pilot study, the effective rates of PRF and stSCS were 45% and 86%, respectively. We then estimated that the sample number was at least 25 in each group, which provided a power of 80% and a level of statistical significance of 0.05 ($\alpha = 0.05$). Considering a potential dropout rate of 5%, we enrolled at least 27 patients in each group. In this study, the blinding method was as follows. All surgical procedures were performed by the same surgeon (Dr. Gong). Pain and function assessments at baseline and at each time point of follow-up were performed by the same investigator who did not know which group the subjects belonged to. The PRF/stSCS instrument was operated by a same nurse who did not participate in any treatment or follow-up.

2.4. Surgical Procedures (PRF and stSCS). The procedures for PRF were as follows. The patient was placed supine (cervical nerve affected) or prone (thoracic and lumbar nerves affected) on the computer tomography (CT) treatment bed. Life signs (blood pressure, heart rate, and oxygen saturation) were continuously monitored. The target intervertebral foramen and the puncture route on the affected side were determined by CT scanning. After satisfactory local anesthesia, radiofrequency needle (20-G, length 100 mm for cervical/thoracic segment and 150 mm for lumbar segment) was inserted according to the predetermined path. Under CT guidance and sensation monitoring (50 Hz, 0.5 V; the radiofrequency instrument, R2000B, Beijing Neo Science Co., Ltd), the needle was slowly advanced until its tip reached the upper edge of the target intervertebral foramen. After withdrawal without blood or cerebrospinal fluid, 2 ml omnipaque contrast medium was injected to confirm the accurate position (the route of the spinal nerve can be visualized). Then, the therapeutic stimulation was performed at the following parameters: temperature, 42°C; frequency, 2 Hz; pulse width, 20 ms; duration, 600 s; and voltage, 40-100 V. The voltage was adjusted gradually from small (40 V) to large (100 V) until the patient felt sensation discomfort. The criterion for parameter adjustment was that the pain area was effectively covered by the electrical-induced

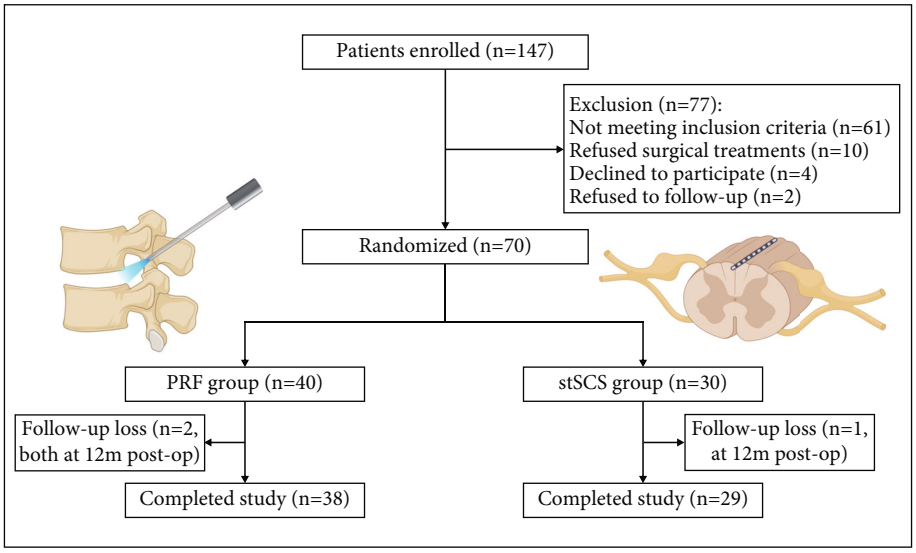

Figure 1: Study flowchart. Seventy patients were randomly assigned to the PRF group and stSCS group. PRF: pulsed radiofrequency; stSCS: short-term spinal cord stimulation.

numbness. The high-voltage, long-duration stimulation was performed twice in each patient, and the duration between two stimulations was 10 minutes.

The procedures for stSCS were as follows. The patient was placed prone on the digital subtraction angiography (DSA) treatment bed. Life signs were routinely monitored. The spinous process was located under fluoroscopy. The target therapeutic segment was determined according preoperative pain dermatome. After local anesthesia, a Tuohy needle was inserted into the epidural space under fluoroscopic guidance, followed by the implantation of a 1×8-contact stimulation electrode (Model: Medtronic 3861, Medtronic, Inc.). The stimulation lead was placed 1-2 mm lateral to the central spinous process (toward the affected side), with its tip adjusted to an appropriate anatomical level. The optimal therapeutic lead position was defined as a pleasant paresthesia coverage of more than 50% of the pain area. Each patient in the stSCS group received only one stimulation lead. After satisfactory positioning, we anchored the lead to the supraspinous ligament and connected it to the pulse generator (Model: Medtronic 3625, Medtronic, Inc.) through an extension cable. Then, a therapeutic short-term electrical stimulation was performed for 2 weeks at the following parameters: voltage, 1-3 V; frequency, 20-80 Hz; and pulse width, 210-450 μs. During the treatment period, patients can control the stimulation level appropriately according to their own response to the paresthesia.

2.5. Pharmacologic Therapies. Before surgical treatments, all patients received a single oral medicine (pregabalin) for pain relief according to their pain severity. The preoperative dose of pregabalin was recorded as the baseline dose. After surgery, all patients were still administered pregabalin for pain management. The pregabalin dose was adjusted according to pain severity. During the clinical trial, all patients avoided other PHN-related pharmacologic therapies.

2.6. Primary Outcome. The primary outcome was the effective rate from baseline to the end of day 360. The effective rate is defined as the proportion of patients with at least a 50% reduction in VAS scores from baseline. The primary outcome was assessed at baseline (before surgery) and at days 1, 7, 30, 90, 180, and 360 after surgery.

2.7. Secondary Outcomes. The secondary outcomes included VAS, SF-36, and pregabalin dosage. The VAS is used to assess pain severity on a scale from 0 (no pain) to 10 (intolerable pain), with higher scores indicating more severe pain. The SF-36 is designed to assess the health status of patients from 8 dimensions. Each dimension was scored from 0 to 100, with higher scores indicating better health. In this study, we assessed the bodily pain and the physical role, the two dimensions most associated with pain. Patients took pregabalin two or three times a day according to their pain severity. The average pregabalin dosage (mg/d) was recorded in both groups. The secondary outcomes were assessed at baseline (before surgery) and at days 30, 90, 180, and 360 after surgery.

2.8. Adverse Events. All adverse events were recorded throughout follow-up, including hematoma at the puncture site, infection, pneumothorax, spinal cord injury, peripheral nerve injury, cerebrospinal fluid leakage, and electrode displacement.

2.9. Statistical Analysis. All statistical analyses were performed using SPSS version 22 (IBM Corp., Armonk, NY). Continuous variables and discrete variables were presented as the mean ± standard deviation and frequency, respectively. For continuous variables, the Shapiro-Wilk test was used to evaluate data normality. An independent-samples t-test or Wilcoxon rank-sum test were used for comparison between groups. One-way repeated measures ANOVA followed by the Bonferroni post hoc test was used to

Table 1: Preoperative characteristics of the patients.

Characteristics	PRF group ($n = 38$)	stSCS group ($n = 29$)	P value
Age (years)	68.29 ± 12.25	70.10 ± 10.24	0.522
Gender (male/female)	19/19	15/14	0.889
Duration of PHN (months)	3.19 ± 2.16	2.94 ± 2.33	0.657
Involved area			0.874
Cervical (%)	7 (18.4)	5 (17.2)	
Thoracic (%)	25 (65.8)	18 (62.1)	
Lumbar (%)	6 (15.8)	6 (20.7)	
VAS scores before surgery	6.66 ± 1.81	7.21 ± 1.78	0.219
Pregabalin dosage before surgery (mg/d)	318.42 ± 110.08	311.21 ± 120.93	0.800

PRF: pulsed radiofrequency; stSCS: short-term spinal cord stimulation; PHN: postherpetic neuralgia; VAS: visual analogue score.

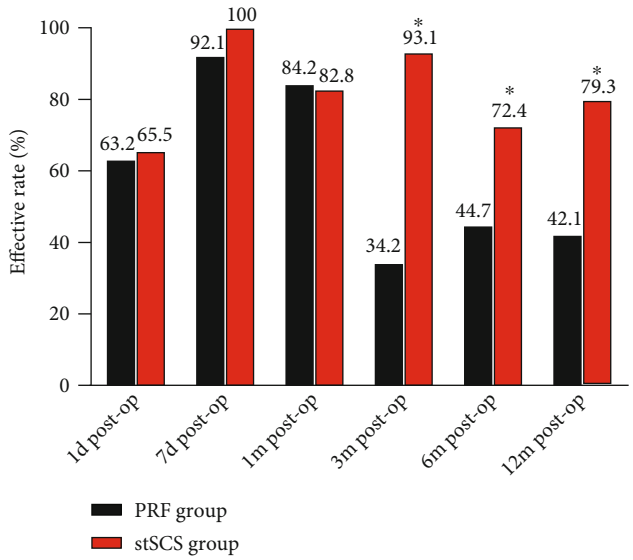

Figure 2: Postoperative effective rate. $^{*}P < 0.05$ indicates the PRF group *vs.* stSCS group.

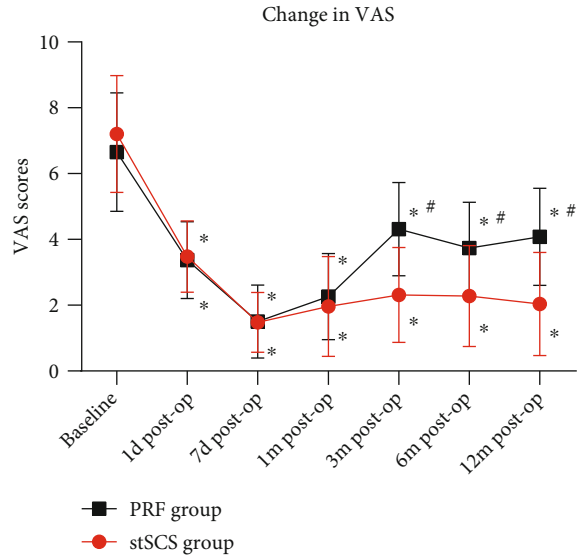

Figure 3: Pre- and postoperative VAS scores. $^{*}P < 0.001$ indicates post-operation *vs.* baseline. $^{\#}P < 0.05$ indicates PRF group *vs.* stSCS group.

compare baseline and postoperative outcomes in each group. For discrete variables, Pearson's chi-square, chi-square continuity correction, or Fisher's exact test was used for comparison between groups. A P value < 0.05 was considered statistically significant.

3. Results

3.1. Patient Demographics. A total of 147 patients with HZ-related pain were enrolled initially, and 77 patients were excluded. Two patients in the PRF group were dropped out at 12 months after surgery, and one patient in the stSCS group was dropped out at 12 months after surgery (Figure 1). Data of these three patients were eliminated. Hence, the final number of patients for analysis was 38 in the PRF group and 29 in the stSCS group (Figure 1). The demographic information included age, gender, duration of PHN, involved area, and preoperative pregabalin dosage. No significant differences in the above characteristics were found between two groups ($P > 0.05$) (Table 1).

3.2. Primary Outcome. The effective rate was significantly higher in the stSCS group compared to the PRF group at months 3, 6, and 12 after surgery ($P < 0.001$, $P = 0.023$, and $P = 0.002$, respectively) (Figure 2). In the PRF group, the effective rate was 44.7% at 6 months after surgery and 42.1% at 12 months after surgery (Figure 2). However, in the stSCS group, the effective rate was 72.4% at 6 months after surgery and 79.3% at 12 months after surgery (Figure 2).

3.3. Secondary Outcomes. The average VAS scores before surgery were 318.42 ± 110.08 and 311.21 ± 120.93 in the PRF group and the stSCS group, respectively. No significant difference in preoperative VAS scores was found between two groups ($P = 0.219$) (Table 1). After surgery, the VAS scores significantly decreased in both groups at each time point, showing an obvious improvement of pain ($P < 0.001$) (Figure 3). However, the VAS scores were significantly lower in the stSCS group compared to the PRF group at months 3, 6, and 12 after surgery ($P < 0.001$) (Figure 3). No significant

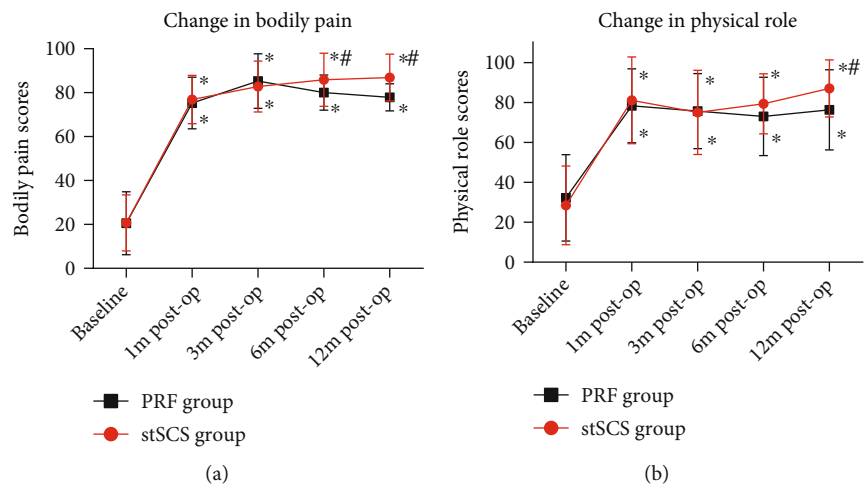

Figure 4: Pre- and postoperative SF-36 scores (bodily pain scores and physical role scores). $^{*}P < 0.001$ indicates postoperation *vs.* baseline. $^{\#}P < 0.05$ indicates PRF group *vs.* stSCS group.

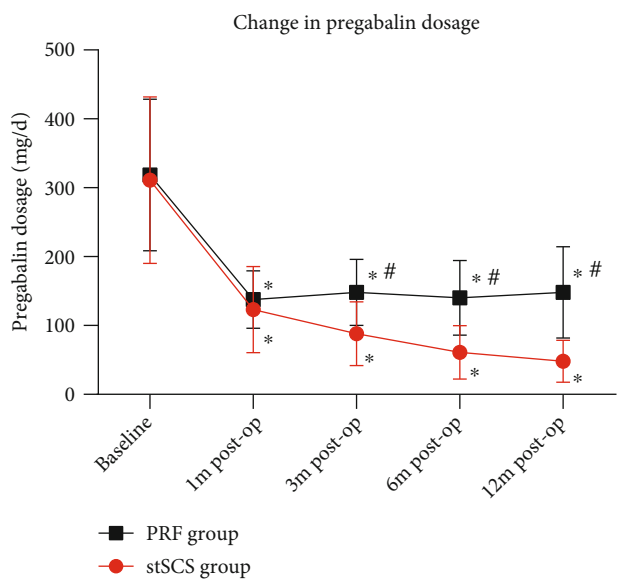

Figure 5: Pre- and postoperative pregabalin dosage. $^{*}P < 0.001$ indicates postoperation *vs.* baseline. $^{\#}P < 0.05$ indicates PRF group *vs.* stSCS group.

differences in preoperative bodily pain scores and physical role scores were found between two groups ($P = 0.962$ and $P = 0.464$, respectively) (Figure 4). After surgery, the scores significantly increased in both groups at each time point ($P < 0.001$) (Figure 4). In terms of bodily pain, the scores were significantly higher in the stSCS group compared to the PRF group at months 6 and 12 after surgery ($P = 0.029$ and $P < 0.001$, respectively) (Figure 4(a)). In terms of physical role, the scores were significantly higher in the stSCS group compared to the PRF group at month 12 after surgery ($P = 0.017$) (Figure 4(b)). After surgery, the pregabalin dosage significantly decreased in both groups at each time point ($P < 0.001$) (Figure 5). However, the dosage was significantly lower in the stSCS group compared to the PRF group at months 3, 6, and 12 after surgery ($P < 0.001$) (Figure 5).

3.4. Adverse Events. Slight hematoma at the puncture site occurred in 2 patients in the PRF group, which gradually subsided within 3 days after the surgery. No patient had infection, pneumothorax, spinal cord injury, peripheral nerve injury, cerebrospinal fluid leakage, electrode displacement, or other serious adverse events after surgical treatments.

4. Discussion

In this prospective randomized controlled study, both PRF and stSCS were effective interventional pain management techniques to relive pain and improve life quality in patients with PHN. The VAS scores were significantly reduced at all-time points of follow-up in both groups. However, the stSCS group showed lower VAS scores at 3, 6, and 12 months after surgery. The SF-36 scores significantly increased at all-time points of follow-up in both groups. Similarly, the stSCS group showed higher SF-36 scores at 12 months after surgery. In addition, the pregabalin dosage in the stSCS group was significantly lower than that in the PRF group at 3, 6, and 12 months after surgery. No serious adverse events occurred in both groups. These results suggested that stSCS provides better and durable pain relief than PRF in PHN patients.

PHN is the most severe complication of herpes zoster. After initial varicella-zoster virus infection, the viral particles invade nerve tissue and remain dormant in somatic sensory ganglia. When the body's cell-mediated immunity changes, the latent varicella-zoster virus can reactivate and replicate along the peripheral sensory nerves, causing neuronal damage and zoster-related pain in dermatomal distributions [5]. The dorsal root ganglion (DRG) is the enlarged tubercle of the dorsal root near each intervertebral foramen, where the cell bodies of first-order sensory afferent neurons are located. The main function of the DRG is to transmit the sensory impulses from peripheral nerve to the spinal cord and brain. DRG is considered to be a novel target for neuromodulation in the treatment of PHN. Here, we used PRF technique to precisely intervene in the function of DRG.

PRF had been proven to be an effective technique for pain management [10–12, 20–22]. PRF technique generates a high-voltage but low-temperature (<40°C) environment around target nerve through high-frequency pulsed current, which can affect the conduction of pain sensory [23]. The underlying mechanism of PRF is attributed to various biological pathways in pain modulation, such as ion channels, neurotransmitters, synaptic function, and immune activity [24]. Since the first application in 1998, numerous studies have demonstrated that PRF on DRG can effectively relieve pain in patients with intractable pain, such as PHN [25]. In previous studies, pain relief started 2 or 3 days after PRF surgery and persisted for 2-6 months in the treatment of PHN [11, 12, 21, 26–28]. In our study, VAS scores decreased significantly at one day after operation. At 3, 6, and 12 months after surgery, the VAS scores showed a slight increase, but it was still significantly lower than baseline. Our results showed that PRF on DRG provided quick and lasting pain relief for PHN patients. In addition, the therapeutic electrical field generated by PRF is high-voltage but low-energy (low frequency and pulse width), which causes no or minimal damage to nerve tissue. Hence, patients did not experience uncomfortable symptoms of surgery-related neurological impairment after surgery. The quality of life also improved significantly after PRF surgery.

SCS is another representative technique of neuromodulation. To date, the exact analgesia mechanism of SCS is still unclear. It is considered that the ascending transmission of pain signals is reduced by electrical stimulation of the dorsal horn of spinal cord [29]. SCS-induced analgesia may also be attributed to the levels of neurotransmitters in the dorsal horn, which reduce zoster-related pain [30]. Since the first clinical application in 1967, SCS technique has developed rapidly [15]. In clinic, SCS is an ideal neuromodulation technique for the treatment of a variety of refractory or recurrent pain. Lots of previous studies have indicated that patients with neuropathic pain can benefit from SCS treatment [8, 17, 18, 21, 31–33]. Our results were consistent with the literature, showing significant pain relief after stSCS treatment. Moreover, the analgesia effect was maintained up to 1 year after operation, which had also been confirmed in some retrospective studies [18, 32]. In the present study, the effective rate was up to 72.4% at half year after surgery and 79.3% at one year after surgery. This result was consistent with a previous randomized controlled study which also showed a 70% effective rate [34]. In the present study, 6 patients in the stSCS group did not meet the criteria of effective rate in 12 months after operation. The preoperative duration of PHN in those six patients was 3.6, 5, 6, 6, 8, and 9.5 months. We considered that the failure to achieve an "effective" was partly due to the course of PHN. Yanamoto et al. reported that patients with a history of PHN less than 6 months could achieve better outcomes with temporary SCS treatment [32]. Hence, we suggested that patients with PHN should receive PRF or stSCS treatments as early as possible, if invasive treatments cannot be avoided [35].

Although postoperative VAS scores decreased significantly in both groups, the pain scores were lower in the stSCS group at 3, 6, and 12 months after treatment, indicating that stSCS therapy had better analgesic effect. This can also be reflected from the effective rate. The effective rate in the stSCS group was as high as 79.3% at one year after treatment, while only 42.1% in the PRF group. The possible reasons are as follows. First, the therapeutic mechanisms of the two techniques are different. The PRF technique is focused on DRG, collection of neuronal cell bodies of peripheral afferent sensory nerves. The stSCS technique is focused on the dorsal horn of spinal cord, the senior nerve center of the DRG. The effective therapeutic area of PRF is limited to the peripheral nerve, while stSCS could suppressed central sensitization. We considered that interventions in the higher-level central nervous system are superior to downstream interventions. Second, the stSCS treatment is a continuous microcurrent stimulation, while the PRF treatment is a temporary pulsed current stimulation. We believed that a 14-day long course of stSCS treatment is better than a 20-minute short course of PRF treatment. Third, the treatment area of PRF involves only one DRG, while the stimulation lead of stSCS has 8 stimulation sites. This indicated that the effective therapeutic dermatomes in the stSCS group were greater than those in the PRF group. In terms of effective rate, a certain number of patients in both groups failed to achieve the efficiency criteria. For patients in the PRF group, if the pain did not improve or recurred, a second PRF procedure or stSCS treatment was suggested [36]. For chronic or refractory PHN, implantation of permanent stimulation lead was recommended after efficacy testing by temporary electrode stimulation.

The main limitation of this trial is that it was a single-center study with a relatively small number of enrolled patients. A multicenter trial with large sample size is needed in the future. Nevertheless, our findings showed preliminary evidence that stSCS was superior to PRF in relieving pain in PHN patients.

5. Conclusions

Both PRF and stSCS could effectively relieve pain for patients with PHN. However, stSCS could provide better analgesic effect, lower pregabalin dosage, and better quality of life than PRF.

Data Availability

The data used to support the findings of present study are available from the corresponding author upon request.

Conflicts of Interest

The authors declared no potential conflicts of interest with respect to the research, authorship, and/or publication of this article.

References

[1] A. Saguil, S. Kane, M. Mercado, and R. Lauters, "Herpes zoster and postherpetic neuralgia: prevention and management," *American Family Physician*, vol. 96, no. 10, pp. 656–663, 2017.

[2] H. J. Forbes, S. L. Thomas, L. Smeeth et al., "A systematic review and meta-analysis of risk factors for postherpetic neuralgia," *Pain*, vol. 157, no. 1, pp. 30–54, 2016.

[3] R. W. Johnson and A. S. Rice, "Postherpetic neuralgia," *The New England Journal of Medicine*, vol. 371, no. 16, pp. 1526–1533, 2014.

[4] G. Luo, Z. Zhang, J. Zhu et al., "Association between the risk of relapse and the type of surgical procedure for herpes zoster-related pain," *Pain Physician*, vol. 24, no. 8, pp. E1227–E1236, 2021.

[5] A. I. Garcia-Gonzalez and O. Rosas-Carrasco, "Herpes zoster and post-herpetic neuralgia in the elderly: particularities in prevention, diagnosis, and treatment," *Gaceta Médica de México*, vol. 153, no. 1, pp. 92–101, 2017.

[6] M. N. Oxman, M. J. Levin, G. R. Johnson et al., "A vaccine to prevent herpes zoster and postherpetic neuralgia in older adults," *The New England Journal of Medicine*, vol. 352, no. 22, pp. 2271–2284, 2005.

[7] C. S. Lin, Y. C. Lin, H. C. Lao, and C. C. Chen, "Interventional treatments for postherpetic neuralgia: a systematic review," *Pain Physician*, vol. 3, no. 22, pp. 209–228, 2019.

[8] T. R. Deer, N. Mekhail, D. Provenzano et al., "The Appropriate Use of Neurostimulation of the Spinal Cord and Peripheral Nervous System for the Treatment of Chronic Pain and Ischemic Diseases: The Neuromodulation Appropriateness Consensus Committee," *Neuromodulation: Technology at the Neural Interface*, vol. 17, no. 6, pp. 515–550, 2014.

[9] B. Wang, Z. du, J. Xia, and H. Zhang, "Efficacy of high-voltage pulsed radiofrequency for the treatment of elderly patients with acute herpes zoster neuralgia," *Revista da Associação Médica Brasileira*, vol. 67, no. 4, pp. 585–589, 2021.

[10] T. Vanneste, A. van Lantschoot, K. van Boxem, and J. van Zundert, "Pulsed radiofrequency in chronic pain," *Current Opinion in Anaesthesiology*, vol. 30, no. 5, pp. 577–582, 2017.

[11] I. Vuka, T. Marciuš, S. Došenović et al., "Efficacy and safety of pulsed radiofrequency as a method of dorsal root ganglia stimulation in patients with neuropathic pain: a systematic review," *Pain Medicine*, vol. 21, no. 12, pp. 3320–3343, 2020.

[12] C. Wu, H. C. Lin, S. F. Chen et al., "Efficacy of pulsed radiofrequency in herpetic neuralgia: a meta-analysis of randomized controlled trials," *The Clinical Journal of Pain*, vol. 36, no. 11, pp. 887–895, 2020.

[13] C. Wan, D. S. Dong, and T. Song, "High-voltage, long-duration pulsed radiofrequency on gasserian ganglion improves acute/subacute zoster-related trigeminal neuralgia: a randomized, double-blinded, controlled trial," *Pain Physician*, vol. 22, no. 4, pp. 361–368, 2019.

[14] M. Raff, R. Melvill, G. Coetzee, and J. Smuts, "Spinal cord stimulation for the management of pain: recommendations for best clinical practice," *South African Medical Journal*, vol. 103, no. 6, pp. 423–430, 2013.

[15] C. N. Shealy, J. T. Mortimer, and J. B. Reswick, "Electrical inhibition of pain by stimulation of the dorsal columns: preliminary clinical report," *Anesthesia and Analgesia*, vol. 46, no. 4, pp. 489–491, 1967.

[16] L. J. Epstein and M. Palmieri, "Managing chronic pain with spinal cord stimulation," *Mount sinai Journal of Medicine: A Journal of Translational and Personalized Medicine*, vol. 79, no. 1, pp. 123–132, 2012.

[17] J. Liu, A. Zhang, X. Ye, X. Hu, R. He, and Z. Jiang, "The effect of short-term spinal cord electrical stimulation on patients with postherpetic neuralgia and its effect on sleep quality," *Neuro Endocrinology Letters*, vol. 42, no. 2, pp. 81–86, 2021.

[18] D. Dong, X. Yu, C. F. Wan et al., "Efficacy of short-term spinal cord stimulation in acute/subacute zoster-related pain: a retrospective study," *Pain Physician*, vol. 20, no. 5, pp. E633–E645, 2017.

[19] L. Lins and F. M. Carvalho, "SF-36 total score as a single measure of health-related quality of life: scoping review," *SAGE Open Medicine*, vol. 4, 2016.

[20] H. Li, Y. Ding, Y. Zhu, Z. Han, and P. Yao, "Effective treatment of postherpetic neuralgia at the first branch of the trigeminal nerve by high-voltage pulsed radiofrequency," *Frontiers in Neurology*, vol. 12, 2021.

[21] M. Ke, F. Yinghui, J. Yi et al., "Efficacy of pulsed radiofrequency in the treatment of thoracic postherpetic neuralgia from the angulus costae: a randomized, double-blinded, controlled trial," *Pain Physician*, vol. 16, no. 1, pp. 15–25, 2013.

[22] C. F. Wan and T. Song, "Comparison of Two Different Pulsed Radiofrequency Modes for Prevention of Postherpetic Neuralgia in Elderly Patients With Acute/Subacute Trigeminal Herpes Zoster," *Neuromodulation: Technology at the Neural Interface*, 2022.

[23] M. C. Chang, "Efficacy of pulsed radiofrequency stimulation in patients with peripheral neuropathic pain: a narrative review," *Pain Physician*, vol. 21, no. 3, pp. E225–E234, 2018.

[24] J. Sam, M. Catapano, S. Sahni, F. Ma, A. Abd-Elsayed, and O. Visnjevac, "Pulsed radiofrequency in interventional pain management: cellular and molecular mechanisms of action-an update and review," *Pain Physician*, vol. 24, no. 8, pp. 525–532, 2021.

[25] M. E. Sluijter, "The effects of pulsed radiofrequency fields applied to the dorsal root ganglion: a preliminary report," *Pain Clinic*, vol. 11, no. 2, pp. 109–117, 1998.

[26] R. C. Maatman, S. M. J. Kuijk, M. A. H. Steegers et al., "A randomized controlled trial to evaluate the effect of pulsed radiofrequency as a treatment for anterior cutaneous nerve entrapment syndrome in comparison to anterior neurectomy," *Pain Practice*, vol. 19, no. 7, pp. 751–761, 2019.

[27] D. Wang, K. Zhang, S. Han, and L. Yu, "PainVision® apparatus for assessment of efficacy of pulsed radiofrequency combined with pharmacological therapy in the treatment of postherpetic neuralgia and correlations with measurements," *BioMed Research International*, vol. 2017, Article ID 5670219, 8 pages, 2017.

[28] A. K. Saxena, K. Lakshman, T. Sharma, N. Gupta, B. D. Banerjee, and A. Singal, "Modulation of serum BDNF levels in postherpetic neuralgia following pulsed radiofrequency of intercostal nerve and pregabalin," *Pain Management*, vol. 6, no. 3, pp. 217–227, 2016.

[29] R. Kuner, "Central mechanisms of pathological pain," *Nature Medicine*, vol. 16, no. 11, pp. 1258–1266, 2010.

[30] J. C. Oakley and J. P. Prager, "Spinal cord stimulation," *Spine (Phila Pa 1976)*, vol. 27, no. 22, pp. 2574–2583, 2002.

[31] H. Harke, P. Gretenkort, H. Ulrich Ladleif, P. Koester, and S. Rahman, "Spinal cord stimulation in postherpetic neuralgia and in acute herpes zoster pain," *Anesthesia & Analgesia*, vol. 94, no. 3, pp. 694–700, 2002.

[32] F. Yanamoto and K. Murakawa, "The Effects of Temporary Spinal Cord Stimulation (or Spinal Nerve Root Stimulation) on the Management of Early Postherpetic Neuralgia from One to Six Months of Its Onset," *Neuromodulation: Technology at the Neural Interface*, vol. 15, no. 2, pp. 151–154, 2012.

[33] K. Moriyama, "Effect of temporary spinal cord stimulation on postherpetic neuralgia in the thoracic nerve area," *Neuromodulation: Technology at the Neural Interface*, vol. 12, no. 1, pp. 39–43, 2009.

[34] B. Liu, Y. Yang, Z. Zhang, H. Wang, B. Fan, and L. Sima, "Clinical study of spinal cord stimulation and pulsed radiofrequency for management of herpes zoster-related pain persisting beyond acute phase in elderly patients," *Pain Physician*, vol. 23, no. 3, pp. 263–270, 2020.

[35] J. Huang, S. Yang, J. Yang et al., "Early treatment with temporary spinal cord stimulation effectively prevents development of postherpetic neuralgia," *Pain Physician*, vol. 23, no. 2, pp. E219–E230, 2020.

[36] C. F. Wan and T. Song, "Efficacy of pulsed radiofrequency or short-term spinal cord stimulation for acute/subacute zoster-related pain: a randomized, double-blinded, controlled trial," *Pain Physician*, vol. 24, no. 3, pp. 215–222, 2021.

Hindawi
Neural Plasticity
Volume 2022, Article ID 9762244, 11 pages
https://doi.org/10.1155/2022/9762244

Research Article

LANCL1 as the Key Immune Marker in Neuropathic Pain

Yu Shi,[1] XueFei Zhang,[1] Qian Fang,[1] Hongrui Zhan,[2] Xianglong Wang,[1] Xiyan Huang,[1] Tao Fan,[1] Wei Liu,[3] and Wen Wu[1]

[1]*Department of Rehabilitation, Zhujiang Hospital, Southern Medical University, Guangzhou 510282, China*
[2]*Department of Rehabilitation, The Fifth Affiliated Hospital of Sun Yat-sen University, Zhuhai 519000, China*
[3]*Department of Rehabilitation, Guangzhou Red Cross Hospital, Jinan University, Guangzhou 510000, China*

Correspondence should be addressed to Tao Fan; fantaokf@163.com, Wei Liu; lw8551082@163.com, and Wen Wu; wuwen66@163.com

Received 1 January 2022; Accepted 21 March 2022; Published 25 April 2022

Academic Editor: Xue-Qiang Wang

Objective. This study is to explore key immune markers and changes of immune microenvironment in neuropathic pain (NeuP). *Method.* The data sets of GSE145199 and GSE145226 in Gene Expression Omnibus (GEO) database was used to analyze, and the key immune markers were verified by GSE70006 and GSE91396, and the infiltration degree of immune cells in different samples were analyzed by CIBERSORT analysis package. *Results.* In this study, we found a key immune marker, namely, LANCL1. Regulatory axis closely related to LANCL1 has also been found, namely, miR-6325/LANCL1 axis. In the immune infiltration analysis, we also found that the LANCL1 is positively correlated with T cells CD4 naïve ($r = 0.880$, $p < 0.05$). *Conclusion.* In this study, we found that LANCL1 may be a protective factor for NeuP, and the miR-6325/LANCL1 axis may be involved in the occurrence and development of NeuP. Cascade reactions including mast cells, macrophages, and T cells may be an important reason for the aggravation of nerve damage.

1. Introduction

Neuropathic pain (NeuP) is a type of pain caused by injury or disease of the nervous system. Its clinical manifestations are hyperalgesia, paresthesia, and spontaneous pain. It is often complicated with sleep disorders, depression, and anxiety [1, 2]. It is estimated that at least 1% -5% of the population suffer from NeuP throughout the year [3]. Because of the diversity of pathogenic factors and the complex pathological mechanism in NeuP, the clinical treatment effect is not satisfactory, which can cause patients to appear serious physiological and psychological disorders, and seriously reduce the quality of life [4, 5]. Therefore, it is of great significance to explore the pathogenesis and prevention of NeuP. Current studies suggest that, imbalance between excitatory and inhibitory somatosensory signals [6], changes in ion channels [7], and variability of pain signals in the central nervous system all have been related with the NeuP. However, the above mechanisms cannot fully explain the occurrence and development of NeuP, and further exploration is needed.

In recent years, researchers have suggested that inflammation and immune mechanisms in the peripheral and central nervous systems play an important role in NeuP [8]. Infiltration of inflammatory cells and activation of innate immune cells activated in response to nervous system damage lead to subsequent production and secretion of various inflammatory mediators. These mediators promote neuroimmune activation and can sensitize primary afferent neurons and cause hypersensitivity to pain [9]. It is well known that nerve injury leads to activation of mast cells and recruitment of neutrophils and macrophages. Tumor necrosis factor (TNF) and interleukin 1 and 6 (IL-1, IL-6) released by immune cells are believed to be closely related to hyperalgesia of NeuP and play an important role in the occurrence and development of NeuP [10]. Some of the molecules

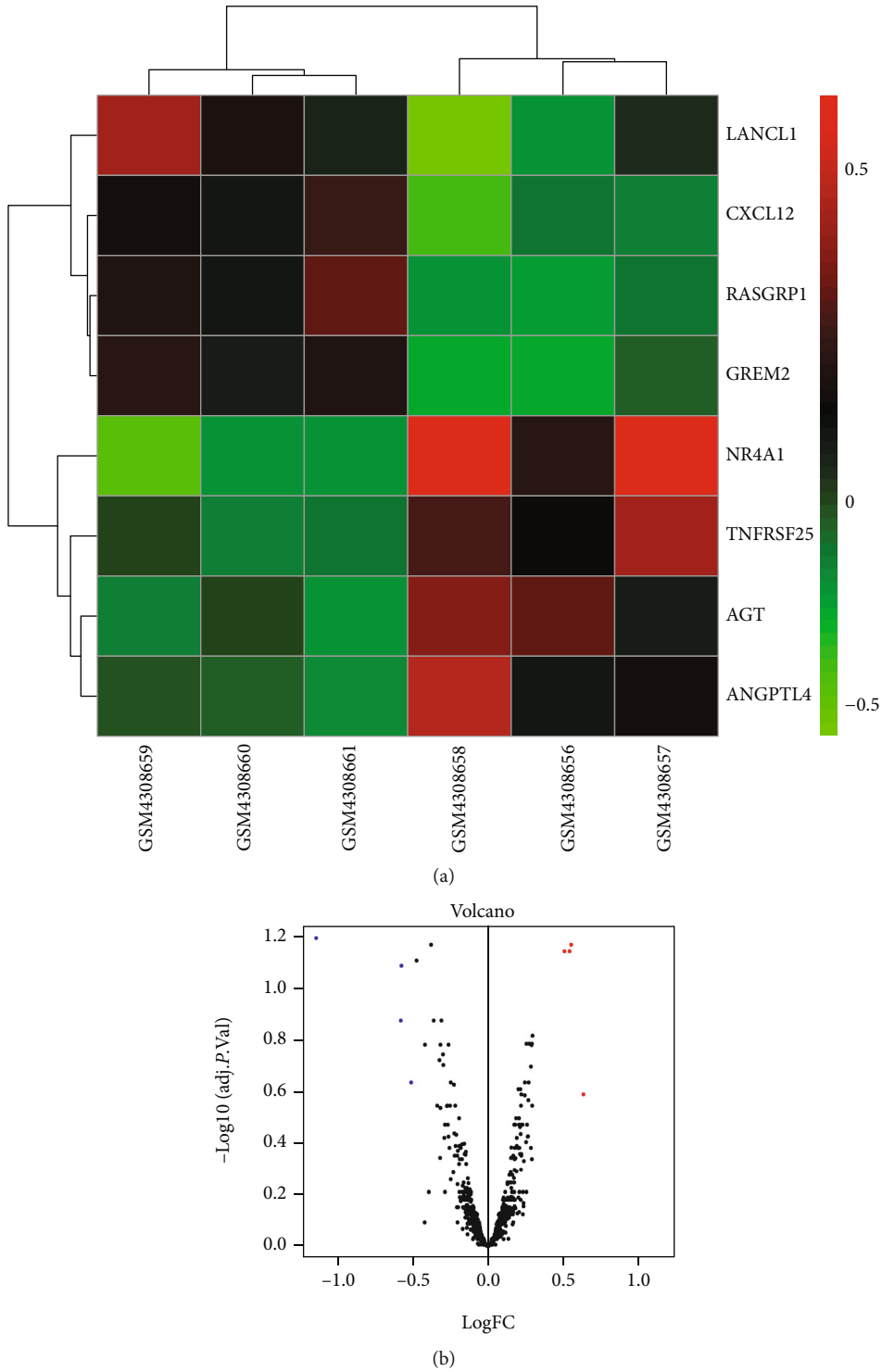

Figure 1: DEGs in the data set: (a) Heatmap of 8 immune DEGs; (b) volcano map of the immune genes; blue represents downregulated immune DEGs, and red represents upregulated immune DEGs.

expressed in gene translation are closely related to immune infiltration and are defined as immune genes [11]. Several immune genes or immune molecules have been shown to play a role in NeuP, such as miRNA-23a/CXCR4 axis [12] and miR-136/IL6R axis [13]. At present, the research on the pathway mechanism of NeuP mainly relies on the verification analysis of the discovered factors, and there is still a lack of screening for the key immune markers of NeuP, leading to the possible omission of the signal axis. Therefore, in order to obtain immune factors closely related to NeuP, we included all immune genes that had been confirmed in the previous studies [14] for screening. At the same time, we

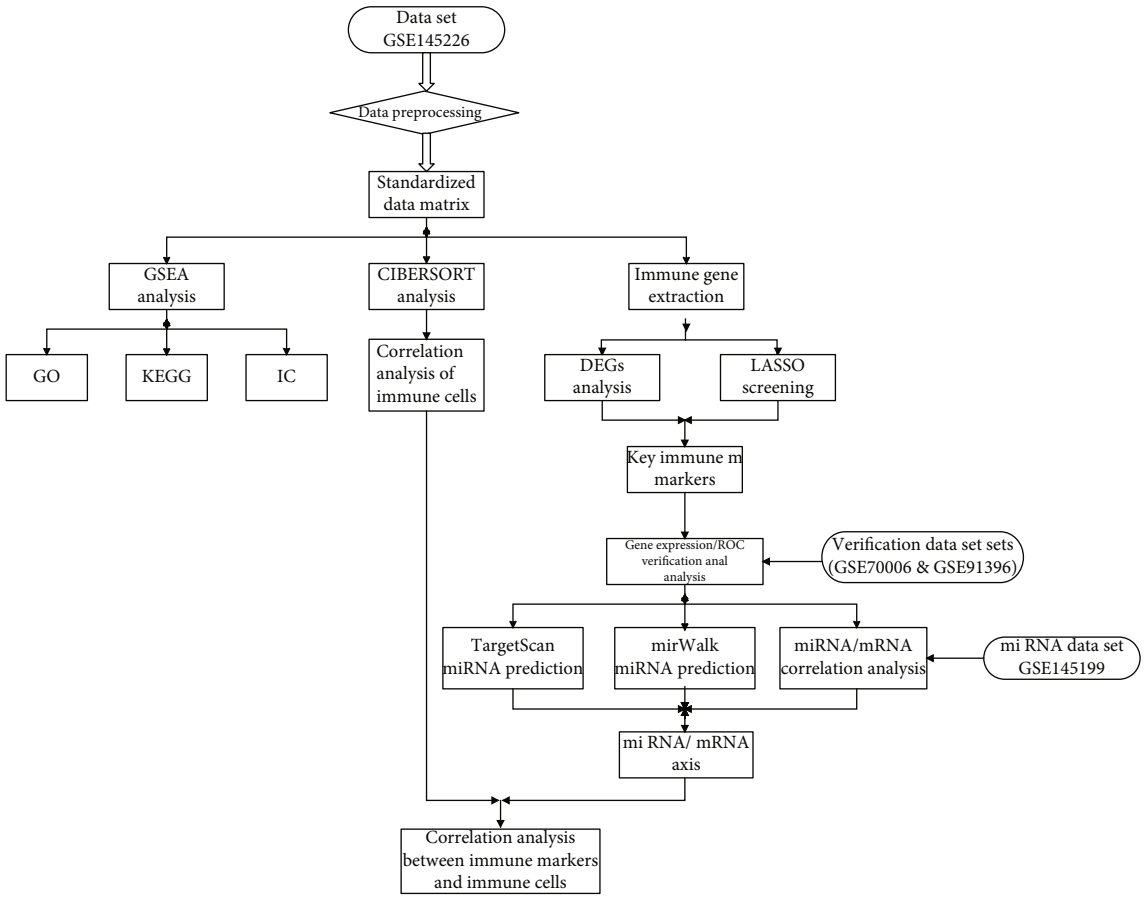

Figure 2: Flow chart of research analysis. GSEA: gene set enrichment analysis; GO: gene ontology; KEGG: Kyoto Encyclopedia of Genes and Genomes; IC: immunological characteristics; DEGs: differential expressed genes; LASSO: least absolute shrinkage and selection operator; ROC: receiver operating characteristic.

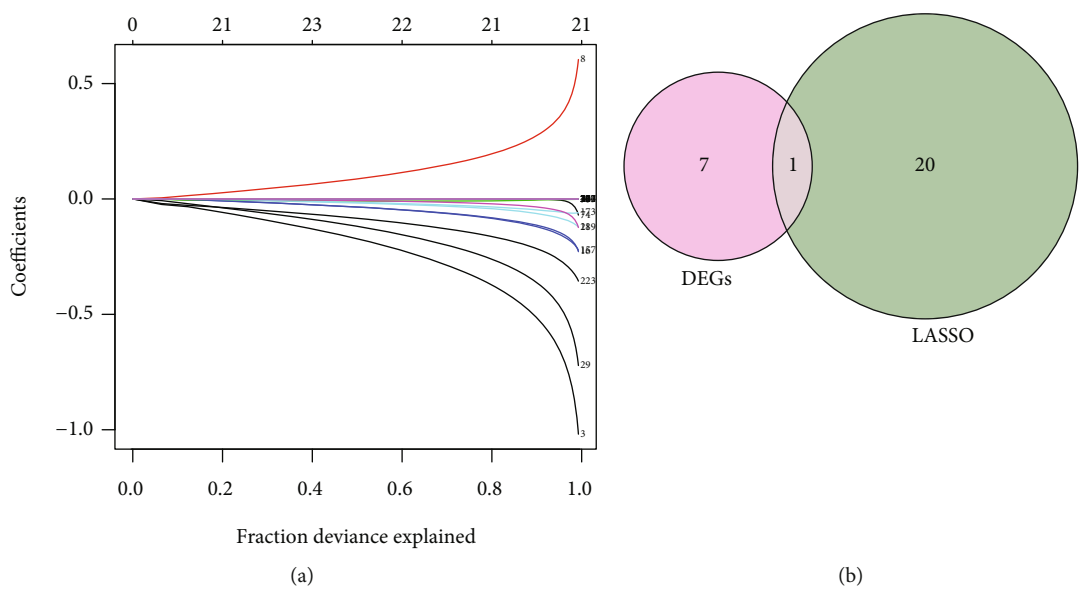

Figure 3: Results of hubgenes screening: (a) the fitted regression curve in LASSO model; (b) Venn diagram of hubgenes screening.

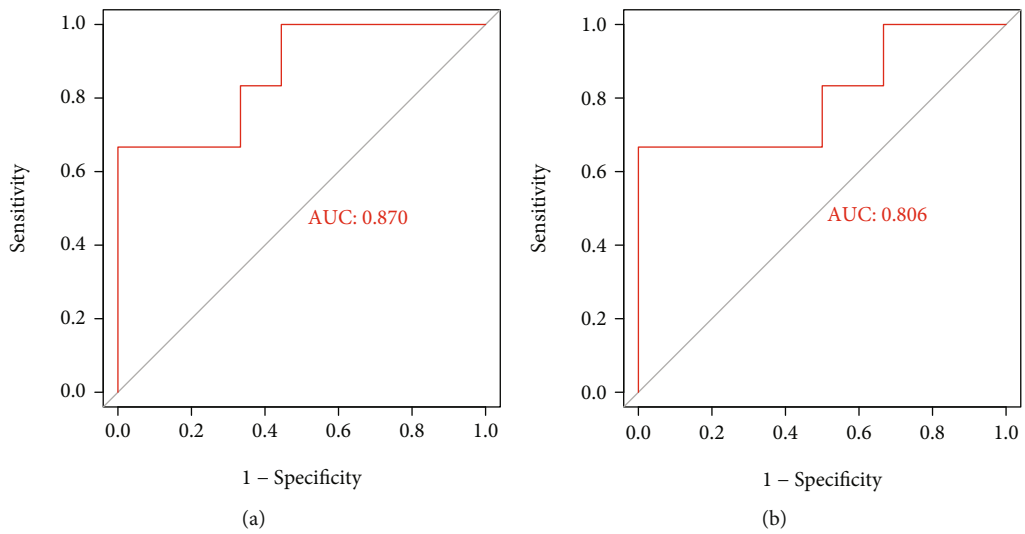

Figure 4: Results of ROC verification: (a) ROC curve of LANCL1 in verification data set of GSE70006; (b) ROC curve of LANCL1 in verification data set of GSE91396.

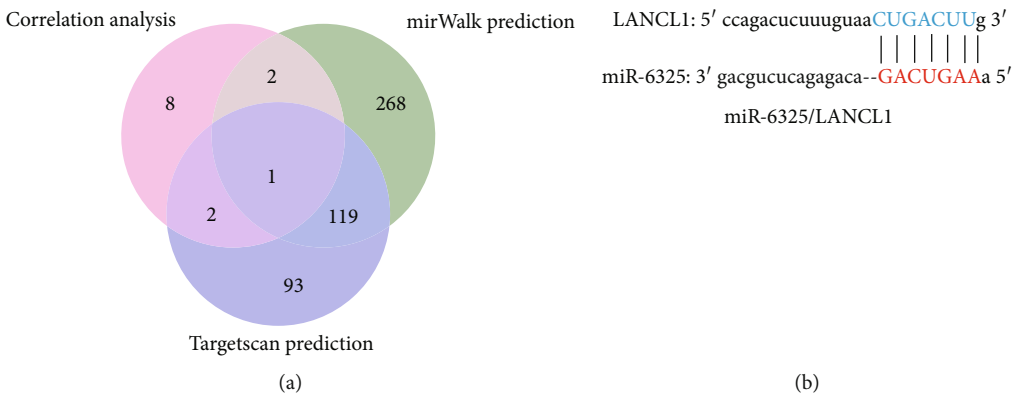

Figure 5: Results of correlation analysis and online database prediction: (a) Venn diagram of miRNA prediction; (b) the binding site of miR-6325/LANCL1 axis.

also included immune infiltration analysis to obtain the infiltration degree of immune cells in different samples to understand the changes in the immune microenvironment of NeuP. It is of great significance to explore the role of key immune markers in immune infiltration and the changes of immune microenvironment from the perspective of immune cell infiltration to reveal the mechanism of NeuP. CIBERSORT [15] is based on immune infiltration data, which allows the use of a transcriptome expression matrix to estimate the abundance of immune cells and other stromal cells in tissue infiltration. CIBERSORT was first used in the analysis of cancer-associated immune infiltration [16] and is now being used in other immune-related studies of nontumor inflammatory responses [17].

In this study, in order to improve the reliability of the research results, we analyzed and estimated mRNA and miRNA data sets sequenced from the same sample set from the Gene Expression Omnibus (GEO) database. Previous studies have shown that neuropathic pain behaviors correlate with synaptic plasticity and limbic cortex alteration [18]. However, the previous screening of key markers of neuropathic pain mostly focused on the inflammatory changes of spinal cord neurons and paid less attention to the inflammatory changes of limbic system. Therefore, we selected the gene data set from limbic cortex for exploration. Key immune markers were obtained through immune gene extraction, differential gene analysis, least absolute shrinkage and selection operator (LASSO) regression model [19] screening, and receiver operating characteristic (ROC) analysis verification. Correlation analysis of mRNAs (key immune markers) and miRNAs was then performed, and online databases (mirWalk and TargetScan) were used to predict the miRNAs likely to bind to key immune markers, and the key miRNA/mRNA signaling axis were obtained after the intersection. Finally, the CIBERSORT analysis package was used to analyze the degree of immune cell infiltration in matrix data and obtain the correlation information between the key immune markers and the immune infiltrated cells. Through this research, we hope to obtain the key immune markers of NeuP and increase the understanding of the immune microenvironment changes in NeuP, so as to provide ideas and help for future research.

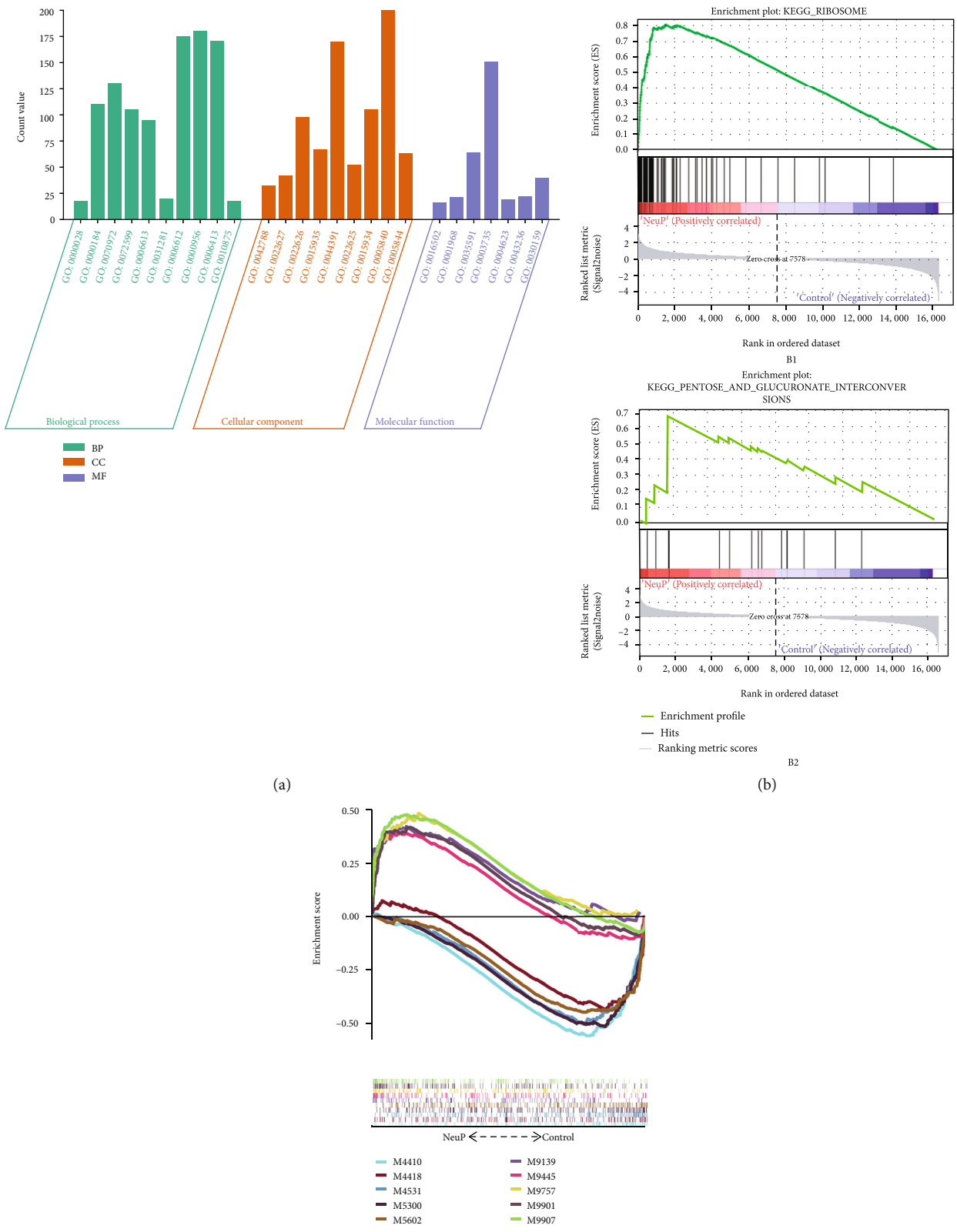

Figure 6: Results of GSEA enrichment analysis: (a) GO term plot of GO enrichment analysis; (b1) enrichment plot of ribosome pathway in KEGG analysis; (b2) enrichment plot of pentose and glucuronate interconversions pathway in KEGG analysis; (c) multiGSEA enrichment plot in IC analysis.

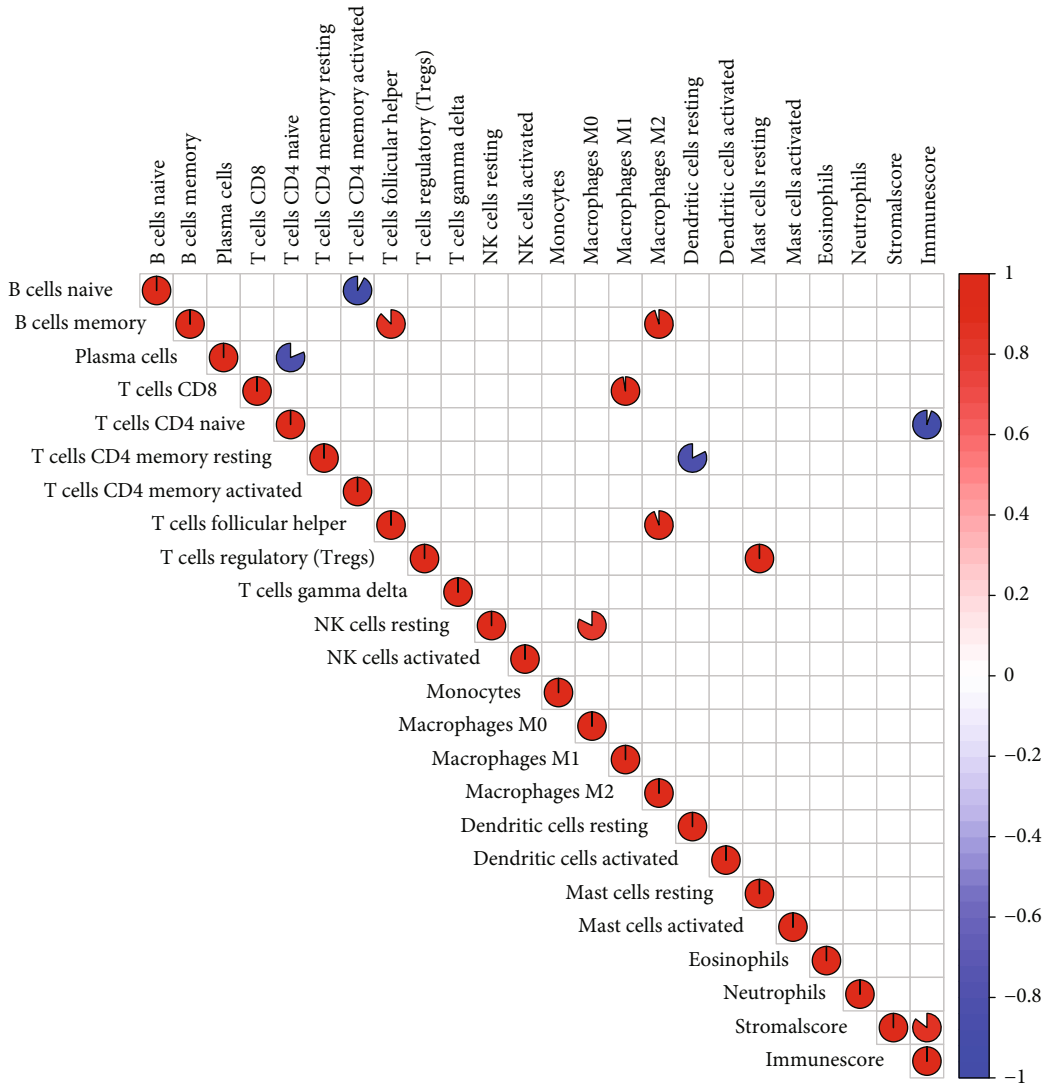

(a)

Figure 7: Continued.

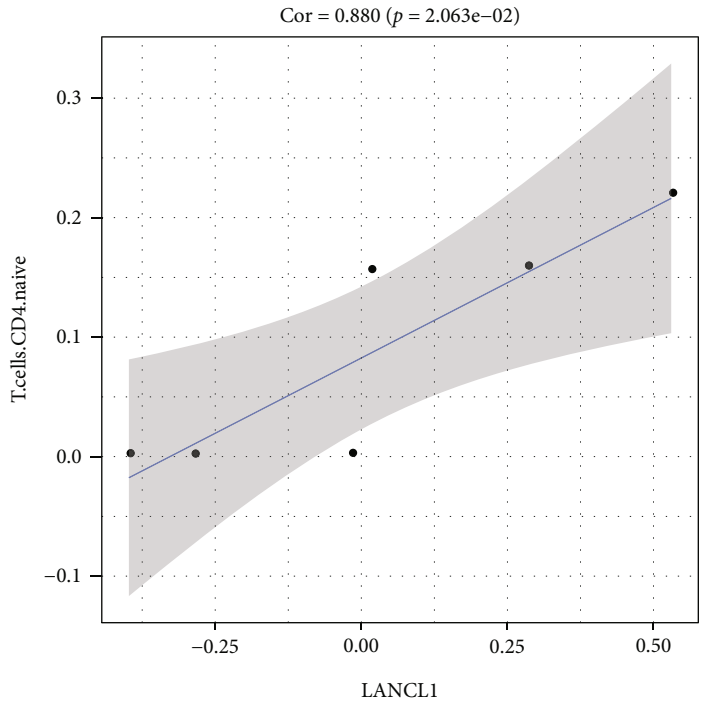

(b)

Figure 7: Correlation analysis results between genes and immune infiltrating cells: (a) correlation analysis of immune infiltrating cells; (b) correlation curve between LANCL1 and T cells CD4 naïve.

2. Methods

2.1. Data Source. In this study, we used the GSE145199 data set (miRNA) [20] and GSE145226 data set (mRNA) [20] in the GEO database as the training set for estimation and analysis and used the data sets GSE70006 and GSE91396 as the verification set to verify the results.

2.2. Data Preprocessing. In this step, we used the R (V4.0.4) software (https://www.r-project.org/) to preprocess the data, including correction and normalization.

2.3. Immune Gene Extraction. In this step, we used the immune gene data provided in the online database ImmPort [14] (https://www.immport.org) to extract the matrix data.

2.4. Differential Expressed Genes (DEGs) Analysis. In this step, we used limma analysis package [21] to perform differential gene analysis on the immune gene data matrix. DEGs with $p < 0.05$ and $|\log2FC| > 0.5$ were considered statistically significant. Then, we used the impute [22] and pheatmap [23] analysis packages to draw the volcano map and heatmap of the DEGs.

2.5. LASSO Analysis Screen. In this step, we performed LASSO regression analysis on immune genomic matrix data using the glmnet [24] analysis package to screen for hubgenes that may be closely associated with NeuP. After that, we intersected the screened hubgenes with DEGs to obtain the key immune markers. And the online website bioinformatics (https://www.bioinformatics.com.cn) was used to draw the Venn diagram.

2.6. ROC Verification of Key Immune Markers. In this step, we used the bioinformatics to perform ROC analysis and draw ROC curve in the verification data sets of GSE70006 [25] and GSE91396 [26]. Hubgenes with $p < 0.05$ and AUC > 0.7 were considered statistically significant; these hubgenes were considered to be key gene markers.

2.7. Correlation Analysis of mRNAs (Key Immune Markers) and miRNAs. In this step, we used the reshape2 [27], dplyr (https://dplyr.tidyverse.org/), and tidyr (https://tidyr.tidyverse.org) analysis packages for the correlation analysis between mRNA and miRNA. According to the binding regulation principle of mRNA and miRNA, correlations with correlation coefficient < -0.4 and $p < 0.05$ were considered statistically significant.

2.8. miRNA Prediction. In this step, we used the online website mirWalk [28] (http://mirwalk.umm.uni-heidelberg.de) and TargetScan (http://www.targetscan.org) to predict miRNAs that may bind to key immune markers. The predicted miRNA/mRNA binding axis was intersected with the miRNA/mRNA correlation axis estimated in the previous step to obtain the key miRNA/mRNA signal axis. The bioinformatics was used to draw the Venn diagram. The miRNA/mRNA signal axis binding sites were also plotted.

2.9. Gene Set Enrichment Analysis (GSEA). In this step, we used the GSEA software [29] to perform Gene Ontology (GO) enrichment analysis, Kyoto Encyclopedia of Genes and Genomes (KEGG) enrichment analysis, and immunological characteristics (IC) analysis on the matrix data. The

results with $p < 0.05$ were considered significant enrichment. The bioinformatics was used to draw the GO term plot, GSEA software was used to draw the GSEA enrichment plot in KEGG, and the ggplot2 [30] analysis package was used to draw the multiGSEA enrichment plot in IC.

2.10. Immune Infiltration Analysis. In this step, we used the CIBERSORT [15] analysis package to estimate the immune infiltration of the data set, and the expression matrix of immune infiltrating cells in different samples was obtained. Then, we used the estimate [31] analysis package to estimate the immune microenvironment of the transcriptome matrix, and the immune scores in different samples was obtained. The corrplot [32] analysis package was used to visualize the correlation between immune infiltrating cells involved in immune microenvironment.

2.11. Correlation Analysis between Key Immune Markers and Immune Infiltrating Cells. The tidyverse [33] analysis package and ggstatsplot [34] analysis package were used to analyze the correlation between the key immune markers and immune infiltrating cells. The correlation coefficient plot was generated. The results with $p < 0.05$ were considered statistically significant.

3. Results

3.1. Results of Data Processing Process. In this study, GSE145199 data set and GSE145226 data set were used for analysis. Firstly, a total of 976 immune genes were extracted from the transcriptome matrix data; secondly, 8 immune DEGs were obtained by differential gene analysis (Figure 1); thirdly, 21 hubgenes were screened by LASSO regression analysis. After crossing with immune DEGs, 1 key immune marker was obtained, namely, LANCL1; fourthly, after correlation analysis and online database prediction, a miRNA/mRNA axis was obtained, namely, miR-6325/LANCL1 axis, and included in the final analysis (Figure 2).

3.2. Results of LASSO Screening. A total of 21 hubgenes were screened out by the LASSO model; the fitted regression curve was shown in Figure 3(a); after the intersection, 1 key immune marker was obtained, namely, LANCL1, as shown in Figure 3(b).

3.3. Results of ROC Verification in Key Immune Marker. The ROC analysis results showed that LANCL1 has good predictability in GSE70006 (AUC = 0.870, $p < 0.05$) and GSE91396 (AUC = 0.806, $p < 0.05$) (Figure 4).

3.4. Results of Correlation Analysis and Online Database Prediction. A total of 13 miRNAs were found to be negatively correlated with LANCL1. Meanwhile, mirWalk database predicted that 390 miRNAs might be bind to LANCL1. TargetScan database predicted that 215 miRNAs might be bind to LANCL1. After intersection, 1 miRNA/mRNA axis was obtained, namely, miR-6325/LANCL1 axis (Figure 5).

3.5. Results of GSEA Analysis. The results of GO enrichment analysis showed that NeuP genes were mainly related to ribosomal small subunit assembly, nuclear-transcribed mRNA catabolic process, nonsense-mediated decay, protein localization to endoplasmic reticulum, establishment of protein localization to endoplasmic reticulum, cotranslational protein targeting to membrane, positive regulation of cyclase activity, protein targeting to membrane, nuclear-transcribed mRNA catabolic process, translational initiation, and positive regulation of cholesterol efflux in biological process (BP); mainly related to polysomal ribosome, cytosolic small ribosomal subunit, cytosolic ribosome, small ribosomal subunit, ribosomal subunit, cytosolic large ribosomal subunit, large ribosomal subunit, ribosome, and polysome in cellular component (CC); and mainly related to nucleotide receptor activity, fibronectin binding, signaling adaptor activity, modified amino acid transmembrane transporter activity, structural constituent of ribosome, phospholipase A2 activity, laminin binding, and signaling receptor complex adaptor activity in molecular function (MF) (Figure 6(a)). The results of KEGG analysis showed that NeuP genes were mainly related to ribosome pathway (Figure 6(b1)) and pentose and glucuronate interconversions pathway (Figure 6 (b2)). The results of IC analysis showed that NeuP genes were mainly related to CD4+ T regulatory cells functions, CD4+ T follicular helper cells functions, dendritic cells (DCs) functions, endogenous retroviruses (ERVs)-related immune response, naive and effector CD8+ T cells functions, and macrophages functions (Figure 6(c)).

3.6. Correlation Analysis Results between Genes and Immune Infiltrating Cells. Correlation analysis results showed that B cells naïve was negatively correlated with T cells memory activated; B cells memory was positively correlated with T cells follicular helper and macrophages M2; plasma cells was negatively correlated with T cells CD4 naïve; T cells CD8 was positively correlated with macrophages M1; T cells CD4 naïve was negatively correlated with immune score; T cells CD4 memory resting was negatively correlated with dendritic cells resting; T cells follicular helper was positively correlated with macrophages M2; T cells regulatory (Tregs) was positively correlated with Mast cells resting; NK cells resting was positively correlated with macrophages M0 (Figure 7(a)). LANCL1 was positively correlated with T cells CD4 naïve ($r = 0.880$, $p < 0.05$) (Figure 7(b)).

4. Discussion

Because of the characteristics of the easily recurrent and difficult treatment of NeuP, it seriously affects the quality of life of the population. Therefore, it is very important to find out the mechanism of NeuP. At present, the mechanism of inflammatory response and the imbalance of immune microenvironment of NeuP has been paid more and more attention by researchers [35]. In this study, we screened the immune genes closely related to NeuP, and estimated the infiltrating degree of immune infiltrating cells in the immune microenvironment. In this study, we found LANCL1 as a key immune marker of NeuP and also found

a miRNA/mRNA axis that closely related to LANCL1, namely, miR-6325/LANCL1 axis. We found the LANCL1 was positively correlated with T cells CD4 naïve. In addition, T cells, B cells, NK cells, macrophages, and dendritic cells have obvious correlation, suggesting the changes of immune microenvironment in NeuP.

In the IC analysis results, we found that the NeuP gene was mainly related the biological process of T cell and macrophages. In the results of immune infiltration analysis, we also found a positive correlation between T cells and macrophages. After peripheral nerve injury, an increase in the number of T cells has been found in the dorsal root ganglia and spinal cord, which suggests that they may play a role in NeuP [36]. After nerve injury occurs, mast cells will be activated first and release too much histamine [37] and TNF [38] and other cytokines, which will lead to nociceptor sensitivity and help the recruitment of neutrophils and macrophages. Both neutrophils and macrophages can produce and release cytokines such as TNF and prostaglandin E2 (PGE2) [39], which can further sensitize nociceptors. The aforementioned cellular activities promote the recruitment of T cells, and T cells can release a variety of cytokines according to their subtypes [40]. The recruitment of immune cells and the release of cytokines aggravate the inflammatory response of nerve injury, leading to NeuP. In our results, T cells, macrophages, and mast cells have an obvious positive correlation, which verifies the important role of the above-mentioned immune cascade in the mechanism of NeuP. The cascade reaction started by the activation of mast cells continuously recruits macrophages and T cells and releases excessive cytokines, leading to the continuous enhancement of the inflammatory response.

CD4+ T cells are helper cells among T cells, which are divided into two subtypes, namely, T helper 1 (Th1) and Th2 cells [41]. Previous studies have shown that Th1 cells produce interleukin-1 (IL-2) and interferon gamma (IFN-γ), which are involved in cell-mediated inflammation; Th2 cells produce IL-4, IL-6, IL-9, IL-10, and IL-13, which are involved in antibody and allergic reactions, and inhibit Th1 cells from synthesizing proinflammatory cytokines [42]. Our results showed that CD4 + T cells were negatively correlated with immune score, suggesting that some CD4 + T cells had protective effect on nerve injury. At the same time, our results also found that LANCL1 was positively correlated with CD4 + T cells, and the expression of LANCL1 was downregulated in NeuP, suggesting that LANCL1 may be a protective factor in the neuroinflammatory response, and LANCL1 may participate in the immune-related signal regulation process. Previous studies have found that LANCL1 has the function of resisting oxidative stress and protecting nerve cells [43, 44]. Decreased expression of LANCL1 affects the protective effect of related pathways on damaged nerves. Downregulation of the miR-6325/LANCL1 axis may be involved in the progression of NeuP. The role of miR-6325 is still unknown, but this gene has also been found in previous NeuP sequencing screening [45], suggesting that miR-6325 may be involved in some regulatory pathways of NeuP. Whether it is only involved in the miR-6325/LANCL1 axis still needs further exploration. Our results also found a negative correlation between B cells and CD4+ T cells. At present, the role of B cells in NeuP is still unclear and needs further exploration [8, 9].

5. Conclusion

In this study, we found that LANCL1 may be a protective factor for NeuP, and the miR-6325/LANCL1 axis may be involved in the occurrence and development of NeuP. Cascade reactions including mast cells, macrophages, and T cells may be an important reason for the aggravation of nerve damage.

Data Availability

The sequencing data used to support the findings of this study have been deposited in the GEO repository (GSE145199, GSE145226, GSE70006, and GSE91396).

Conflicts of Interest

The authors have no conflict of interest.

Authors' Contributions

Study concept and design were proposed by Y.S. and W.W. Acquisition, analysis, or interpretation of data was performed by Y.S., Q.F., and X.W. Drafting of the manuscript was designed by Y.S. and W.W. Critical revision of the manuscript was contributed by T.F., W.L., and W.W. Statistical analysis was conceived and designed by Y.S., Q.F., and X. W. Technical support was contributed by W.W. Study supervision was initiated by W.W. and W.L. Yu Shi, Xuefei Zhang, and Qian Fang contributed to the work equally and should be regarded as co-first authors.

Acknowledgments

This work was supported by the National Natural Science Foundation of China (NNSFC), China. contract grant number: 82102645, 82172526, 81772430, 81801119; Clinical Research Foundation of Southern Medical University, China, contract grant number: LC2016PY037; Guangdong Basic and Applied Basic Research Foundation, China, contract grant number: 2021A1515011042, 2019A1515110739, 2018A030313952, 2021A1515010135; and China Postdoctoral Science Foundation, China, contract grant number: 2019M662995. Project of Administration of Traditional Chinese Medicine of Guangdong Province, China; Contract grant number: 20201066. We thank Cai G. et al., Szyf M. et al., and Descalzi G. et al. for the data sets they shared in GEO (GSE145199, GSE145226, GSE70006 and GSE91396).

References

[1] J. Scholz, N. B. Finnerup, N. Attal et al., "The IASP classification of chronic pain for ICD-11: chronic neuropathic pain," *Pain*, vol. 160, no. 1, pp. 53–59, 2019.

[2] S. P. Cohen and J. Mao, "Neuropathic pain: mechanisms and their clinical implications," *BMJ*, vol. 348, no. feb05 6, 2014.

[3] A. Ellis and D. Bennett, "Neuroinflammation and the generation of neuropathic pain," *British Journal of Anaesthesia*, vol. 111, no. 1, pp. 26–37, 2013.

[4] D. Bouhassira, M. Lanteri-Minet, N. Attal, B. Laurent, and C. Touboul, "Prevalence of chronic pain with neuropathic characteristics in the general population," *Pain*, vol. 136, no. 3, pp. 380–387, 2008.

[5] R. Baron, "Mechanisms of disease: neuropathic pain—a clinical perspective," *Nature Clinical Practice Neurology*, vol. 2, no. 2, pp. 95–106, 2006.

[6] L. Colloca, T. Ludman, D. Bouhassira et al., "Neuropathic pain," *Nature Reviews Disease Primers*, vol. 3, no. 1, pp. 1–19, 2017.

[7] R. Amir, C. E. Argoff, G. J. Bennett et al., "The role of sodium channels in chronic inflammatory and neuropathic pain," *The Journal of Pain*, vol. 7, no. 5, pp. S1–S29, 2006.

[8] G. Moalem and D. J. Tracey, "Immune and inflammatory mechanisms in neuropathic pain," *Brain Research Reviews*, vol. 51, no. 2, pp. 240–264, 2006.

[9] M. A. Thacker, A. K. Clark, F. Marchand, and S. B. McMahon, "Pathophysiology of peripheral neuropathic pain: immune cells and molecules," *Anesthesia and Analgesia*, vol. 105, no. 3, pp. 838–847, 2007.

[10] P.-C. Huang, K.-L. Tsai, Y.-W. Chen, H.-T. Lin, and C.-H. Hung, "Exercise combined with ultrasound attenuates neuropathic pain in rats associated with downregulation of IL-6 and TNF-α, but with upregulation of IL-10," *Anesthesia and Analgesia*, vol. 124, no. 6, pp. 2038–2044, 2017.

[11] S. Bhattacharya, S. Andorf, L. Gomes et al., "ImmPort: disseminating data to the public for the future of immunology," *Immunologic Research*, vol. 58, no. 2-3, pp. 234–239, 2014.

[12] Z. Pan, Q. Shan, P. Gu et al., "miRNA-23a/CXCR4 regulates neuropathic pain via directly targeting TXNIP/NLRP3 inflammasome axis," *Journal of Neuroinflammation*, vol. 15, no. 1, pp. 1–19, 2018.

[13] D. Zhang, J. Y. Mou, F. Wang, J. Liu, and X. Hu, "CRNDE enhances neuropathic pain via modulating miR-136/IL6R axis in CCI rat models," *Journal of Cellular Physiology*, vol. 234, no. 12, pp. 22234–22241, 2019.

[14] S. Bhattacharya, P. Dunn, C. G. Thomas et al., "ImmPort, toward repurposing of open access immunological assay data for translational and clinical research," *Scientific Data*, vol. 5, no. 1, pp. 1–9, 2018.

[15] A. M. Newman, C. L. Liu, M. R. Green et al., "Robust enumeration of cell subsets from tissue expression profiles," *Nature Methods*, vol. 12, no. 5, pp. 453–457, 2015.

[16] B. Chen, M. S. Khodadoust, C. L. Liu, A. M. Newman, and A. A. Alizadeh, "Profiling Tumor Infiltrating Immune Cells with CIBERSORT," in *Methods in Molecular Biology*, Cancer systems biology, pp. 243–259, Springer, 2018.

[17] Y.-J. Deng, E.-H. Ren, W.-H. Yuan, G.-Z. Zhang, Z.-L. Wu, and Q.-Q. Xie, "GRB10 and E2F3 as diagnostic markers of osteoarthritis and their correlation with immune infiltration," *Diagnostics*, vol. 10, no. 3, p. 171, 2020.

[18] F. Guida, M. Iannotta, G. Misso et al., "Long-term neuropathic pain behaviors correlate with synaptic plasticity and limbic circuit alteration: a comparative observational study in mice," *Pain*, vol. Publish Ahead of Print, 2021.

[19] J. Ranstam and J. Cook, "LASSO regression," *Journal of British Surgery*, vol. 105, no. 10, p. 1348, 2018.

[20] G. Cai, Y. Zhu, Y. Zhao et al., "Network analysis of miRNA and mRNA changes in the prelimbic cortex of rats with chronic neuropathic pain: pointing to inflammation," *Frontiers in Genetics*, vol. 11, p. 612, 2020.

[21] M. E. Ritchie, B. Phipson, D. Wu et al., "limma powers differential expression analyses for RNA-sequencing and microarray studies," *Nucleic acids research*, vol. 43, no. 7, article e47, 2015.

[22] T. Hastie, R. Tibshirani, B. Narasimhan, and G. Chu, "impute: Imputation for microarray data," *R package version 1.68.0*, vol. 1, no. 62, 2021.

[23] R. Kolde and M. R. Kolde, "Package 'pheatmap'," *R package*, vol. 1, no. 7, p. 790, 2015.

[24] T. Hastie and J. Qian, "Glmnet vignette," *Retrieved June*, vol. 9, no. 2016, pp. 1–30, 2014.

[25] K. M. Kober, M.-C. Lee, A. Olshen et al., "Differential methylation and expression of genes in the hypoxia-inducible factor 1 signaling pathway are associated with paclitaxel-induced peripheral neuropathy in breast cancer survivors and with preclinical models of chemotherapy-induced neuropathic pain," *Molecular Pain*, vol. 16, 2020.

[26] G. Descalzi, V. Mitsi, I. Purushothaman et al., "Neuropathic pain promotes adaptive changes in gene expression in brain networks involved in stress and depression," *Science signaling*, vol. 10, no. 471, 2017.

[27] H. Wickham, "reshape2: Flexibly reshape data: a reboot of the reshape package," *R package version*, vol. 1, no. 2, 2012.

[28] C. Sticht, C. De La Torre, A. Parveen, and N. Gretz, "miRWalk: an online resource for prediction of microRNA binding sites," *PloS One*, vol. 13, no. 10, article :e0206239, Article ID e0206239, 2018.

[29] A. Subramanian, H. Kuehn, J. Gould, P. Tamayo, and J. P. Mesirov, "GSEA-P: a desktop application for gene set enrichment analysis," *Bioinformatics*, vol. 23, no. 23, pp. 3251–3253, 2007.

[30] H. Wickham, W. Chang, and M. H. Wickham, "Package 'ggplot2'," *Create Elegant Data Visualisations Using the Grammar of Graphics Version*, vol. 2, no. 1, pp. 1–189, 2016.

[31] K. Yoshihara, M. Shahmoradgoli, E. Martínez et al., "Inferring tumour purity and stromal and immune cell admixture from expression data," *Nature Communications*, vol. 4, no. 1, pp. 1–11, 2013.

[32] T. Wei, V. Simko, M. Levy, Y. Xie, Y. Jin, and J. Zemla, "Comment on diagnosis of unilateral trapezius muscle palsy: 54 cases," *Muscle & Nerve*, vol. 56, no. 3, article e24, 2017.

[33] H. Wickham, M. Averick, J. Bryan et al., "Welcome to the Tidyverse," *Journal of Open Source Software*, vol. 4, no. 43, p. 1686, 2019.

[34] I. Patil and C. Powell, "ggstatsplot:"ggplot2" based plots with statistical details," *CRAN*, 2018.

[35] M. Calvo, J. M. Dawes, and D. L. Bennett, "The role of the immune system in the generation of neuropathic pain," *The lancet neurology*, vol. 11, no. 7, pp. 629–642, 2012.

[36] P. Hu and E. McLachlan, "Macrophage and lymphocyte invasion of dorsal root ganglia after peripheral nerve lesions in the rat," *Neuroscience*, vol. 112, no. 1, pp. 23–38, 2002.

[37] Y. A. Mekori and D. D. Metcalfe, "Mast cells in innate immunity," *Immunological Reviews*, vol. 173, no. 1, pp. 131–140, 2000.

[38] H. Junger and L. S. Sorkin, "Nociceptive and inflammatory effects of subcutaneous TNF α," *Pain*, vol. 85, no. 1, pp. 145–151, 2000.

[39] H. Baba, T. Kohno, K. A. Moore, and C. J. Woolf, "Direct activation of rat spinal dorsal horn neurons by prostaglandin E2," *Journal of Neuroscience*, vol. 21, no. 5, pp. 1750–1756, 2001.

[40] G. Moalem, K. Xu, and L. Yu, "T lymphocytes play a role in neuropathic pain following peripheral nerve injury in rats," *Neuroscience*, vol. 129, no. 3, pp. 767–777, 2004.

[41] S. Sad, R. Marcotte, and T. R. Mosmann, "Cytokine-induced differentiation of precursor mouse $CD8^+$ T cells into cytotoxic $CD8^+$ T cells secreting Th1 or Th2 cytokines," *Immunity*, vol. 2, no. 3, pp. 271–279, 1995.

[42] T. R. Mosmann and S. Sad, "The expanding universe of T-cell subsets: Th1, Th2 and more," *Immunology Today*, vol. 17, no. 3, pp. 138–146, 1996.

[43] C. Huang, M. Chen, D. Pang et al., "Developmental and activity-dependent expression of LanCL1 confers antioxidant activity required for neuronal survival," *Developmental Cell*, vol. 30, no. 4, pp. 479–487, 2014.

[44] H. Tan, M. Chen, D. Pang et al., "LanCL1 promotes motor neuron survival and extends the lifespan of amyotrophic lateral sclerosis mice," *Cell Death and Differentiation*, vol. 27, no. 4, pp. 1369–1382, 2020.

[45] K. K. Bali, M. Hackenberg, A. Lubin, R. Kuner, and M. Devor, "Sources of individual variability: miRNAs that predispose to neuropathic pain identified using genome-wide sequencing," *Molecular Pain*, vol. 10, pp. 1744–8069, 2014.